THE PREPARATION AND PROPERTIES OF DENDRITIC AND HYPERBRANCHED POLYESTERS AND THEIR BLENDS WITH PET

Neil McVean Stainton

A thesis submitted for the degree of
Doctor of Philosophy at the University of Durham

July 1994

1 1 ^ T 1 ^4

Abstract

The Preparation and Properties of Dendritic and
Hyperbranched Polyesters and their Blends with PET

A convergent synthesis of aryl ester dendrimers with flexible spacer units via a series of "dendron wedges" of increasing size is described. The development of a high yield iterative protection scheme for phenolic groups as acetates, in the presence of aryl esters, enables dendrimers to be assembled using this approach. These molecules have been blended with PET and the structure-property relationship of the blends investigated. Although dielectric studies show relatively small effects on the T_g relaxation process, the addition of dendrimers to PET produces a significant modification of the tensile drawing behaviour which can be interpreted in terms of the stretching of a molecular network. A small dendrimer acts as a plasticiser and reduces the entanglement density whereas a larger dendrimer acts as an antiplasticising agent and increases the entanglement density.

A new approach to the controlled synthesis of hyperbranched polyesters is demonstrated. This technique facilitates the production of new families of hyperbranched materials without the need to resort to the laborious and time-consuming methods employed in the synthesis of their dendrimer analogues. This work allows for an experimental assessment of some of the points made in the theoretical treatment of the subject and also describes the use of such extensively branched materials to replicate the unusual properties of dendrimer molecules whilst avoiding the difficulties associated with their step-wise synthesis.

Contents

Acknowledgements

Memorandum

The work reported in this thesis has been carried out at the Durham and Leeds sites of the Interdisciplinary Research Centre in Polymer Science and Technology between October 1991 and June 1994. This work has not been submitted for any other degree either in Durham or elsewhere and is the original work of the author except where acknowledged by means of an appropriate reference.

Statement of Copyright

The copyright of this thesis rests with the author. No quotation from it should be published without the prior written consent and information derived from it should be acknowledged.

Financial Support

CHAPTER 1

An Introduction to Dendritic Polymers

An Introduction to Dendritic Polymers

Polymer chemistry is traditionally regarded as the synthesis and characterisation of macromolecular materials which display a distribution in molecular weight and structure. A great deal of emphasis has been put on the understanding and rationalisation of the physical and chemical properties of such materials.

In recent years, there has been significant interest in well-defined, highly ordered species with unusual characteristics that arise as a consequence of their novel topological or molecular geometries. As a result, considerable progress has been made in the study of such materials and their development for a host of speciality applications. In numerous cases, Mother Nature has provided the inspiration behind many ingenious advances.

The natural world abounds with examples of complex, extensively branched self-assembly species, such as trees and coral. Even within our own bodies, the circulation of the blood and operation of neural networks are critically dependent on hyperbranched pathways. It then comes as no surprise to learn that such structures have provided prototype models to be mimicked and investigated at a molecular level, bearing in mind the new properties and phenomena that may be revealed during the course of such work.

The current interest in multibranched polymeric structures may be traced back to the pioneering work of Flory.[1] As early as 1952, he produced a theoretical paper discussing the preparation of polymers from monomer units having a single type A functional group and two or more type B functional groups, so-called AB_x monomers, reactions being restricted to those between a type A and type B group. Each polymer molecule would contain at most one unreacted A functionality and exactly one provided that no intramolecular reaction took place. Although extensively branched, such structures would not form cross-linked network systems and as such, the "branch-on-branch" growth approach could be used to build up a new class of polymeric materials (Figure 1.1).
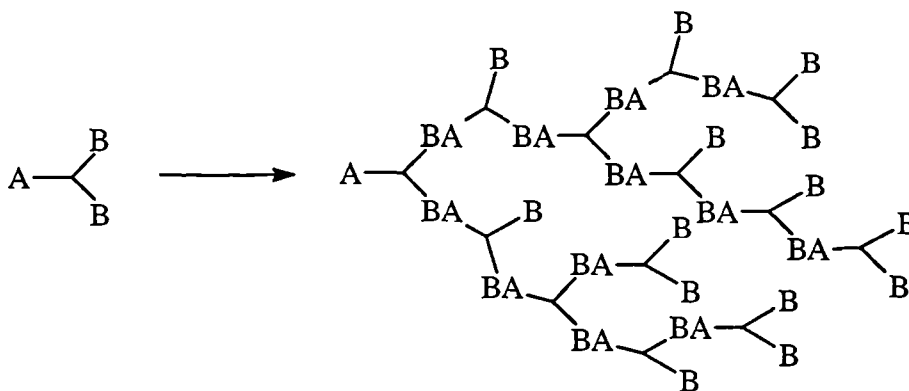
Figure 1.1 A Schematic View of AB_2-type Polymerisation.

It was not until 1978 that Vögtle et al.[2] reported the preparation of a series of "cascade" molecules, utilising a protection/deprotection sequence. The reaction of a monoamine with acrylonitrile introduced nitrile-terminated branching units. These were reduced to amines which upon further treatment with acrylonitrile and subsequent nitrile reduction yielded the cascade structure shown below (Figure 1.2).
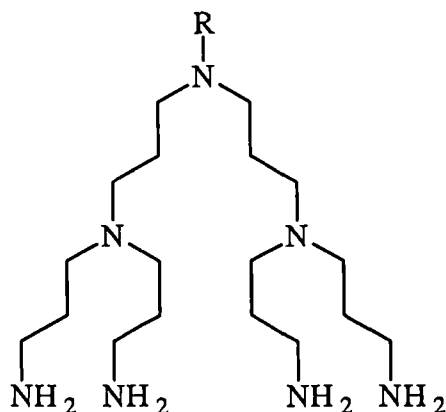
Figure 1.2 The Vögtle Cascade Structure.

Despite this isolated example, the growth of interest in the synthesis of macromolecular three-dimensional species with hyperbranched architecture commenced only as recently as the mid-Eighties. By this time, two research groups, those of Newkome[3-5] and of Tomalia,[6-8] had published reports on their progress towards cascade synthesis. The Newkome group named such structures arborols, a Latin term drawing the analogy of the extensively branched topology of such species

3

to that of trees. In a similar way, Tomalia called such materials "starburst" polymers or dendrimers, (from the Greek word *dendritic* = treelike), the term that has become widely used to describe all species having molecular geometry of this type. In recent literature,[9,10] it has been increasingly common for random, ill-defined polymers having an extensively branched nature to be termed dendrimers or dendritic polymers. In this work, such species will be identified by the alternative term of "hyperbranched polymer". The term "dendrimer" will be exclusively reserved to describe monodisperse species with well-defined topologies and controlled, regular branching units that are coupled to a central core unit. These two kinds of structure are shown diagrammatically in Figure 1.3.

(a)   (b)
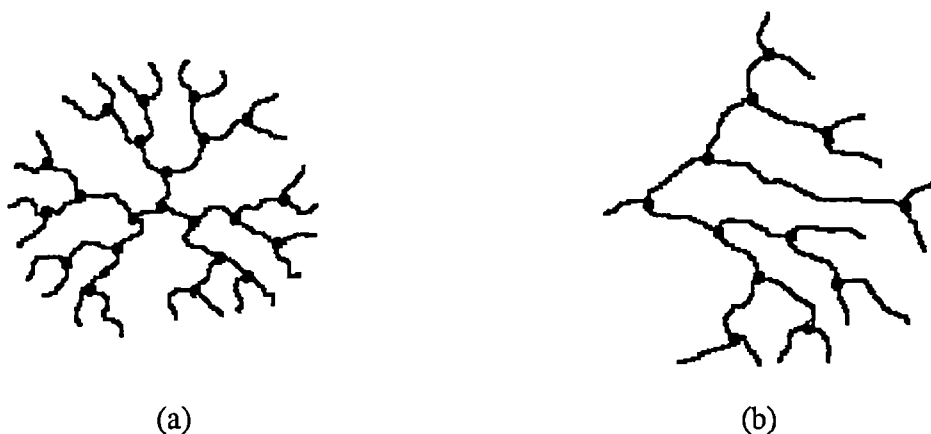
Figure 1.3 Schematic Representation of a) a typical dendrimer

b) a hyperbranched polymer.

In the synthesis of the polyamidoamine (PAMAM) dendrimers,[6] Tomalia and co-workers reacted ammonia with methyl acrylate by exhaustive Michael addition to yield a triester. The subsequent addition of a large excess of ethylenediamine produced a terminal triamine. The reiteration of these two steps was used to build up larger dendritic molecules (Figure 1.4).
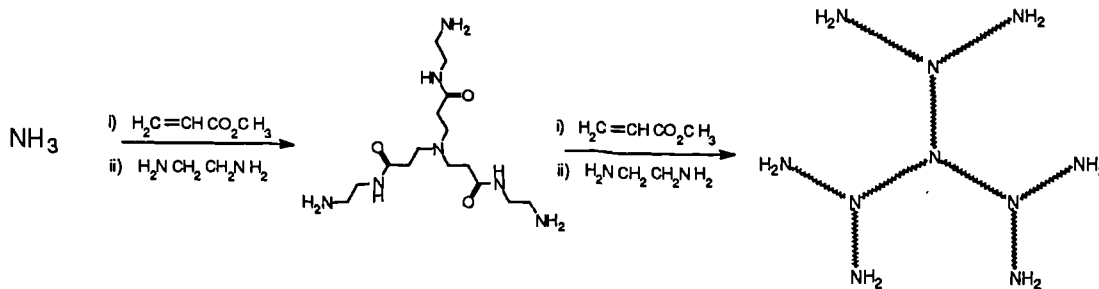
Figure 1.4 Synthetic Scheme for PAMAM Dendrimers.[6]

In the course of (PAMAM) dendrimer synthesis, Tomalia identified many of the general principles involved in the construction of dendrimers and introduced much of the terminology in current usage in this field.[7,11]

Each series of dendrimers consists of a number of macromolecules of increasing size, or "generation". Every member of the series consists of a polyfunctional core to which are attached an increasing number of highly symmetrical layers of branching units (Figure 1.5).

Generation No.	1	2	3	4	5
Terminal Groups	3	6	12	24	48
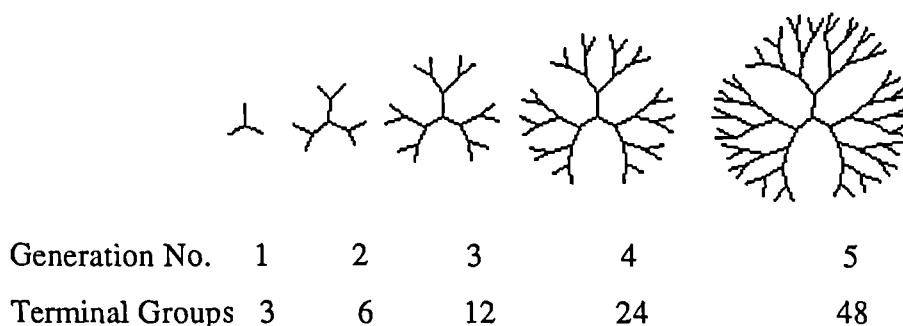
Figure 1.5 A Schematic Dendrimer Series Illustrating the Growth in Size as a Function of Generation.

In the original method for the synthesis of dendrimer molecules, the so-called divergent route, growth commences at the central core molecule by reaction with two or more masked or protected branching units. Subsequently, the protective groups are removed to reveal a dendrimer with reactive terminal functionality. This may be coupled to further branching units and the iterative step-wise growth procedure repeated until a dendrimer of the desired size is prepared. Clearly, the number of

terminal groups added in the formation of each successive generation increases rapidly, following a geometric progression and hence high molecular mass species are readily attained (Figure 1.6).
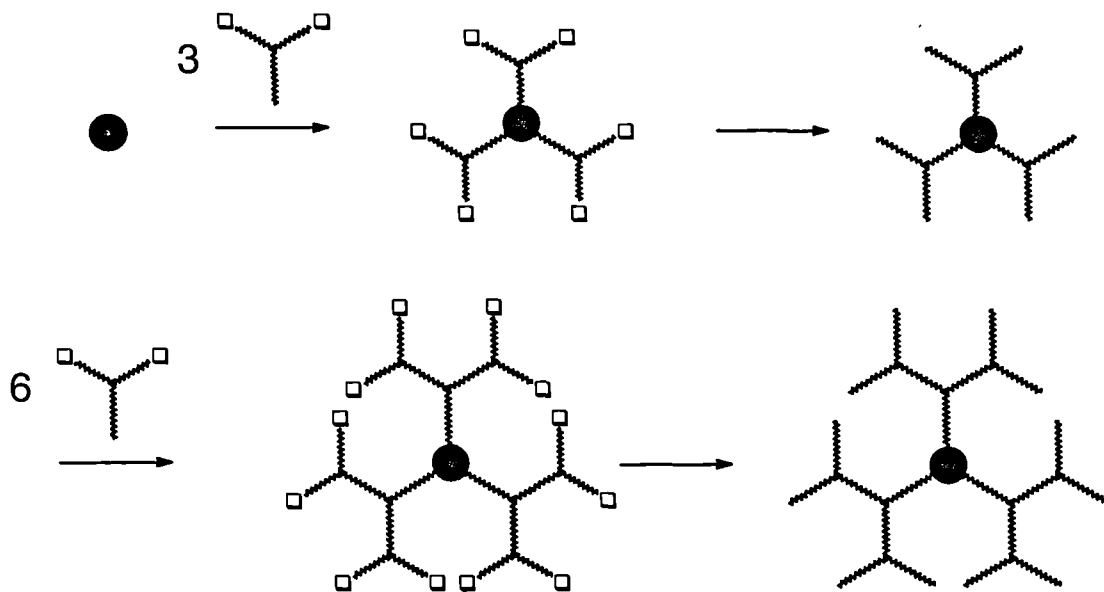
Figure 1.6 A Schematic Representation of the Divergent Route.
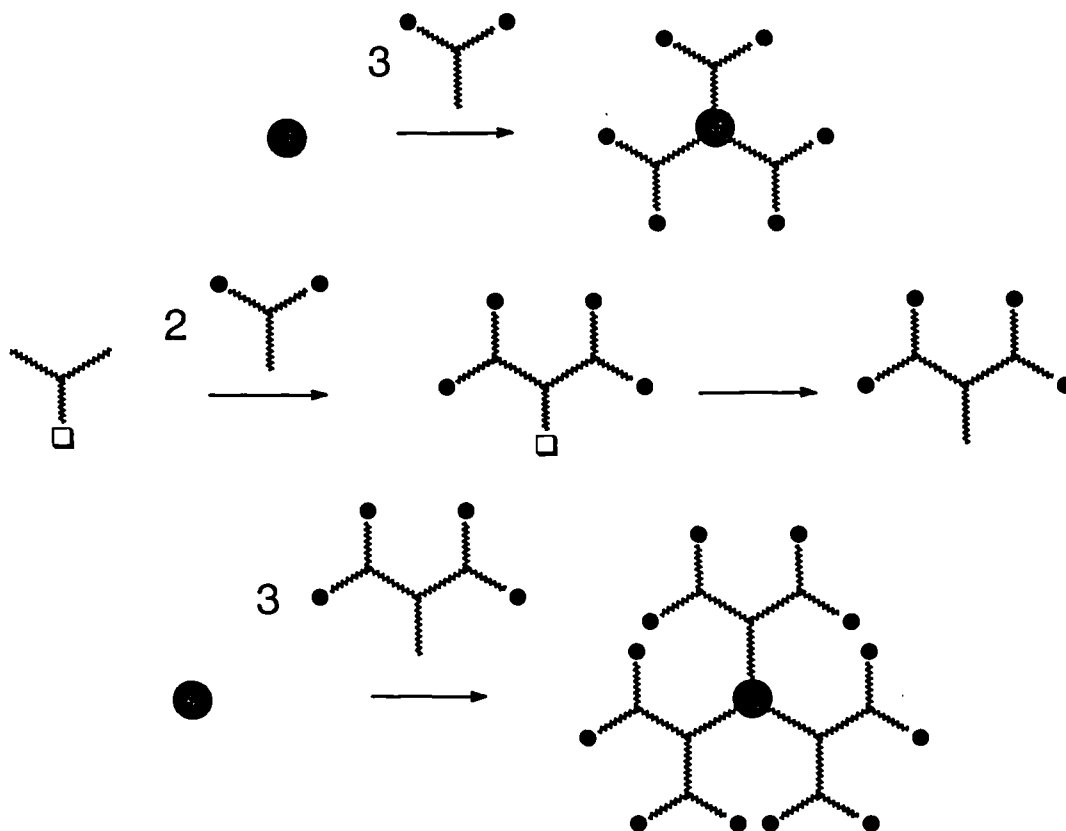
Figure 1.7 A Schematic Representation of the Convergent Route.

More recently, convergent techniques have been used by a number of groups working in this field,[12-16] notably that of Fréchet, in which dendrimer construction commences at what will ultimately be the periphery of the molecule and grows inwards via a series of "dendron wedges" of increasing size that are eventually attached to the core molecule (Figure 1.7). In contrast to growth by the divergent route, convergent growth of each dendron wedge requires only a limited number of reactions to be carried out in each generation growth step. As such, the convergent methodology readily overcomes the problems associated with incomplete or undesirable reactions at congested surfaces. These result in a variety of defects and structural abnormalities, such as branching irregularity and inter dendrimer branching, which are features responsible for the breakdown of ideal divergent growth. The convergent approach has become the preferred mode of synthesis since a monodisperse dendrimer is generally more readily obtained in this way. Two examples of the synthesis of dendron wedges are shown in Figure 1.8. In both cases, dendrimer synthesis would be completed by coupling to an appropriate core molecule.

A major disadvantage associated with convergent growth is the limitation in the ultimate size of dendrimers that can be obtained. With increasing wedge size, the degree of steric inhibition at the focal point rises substantially and the resultant diminished reactivity restricts the size of monodisperse macromolecules that can be prepared in this way. In order to overcome such problems, a number of approaches have been taken to generate larger dendrimers by the convergent route. For example, a "double stage" convergent growth technique[17] has been developed. This involves the preparation of dendrimers having a reactive functional group at each peripheral chain end. Such molecules can then be used as "hypercores" to which other large dendron wedges may be attached although it is quite conceivable that branching irregularity may occur as a result. More recently, this concept has been adapted to facilitate accelerated fully convergent growth by replacement of conventional AB_2-type monomers with double-generation $A(BA)_2B_4$ branches.[18] This significantly reduces the number of stages required for the synthesis of higher dendrimer generations.
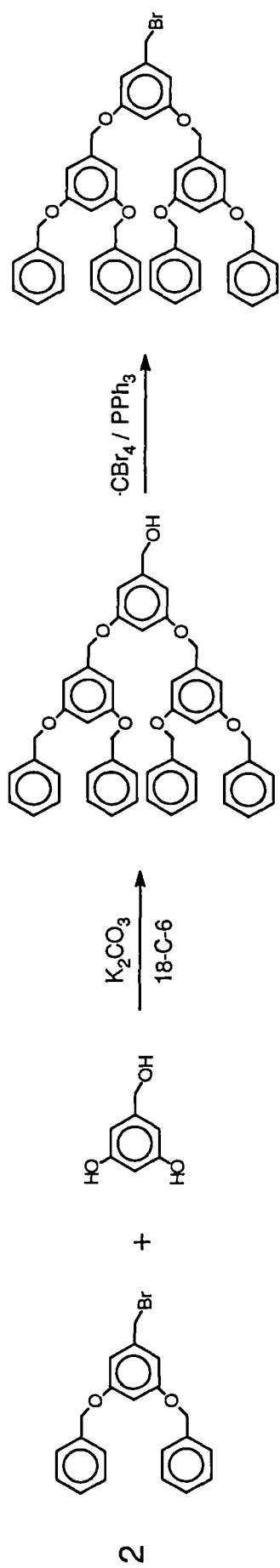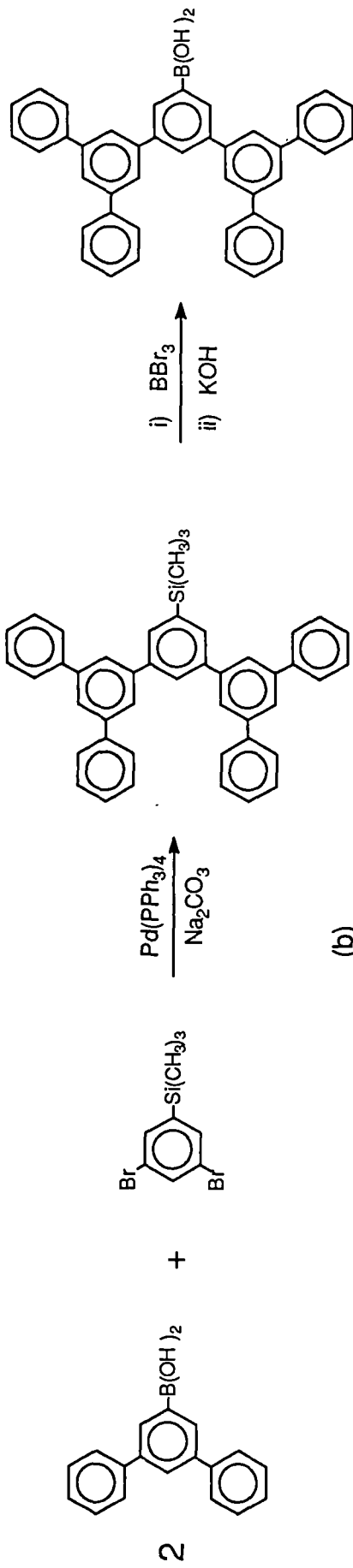
Figure 1.8 Examples of Dendron Wedge Synthesis for

a) Polyether Dendrimers[13]   b) Hydrocarbon Dendrimers[15]

The negligibly small molecular weight distribution of these materials makes them particularly attractive for application as calibration standards for size exclusion chromatography. Unlike more traditional standards, prepared by anionic methods and/or fractionation, it is possible to determine their precise mass and dimensions unambiguously, which has aroused considerable interest in the field.[19]

The greater degree of control of the convergent technique in comparison to divergent methods facilitates easier purification of intermediates and products, particularly for the larger molecules, and allows the preparation of unusual dendrimer-derived species that are unobtainable via the divergent route. Amongst such developments have been numerous examples of novel block copolymer structues exhibiting a wide range of topological features. A host of different architectures may be adopted by dendritic copolymers as a consequence of the constraints imposed by their novel structures. The Fréchet group have recently provided a number of examples in this area.[20-23]

Some of these copolymers are obtained by the incorporation of dendritic fragments into conventional polymer synthesis; for example the use of polyether wedges to end-cap poly(ethylene glycol) chains[21] (Figure 1.9a) or to terminate the free-radical polymerisation of styrene[22] to yield bar bell-like triblock copolymers. The copolymerisation of styrene with polyether wedge-functionalised styrene under free-radical conditions has lead to the formation of graft copolymers with dendron wedges as pendant groups on a mainchain polystyrene backbone[23] (Figure 1.9b).

More unusual block copolymers have been made by combination of polyether[13] and polyester[24] chemistry, both of which have been used independently for dendrimer synthesis by the convergent route. One such topological assembly involves the growth of successive concentric layers of differing branching units onto dendrimer wedges that are then attached to a central core. Bearing in mind that the chemistry required to form the inner layers must be compatible with the existing outer layers, the structure can be varied with respect to the width, structure and number of layers to form a so-called dendritic layer-block copolymer[20] (Figure 1.9c).

A different molecular architecture, the segment-block copolymer, incorporates dendron wedges of different types coupled to the same core[20] (Figure 1.9d) thus emphasising the versatility and high degree of control over internal structure in dendrimer synthesis.
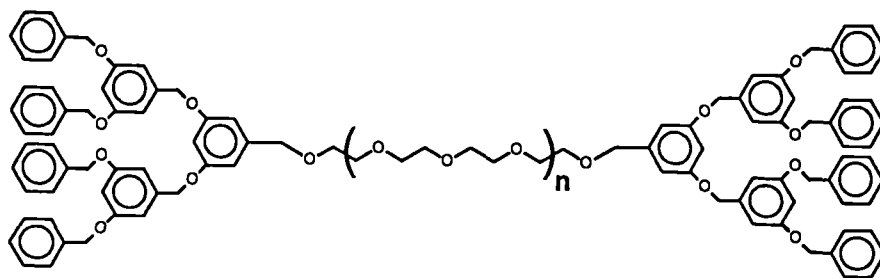
(a) bar-bell triblock copolymer [21]
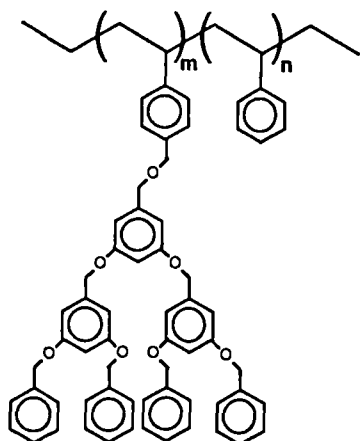
(b) pendant group copolymer [23]
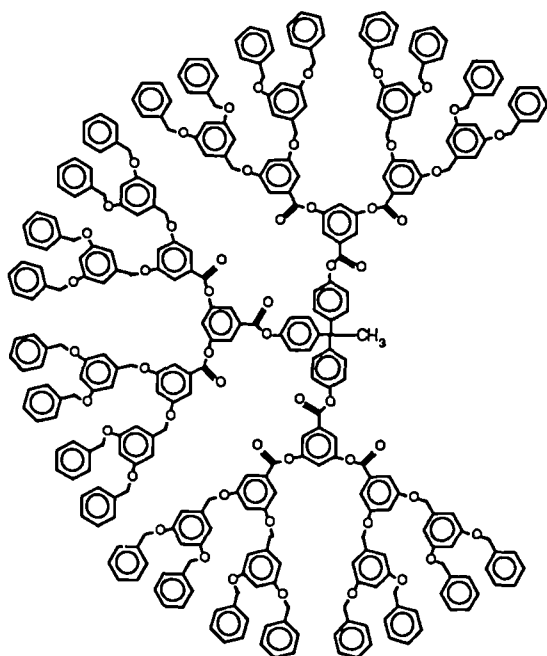
(c) layer-block copolymer [20]
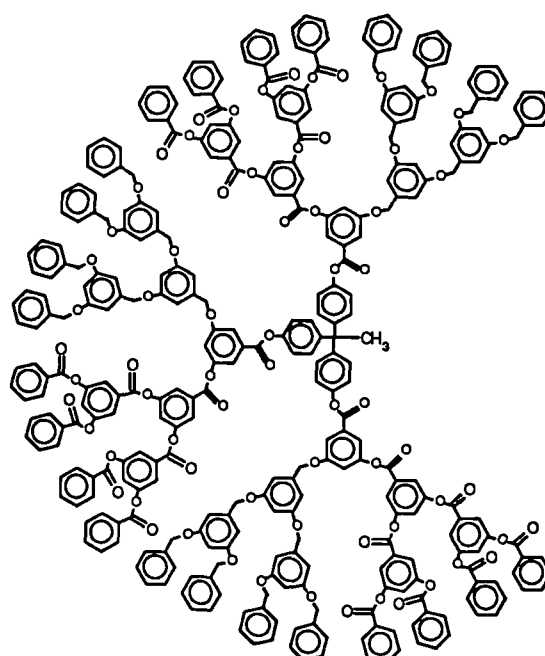
(d) segment-block copolymer [20]

Figure 1.9 Some unusual dendrimer-based copolymers.

There are three distinct architectural features common to dendritic molecules. Although they are inter-related as a consequence of molecular connectivity, useful qualitative information may be elicited by examining each independently.

The Core

This is the focal point of any dendrimer and provides the template to which dendron wedges are attached. Its size, shape and multiplicity will have a profound influence on molecular geometry.

Interior Zones

The control and development of internal structure is closely linked to the iterative sequencing of branch junctions and the spacers between them. The uniform, concentric growth brought about by an absence of structural defects enables highly ordered species of relatively low aspect ratio yet of variable size and flexibility to be constructed.

The influence of internal structure modification has been demonstrated by Moore and Xu.[25,26] Whilst convergent growth of arylacetylenic dendrimers proceeds as expected for the smaller members of the series, larger wedges were unable to be prepared by this route. Despite the addition of terminal functionalities to aid solubility, only low yields of the larger wedges were obtained. Molecular modelling of such fragments has suggested that the problem arises from the steric constraints imposed by the rigidity of the system. By the incorporation of larger rigid spacer units between the branch junctions, appreciably enhanced yields have been reported in the synthesis of larger dendrimers. This has been attributed to the significant reduction in steric inhibition caused by the interaction of adjacent wedge segments and led to the suggestion that provided monomer size increases at a sufficient rate then in principle, rigid dendrimer growth could continue indefinitely (Figure 1.10).
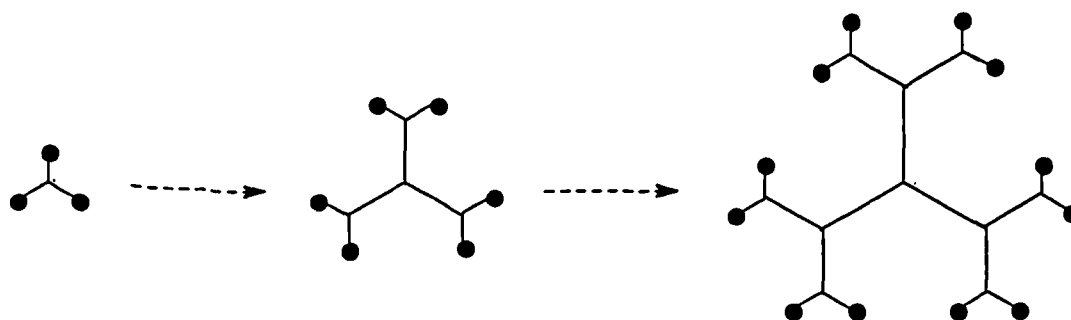
Figure 1.10 Increasing the monomer size as a function of generation could allow rigid dendrimer growth to continue indefinitely.[26]

In another development, the Nagasaki group[27] has introduced crown ether molecules as spacer groups into dendritic molecules. Such structures would be expected to exhibit selective binding properties towards alkali metal ions.

Whereas the chemical nature and multiplicity of branch points determine bond angles, the more subtle influences of hydrogen bonding and steric constraints control the secondary structure, as is found to be the case in proteins and more conventional linear polymers.

Exterior Surface Region

The identical connectivity paths linking all parts on the periphery to the core lead to a multitude of similar terminal environments. Complete and partial surface functionalisation have already been extensively studied. In many cases, such modification brings about a radical changes in physical properties such as solubility and phase transition temperature.[24,28-31] Dendrimers with selectively hydrophilic and hydrophobic surface regions would be expected to reveal unusual properties at interfaces.

There have been many reports in the literature of the synthesis of monodisperse dendritic polymers however relatively few of these have shown any appreciable consideration of the physical aspects of dendrimer growth. On the basis of computer-aided molecular modelling, it was proposed that with increasing dendrimer size, there is a pronounced transition from flexible, disc-like species to more rigid structures, with densely packed surface groups enclosing a near-hollow interior comprising of a

number of voids and channels.[32] This hypothesis has been given some support by the use of photochemical relaxation techniques to probe surface structure.[33]

In this way, dendrimers have been likened to classical micelles, aggregates of amphipathic molecules that are arranged in such a way so as to present a uniform spherical exterior surface. Such molecules may find ready acceptance as surfactants and solubilising agents. In contrast to micelles, that are held together by intermolecular interactions, dendrimers are single molecules containing covalent chemical bonds. As such, dendrimers are generally more robust than their natural counterparts. As the number of generations increases, dendrimer molecules begin to take on the characteristics of biological entities and consequently, given the ease with which their size, shape, flexibility and surface features may be controlled, interest has been aroused in their potential to mimic the activities and functions carried out by living systems at a microscopic level.[34,35]

The Concept of a Limiting Generation

Since the number of terminal groups grows exponentially with increasing dendrimer generation whilst the molecular radius can, to a first approximation, be considered to grow at a constant rate, it is clear that growth cannot continue indefinitely. Consequently, there must be a limiting, dense-packed generation beyond which the effects of steric inhibition prevent further ideal growth.

If the spacers between branch points are sufficiently short then it is reasonable to suppose that the limiting generation may be estimated from a consideration of the geometry and steric constraints at such points. In contrast, for large spacers, it is to be expected that the limiting generation is an increasing function of spacer length.

Theoretical Models

In an attempt to understand the structural characteristics of dendritic molecules, two theoretical models have been put forward:-

That of de Gennes and Hervet[36] is based on the Maciejewski "cast shell" model.[37] This approach assumes that all the wedges grow radially outwards from the core and consequently, all terminal groups are found on the periphery of the molecule. By consideration of the free energy of the system, the Edwards self-consistent field

method[38,39] is used to predict the dependence of molecular dimensions and limiting generation on spacer length, given that all the branch points are fully reacted and the spacers are sufficiently large for branch structure to be unimportant. It is clear that in this model, low generations are more flexible than higher ones. The growing density as a function of radius leads to increased rigidity and it is the resultant space-filling considerations that bring about the inhibition of regular growth.

In contrast, Lescanec and Muthukumar[40] have developed a numerical simulation of kinetic growth using a self-avoiding walk algorithm. The major difference between this model and that of de Gennes and Hervet is the prediction that folding back of branches on themselves may occur. Chain ends may be buried within the molecule and not necessarily reside solely on the outer surface.

Although there is only limited experimental data available and the systems studied to date have significantly different structural characteristics, preliminary reports[41] suggest that providing the dendrimers are sufficiently flexible, the kinetic simulation of Lescanec and Muthukumar most accurately predicts the experimental situation. This must not however be taken as a firm endorsement of the kinetic model and further work is required to establish the nature of the branching structure.

There is no doubt that the new and flourishing discipline of dendrimer science represents a significant advance of the precision in synthesis of macromolecular species. Although still in its infancy, it is anticipated that this will be a major area of interest with the adaptation of dendrimers to perform a wide range of specific tasks. It is the detailed characterisation, understanding and utilisation of such materials that may ultimately lead to the transformation of dendritic polymers from their current chemical curiosity status to highly specialised species for commercial exploitation.

This Work

Many of the early reports on the synthesis of dendritic polymers were largely of interest on account of the novel topological arrays described therein and their departure from the realm of conventional polymer science. More recently, structural studies have revealed that such structures may be readily adapted for a host of speciality applications.

This work describes the synthesis and characterisation of a series of polyester dendrimers. Some of these have been blended with a linear polymer to investigate their effect on the modification of its mechanical properties. In a further study, a number of structurally similar hyperbranched polymers have been prepared with a view to assessing their potential for technological applications.

References

1.   Flory, P.J., J.Am.Chem.Soc. 2718 (1952)

2.   Buhleier, E., Wehner, W. and Vögtle, F., Synthesis 155 (1978)

3.   Newkome, G.R., Yao, Z., Baker, G.R. and Gupta, V.K., J.Org.Chem. 50, 2003 (1985)

4.   Newkome, G.R., Yao, Z., Baker, G.R., Gupta, V.K., Russo, P.S. and Saunders, M.J., J.Am.Chem.Soc. 108, 849 (1986)

5.   Newkome, G.R., Baker, G.R., Saunders, M.J., Russo, P.S., Gupta, V.K., Yao, Z., Miller, J.E. and Bouillion, K., J.Chem.Soc.,Chem.Commun. 752 (1986)

6.   Tomalia, D.A., Baker, H., Dewald, J., Hall, M., Kallos, G., Martin, S., Roeck, J., Ryder, J. and Smith, P., Polym.J.(Tokyo) 17, 117 (1985)

7.   Tomalia, D.A., Baker, H., Dewald, J., Hall, M., Kallos, G., Martin, S., Roeck, J., Ryder, J. and Smith, P., Macromolecules 19, 2466 (1986)

8.   Padias, A.B., Hall, H.K.(Jr.), Tomalia, D.A. and M^{C}Connell, S.R., J.Org.Chem. 52, 5305 (1987)

9.   Percec, V. and Kawasumi, M., Macromolecules 25, 3843 (1992)

10.   Suzuki, M., Ii, A. and Saegusa, T., Macromolecules 25, 7071 (1992)

11.   Tomalia, D.A., Naylor, A.M. and Goddard, W.A.III, Angew.Chem.Int.Ed.Engl. 29, 138 (1990)

12.   Hawker, C.J. and Fréchet, J.M.J., J.Chem.Soc.,Chem.Commun. 1010 (1990)

13.   Hawker, C.J. and Fréchet, J.M.J., J.Am.Chem.Soc. 112, 7638 (1990)

14.   Miller, T.M., Kwock, E.W. and Neenan, T.X., Macromolecules 25, 3143 (1992)

15.   Miller, T.M., Neenan, T.X., Zayes, R. and Bair, H.E., J.Am.Chem.Soc. 114, 1018 (1992)

16.   Uhrich, K.E. and Fréchet, J.M.J., J.Chem.Soc.,Perkin Trans.1 1623 (1992)

17.   Wooley, K.L., Hawker, C.J. and Fréchet, J.M.J., J.Am.Chem.Soc. 113, 4252 (1991)

18.   Wooley, K.L., Hawker, C.J. and Fréchet, J.M.J., Angew.Chem.Int.Ed.Engl. 33, 82 (1994)

19. Dubin, P.L., Edwards, S.L., Kaplan, J.I., Mehta, M.S., Tomalia, D.A. and Xia, J., Anal.Chem. 64, 2344 (1992)

20. Hawker, C.J. and Fréchet, J.M.J., J.Am.Chem.Soc. 114, 8405 (1992)

21. Gitsov, I., Wooley, K.L. and Fréchet, J.M.J., Angew.Chem.Int.Ed.Engl. 31, 1200 (1992)

22. Gitsov, I., Wooley, K.L., Hawker, C.J. and Fréchet, J.M.J. ACS Polym.Prep. 32(3), 631 (1991)

23. Wooley, K.L., Hawker, C.J., Lee, R. and Fréchet, J.M.J., Polym.Mater.Sci.Eng. 64, 73 (1991)

24. Hawker, C.J., Fréchet, J.M.J., J.Chem.Soc.Perkin Trans.1 2459 (1992)

25. Moore, J.S. and Xu, Z., ACS Polym.Prep. 32(3), 629 (1991)

26. Moore, J.S. and Xu, Z., Macromolecules 24, 5893 (1991)

27. Nagasaki, T., Masakatsu, U., Arimori, S. and Shinkai, S., J.Chem.Soc.,Chem.Commun. 608 (1992)

28. Wooley, K.L., Hawker, C.J., Pochan, J.M. and Fréchet, J.M.J., Macromolecules, 26, 1514 (1993)

29. Newkome, G.R.,Young, J.K., Baker, G.R., Potter, R.L., Audoly, L., Cooper, D., Weis, C.D., Morris, K. and Johnson, C.S. Jr., Macromolecules 26, 2394 (1993)

30. Hawker, C.J., Wooley, K.L. and Fréchet, J.M.J., J.Chem.Soc.Perkin Trans.1 1287 (1993)

31. Hawker, C.J. and Fréchet, J.M.J., Macromolecules 23, 4726 (1990)

32. Naylor, A.M., Goddard, W.A.III, Kiefer, G.E. and Tomalia, D.A., J.Am.Chem.Soc. 111, 2339 (1989)

33. Moreno-Bondi, M.C., Orellana, G., Turro, N.J. and Tomalia, D.A., Macromolecules 23, 910 (1990)

34. Jin, R.; Aida, T. and Inove, S., J.Chem.Soc.,Chem.Commun. 1260 (1993)

35. Posnett, D.S., McGraith, H. and Tam, J.P., J.Biol.Chem. 263, 1719 (1988)

36. de Gennes, P.G. and Hervet, H.J., J.Phys.Lett. 44, L-351 (1983)

37. Maciejewski, M., J.Macromol.Sci.Chem. A17, 689 (1982)

38. Edwards, S.F., Proc.Phys.Soc.(London) 85, 613 (1965)

39. de Gennes, P.G., Rep.Prog.Phys. 32, 187 (1969)

40. Lescanec, R.L. and Muthukumar, M., Macromolecules <u>23</u>, 2280 (1990)

41. Mourey, T.H., Turner, S.R., Rubinstein, M., Fréchet, J.M.J., Hawker, C.J. and Wooley, K.L., Macromolecules <u>25</u>, 2401 (1992)

CHAPTER 2

Synthesis and Characterisation of
Extended Aryl Ester Dendrimers

Synthesis and Characterisation of Extended Aryl Ester Dendrimers

Background

Many examples of dendritic polyethers,[1] polyesters,[2,3] polyamides[4] and hydrocarbon[5,6] dendrimers have been prepared using 1,3,5-substituted benzenes because of the ready availability of a wide variety of such structural units and the ease with which they are adapted to provide symmetrical branch points.

At the beginning of this project, attempts to prepare a new series of dendritic polymers via a convergent route were based on the chalcone-forming chemistry of benzaldehyde and acetophenone using the branching unit 3,5-diacetylbenzaldehyde. Difficulties were experienced during monomer preparation and diacetylation could only be carried out by use of the multiple Fries rearrangement of the respective aryl acetates and low yields were attained at several stages. Such problems were considered to be incompatible with the high yielding iterative processes required for dendrimer synthesis.

Later work focused on the preparation of phenoxyhexyl ester dendrimers, a series of poly(ester-ether) dendrimers incorporating 5-hydroxyisophthalic acid-derived branch points separated by flexible alkyl chains. Despite the relatively straightforward preparation of the smallest member of this series, tris(6-phenoxyhexyl)trimesic ester, the synthesis of the second generation wedge, di-(6-phenoxyhexyl)-5-(6-hydroxyhexyl) isophthalate, proceeded only in low yield. The attempted coupling of this to the dendrimer core, 1,3,5-benzenetricarbonyl trichloride, yielded a viscous mixture of products that arose as a consequence of incomplete reaction and it was not possible to isolate the pure second generation dendrimer. This scheme was discontinued.

As a result of the unsuccessful initial schemes undertaken, it has been recognised that in the course of dendrimer synthesis, it is necessary to bear in mind the prerequisites of polymer chemistry for more traditional systems, namely the ease of monomer production, high yielding conversions and the minimisation of side reactions.

The synthesis of aryl ester dendrimers incorporating linear aromatic spacer or extension units between successive branch junctions is reported here. In this way, the concept of dendritic layer-block copolymers of Hawker and Fréchet[7] is combined with aryl ester dendrimer synthesis similar to that of Miller, Kwock and Neenan.[3] The

Miller polyester route involves the preparation of a series of dendron wedges based on 5-hydroxyisophthalic acid via a convergent route. Unlike their linear analogue, poly(p-hydroxybenzoic acid), which is essentially infusible and insoluble and consequently extremely difficult to process, such dendrimers have been found to be highly soluble in a wide range of common organic solvents.

Synthesis

A series of three aryl ester dendrimers, having 7, 16 and 19 aromatic rings, have been prepared via a convergent route.

[7]   **[16]**   **[19]**
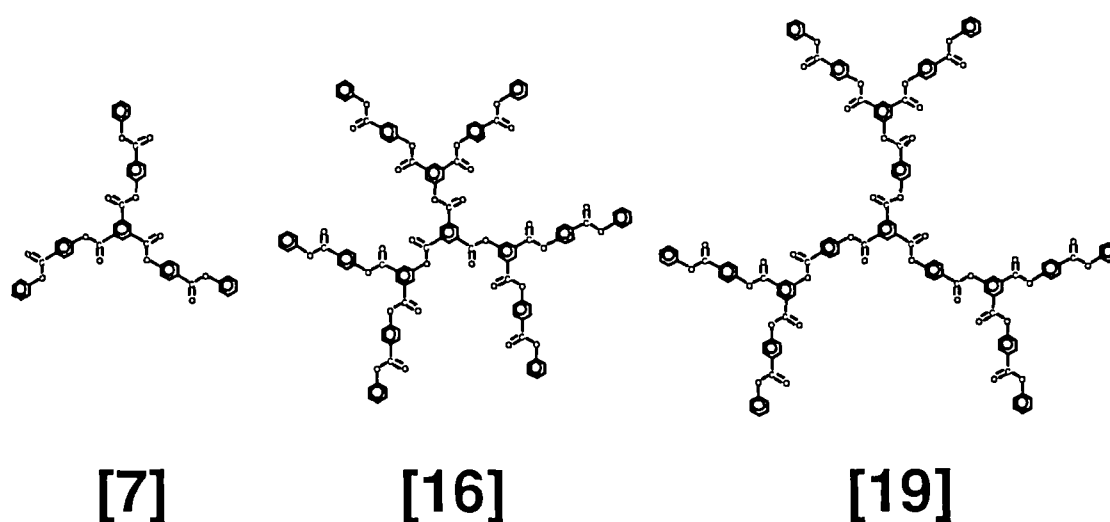
Figure 2.1 The Extended Aryl Ester Dendrimer Series.

One of the major differences between this route and that of Miller is in the selection of an appropriate iterative protection scheme for the phenolic group at the focal point of each dendron wedge. The Miller route involves the protection of both the hydroxyl and carboxyl groups of the branch junction precursor, 5-hydroxyisophthalic acid, with t-butyldimethylsilyl chloride to yield bis(t-butyldimethylsilyl)-5-(t-butyldimethylsiloxy) isophthalate, selective hydrolysis of the ester groups to give the corresponding diacid and conversion to the acid chloride by treatment with thionyl chloride in an overall yield of ~ 60%.[3]

Our novel approach to dendrimer synthesis utilises acetates as protecting groups in the preparation of polyaryl esters. The synthesis is based on reactions

involving 5-acetoxyisophthaloyl dichloride **2** (the branching unit) and 4-acetoxybenzoyl chloride **1** (the spacer unit) with a series of phenolic "dendron wedges" and subsequent selective ester cleavage to yield wedges of increasing size. The acid chlorides are prepared in a two-step process from the appropriate hydroxyacids, 5-hydroxyisophthalic acid and 4-hydroxybenzoic acid, both of which are commercially available. Initial acetylation of the phenol groups with acetic anhydride in basic aqueous solution is followed by conversion to the acid chloride by reaction with phosphorus pentachloride. Overall yields of typically 86 - 89% have been obtained (see Scheme 2.1).
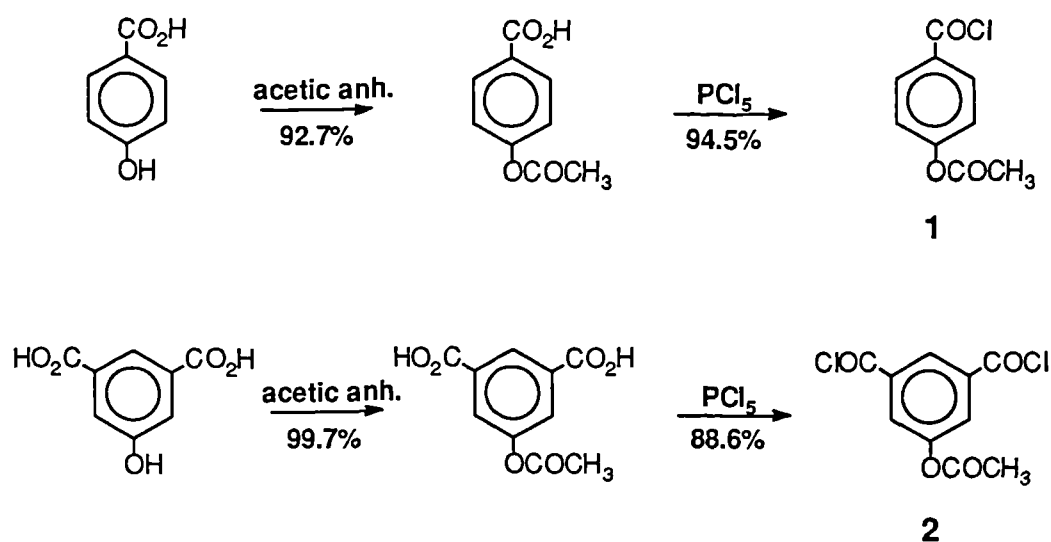
Scheme 2.1 Synthesis of the Acetoxyacid Chlorides.

To overcome the increasingly cumbersome nomenclature for the larger aromatic molecules, these are named with reference to the number of aromatic rings in the structure followed by an abbreviation indicating the reactive functional group (see Scheme 2.2).

[7]

[16]

[19]

c
75.8%

f
24.7%

f
16.9%

[2]-OH

[5]-OH

[6]-OH

b
43.5%

e
86.6%

e
86.7%

[2]-OAc

[5]-OAc

[6]-OAc

a
92.5%

d
93.0%

a
83.1%

[2]-OH

[5]-OH

a   CH₃COO—⟨⟩—COCl 1, pyridine, DMAP

b   KOH, EtOH

c   ClOC—COCl / COCl   3, pyridine, DMAP

d   ClOC—COCl / OCOCH₃   2, pyridine, DMAP

e   H⁺, thf

f   3, N,N-dimethylaniline
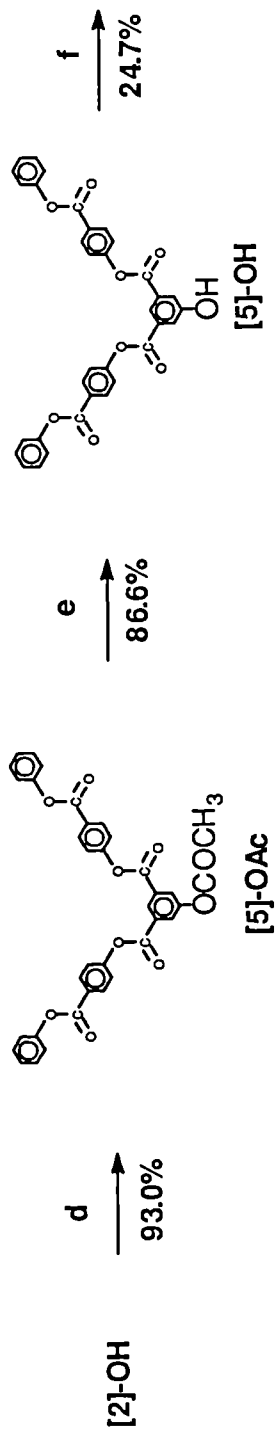
Scheme 2.2 Outline routes to dendrimers [7], [16] and [19].

23

Reaction of 4-acetoxybenzoyl chloride 1 with phenol in a solution of dichloromethane and pyridine with 4-dimethylaminopyridine (DMAP) catalysis yields phenyl-(4-acetoxybenzoate), [2]-OAc (see Scheme 2.2). The conversion of [2]-OAc to the extended terminal unit, phenyl-(4-hydroxybenzoate) [2]-OH, was first attempted by selective reduction with sodium borohydride in monoglyme under mild conditions,[8] a technique successfully employed by ourselves in related work involving acetoxyalkyl benzoates. Despite prolonged reaction times, no change was detected and the [2]-OAc remained intact. On reaction of [2]-OAc with ethanolic potassium hydroxide on a small scale at 0°C, yields of the desired product are obtained in excess of 70% however on scaling up this process, significant phenol contamination is observed, indicating the lack of specificity of the reaction. Following purification by vacuum sublimation, [2]-OH is obtained in low yield. Reaction of the trifunctional core molecule, 1,3,5-benzenetricarbonyl trichloride 3, with the deprotected product, [2]-OH, in dichloromethane/pyridine solution with DMAP ca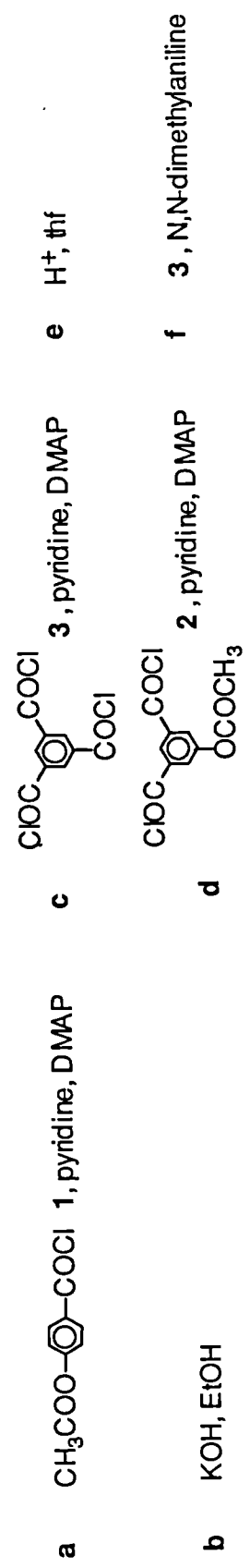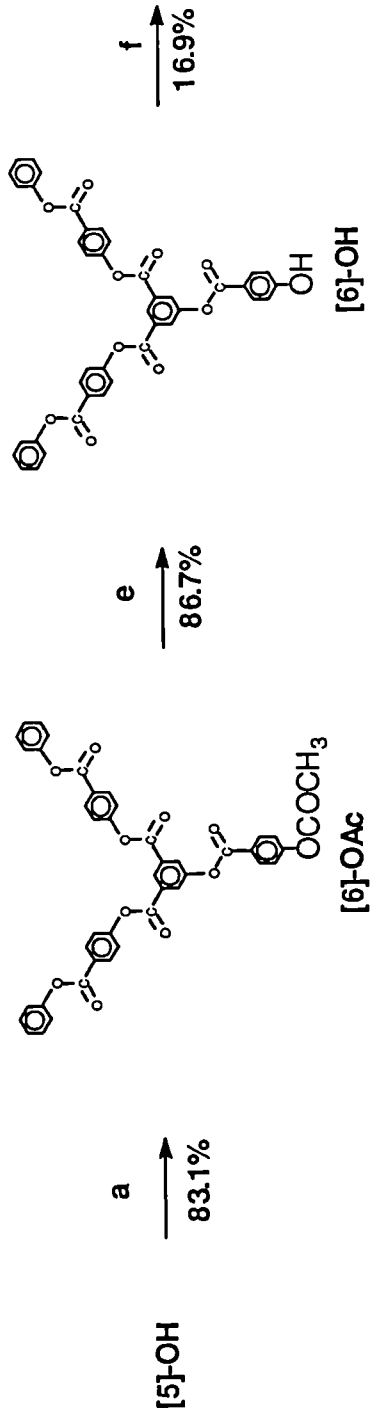talysis yields [7], the extended first generation dendrimer in high yield and without the need for purification by column chromatography.

In a similar manner, [5]-OAc, the protected second generation wedge is prepared by reaction of [2]-OH with 5-acetoxyisophthaloyl dichloride 2 in excellent yield. The deacetylation of [5]-OAc was initially attempted using borohydride reductive hydrolysis. Analysis of the products revealed a significant proportion of phenyl-(4-hydroxybenzoate), [2]-OH, indicating aryl benzoate hydrolysis. Other basic hydrolysis techniques were equally unsuccessful and resulted in undesirable fragmentation. Investigation of acid catalysed deacetylation showed that a 10% v/v aqueous hydrochloric acid solution and tetrahydrofuran mixture is suitably regiospecific and gives [5]-OH cleanly and in high yield. Adaptation of this procedure for [2]-OH synthesis is only partially successful and an appreciable quantity of phenol is produced, indicating a lack of reaction selectivity. The yield of [2]-OH did not justify changing from the preferred mode of synthesis as previously described.

From the experience of other researchers,[3] who concluded that the coupling of large branched aryl ester wedges to an aromatic core could not be accomplished cleanly using either pyridine or DMAP and resulted in significant ester exchange, the weaker, less nucleophilic base, N,N-dimethylaniline, has been used to catalyse the

reaction of [5]-OH with 1,3,5-benzenetricarbonyl trichloride 3 to produce [16], the second generation dendrimer, after purification by column chromatography.

The extended second generation wedge, [6]-OH, is prepared by the reaction of 4-acetoxybenzoyl chloride 1 with [5]-OH in dichloromethane/pyridine solution with DMAP to yield [6]-OAc followed by acid catalysed deacetylation. This wedge is attached to the core molecule, 1,3,5-benzenetricarbonyl trichloride 3 using the method described above, to yield [19], the extended second generation dendrimer.

Unsuccessful attempts have been made to prepare larger dendrimers using this route. The synthesis of [13]-OAc, the protected third generation wedge, from [6]-OH with 5-acetoxyisophthaloyl dichloride 2 can be carried out in low yield but without difficulty however attempts to deprotect this in aqueous acid/THF solution have failed. Infra-red spectroscopy of the product indicates appreciable aryl ester hydrolysis. It is perhaps significant that similar problems have been experienced in related systems for wedges of a comparable size. Miller reported the undesirable aryl ester hydrolysis of a silyloxy-protected polyester wedge of a similar size and under similar deprotection conditions to those attempted in this work.[3] This was attributed to the competitive hydrolysis of the ester linkages with respect to the removal of the silyl protecting group and resulted in the termination of dendrimer growth by this route.

It is possible that the increasing extent of aryl ester hydrolysis with increasing size of wedge, as compared to removal of the protecting group, may be attributed at least in part to the folding back of the large dendrimer branches towards the focal point of the wedge, thus congesting the reactive site and compounding the already serious problem of undesirable aryl ester hydrolysis as a consequence of the increasing aryl ester : acetate ratio.

Characterisation of the Dendrimers

Unambiguous proof of dendrimer molecule structure required the use of a wide variety of analytical techniques.

N.M.R. Spectroscopy

On account of the high symmetry of the dendrimers, both ^{1}H and ^{13}C n.m.r. spectroscopy have proved invaluable in their characterisation and that of their component wedges. It has been particularly useful to note that an individual proton or carbon atom has a resonance position that varies only slightly when the molecule of which it is a part is incorporated into a larger wedge or dendrimer. In this way, the smaller wedges have served as model compounds to aid in the assignment of the larger molecules. Unlike ^{1}H spectra, conventional ^{13}C spectra are not quantitative since the relaxation time of a carbon nucleus to its equilibrium state is heavily dependent on its chemical environment. Despite this apparent complication, it has been found that the relative intensities of the peaks in broadly similar environments are largely proportional to the number of nuclei within those environments since the relaxation times are comparable. This is of great benefit in the assignment of the larger wedges and dendrimers of the series in which well-defined ratios of carbon nuclei exist in very similar environments.

Because of the lack of multiplicity in conventional ^{13}C spectra, it is often difficult to assign individual carbon resonances and it is useful to be able to identify the carbon atom to which each proton is attached. Multipulse two-dimensional heteronuclear correlation (hetcor) spectroscopy has been extensively utilised for the unambiguous assignment of individual proton and carbon resonances within the structures. Unlike a conventional n.m.r. spectrum, that displays peak intensity as a function of a single frequency dimension, a hetcor spectrum correlates ^{13}C spectrum signals with ^{1}H spectrum signals arising from directly bonded proton and carbon atoms. The result is displayed as a contour plot in two-dimensional frequency space.

The peak assignments for all the compounds follow in a straightforward way from their spectra, bearing in mind relative peak intensities and the use of correlation tables of chemical shifts of related compounds (Figures 2.2 and 2.3).
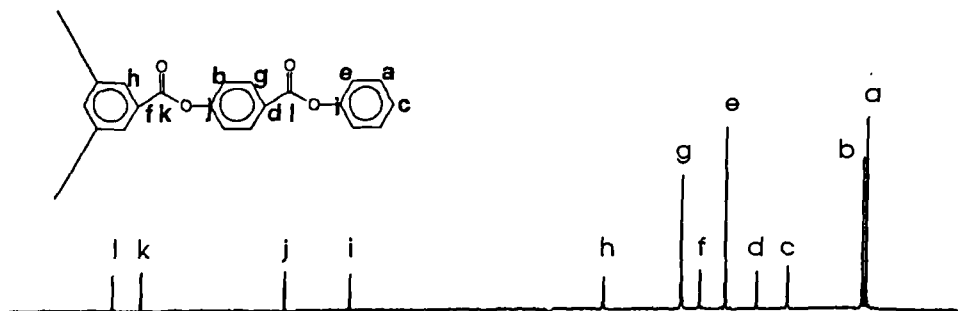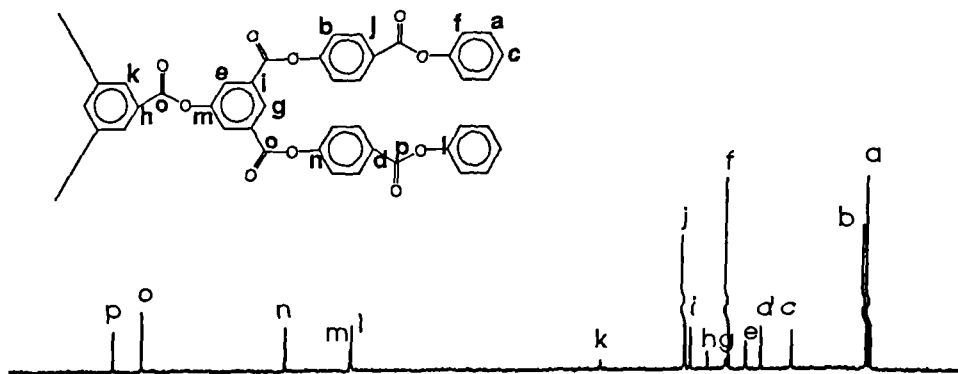
Figure 2.2 ^{13}C n.m.r. spectra of dendrimers in CDCl$_3$.

Figure 2.3 2-D heteronuclear correlation spectrum of [16] in CDCl₃.

28

Gel Permeation Chromatography (GPC)

Gel permeation chromatography is a widely used characterisation technique for the routine analysis of molecular weight distribution of soluble polymers based on their separation according 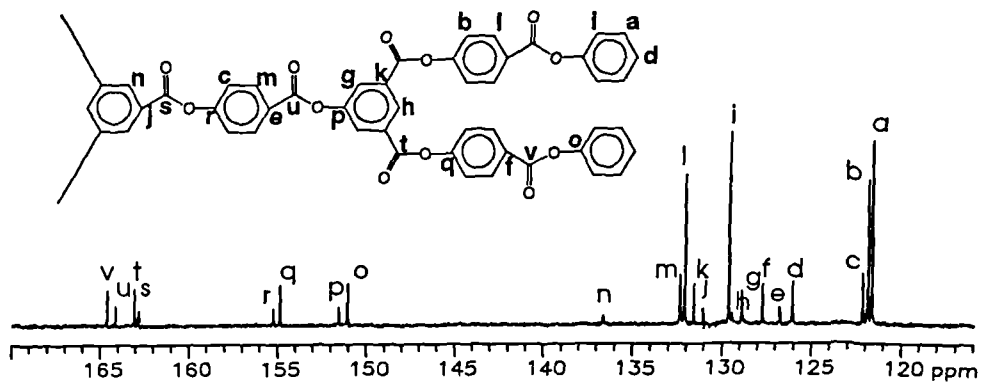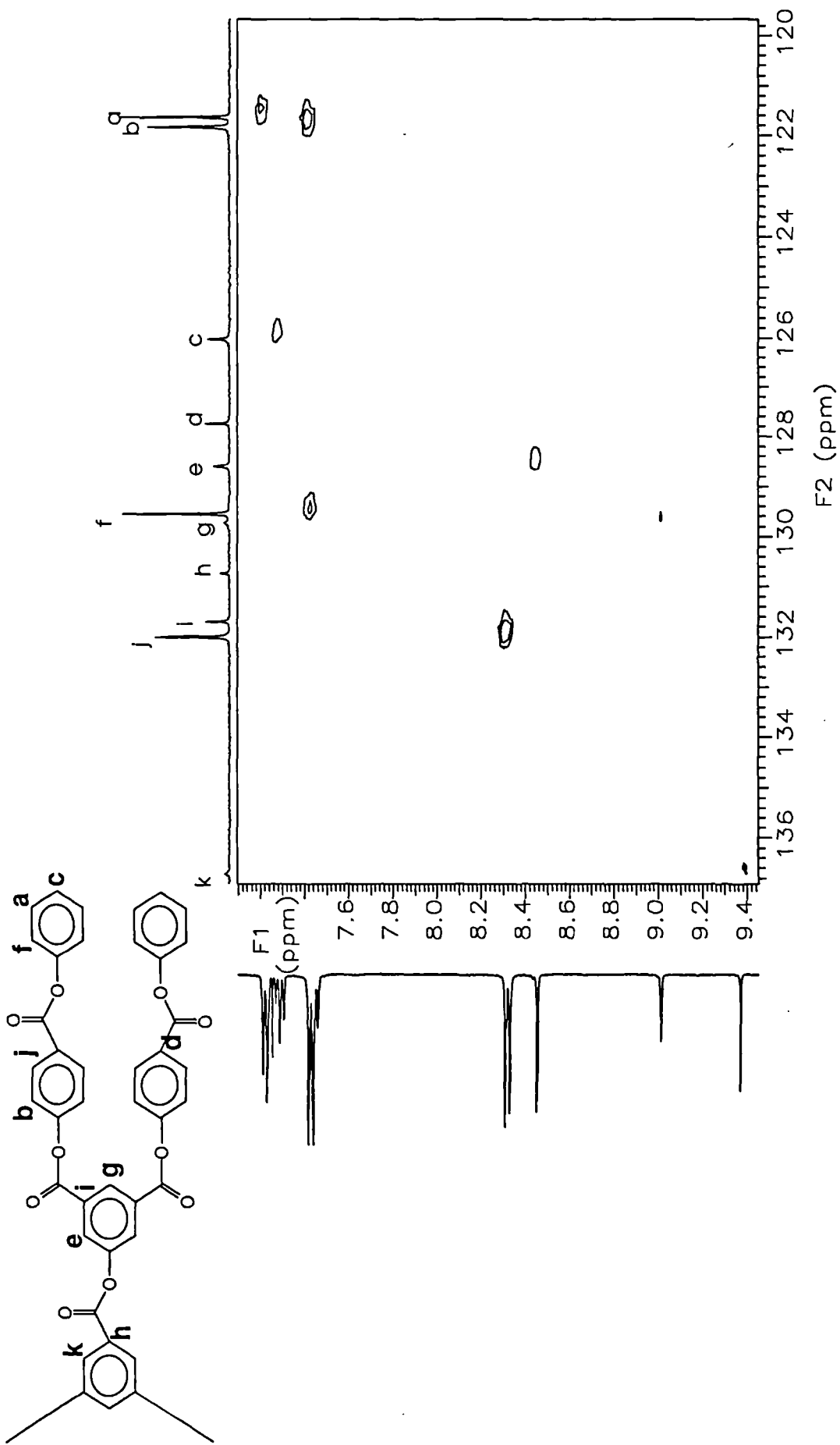to hydrodynamic volume. It is particularly effective in the analysis of dendrimers and especially those prepared via a convergent route since the molecular mass and thus the expected molecular size in solution, changes drastically at each growth step.

Analysis of both dendrimer [7] and [16] by GPC reveals a single peak in each case. Ideally, such monodisperse molecules with a well-defined molecular mass should elute from a GPC column at a single elution time however in practice, elution peaks have finite width due to factors such as diffusion and axial dispersion within the column and the need for a finite injection volume of polymer solution for analysis.[9] The calculated polydispersity ratio of each dendrimer is typically 1.04, which is comparable with that of the polystyrene calibration standards, thus supporting the expected monodisperse nature of the dendrimers. GPC analysis of dendrimer [19] indicates the presence of a small quantity of impurity that could not be removed by column chromatography. Superposition of the GPC traces for dendrimers [7], [16] and [19] indicates that this impurity is of comparable mass to dendrimer [7] and is consistent with the hypothesis that it is a trace of the unreacted wedge material [6]-OH (Figure 2.4).

Although GPC is useful for the comparison of relative molecular mass distribution, it is frequently used for the determination of absolute mass values which can often lead to considerable misinterpretation of the data. Its use in the analysis of well-defined species such as dendrimers shows that absolute mass values cannot necessarily be determined by routine GPC analysis. This point is illustrated in our own data (Table 2.1).
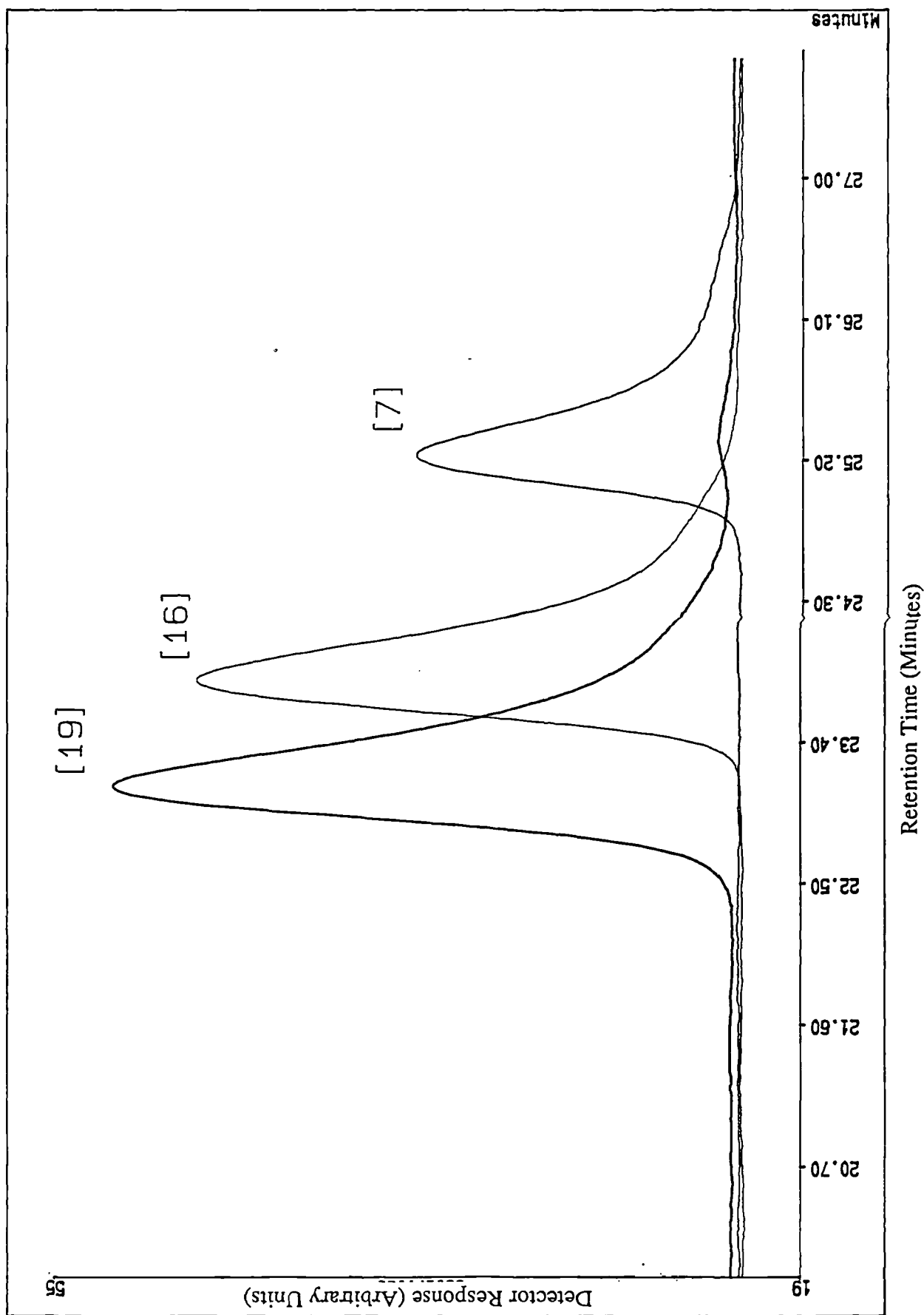
Figure 2.4 GPC of dendrimers [7], [16] and [19]

Compound	Nominal Mass	M_n (GPC)
[7]	798	915
[13]-OAc	1576	2310
[16]	1878	2530
[19]*	2238	3370

* - analysis of major peak

Table 2.1 Comparison of Nominal and Calculated Mass Values
as measured by chloroform GPC.

The data presented in the above table indicates that the aryl ester dendrimers have shorter retention times within the GPC column and thus larger hydrodynamic radii than polystyrene equivalents of the same molecular mass. This is in contrast to the published results of Fréchet[10] in the investigation of dendritic polyethers in which lower than expected mass values were determined by GPC. These observations can be rationalised on the basis of the hypothesis that the aryl ester dendrimers are less able and the polyether dendrimers more able to penetrate the column pores than their polystyrene equivalents of the same molecular mass which is consistent with the aryl ester dendrimers having a relatively rigid, extended structure as compared to polystyrene whereas the more flexible polyether dendrimers in the Fréchet series occupy a smaller volume than polystyrene standards of the same molecular weight.

Other Characterisation Techniques

Elemental analysis of [7] and [16] shows close agreement with the calculated values whereas that of [19] confirms the presence of a slight impurity as noted by GPC. Characterisation by mass spectroscopy has also been attempted using conventional C.I. and E.I. techniques however both of these have resulted in fragmentation to species containing only single aromatic units and no molecular ions have been detected. The dendrimers are highly soluble in organic solvents such as chloroform, dichloromethane and tetrahydrofuran, contrasting markedly with their linear analogue poly(p-hydroxybenzoic acid), which is virtually insoluble in common organic solvents. Thermogravimetric analysis has shown that at a constant heating rate

of 10°C/min in a nitrogen atmosphere, the dendrimers [16] and [19] retain 98 % of their mass up to around 400°C whereas the smaller dendrimer [7] is apparently less stable or more volatile. Wide angle X-ray powder diffraction indicates that [7] is crystalline whereas both **[16]** and **[19]** are less well-ordered compounds (Figure 2.5). Heat of fusion measurements by differential scanning calorimetry support this view (Table 2.2 and Figure 2.6).

Dendrimer	RMM	Solubility (chloroform, 25°C)	Melting Point (DSC)	Enthalpy of Fusion	Thermo-gravimetry (2% wt. loss)
[7]	798	297 g/l	190°C	71 J/g	278°C
[16]	1878	156 g/l	152°C	20 J/g	389°C
[19]	2238	174 g/l	136°C	13 J/g	405°C

Table 2.2 Physical Properties of Dendrimers [7], [16] and [19].
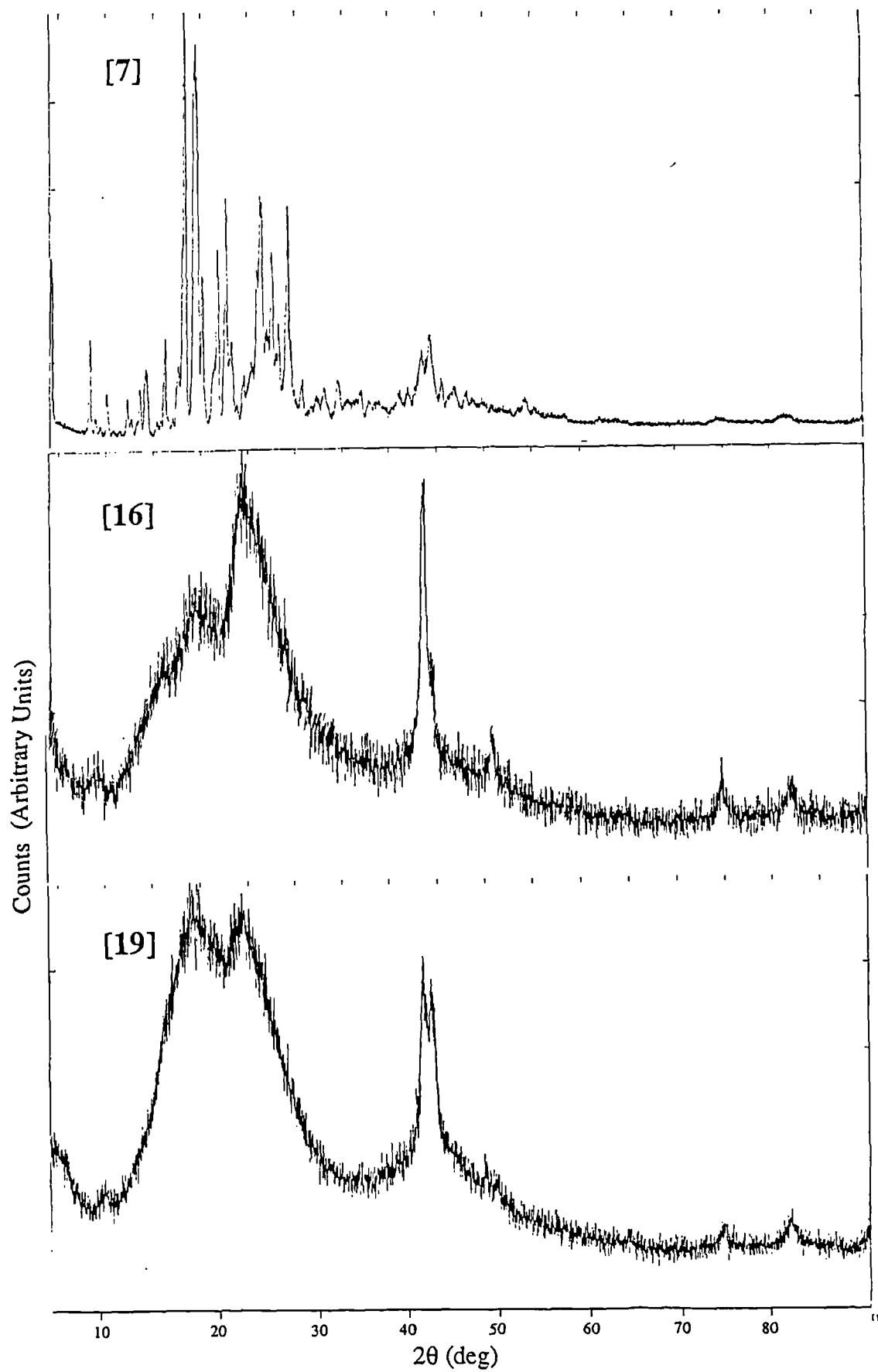
Figure 2.5 Wide Angle X-ray Diffraction Traces of [7], [16] and [19]

Normalised Differential Scanning Calorimetry Traces for Dendrimers (7), (16) and (19)

[7]

[16]

[19]

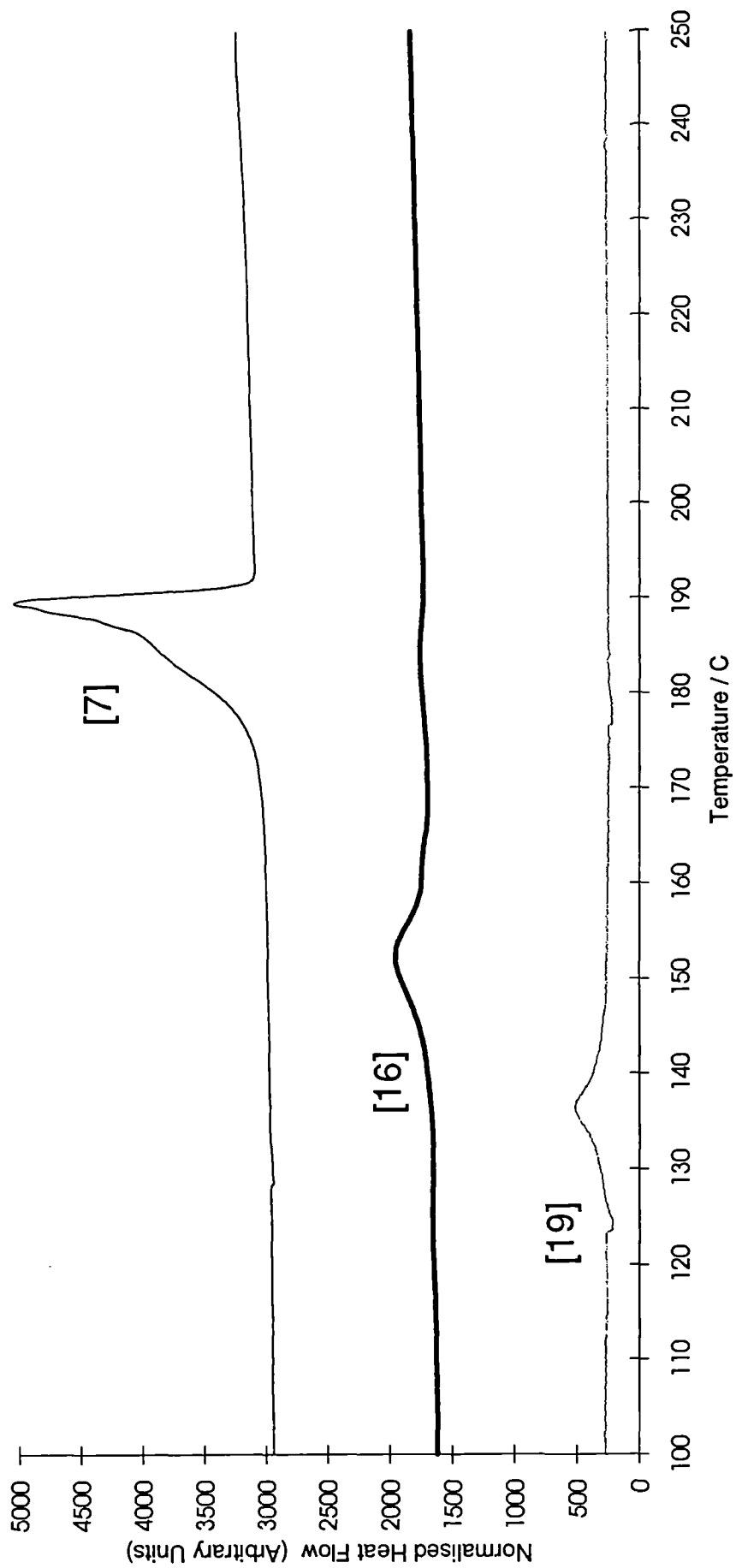Normalised Heat Flow (Arbitrary Units)

Temperature / C

Figure 2.6

Experimental

All organic reagents were obtained from Aldrich Chemical Co. and used without further purification. Melting points were obtained on an Electrothermal digital melting point apparatus unless otherwise stated and reported without correction. Infra-red spectra were recorded on a Perkin-Elmer 1600 series FTIR. Thermogravimetric analyses were carried out using a Shimadzu TGA-50. Differential scanning calorimetry was performed on a Perkin-Elmer DSC-7 at a scanning rate of 10°C/min (Figure 2.6). ^{1}H and ^{13}C n.m.r. spectra were recorded on a Varian 200MHz Gemini or Varian 400MHz spectrometer as indicated and were referenced to TMS. Gel permeation chromatography was carried out in chloroform using three 5µm columns of PL gel with pore size 100Å, 10^3Å and 10^5Å and a Waters differential refractometer detector (Figure 2.4). X-Ray diffraction was carried out on a Siemens Diffraktometer D5000 (Figure 2.5).

The I.R. and n.m.r. spectra for all compounds are shown in Appendix 1.

Synthesis of 4-acetoxybenzoic acid. To a stirred solution of 4-hydroxybenzoic acid (225.00g,1.63mol) in aqueous sodium hydroxide solution (2.7l,2.5M) cooled in an ice-water bath, acetic anhydride (750ml) was added slowly. Stirring was continued until the mixture solidified, upon which the flask was shaken for 10 minutes and the contents acidified to pH1 using concentrated hydrochloric acid. The white slurry was filtered and the filtrate extracted with ethyl acetate (4× 300ml). A further portion of ethyl acetate (900ml) was added to this and the filtered residue was dissolved in it. The resulting solution was washed with water (5×1l) and the combined aqueous washings extracted with ethyl acetate (500ml). The organic portions were combined, dried (MgSO$_4$), the solvent removed by evaporation and the residue dried under vacuum at 80°C for 4h. to yield 4-acetoxybenzoic acid as a white powdery solid (272.04g,1.51mol,92.7%,mp.188.0-189.5°C lit.[11] 187.5°C) which was characterised by ^{1}H n.m.r. (CDCl$_3$, 200MHz) δ2.34 (s,3H,CH$_3$), δ7.21 (d,8.96Hz,2H,ArH), δ8.15 (d,8.90Hz,2H,ArH), ^{13}C n.m.r. (CDCl$_3$, 50MHz) δ21.66 (CH$_3$), δ122.26 (aromatic C-H), δ127.31 (aromatic C-R), δ132.37 (aromatic C-H), δ 155.48 (aromatic C-O), δ169.35 (ArCO$_2$H), δ171.83 (COCH$_3$), I.R. (KBr disc) 2996.0

cm^{-1} (broad, carboxylic acid O-H, aryl-H and saturated C-H stretch), 1754.5 cm^{-1} (s, ester C=O absorption), 1681.6 cm^{-1} (s, carboxylic acid C=O absorption).

Synthesis of 4-acetoxybenzoyl chloride. An intimate mixture of 4-acetoxybenzoic acid (304.88g,1.69mol) and phosphorus pentachloride (358.01g,1.72mol) in a flask fitted with a reflux condenser and gas absorption device was warmed gently with a heat gun to initiate the reaction and shaken occasionally until the vigorous evolution of hydrogen chloride had ceased. The reaction mixture was stirred for a further ½h. at room temperature to form a pale yellow homogeneous oil. After removal of phosphorus oxychloride by distillation at atmospheric pressure, the residue was distilled at reduced pressure (107°C,0.4mmHg) to produce a clear oil that on cooling yielded 4-acetoxybenzoyl chloride as a white crystalline solid (317.51g,1.60mol,94.5%,mp. 29.5-30.5°C lit[11] 29-30°C) which was characterised by ^{1}H n.m.r. (d^6-acetone, 200MHz) δ2.33 (s,3H,C$\underline{H}_3$), δ7.41 (d,9.08Hz,2H,Ar$\underline{H}$), δ8.20 (d,9.00Hz,2H,Ar$\underline{H}$), ^{13}C n.m.r. (d^6-acetone, 50MHz) δ21.42 ($\underline{C}H_3$), δ124.05 (aromatic $\underline{C}$-H), δ131.35 (aromatic $\underline{C}$-R), δ134.26 (aromatic $\underline{C}$-H), δ158.11 (aromatic $\underline{C}$-O), δ 168.00 ($\underline{C}$OCl), δ169.42 ($\underline{C}$OCH$_3$), I.R. (liquid) 1773.8 cm^{-1} (s, acid chloride and ester C=O absorptions), 1597.4 cm^{-1} (s, aryl-H C-H vibration), 1499.3 cm^{-1} (m, aryl-H C-H vibration), 1370.3 cm^{-1} (m, CH$_3$ C-H symmetrical deformation), 1199.4 cm^{-1} (s, aromatic C-O stretch), 1162.1 cm^{-1} (s, aromatic C-O stretch).

Synthesis of phenyl-(4-acetoxybenzoate). To a suspension of 4-acetoxybenzoyl chloride (315.75g,1.59mol) in pyridine (1350ml) were added phenol (179.47g,1.91mol), 4-dimethylaminopyridine (9.74g,0.080mol) and dichloromethane (650ml). The mixture was stirred at room temperature for 48h. The resulting solution was washed with aqueous hydrochloric acid solution (15×400ml,10%v/v) followed by aqueous sodium hydroxide solution (15×400ml,1.0M) and aqueous potassium carbonate solution (2×300ml,1.0M), dried (MgSO$_4$), the solvent removed by evaporation and the residue dried under vacuum to yield phenyl-(4-acetoxybenzoate) as a light tan solid (376.79g,1.47mol,92.5%,mp.83.5-85.5°C) which was characterised by ^{1}H n.m.r. (CDCl$_3$, 200MHz) δ2.33 (s,3H,C$\underline{H}_3$), δ7.22 (m,5H,Ar$\underline{H}$), δ7.43 (m, 2H,Ar$\underline{H}$), δ8.23 (d,8.58Hz,2H,Ar$\underline{H}$), ^{13}C n.m.r. (CDCl$_3$,

50MHz) δ21.67 ($\underline{C}H_3$), δ122.19, δ122.38, δ126.47 (all aromatic $\underline{C}$-H), δ127.59

(aromatic $\underline{C}$-R), δ130.03, δ132.30 (both aromatic $\underline{C}$-H), δ151.36, δ155.32 (both

aromatic $\underline{C}$-O), δ164.89 (Ar$\underline{C}$=O), δ169.32 (CH$_3\underline{C}$=O), I.R. (KBr disc) 3068.0 cm^{-1}

(w, acetate C-H absorption), 1755.2 cm^{-1} (s, alkyl ester C=O absorption), 1728.9 cm^{-1}

(s, aryl ester C=O absorption), 1601.5 cm^{-1} (s, aryl-H C-H vibration), 1501.9 cm^{-1} (s,

aryl-H C-H vibration), 1485.2 cm^{-1} (s, aryl-H C-H vibration).

Synthesis of phenyl-(4-hydroxybenzoate). Phenyl-(4-acetoxybenzoate)

(199.44g,0.779mol) was added to an ice-cold solution of sodium hydroxide

(31.16g,0.779mol) in ethanol (1.3l) and the mixture stirred at 0°C for ½h. After

filtration, water (6l) was added to the filtrate and the solution acidified to pH1 with

concentrated hydrochloric acid. The resultant precipitate was collected by filtration,

washed with aqueous hydrochloric acid (10%v/v) then hexane and dried under

vacuum. The filtrate was extracted with ethyl acetate, the organic layers combined,

dried (MgSO$_4$) and the solvent removed by evaporation to yield a white residue that

was dried under vacuum. The crude product portions were combined and purified by

vacuum sublimation (~210°C,0.3mmHg) followed by recrystallisation from hot

toluene and washed with cold toluene and hexane to yield phenyl-(4-

hydroxybenzoate) as a white crystalline solid (72.57g,0.339mol,43.5%, mp.184.0-

185.0°C lit^{12} 173-175°C) which was characterised by ^{1}H n.m.r. (d^6-acetone, 400MHz)

δ7.01 (d,9.2Hz,2H,Ar$\underline{H}$), δ7.26 (m,3H,Ar$\underline{H}$), δ7.45 (m,2H,Ar$\underline{H}$), δ8.06

(d,8.8Hz,2H,Ar$\underline{H}$), δ9.36 (s,1H,O$\underline{H}$), ^{13}C n.m.r. (d^6-acetone, 100MHz)

δ116.31 (aromatic $\underline{C}$-H), δ121.66 (aromatic $\underline{C}$-R), δ122.82,δ126.38,δ130.18,δ133.12

(all aromatic $\underline{C}$-H), δ152.30 (aromatic $\underline{C}$-O), δ163.25 (aromatic $\underline{C}$-OH), δ165.21

($\underline{C}$=O), I.R. (KBr disc) 3397.6 cm^{-1} (broad, H-bonded O-H stretch), 3055.9 cm^{-1} (w,

aryl-H C-H stretch), 1698.8 cm^{-1} (s, ester C=O absorption), 1603.4 cm^{-1} (s, aryl-H C-

H vibration), 1585.3 cm^{-1} (s, aryl-H C-H vibration), 1509.6 cm^{-1} (s, aryl-H C-H

vibration), 851.8 cm^{-1} (s, aryl-H C-H out of plane vibration).

Synthesis of [7], the extended 1st generation dendrimer. To a solution of

1,3,5-benzenetricarbonyl trichloride (5.31g,0.0200mol) in pyridine (220ml) were

added phenyl-(4-hydroxybenzoate) (15.00g,0.0701mol), 4-dimethylaminopyridine

(0.40g,0033mol) and dichloromethane (80ml). The resulting solution was stirred at room temperature for 4 days.

After addition of a further portion of dichloromethane (250ml), the solution was washed with aqueous hydrochloric acid solution (4×250ml,10%v/v), aqueous sodium hydroxide solution (3×250ml,1.0M) and brine (2×250ml), dried (MgSO$_4$) and the solvent removed by evaporation. The residue was recrystallised from a mixture of ethyl acetate and ethanol (3:1). The product was dried under vacuum at 100°C overnight to yield dendrimer [7] as a white powdery solid (12.10g,0.0152mol,75.8%,mp.191.5-193.0°C); Found C, 72.36%; H, 3.77%; O, 23.87%. C$_{48}$H$_{30}$O$_{12}$ requires C, 72.18%; H, 3.76%; O, 24.06%. ^{1}H n.m.r. (CDCl$_3$, 400MHz) δ7.23 (d,8.4Hz,6H,ArH), δ7.29 (m,3H,ArH), δ7.44 (m,12H, ArH), δ8.33 (d,8.8Hz,ArH), δ9.29 (s,3H,ArH), ^{13}C n.m.r. (CDCl$_3$, 100MHz) δ121.61, δ121.82, δ126.01 (all aromatic C-H), δ127.75 (aromatic C-R), δ129.52 (aromatic C-H), δ130.94 (aromatic C-R), δ131.99, δ136.37 (both aromatic C-H), δ 150.76, δ154.45 (both aromatic C-O), δ162.59, δ164.19 (both C=O), I.R. (KBr disc) 3065.9 cm^{-1} (w, aryl-H C-H stretch), 1734.7 cm^{-1} (s, ester C=O absorption), 1591.8 cm^{-1} (s, aryl-H C-H vibration), 1502.8 cm^{-1} (s, aryl-H C-H vibration).

Synthesis of 5-acetoxyisophthalic acid. To a stirred solution of 5-hydroxyisophthalic acid (100.00g,0.594mol) in aqueous sodium hydroxide solution (1l,2.5M) cooled in an ice-water bath, acetic anhydride (200ml) was added slowly. Stirring was continued for 2 hours, upon which the flask was shaken for 10 minutes and the contents acidified to pH1 using concentrated hydrochloric acid. The white slurry was filtered and the filtrate extracted with ethyl acetate (6×300ml). A further portion of ethyl acetate (900ml) was added to this and the filtered residue was dissolved in it. The resultant solution was washed with water (5×500ml) and the combined aqueous washings extracted with ethyl acetate (500ml). The organic portions were combined, dried (MgSO$_4$), the solvent removed by evaporation and the residue dried under vacuum at 80°C for 4h. to yield 5-acetoxyisophthalic acid as a white powdery solid (122.56g,0.547mol,99.7%,mp.246-247°C) which was characterised by ^{1}H n.m.r. (d^6-acetone, 200MHz) δ2.35 (s,3H,CH$_3$), δ8.00 (d,1.52Hz,2H,ArH), δ8.56 (t,1.52Hz,1H,ArH), ^{13}C n.m.r. (d^6-acetone, 50MHz)

δ21.30 ($\underline{C}H_3$), δ128.44 (aromatic $\underline{C}$-H), δ128.89 (aromatic $\underline{C}$-H), δ133.73 (aromatic $\underline{C}$-R), δ152.46 (aromatic $\underline{C}$-O), δ166.50 (ArCO$_2$H), δ170.06 ($\underline{C}$OCH$_3$), I.R. (KBr disc) 3100 - 2600 cm^{-1} (broad, H-bonded O-H, aryl-H and saturated C-H stretches), 1770.4 cm^{-1} (s, ester C=O absorption), 1693.8 cm^{-1} (s, carboxylic acid C=O absorption).

Synthesis of 5-acetoxyisophthaloyl dichloride. An intimate mixture of 5-acetoxyisophthalic acid (98.93g,0.492mol) and phosphorus pentachloride (213.2g,1.024mol) in a flask fitted with a reflux condenser and gas absorption device was warmed gently with a heat gun to initiate the reaction and shaken occasionally until the vigorous evolution of hydrogen chloride had ceased. To ensure complete reaction, the reaction mixture was stirred for a further hour at room temperature to form a pale yellow homogeneous oil. After removal of phosphorus oxychloride by distillation at atmospheric pressure, the residue was distilled at reduced pressure (132-134°C,0.3mmHg) to produce a clear oil that on cooling yielded 5-acetoxyisophthaloyl dichloride as a white crystalline solid (113.75g,0.436mol,88.6%, mp.51.5-52.5°C) which was characterised by ^{1}H n.m.r. (d^6-acetone,200MHz) δ2.37 (s,3H,$\underline{C}H_3$), δ8.28 (s,2H,Ar$\underline{H}$), δ8.65 (s,1H,Ar$\underline{H}$), ^{13}C n.m.r. (d^6-acetone,50MHz) δ21.29 ($\underline{C}H_3$), δ131.33 (aromatic $\underline{C}$-H), δ132.03 (aromatic $\underline{C}$-H), δ136.44 (aromatic $\underline{C}$-R), δ153.07 (aromatic $\underline{C}$-O), δ167.46 ($\underline{C}$OCl), δ169.78 ($\underline{C}$OCH$_3$), I.R. (liquid) 3092.6 cm^{-1} (m, aryl-H C-H stretch), 3028.7 cm^{-1} (w, aryl-H C-H stretch), 1774.7 cm^{-1} (s, acid chloride and ester C= absorptions).

Synthesis of [5]-OAc, the protected 2nd generation wedge. Phenyl-(4-hydroxybenzoate) (114.00g,0.533mol), 4-dimethylaminopyridine (1.50g,0.012mol) and dichloromethane (330ml) were added to a suspension of 5-acetoxyisophthaoyl dichloride (68.02g,0.261mol) in pyridine (1l). After stirring at room temperature for 36h., dichloromethane (1.6l)was added and the solution washed with aqueous hydrochloric acid solution (10%v/v,12×600ml) and aqueous sodium hydroxide solution (1.0M,12×600ml), dried (MgSO$_4$), the solvent removed by evaporation and the residue dried under vacuum to yield [5]-OAc as a white powdery solid (149.52g,0.243mol,93.0%,mp.194.5-196.5°C) which was characterised by ^{1}H n.m.r. (CDCl$_3$, 400MHz) δ2.40 (s,3H,$\underline{C}H_3$), δ7.23 (m,4H,Ar$\underline{H}$), δ7.29 (m,2H,Ar$\underline{H}$), δ7.43

(m,8H,Ar$\underline{H}$), δ8.24 (d,1.6Hz,2H,Ar$\underline{H}$), δ8.32 (d,8.4Hz,4H,Ar$\underline{H}$), δ8.91

(t,1.6Hz,1H,Ar$\underline{H}$), [13]C n.m.r. (CDCl$_3$, 100MHz) δ20.95 ($\underline{C}$H$_3$), δ121.62, δ121.83, δ

125.97 (all aromatic $\underline{C}$-H), δ127.58 (aromatic $\underline{C}$-R), δ128.71, δ129.09, δ129.50 (all

aromatic $\underline{C}$-H), δ131.27 (aromatic $\underline{C}$-R), δ131.93 (aromatic $\underline{C}$-H), δ150.78, δ151.07,

δ154.56 (all aromatic $\underline{C}$-O), δ162.72, δ164.24 (both aromatic $\underline{C}$=O), δ168.89

(O$\underline{C}$OCH$_3$), I.R. (KBr disc) 3078.6 cm^{-1} (w, aryl-H C-H stretch), 1773.3 cm^{-1} (s,

alkyl ester C=O absorption), 1743.8 cm^{-1} (s, aryl ester C=O absorption), 1590.5 cm^{-1}

(m, aryl-H C-H vibration), 1503.1 cm^{-1} (m, aryl-H C-H vibration), 746.4 cm^{-1} (m,

aryl-H C-H out of plane vibration).

Synthesis of [5]-OH, the 2nd generation wedge. The protected wedge, [5]-

OAc (147.73g,0.240mol) was added to a mixture of aqueous hydrochloric acid

solution (10%v/v,700ml) and tetrahydrofuran (2.1l) and the solution refluxed for 18h.

After cooling, the tetrahydrofuran was removed by evaporation and the residue

extracted with ethyl acetate (4×500ml), dried (MgSO$_4$) and the solvent removed by

evaporation. The residue was recrystallised from hot toluene, washed with hexane

and dried under vacuum to yield [5]-OH as a fine white powder

(119.34g,0.208mol,86.6%,mp. 202.0-205.5°C) which was characterised by [1]H n.m.r.

(d^6-acetone, 400MHz) δ7.33 (m,6H,Ar$\underline{H}$), δ7.49 (m,4H,Ar$\underline{H}$), δ7.59

(d,8.8Hz,4H,Ar$\underline{H}$), δ7.98 (d,1.6Hz,2H,Ar$\underline{H}$), δ8.31 (d,9.2Hz,4H,Ar$\underline{H}$), δ8.49

(t,1.6Hz,1H,Ar$\underline{H}$), δ9.50 (broad,1H,O$\underline{H}$), [13]C n.m.r. (d^6-acetone, 100MHz)

δ122.57, δ122.77, δ123.28, δ123.36, δ126.75 (all aromatic $\underline{C}$-H), δ128.38 (aromatic

C-R), δ130.32 (aromatic $\underline{C}$-H), δ132.22 (aromatic $\underline{C}$-R), δ132.47 (aromatic $\underline{C}$-H), δ

152.11, δ156.08, δ159.03 (all aromatic $\underline{C}$-O), δ164.22, δ164.79 (both aromatic $\underline{C}$=O),

I.R. (KBr disc) 3386.1 cm^{-1} (broad, H-bonded O-H stretch), 3071.1 cm^{-1} (w, aryl-H

C-H stretch), 1736.7 cm^{-1} (s, aryl ester C=O absorption), 1708.8 cm^{-1} (s, aryl ester

C=O absorption), 1601.2 cm^{-1} (s, aryl-H C-H vibration), 1498.0 cm^{-1} (s, aryl-H C-H

vibration), 744.7 cm^{-1} (s, aryl-H out of plane vibration).

Synthesis of [16], the 2nd generation dendrimer. 1,3,5-Benzenetricarbonyl

trichloride (0.58g,0.00218mol) was added to a stirred solution of [5]-OH

(4.50g,0.00784mol) in dichloromethane (30ml) and N,N-dimethylaniline (1.5ml) and

the mixture stirred at room temperature for 40h. After addition of dichloromethane

(60ml), the solution was washed with aqueous hydrochloric acid solution (10%v/v,3×

50ml) and brine (2×50ml), dried (MgSO$_4$), the solvent was removed by evaporation

and the residue purified by column chromatography (dichloromethane/1% ethyl

acetate/silica (Merck silica gel 60)) followed by recrystallisation (1:1 ethanol/ethyl

acetate mixture) to yield dendrimer [16] as a white powder

(1.01g,0.000538mol,24.7%,mp.162.5-164.0°C); Found C, 70.61%; H, 3.46%; O,

25.93%). C$_{111}$H$_{66}$O$_{30}$ requires C, 70.93%; H, 3.51%; O, 25.56%. [1]H n.m.r. (CDCl$_3$,

400MHz) δ7.22 (d,8.8Hz,12H,ArH), δ7.29 (m,6H,ArH), δ7.44 (m,24H,ArH), δ8.32

(d,8.8Hz,12H,ArH), δ8.45 (d,1.6Hz,6H,ArH), δ9.01 (t,1.2Hz,3H,ArH), δ9.37

(s,3H,ArH), [13]C n.m.r. (CDCl$_3$, 100MHz) δ121.63, δ121.84, δ126.05 (all aromatic C-

H), δ127.74 (aromatic C-H), δ128.60, δ129.55,δ129.73 (all aromatic C-H), δ130.74,

δ131.70 (both aromatic C-R), δ132.01, δ136.72 (both aromatic C-H), δ150.78, δ

150.84, δ154.51 (all aromatic C-O), δ162.60 (2×aromatic C=O), δ164.23 (aromatic

C=O), I.R. (KBr disc) 3073.6 cm^{-1} (w, aryl-H C-H stretch), 1739.3 cm^{-1} (s, ester

C=O absorption), 1599.9 cm^{-1} (s, aryl-H C-H vibration), 1503.4 cm^{-1} (s, aryl-H C-H

vibration), 742.0 cm^{-1} (s, aryl-H C-H out of plane vibration).

Synthesis of [6]-OAc, the protected extended 2nd generation wedge. To a

stirred solution of 4-acetoxybenzoyl chloride (5.42g,0.0273mol) in pyridine (250ml)

were added [5]-OH (12.50g,0.0218mol), dichloromethane (80ml) and 4-

dimethylaminopyridine (0.18g,0.0015mol). After stirring at room temperature for 48

hours, dichloromethane (250ml) was added and the solution washed with aqueous

hydrochloric acid solution (10%v/v,6×300ml) and aqueous sodium hydroxide

solution (1.0M,9×300ml),dried (MgSO$_4$), the solvent removed by evaporation and the

residual oil dried under vacuum to yield [6]-OAc as a fine white powder

(13.34g,0.0181mol,83.1%,mp.75.0-76.0°C) which was characterised by [1]H n.m.r.

(CDCl$_3$, 400MHz) δ2.36 (s,3H,CH$_3$), δ7.22 (m,4H,ArH), δ7.30 (m,4H,ArH), δ7.43

(m,8H,ArH), δ8.28 (d,8.8Hz,2H,ArH), δ8.32 (d,8.8Hz,4H,ArH), δ8.36

(d,1.6Hz,2H,ArH), δ8.96 (t,1.6Hz,1H,ArH), [13]C n.m.r. (CDCl$_3$, 100MHz) δ21.18

(CH$_3$), δ121.66, δ121.88, δ122.14 (all aromatic C-H), δ125.91 (aromatic C-R), δ

126.01 (aromatic C-H), δ127.62 (aromatic C-R), δ128.84, δ129.29, δ129.54 (all

aromatic $\underline{C}$-H), δ131.41 (aromatic $\underline{C}$-R), δ131.98, δ132.00 (both aromatic $\underline{C}$-H), δ 150.82, δ151.35, δ154.62, δ155.33 (all aromatic $\underline{C}$-O), δ162.77, δ163.94, δ164.29 (all aromatic $\underline{C}$=O), δ168.69 (O$\underline{C}$OCH$_3$), I.R. (KBr disc) 3074.3 cm^{-1} (w, aryl-H C-H stretch), 1738.3 cm^{-1} (s, ester C=O absorption), 1601.2 cm^{-1} (s, aryl-H C-H vibration), 1503.7 cm^{-1} (m, aryl-H C-H vibration), 742.1 cm^{-1} (m, aryl-H C-H out of plane vibration).

Synthesis of [6]-OH, the extended 2nd generation wedge. Aqueous hydrochloric acid solution (10%v/v,0.5l) was added to a solution of [6]-OAc (97.51g,0.132mol) in tetrahydrofuran (1.5l) and the mixture refluxed for 24h. On cooling, water (300ml) was added and the tetrahydrofuran removed by evaporation. The residue was extracted with ethyl acetate (3×400ml) and the combined organic layers washed with aqueous hydrochloric acid solution (10%v/v,3×300ml), dried (MgSO$_4$) and the solvent removed by evaporation. The residual oil was dried under vacuum to give a white solid that was recrystallised from toluene, washed with hexane and dried under vacuum (120°C) overnight to yield [6]-OH as a white powdery solid (79.44g,0.114mol,86.7%,mp.215.5-216.0°C) which was characterised by ^{1}H n.m.r. (d^6-acetone, 400MHz) δ7.04 (d,8.8Hz,2H,Ar$\underline{H}$), δ7.32 (m,6H,Ar$\underline{H}$), δ 7.49 (m,4H,Ar$\underline{H}$), δ7.62 (d,8.8Hz,4H,Ar$\underline{H}$), δ8.14 (d,8.8Hz,2H,Ar$\underline{H}$), δ8.31 (d,8.8Hz,4H,Ar$\underline{H}$), δ8.44 (d,1.6Hz,2H,Ar$\underline{H}$), δ8.86 (t,1.6Hz,1H,Ar$\underline{H}$), δ9.54 (broad,1H,O$\underline{H}$), ^{13}C n.m.r. (d^6-acetone, 100MHz) δ116.38 (aromatic $\underline{C}$-H), δ116.47 (aromatic $\underline{C}$-R), δ122.76, δ123.26, δ126.74 (all aromatic $\underline{C}$-H), δ128.45 (aromatic $\underline{C}$-R), δ129.20, δ129.63, δ130.31 (all aromatic $\underline{C}$-H), δ132.30 (aromatic $\underline{C}$-R), δ132.47, δ133.53 (both aromatic $\underline{C}$-H), δ152.07, δ152.78, δ155.93 (all aromatic $\underline{C}$-O), δ163.64 (aromatic $\underline{C}$=O), δ163.75 (aromatic $\underline{C}$-OH), δ164.76, δ165.02 (both aromatic $\underline{C}$=O), I.R. (KBr disc) 3392.1 cm^{-1} (broad, O-H stretch), 3072.5 cm^{-1} (w, aryl-H C-H stretch), 1739.3 cm^{-1} (s, ester C=O absorption), 1591.0 cm^{-1} (s, aryl-H C-H vibration), 1503.5 cm^{-1} (s, aryl-H C-H vibration), 744.0 cm^{-1} (s, aryl-H C-H out of plane vibration).

Synthesis of [19], the extended 2nd generation dendrimer. To a stirred solution of [6]-OH (1.55g,0.00223mol) in dichloromethane (12ml) and N,N-dimethylaniline (0.4ml) was added 1,3,5-benzenetricarbonyl trichloride

(0.169g,0.000636mol) and the mixture stirred at room temperature for 40 hours. After addition of dichloromethane (30ml), the solution was washed with aqueous hydrochloric acid solution (10%v/v,5×50ml) and brine (2×50ml), dried (MgSO$_4$) and the solvent removed by evaporation. The residue was purified by column chromatography (dichloromethane/1%ethyl acetate/silica (Merck silica gel 60)) to produce a white solid that was recrystallised from a 1:1 mixture of ethanol and ethyl acetate then dried under vacuum (120°C,overnight) to yield dendrimer [19] as a white powder (0.24g, 0.000107mol,16.9%); Found C,68.94%; H,3.40%; O,27.66%. $C_{132}H_{78}O_{36}$ requires C,70.78%; H,3.49%; O, 25.73%. ^{1}H n.m.r. (CDCl$_3$, 400MHz) δ7.24 (d,8.4Hz,12H,ArH), δ7.30 (m,6H,ArH), δ7.45 (m,24H,ArH), δ7.53 (d,8.4Hz,6H,ArH), δ8.34 (d,8.4Hz,12H,ArH), δ8.40 (m,12H,ArH), δ9.00 (s,3H,ArH), δ9.33 (s,3H,ArH), ^{13}C n.m.r. (CDCl$_3$, 100MHz) δ121.76, δ121.98, δ 122.25, δ126.14 (all aromatic C-H), δ126.82, δ127.78 (both aromatic C-R), δ128.92, δ129.47, δ129.66 (all aromatic C-H), δ131.07, δ131.59 (both aromatic C-R), δ 132.10, δ132.38, δ136.61 (all aromatic C-H), δ150.92, δ151.40, δ154.71, δ155.10 (all aromatic C-O), δ162.62, δ162.86, δ163.91, δ164.38 (all aromatic C=O), I.R. (KBr disc) 3071.9 cm^{-1} (w, aryl-H C-H stretch), 1738.7 cm^{-1} (s, ester C=O absorption), 1599.8 cm^{-1} (m, aryl-H C-H stretch), 1504.1 cm^{-1} (m, aryl-H C-H out of plane vibration).

Synthesis of [13]-OAc, the protected 3rd generation wedge. To a suspension of 5-acetoxyisophthaoyl dichloride (2.68g,0.0103mol) in pyridine (250ml) were added [6]-OH (15.00g,0.0216mol), 4-dimethylaminopyridine (0.15g,0.0012mol) and dichloromethane (80ml). After stirring at room temperature for 4 days, dichloromethane (250ml) was added and the solution washed with aqueous hydrochloric acid solution (10%v/v,15×200ml) and aqueous sodium hydroxide solution (1.0M,15×200ml), dried (MgSO$_4$), the solvent removed by evaporation and the residue dried under vacuum (90°C,4 hours) to yield [13]-OAc as a white powdery solid (7.11g,0.00451mol,41.8%) which was characterised by ^{1}H n.m.r. (CDCl$_3$,400MHz) δ2.40 (s,3H,CH$_3$), δ7.24 (m,8H,ArH), δ7.29 (m,4H,ArH), δ 7.44 (m,20H,ArH), δ8.25 d,1.6Hz,2H,ArH), δ8.32 (d,8.4Hz,8H,ArH), δ8.36 (d,8.8Hz,4H,ArH), δ8.39 (d,1.6Hz,4H,ArH), δ8.92 (t,1.6Hz,1H,ArH), δ8.97

(t,1.6Hz,2H,ArH), ^{13}C n.m.r. (CDCl$_3$, 100MHz) δ20.97 (CH$_3$), δ121.62, δ121.84, δ 122.13, δ125.99 (all aromatic C-H), δ126.46, δ127.60 (both aromatic C-R), δ128.80 (2×aromatic C-H), δ129.17, δ129.37, δ129.51 (all aromatic C-H), δ131.18, δ131.42 (both aromatic C-R), δ131.95, δ132.16 (both aromatic C-H), δ150.76, δ151.12, δ 151.28, δ154.57, δ155.08 (all aromatic C-O), δ162.61, δ162.72, δ163,81, δ164.25 (all aromatic C=O), δ168.91 (OCOCH$_3$), I.R. (KBr disc) 3075.9 cm^{-1} (w, aryl-H C-H stretch), 1740.4 cm^{-1} (s, ester C=O absorption), 1600.5 cm^{-1} (s, aryl-H C-H vibration), 1503.4 cm^{-1} (s, aryl-H C-H vibration), 742.8 cm^{-1} (m, aryl-H C-H out of plane vibration).

References

1. Hawker, C.J. and Fréchet, J.M.J., J. Chem. Soc.,Chem. Commun. 1010 (1990)

2. Hawker, C.J. and Fréchet, J.M.J., J. Chem. Soc.,Perkin Trans.1 2459 (1992)

3. Miller, T.M., Kwock, E.W. and Neenan, T.X., Macromolecules 25, 3143 (1992)

4. Bayliff, P.M., Feast, W.J. and Parker, D., Polymer Bulletin 29, 265 (1992)

5. Miller, T.M., Neenan, T.X., Zayes, R. and Bair, H.E., J. Am. Chem. Soc. 114, 1018 (1992)

6. Xu, Z. and Moore, J.S., Angew. Chem. Int. Ed. Engl. 32, 1354 (1993)

7. Hawker, C.J. and Fréchet, J.M.J., J. Am. Chem. Soc. 114, 8405 (1992)

8. Quick, J. and Crelling, J.K., J. Org. Chem. 43, 155 (1978)

9. Holding, S.R. in "Size Exclusion Chromatography", Hunt, B.J. and Holding, S.R. (eds.), Blackie (1989)

10. Hawker, C.J. and Fréchet, J.M.J., J. Am. Chem. Soc. 112, 7638 (1990)

11. Linnell, W.H. and Roushdi, I.M., Quart. J. Pharm. Pharmacol. 14, 270 (1941)

12. Ogata, Y. and Furuta, M., J. Org. Chem. 39, 216 (1974)

CHAPTER 3

Polymer Blends

Polymer Blends

Introduction

Given that only relatively small quantities of dendrimers can be prepared by the iterative synthetic procedures outlined earlier, it is clear that if such materials are to be of any practical advantage then applications must be sought in two key areas. The first of these is in the general field of "smart technology", such as nanoengineering and pharmaceutical applications, in which dendrimers must be activated to carry out highly specific tasks by the incorporation of appropriate functionality. Secondly, as passive molecules, dendrimers may find application as additives in conventional materials for the enhancement of physical properties and modification of processing techniques. In the course of this project, the aryl ester dendrimers have been considered as candidates to be blended with poly(ethylene terephthalate) (PET) (Figure 3.1). PET is a commercially important bulk polymer with a wide range of uses encompassing packaging materials, films and fibres on account of its remarkable combination of desirable mechanical and barrier properties and aesthetic acceptability.[1]
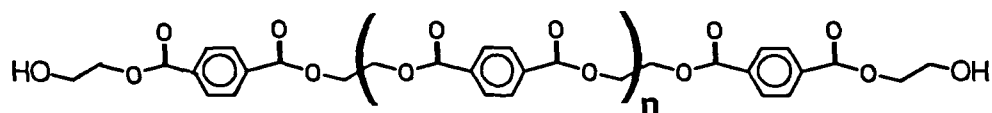

Figure 3.1 Poly(ethylene terephthalate).

Polymer Blends

A polymer blend can be defined as an intimate mixture of two or more types of polymer, differing in their constitution or configurational composition.[2] The resultant material may possess mechanical, thermal or other physical properties that are substantially different from those of its components. Blends that exhibit enhanced properties or replicate those of existing materials whilst incorporating significant cost or processing advantages are of considerable practical importance in a commercial environment, particularly since minimal development costs are incurred by combining existing polymers with respect to those involved in producing new monomers and polymerisation techniques. Blends are also of interest from an academic standpoint

since the study of such materials has lead to a greater understanding of polymer chain interactions and the development of solid state mixing theory.[3-5]

Miscibility of Polymer Blends[1,4,6]

On mixing any two polymers, the resultant blend can be described in terms of the miscibility or compatibility of the components. Although these terms are frequently regarded as synonymous, miscibility and compatibility are technologically distinct from one another. A blend is said to be compatible if there is a beneficial change in an observed parameter with respect to those of its constituents. Clearly the compatibility or otherwise of a blend , which may be a single or multiphase system, is to some extent determined by the intended application. In contrast, a miscible blend has a single homogeneous phase except in the case in which one or both of the components are crystallisable, in which case the amorphous regions of the blend must be homogeneous. Compatible blends may be miscible or immiscible. For polymeric plasticisers, complete miscibility is highly desirable whereas in rubber-like impact resistant materials, this is not the case. In order to understand more fully the concept of miscibility, it is necessary to consider a thermodynamic approach to the mixing of blend components at a molecular level. For any favourable mixing process, the free energy of mixing must be negative, i.e. $\Delta G_{mix} < 0$. This is a necessary but not a sufficient condition for miscibility. ΔG_{mix} is given by

$$\Delta G_{mix} = \Delta H_{mix} - T\Delta S_{mix} \qquad \text{(eqn. 3.1)}$$

where ΔH_{mix} and ΔS_{mix} are the enthalpy and entropy of mixing respectively and T is the absolute temperature. The Flory-Huggins theory of polymer solutions, which takes the interaction between the blend components into account, specifies the additional requirement[7]

$$\left(\frac{\partial^2 G_{mix}}{\partial \phi_i^2}\right)_{T,P} > 0 \qquad \text{(eqn. 3.2)}$$

to ensure stability against phase segregation, where ϕ_i is the volume fraction of component i in the mixture and P is the pressure.

On the strength of thermodynamic considerations, blend miscibility can be predicted to occur in the following cases.

i) If the polymers are of sufficiently low molecular mass, the entropy of mixing is relatively high and may outweigh any unfavourable endothermic enthalpy of mixing.

ii) If the enthalpy of mixing is positive but small, even polymers of high molecular mass may have sufficient entropy of mixing to promote miscibility.

iii) If the enthalpy of mixing is negative, the blend components are expected to be miscible irrespective of molecular mass. This is the case when there are specific interactions between the blend components.

Many techniques have been utilised in the investigation of miscibility.[3,8] In principle, the simplest of these is the direct measurement of the enthalpy of mixing on combination of blend components however due to the practical difficulties involved, its use is restricted to oligomers or low viscosity materials. One of the most common techniques for the determination of blend miscibility is glass transition (T_g) analysis. Miscible polymer blends exhibit a single glass transition at a temperature between those of the blend components. If however the components have similar glass transition temperatures, resolution of individual transitions is often poor thus restricting the usefulness of this method.

The Interaction Parameter χ

A quantitative measure of blend miscibility can be determined by calculation of the interaction parameter χ. It has been proposed that any pair of blend components with a negative interaction parameter will form a miscible blend. Consequently, in determining the miscibility of polymer blends, attention has focused on the measurement of the interaction parameter χ.

In recent years, small angle neutron scattering has become increasingly important in the determination of blend miscibility. Not only is this an absolute technique but it also allows the temperature dependence of the interaction parameter to

be determined. Although an extremely powerful tool in the investigation of polymer blends, neutron scattering has two distinct limitations. In order to obtain acceptable scattering contrast, it is necessary to have one of the blend components deuterated thus restricting the range of blends that may be easily studied. There are also a limited number of neutron sources available on which such experiments can be performed.

If one of the components of a polymer blend can crystallise, a separate crystalline phase may form even though the components form a miscible blend. The observed melting point depression of the crystalline phase can be related to the interaction between the blend components. Based on the Flory-Huggins thermodynamic theory of mixing, Nishi and Wang[5] extended the work of Scott[9] to derive the equation

$$\left(\frac{1}{T_{mb}^0} - \frac{1}{T_m^0}\right) * T_{mb}^0 = -\frac{B\phi_1^2 \overline{V_{2u}}}{\Delta H_{2u}} \qquad \text{(eqn 3.3)}$$

where T_{mb}^0 is the equilibrium melting point of the semi-crystalline component in the blend, T_m^0 is the equilibrium melting point of the pure semi-crystalline polymer and $\overline{V_{2u}}$ is the molar volume of a 100% crystalline sample of the semi-crystalline component per repeat unit in the sample, i.e. the volume occupied by one mole of repeat units in a fully crystalline sample. ΔH_{2u} is the molar enthalpy of fusion per repeat unit of a 100% crystalline sample of the pure semi-crystalline polymer, ϕ_1 is the volume fraction of the amorphous component and B is the free energy density of the system, which is related to the interaction parameter χ by the expression

$$\chi = \frac{B\overline{V_{1u}}}{RT_{mb}^0} \qquad \text{(eqn 3.4)}$$

where $\overline{V_{1u}}$ is the molar volume of the amorphous component per repeat unit in the blend and R is the gas constant.

Blend Mixing

Melt mixing, solvent casting and blend precipitation are the major ways in which blends may be prepared from their component polymers.[7] The first of these is particularly useful in an industrial environment where intimate mixing in the molten state facilitates the manufacture of blended materials in a continuous process. Solution methods are more applicable to the preparation of small quantities of material, where melt processing is not practical. One of the most significant disadvantages of the solvent casting technique is the potential for components to form two-phase systems despite being a miscible combination. This is often observed if the blend constituents have greatly differing solubility in the casting solvent. Blend precipitation overcomes this problem by precipitation into a non-solvent and can be of use in the removal of solvent if this is difficult to remove by the conventional solvent casting technique.

Preparation of Dendrimer/PET Blends

Separate solutions of known concentrations of dendrimers [7], [16] and of PET in dichloroacetic acid ($CHCl_2CO_2H$) were prepared and mixed in the appropriate ratios so as to form 2.5%, 5%, 10% and 20% w/w dendrimer/PET solutions. After stirring to ensure complete mixing, each solution was poured into a large excess of distilled water from which a white leathery solid was precipitated. This was collected by filtration, washed several times with water and extracted using a Soxhlet apparatus with distilled water for 24 hours to remove any residual traces of dichloroacetic acid. The solid was dried under vacuum (50°C, 0.1Torr) to constant mass. A sample of pure PET was prepared in a similar manner in order to provide an appropriate reference material. PET ($M_W \approx 20,000$) was supplied by ICI p.l.c.

Thermal Characterisation and Determination of the Interaction Parameter

Since PET is a semi-crystalline polymer, the measurement of melting point depression of the crystalline component as a function of blend composition provides a convenient method for the determination of the interaction parameter χ. The dendrimer acts as a diluent or impurity and has the effect of reducing the observed crystalline PET melting point as calculated by Nishi and Wang[5] and described earlier.

51

Melting points were determined by differential scanning calorimetry (DSC) using a Perkin-Elmer DSC-7 model. In accordance with equation 3.3, equilibrium melting points should be used in all cases by application of the Hoffman-Weeks equation[2] (see Supplement 3.2) as emphasised by Runt and Gallagher[10] in their recent review of the field however Nishi and Wang inferred that this had no significant influence on the melting point depression.[5] Consequently, uncorrected experimental melting point values have been used in the course of this work.
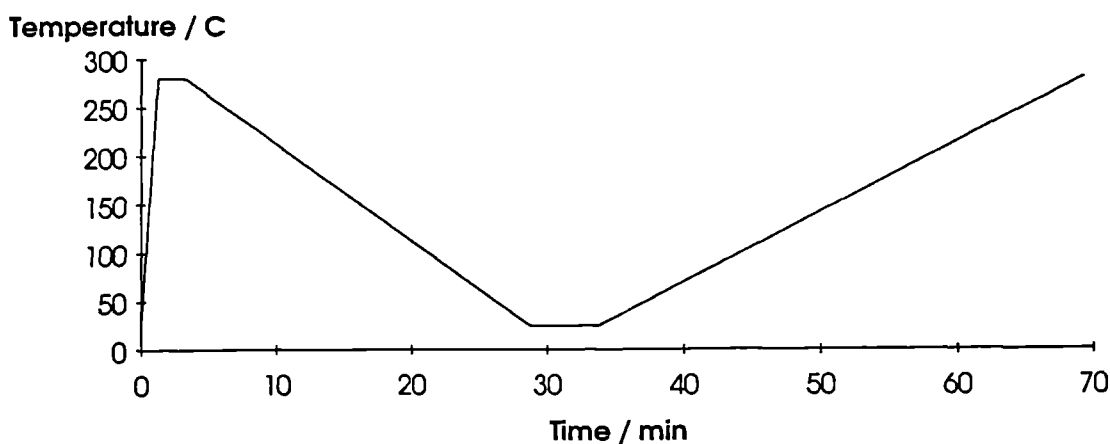
Temperature / C

Figure 3.2 DSC Temperature Profile for Melting Point Determination.

Each sample was heated at a rate of 200°Cmin^{-1} to 280°C, around 15°C above the literature equilibrium melting point of PET,[11] at which it was held for 2 minutes. After cooling at a rate of 10°Cmin^{-1} to 25°C, where it was held for a further 5 minutes, a DSC thermogram was recorded at a heating rate of 10°Cmin^{-1} to 280°C (Figure 3.2). This procedure was repeated twice for each blend composition, using a new specimen each time. The recorded melting point for each sample is the peak value of the melting endotherm, the values of which are shown in Table 3.1 and illustrated in Figures 3.3 and 3.4.

Sample	Melting Point / °C	Mean Melting Point / °C
PET	252.08 251.75 252.32	252.05 ± 0.23
2.5% [7]/PET	251.87 251.63 252.20	251.90 ± 0.23
5% [7]/PET	250.68 251.06 252.19	251.31 ± 0.64
10% [7]/PET	248.16 248.33 248.70	248.40 ± 0.23
20% [7]/PET	245.38 245.49 245.58	245.48 ± 0.08
2.5% [16]/PET	251.40 250.69 251.54	251.21 ± 0.37
5% [16]/PET	251.36 250.33 251.00	250.90 ± 0.43
10% [16]/PET	249.15 249.41 249.08	249.21 ± 0.14
20% [16]/PET	244.71 243.75 244.37	244.28 ± 0.40

Table 3.1 DSC Melting Point Depression of Dendrimer / PET Blends.

TEMPERATURE / C
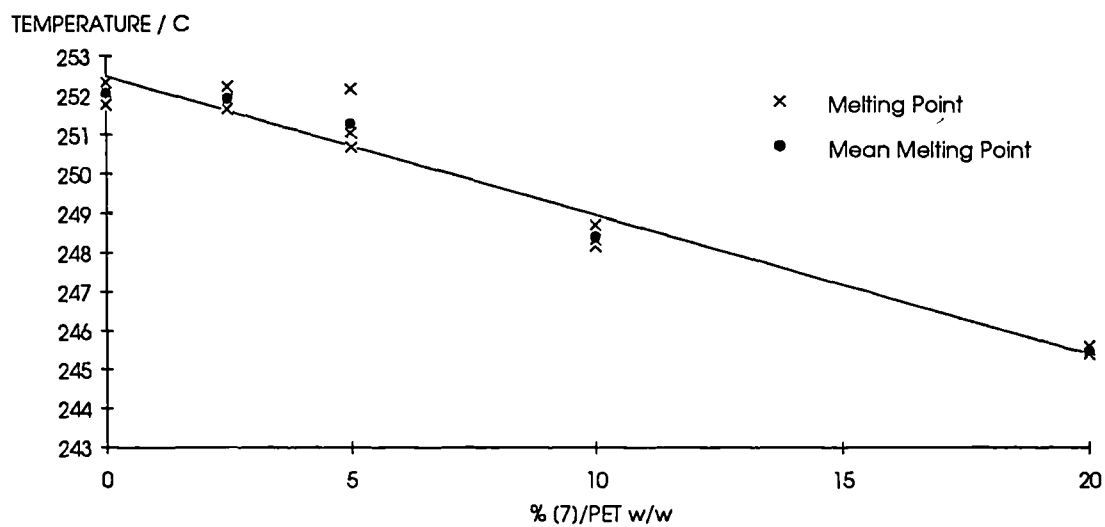
Figure 3.3 Melting Point Depression of Dendrimer [7] / PET Blends.

TEMPERATURE / C
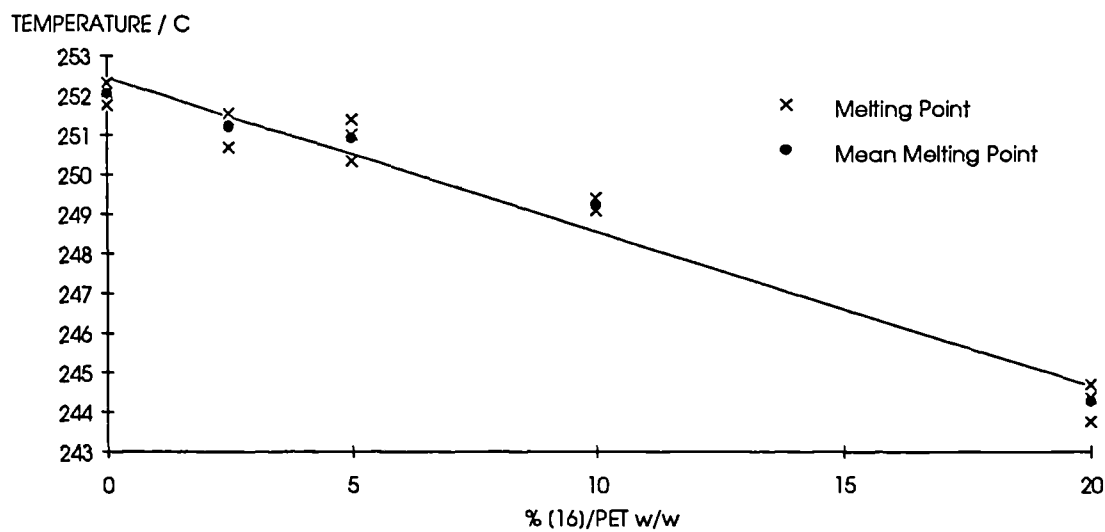
Figure 3.4 Melting Point Depression of Dendrimer [16] / PET Blends.

It is noted from Figures 3.3 and 3.4 that the melting point depression of PET on blending with dendrimers [7] and [16] is approximately linear with respect to the weight fraction of dendrimer in the blend. Furthermore, comparison of the two figures indicates that the melting point depression is largely unaffected by dendrimer size (i.e. [7] or [16]) for a given dendrimer/PET composition.

According to the classical expression for the melting point depression by low molecular weight diluents, it would be expected that for a fixed dendrimer/PET composition by weight, a larger depression of melting temperature would be observed for dendrimer [7] than for dendrimer [16] since melting point depression is regarded as a colligative property.[6]

	Dendrimer [7]	Dendrimer [16]
RMM	798	1878
No. of ester links / molecule	6	15
No. of rings / molecule	7	16
RMM / no. of ester links	133	126
RMM / no. of rings	114	117

Table 3.2 Comparison of dendrimer [7] and [16] composition.

With reference to the table above (Table 3.2), consideration of dendrimer/PET blend melting point depression in terms of specific interactions between carbonyl groups and aromatic rings indicates that both the number of ester links and aromatic rings per unit mass are similar for the two dendrimers. Since melting point depression is not significantly affected by dendrimer type but only by percentage weight incorporation of dendrimer, this suggests that specific interaction between ester carbonyl groups and aromatic rings is a dominant factor and is proposed as a plausible rationalisation of the observed melting point behaviour.

In earlier studies involving the blending of PET with poly(butylene terephthalate) (PBT) and polycarbonates, the apparent miscibility of the components has also been attributed to dipolar interaction between ester carbonyl groups and aromatic rings.[12]

In order to evaluate the free energy density B and the interaction parameter χ from equation 3.3, it is necessary to determine $\overline{V_{[7]u}}$, $\overline{V_{[16]u}}$ and $\overline{V_{PETu}}$, the molar volume per repeat unit of dendrimers [7], [16] and PET in the sample respectively and ϕ_1, the volume fraction of dendrimer in each blend composition. These in turn require the measurement of the densities of all the blend components using a density gradient column (see Supplement 3.1).

The relative densities of both PET and dendrimer [7] were determined to be 1.369 and that of dendrimer [16] to be 1.322. This is consistent with wide-angle X-ray diffraction data (see Chapter 2) which indicated that dendrimer [16] is largely amorphous whereas dendrimer [7] is appreciably crystalline. The assumption was made that the densities of the free components do not differ appreciably from those in the blends.

Evaluation of $\overline{V_{[7]u}}$, $\overline{V_{[16]u}}$ and $\overline{V_{PETu}}$ yield values of 97.2 cm^{3}mol^{-1}, 94.7 cm^{3}mol^{-1} and 126.7 cm^{3}mol^{-1} respectively. For each dendrimer, this value has been calculated by dividing the dendrimer mass per ester linkage in the structure by the experimentally determined density. For the PET, this is simply the molecular mass of a PET repeat unit (192g mol^{-1}) divided by the density of 100% crystalline PET sample (1.515g cm^{-3}).[11]

The volume fraction of dendrimer [7] in the blends is equal to its weight fraction since the density of dendrimer [7] and that measured for the PET used in this experiment are equal. The volume fraction of dendrimer [16] in the blends is calculated to reflect the differing densities of the two components in the dendrimer [16]/PET blend compositions. ΔH_{PETu}, the molar enthalpy of fusion per repeat unit of 100% crystalline PET is taken to be 2.69 kJmol^{-1}.[13]
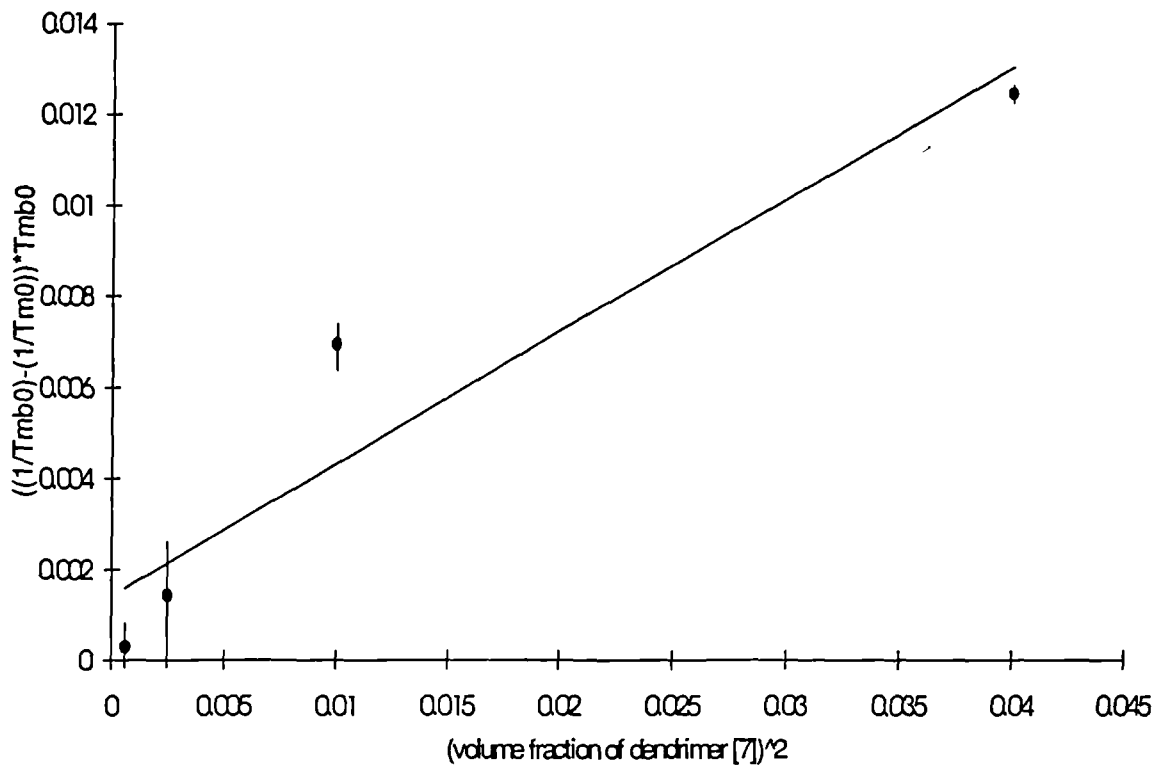
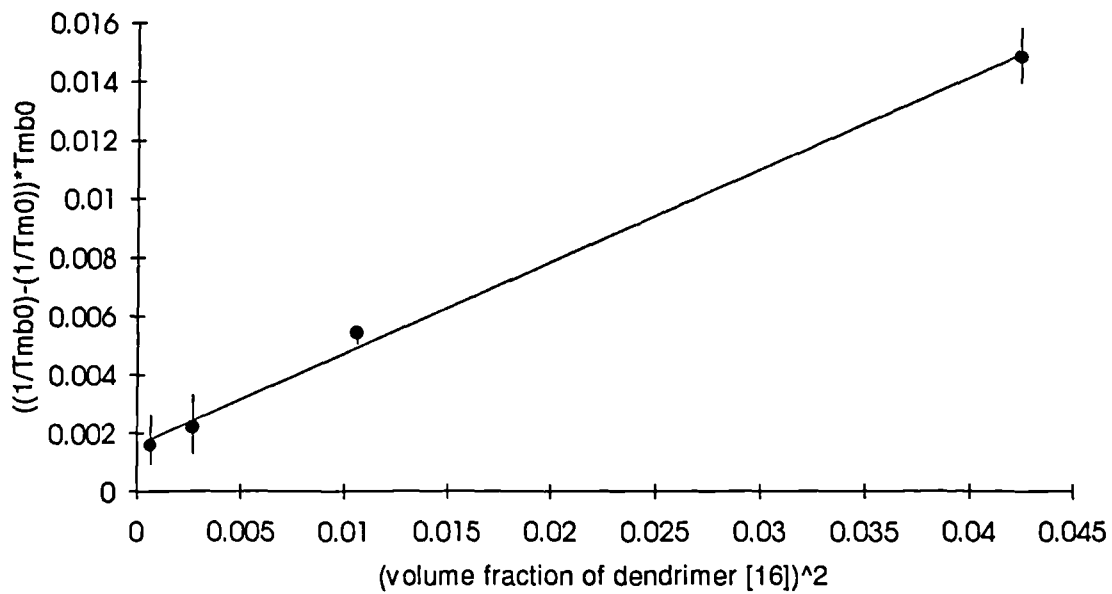**Figure 3.5**   Simple Nishi-Wang Plot for Dendrimer [7] / PET Blends.

Figure 3.6 Simple Nishi-Wang Plot for Dendrimer [16] / PET Blends.

Figures 3.5 and 3.6 show the melting point depression data for dendrimer [7]/PET and dendrimer [16]/PET blends respectively plotted according to equation 3.3. The free energy density B and the interaction parameter at the melting point χ have been calculated from a least squares fit of the data in each case and summarised below (Table 3.3).

	B /Jcm^{-3}	χ
Dendrimer [7]/PET	-6.20	-0.14
Dendrimer [16]/PET	-6.67	-0.15

Table 3.3 Free energy density B and interaction parameter values for the dendrimer/PET blends.

In each case, the negative sign of χ indicates that the system forms a miscible and thermodynamically stable blend near the melting point and demonstrates that the melting point depression can be accounted for in terms of the thermodynamic theory of mixing. The magnitude of χ is quite reasonable in comparison with data from other miscible polymer mixtures. Poly(vinylidene fluoride) - poly(methyl methacrylate)[5] and poly(ethylene oxide)-poly(methyl methacrylate)[14] blends have interaction parameters of -0.30 and -0.16 respectively as measured by melting point depression analysis.

The finite positive intercepts in Figures 3.5 and 3.6 are an indication that entropic contributions to the melting point depression have been neglected in the simplified Nishi-Wang expression, equation 3.3. Although it is possible to use a more elaborate expression for interaction parameter evaluation incorporating entropic terms, it is questionable as to whether such a treatment would provide a significant benefit in dealing with blends incorporating multibranched structures with novel topologies.

It is also noted that in comparison with Figure 3.6, Figure 3.5 has a substantially greater deviation from linearity. Although no full explanation of this observation is attempted, it is suggested that the appreciable crystallinity of pure dendrimer [7] may in some way influence the interaction between the blend components and has not been fully dealt with in this simplified treatment however no

evidence of crystalline dendrimer [7] has been found within the blends by wide-angle X-ray diffraction analysis.

Transesterification

During the course of melt blending mixtures incorporating polyester components, it is known that the blending process can result in appreciable ester interchange such that the amorphous region may be in part copolymeric thus giving a misleading indication of the blend miscibility.[1] If the dendrimer / polyester blends were to undergo significant transesterification during formulation or subsequent processing, the ester exchange would lead to the formation of an extensively cross-linked network.

In order to investigate the possibility of blend transesterification, attempts were made to extract unchanged dendrimer from the blended materials as prepared earlier, after heating the blends at 150°C under vacuum for 24 hours and from free-standing films cast from dichloroacetic acid solution and remelted at 280°C (see Chapter 4). For both dendrimer [7] and [16]/PET blends, a known mass of sample was extracted using a Soxhlet apparatus and chloroform as a solvent for 48 hours after which the solvent was evaporated and the residue dried under reduced pressure before weighing and analysis by n.m.r. In all cases, the mass of the residue was slightly in excess of that calculated for the dendrimer content of the initial sample. N.m.r. analysis in deuterated chloroform indicated that in all cases, the residues comprised of two components. The greater part of the residue as determined by peak integration was identified as unchanged dendrimer by reference to the spectra of the pure dendrimers. The additional component gave rise to two ^{1}H n.m.r. peaks at $\delta 8.1$ and $\delta 4.7$ of approximately equal intensity. These have been attributed to aromatic and methylene proton resonances respectively from chloroform-soluble PET oligomers which would account for the greater than expected residue masses. Such peaks have also been found on extraction of the pure PET reference material.

The blend extraction study described above indicates that unaltered dendrimer components can be extracted from blends and provides no evidence of blend transesterification during the formulation process, on heating at 150°C for 24 hours or during the preparation of dendrimer / PET films.

Conclusion

Thermal characterisation of the dendrimer / PET blends has enabled the interaction parameter, χ, to be determined in each case. The results show that both dendrimer [7] and dendrimer [16] can be blended with PET in proportions up to and including 20% by weight to form miscible and thermodynamically stable blends. Essentially quantitative dendrimer extraction from blended material indicates that no appreciable transesterification takes place during the preparation or subsequent processing of the blends to form thin films.

References

1. Goodman I. in "Encyclopedia of Polymer Science and Engineering V12" (2nd edn.), Mark, H.F., Bikales, N.M., Overberger, C.G. and Menges, G. (Eds.), Wiley Interscience (1988)

2. Sperling, L.H., "Introduction to Physical Polymer Science" (2nd edn.), Wiley Interscience (1992)

3. Olabisi, O., Robeson, L.M. and Shaw, M.T., "Polymer-Polymer Miscibility", Academic Press (1979)

4. Paul, D.R. in "Polymer Blends V1", Paul, D.R., Newman, S. (Eds.), Academic Press   (1978)

5. Nishi, T. and Wang, T.T., Macromolecules $\underline{8}$, 909 (1975)

6. Walsh, D.J. in "Comprehensive Polymer Science V2", Allen, G. and Bevington, J.C.   (Eds.), Pergamon (1989)

7. Barlow, J.W. in "Encyclopedia of Polymer Science and Engineering V12" (2nd edn.), Mark, H.F., Bikales, N.M., Overberger, C.G. and Menges, G. (Eds.), Wiley Interscience (1988)

8. Clough, N.E. and Richards, R.W., Polymer $\underline{35}$, 1044 (1994)

9. Scott, R.L., J.Chem.Phys. $\underline{17}$, 279 (1949)

10. Runt, J. and Gallagher, K.P., Polymer Communications $\underline{32}$, 180 (1991)

11. Lawton, E.L. and Ringwald, E.L. in "Polymer Handbook" (3rd edn.), Brandrup, J., and Immergut, E.H. (Eds.), Wiley Interscience (1975)

12. Cruz, C.A., Barlow, J.W. and Paul, D.R., Macromolecules $\underline{12}$, 726 (1979)

13. Mehta, S., Gaur, U. and Wunderlich, B., J.Polym.Sci.,Polym.Chem.Ed. $\underline{16}$, 289 (1978)

14. Liberman, S.A., Gomes, A.deS. and Macchi, E.M., J.Polym.Sci.,Polym.Chem.Ed. $\underline{22}$, 2809 (1984)

Supplement 3.1 Density Measurement of Blend Components

Density measurements were made using a graduated aqueous zinc chloride density column at 23°C. Calibration of the column was carried out using beads of known density. A graph of bead height within the column as a function of relative density yielded a straight line, indicating a uniform density gradient.

Density gradient columns are surprisingly stable provided that disturbances producing convection currents are minimised. This particularly true if the column is well insulated and the density range is small since under such circumstances the diffusion rate is minimal and a linear concentration gradient may be maintained for up to 6 months.

All samples were suspended in methanol and the suspensions degassed under reduced pressure to remove air bubbles from the particle surfaces. On decanting the supernatant liquid, the samples were added to the top of the density column and left for several hours to settle to constant height. The relative density of each sample was determined with reference to the calibration graph shown below (Figure S3.1.1).
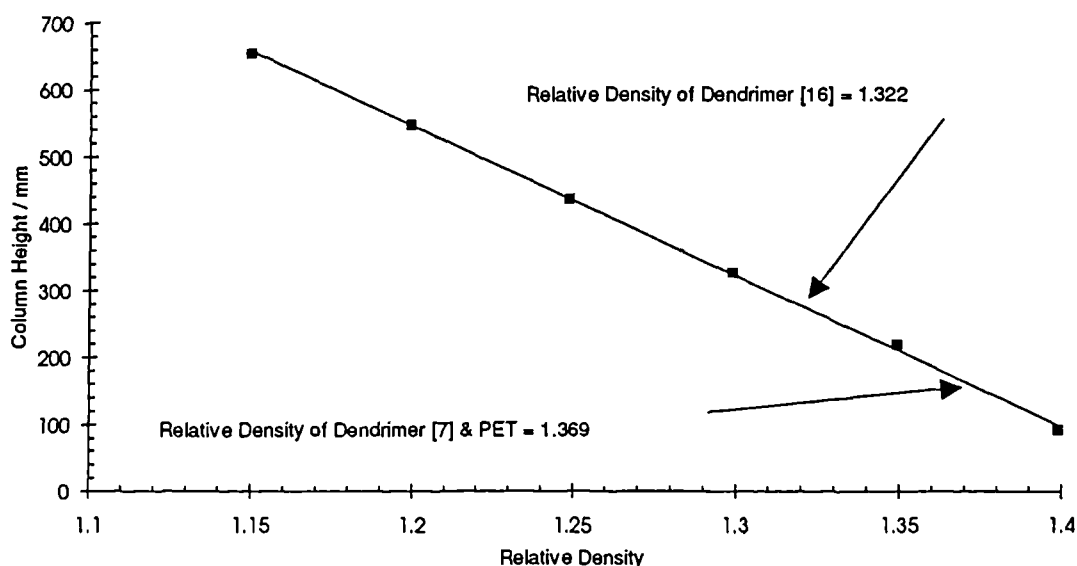
Figure S3.1.1 Calibration Graph for Density Column.

Supplement 3.2 Hoffman-Weeks Evaluation of Equilibrium Melting Point

The equilibrium melting temperature T_m° of a polymer may be defined as the melting temperature of an assembly of perfect crystals of sufficient size such that surface effects are negligible. In practice, polymers melt below T_m° because the crystals are small and imperfect. As a result, the crystallisation temperature T_c has a significant influence on the experimentally measured melting point T_m.[1]

In a series of experiments to determine the effect of T_c on T_m Hoffman and Weeks[2] developed the relationship

$$T_m^\circ - T_m = \phi \, (T_m^\circ - T_c)$$

where ϕ is a stability parameter dependent on crystal size and perfection. For a higher isothermal crystallisation temperature T_c, more perfect crystals are formed and so the experimental melting point T_m increases.

To determine the equilibrium melting temperature T_m° it is necessary to measure T_m as a function of T_c. The intersection of the line $T_m = T_c$ with the extrapolation of the experimental data gives the value of T_m°. Crystals formed at a T_c much lower than T_m° thicken during the thermal characterisation procedure leading to a higher experimental T_m than the true value. At higher T_c the effect of lamellar thickening is reduced and the experimental T_m is nearer the true value.[3] For this reason, isothermal crystallisation is carried out over a narrow temperature range below the measured melting temperatures.

As an illustration of the significant difference in T_m and T_m° for PET used in the formulation of the dendrimer / PET blends, PET reference samples were characterised by differential scanning calorimetry in order to determine T_m°. Each sample was heated from 25°C at a rate of 200°C min^{-1} to 280°C where it was held for five minutes. After cooling at the same rate to the isothermal crystallisation temperature T_c, where it was held for a further 60 minutes, a DSC thermogram was recorded at a heating rate of 10°C min^{-1} to 280°C.

T_c / °C	220	225	230	232.5	235	237.5	240
T_m / °C	247.27	246.25	253.11	254.45	254.96	256.19	257.15

Table S3.2.1 Experimental Melting Temperature as Measured by

DSC as a Function of Crystallisation Temperature.
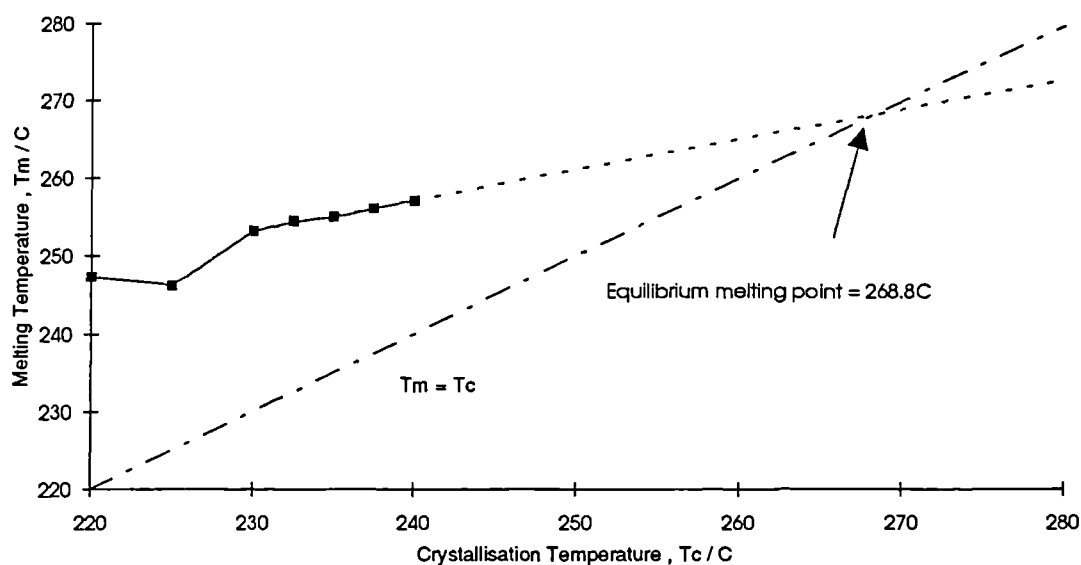
Figure S3.1.1 Hoffman-Weeks plot for PET.

The equilibrium melting temperature $T_{m°}$ for PET is calculated to be 268.8°C, somewhat higher than the experimentally measured value of 252.05°C in Chapter 3.

References

1.   Sperling, L.H., "Introduction to Physical Polymer Science" (2nd edn.), Wiley Interscience (1992)

2.   Hoffman, J.D. and Weeks, J.J., J. Res. Natl. Bur. Stand. 66A, 13 (1962)

3.   Runt, J. and Gallagher, K.P., Polymer Communications 32, 180 (1991)

CHAPTER 4

Dielectric and Mechanical Characterisation
of Dendrimer / PET Blends

Dielectric and Mechanical Characterisation of Dendrimer / PET Blends

Introduction

In the course of the author's work on dendrimer/PET blends, the dependence of the properties of the blends on dendrimer structure and blend composition have been investigated using dielectric and thermally stimulated current techniques followed by drawing experiments and measurement of mechanical properties.

Karasz and co-workers have recently prepared extended aryl ester dendrimers using a convergent scheme similar to that used in this work and the blending of such molecules with polycarbonate has been investigated with a view to determining the effect of dendrimer incorporation on the relaxation processes of the linear polymer.[1] Characterisation of the blends using dielectric thermal analysis techniques has shown that the dendrimers have an appreciable influence on both segmental chain motion and localised subambient relaxation behaviour.

With increasing dendrimer content, the polycarbonate glass transition is progressively reduced whilst the magnitude and width of the subambient transition are greatly enhanced. Both of these observations have been attributed to the increase in free volume of the system brought about by the branched nature of the dendrimer molecules. The T_g depression suggests that the dendrimers serve to plasticise the polycarbonate yet do not suppress localised relaxation processes. Relaxation suppression in some polycarbonate blends due to plasticiser addition leads to mechanical embrittlement and reduced impact resistance.

Dielectric Analysis[2,3]

If two conductors are enclosed within a vacuum and charged by application of a potential difference V across them, the conductors will carry equal and opposite charges +q and -q, q is related to V by the expression

$$q = CV \qquad \text{(eqn. 4.1)}$$

where C, the constant of proportionality, is the capacitance of the system. Capacitance is measured in Farads (F), after Faraday who laid the foundations in this field.

For a parallel plate capacitor, in which the two plates each have area A and are separated by a distance d,

$$C = \frac{\varepsilon_0 A}{d} \qquad \text{(eqn. 4.2)}$$

where ε_0 is the dielectric permittivity of free space, 8.85×10^{-12} Fm^{-1}. The electric field E between the plates is given by

$$E = \frac{V}{d} \qquad \text{(eqn. 4.3)}$$

If the vacuum separating the plates is replaced by an insulator, or dielectric material, the amount of charge stored on the plates for a given potential difference, i.e. the capacitance, is increased such that

$$C = \frac{\varepsilon \varepsilon_0 A}{d} \qquad \text{(eqn. 4.4)}$$

where ε is the relative permittivity, or dielectric constant of the material.

Material	Relative Permittivity
Vacuum	1.00000
Air	1.00054
Polyethylene	2.3
Polystyrene	2.6
Bakelite	4.8
Titanium Dioxide	100

Table 4.1 Relative permittivities for some dielectrics at room temperature for constant field strength E.[2]

In order to derive useful information relating to the structure and dynamics of dielectric materials, it is necessary to understand the effect of an applied electric field on such materials in terms of atomic and molecular motion.

The permittivity of a dielectric medium reflects the extent to which an applied electric field can polarise the localised charge distribution within the sample. For non-polar samples, there are two distinct means by which charge separation may occur, namely electronic and atomic polarisation. Electronic polarisation involves the distortion of an electron cloud with respect to the nucleus whereas atomic polarisation involves the displacement of an atomic nucleus relative to other nuclei.

In polar molecules, additional polarisation may be afforded by orientation of permanent electric dipoles with the applied field. Since all molecules are in a state of constant thermal agitation, complete alignment may never be achieved however the degree of alignment may be enhanced as the field strength is increased or the temperature is decreased.

(a)   (b)
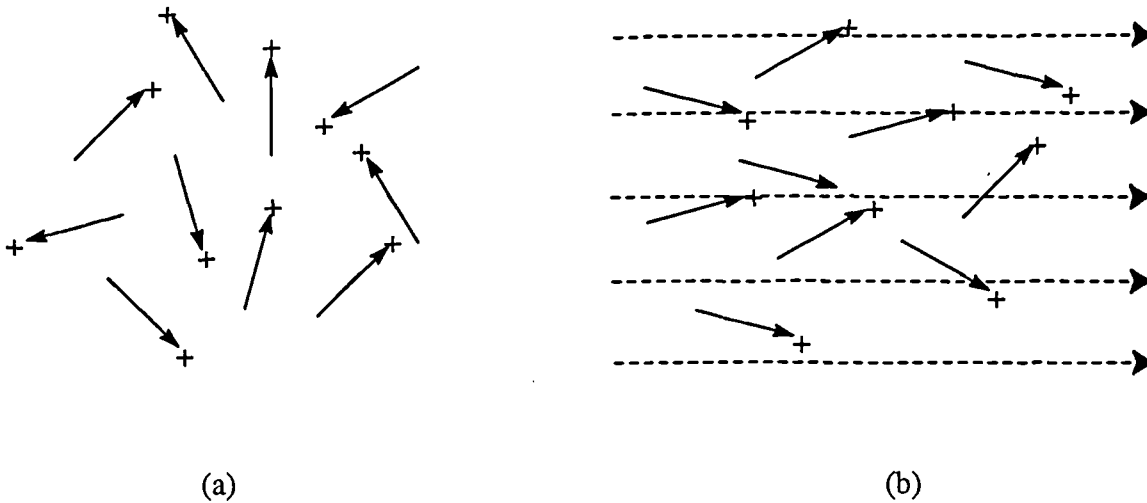
Figure 4.1 (a) Random orientation of molecules with a permanent electric dipole

moment in the absence of an external electric field.

(b) Partial alignment of permanent dipoles under the influence of an applied

electric field. Thermal agitation prevents complete alignment.[2]

Hence the total polarisability α_t is the sum of three components

$$\alpha_t = \alpha_e + \alpha_a + \alpha_o \qquad \text{(eqn. 4.5)}$$

where α_e, α_a and α_o are the electronic, atomic and orientational polarisabilities respectively.

The net effect of the polarisation of a dielectric material is the separation of the centres of positive and negative charge and the accumulation of charge on the dielectric faces. Although the material remains electrically neutral overall, there is a small displacement of electrons from their equilibrium position. No electrons are transferred over macroscopic distances.

In non-polar solids, the permittivity is virtually independent of temperature and changes only slightly on melting, indicating that dipole induction is largely unaffected by the substantial structural transition involved in the change of state. In most solids comprising of polar molecules, the permanent electric dipoles have no rotational

69

freedom and are unable to align themselves with an applied field. On freezing a polar liquid, the permittivity falls abruptly to a value typical for non-polar materials as molecular reorientation is restricted.

In solid polymeric materials containing polar groups, rotational freedom is often retained even at low temperatures and for the purposes of dielectric characterisation, such polymers can be considered to behave more like viscous liquids than conventional solids.

Provided that a polymer is sufficiently mobile, i.e. above the glass transition temperature T_g, polarisation may be induced by interaction with an electric field. By cooling the material to a sufficiently low temperature with the field still in place, it is possible to freeze the dipolar orientational order within the structure. Removal of the applied potential difference has little effect on polarisation since molecular motion has effectively ceased. The charge distribution remains dormant unless discharged by thermal relaxation.

On putting a short circuit across the plates of the capacitor, the dielectric relaxation may be monitored by observing the rate at which charge flows between the plates, that is, the discharge current, as a function of increasing temperature. The temperature at which a molecular relaxation process takes place is determined by the localised spatial constraints imposed by neighbouring molecules. This forms the basis of thermally stimulated current analysis (TSC), or thermally stimulated discharge current analysis (TSDC) as it is sometimes known, developed to investigate the structure and properties of dielectric materials under static electrical strain conditions. The sensitivity is such that it is possible to detect individual molecular relaxation processes and thus aids the development of a model for polymeric materials at a molecular level.[4]
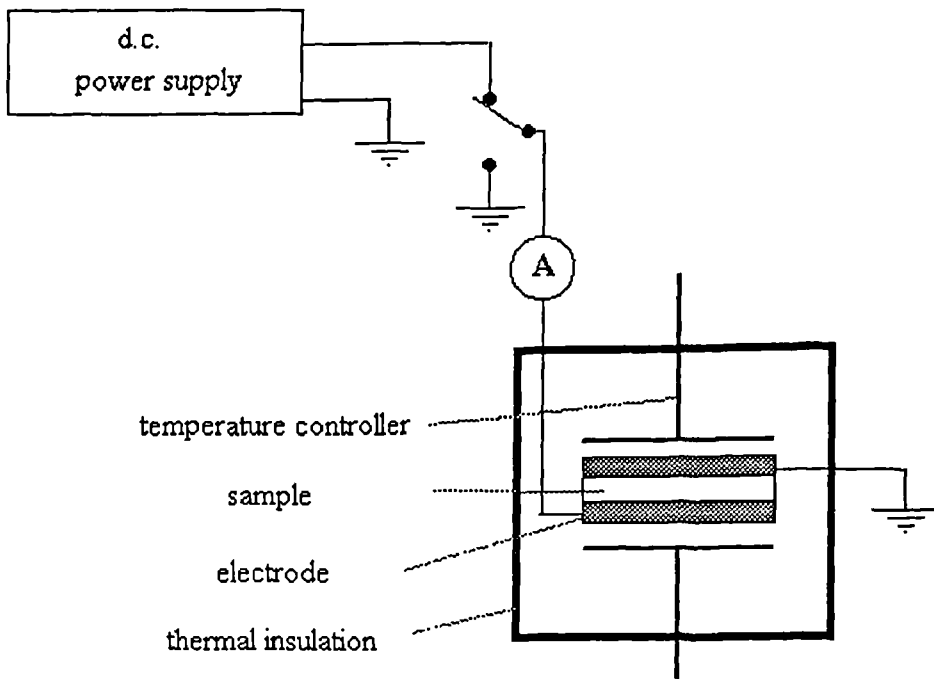
Figure 4.2 Schematic Arrangement of TSC Apparatus.[4]
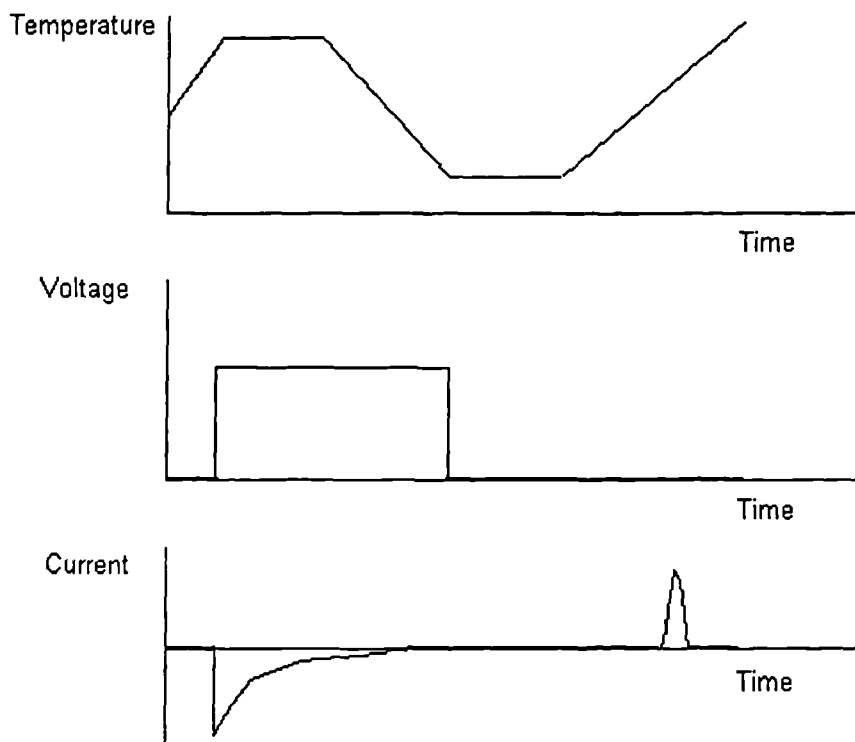
Figure 4.3 Schematic Temperature, Voltage and Current Profile

of a TSC Experiment.

When an electric field is applied across a polymer dielectric, it takes a finite time to induce polarisation in the material. Although atomic and electronic polarisation occur virtually instantaneously, orientation of permanent dipoles has a much greater response time and so there is a time lag between the application of the field and the maximum dipolar alignment. This may be seen as an effect of the drag imposed as the dipoles rotate through the viscous medium.

If an alternating potential difference is applied across the plates of the capacitor, dielectric polarisation constantly changes with the oscillating electric field. As the frequency of the alternating field increases, the permanent dipoles become less able to align fast enough, on account of their high orientational response time. The phase of the orientational polarisation lags behind the driving field and the maximum polarisability falls below that of the d.c. or low frequency value.

For practical purposes, α_a and α_e may be regarded as independent of frequency since atomic polarisation response times are of the order of 10^{-14}s and those for electronic polarisation are even lower.

Dielectric polarisation P may be regarded as comprising of two components, P_1 ($= \chi_1 E(t)$), a frequency-independent contribution from atomic and electronic polarisation and P_2, a frequency-dependent term from the orientational polarisation.

$$P = P_1 + P_2 \qquad \text{(eqn. 4.6)}$$

If at any time t, P_2 approaches the low frequency value $\chi_2 E(t)$ at a rate proportional to $(\chi_2 E - P_2)$, where χ_1 and χ_2 are constants and not to be confused with the interaction parameter symbol χ used in the previous chapter, the differential equation

$$\frac{dP_2}{dt} = \frac{1}{\tau}\left(\chi_2 E - P_2\right) \qquad \text{(eqn. 4.7)}$$

can be constructed, where τ is the dielectric relaxation time constant. Solution of the above equation in an alternating field yields

$$P = P_1 + P_2 = \left(\chi_1 + \frac{\chi_2}{1 + i\omega t}\right)E \qquad \text{(eqn. 4.8)}$$

where ω is the angular frequency of oscillation and i is the complex number $\sqrt{-1}$. This result corresponds to there being a complex permittivity ε^* that may be separated into real and imaginary components ε' and ε'' respectively such that

$$\varepsilon^* = \varepsilon' - i\varepsilon'' \qquad \text{(eqn. 4.9)}$$

where ε' represents the relative permittivity at a particular frequency and ε'' is the dielectric loss factor. The phase lag between the alternating field and the orientational polarisation leads to the dissipation of energy as heat. The rate of conversion of electrical energy to thermal energy is represented by ε''. The term $\varepsilon''/\varepsilon'$, otherwise known as tan δ or the dissipation factor, is the ratio of energy loss:energy storage within the system.
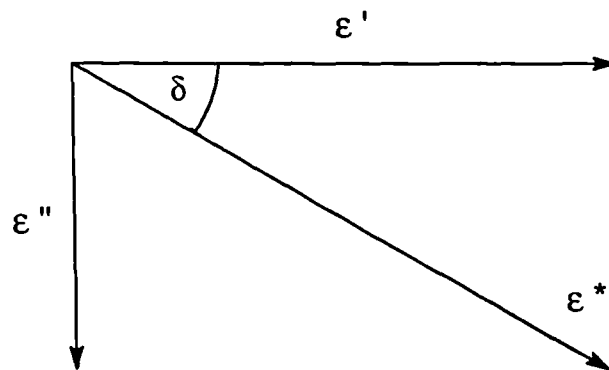
Figure 4.4 Argand diagram illustrating the relationship between ε', ε'' and ε^*.[5]
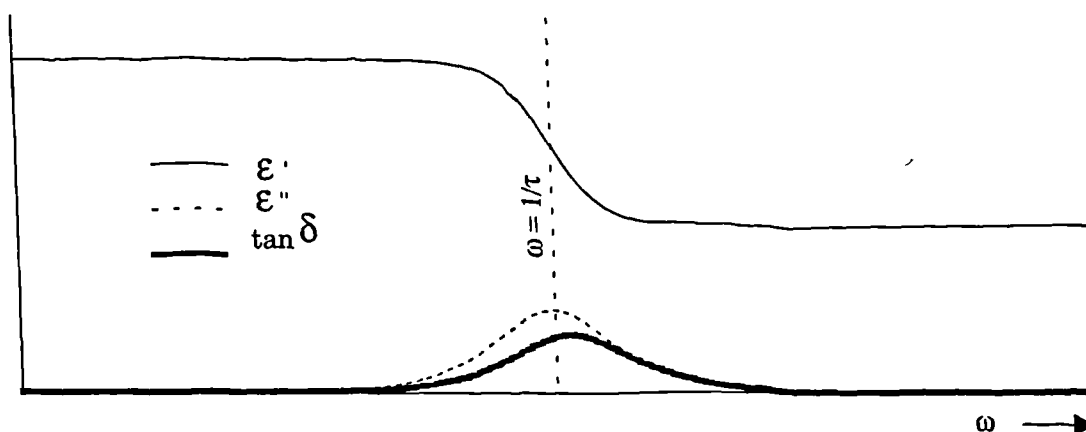
Figure 4.5 Schematic plot of real (ε') and imaginary (ε'') permittivity and the dielectric loss angle tan δ against frequency.[6]

At low frequency, dipole orientation can keep up with the oscillating field and little energy is lost (high ε' and low loss, ε'') (Figure 4.5). As the frequency increases, the phase lag between the oscillating field and the permanent dipole alignment increases. The phase lag and consequent energy loss reach a maximum at $\omega = 1/\tau$. At very high frequencies, the dipoles hardly move and again, little energy is lost (lower ε' and low loss, ε'').

Since dipolar relaxations within polymer dielectrics may take place over many orders of magnitude of frequency at a given temperature, it is often more convenient for dielectric properties to be measured at a fixed frequency over a wide temperature range. Low temperatures correspond to high frequencies and high temperatures to low frequencies. At low temperature, permanent dipoles are unable to move and do not contribute to the overall permittivity whereas at high temperature, the dipoles are able to oscillate with negligible loss.

The measurement of relative permittivity ε' and loss angle δ over a wide temperature range at a fixed frequency forms the basis of dielectric thermal analysis (DETA) which when used in conjunction with other characterisation techniques can yield useful information regarding polymer mobility and dynamics in the solid state.

Dielectric Analysis of PET

The highly polar nature of poly(ethylene terephthalate) (PET) makes investigation of the structural motion of this polymer relatively straightforward using dielectric characterisation techniques such as thermally stimulated current analysis (TSC) and dielectric thermal analysis (DETA). To assess the changes in dielectric relaxation behaviour of dendrimer [7] and dendrimer [16]/PET blends (see Chapter 3) with respect to pure PET, both TSC and DETA characterisation techniques have been used. Significant changes in relaxation behaviour are often indicative of appreciable modification of mechanical properties.

Sample Preparation for TSC and DETA

To a thin glass cover slip coated with an aluminium electrode of thickness 30nm was cast a solution of dendrimer/PET blend in dichloroacetic acid (10% w/w) to form a thin, even film of the blend over the electrode surface. The film was dried on a hotplate for 3 hours at 60°C followed by further drying in a vacuum oven at 140°C overnight. The opaque sample was melted on a hotplate at 280°C for 5 seconds before removing and cooling rapidly in a stream of compressed air to minimise crystallisation. A further aluminium electrode of thickness 30nm was evaporated on the polymer film and the film thickness measured using a micrometer gauge. Typical film thickness was in the range 10 - 15μm.

Experimental TSC Analysis

On rapidly heating the polymer film from room temperature to 80°C, slightly above the reported glass transition temperature of PET,[7] a d.c. voltage V (~ 40 - 60V) was applied across the film in order to induce dipolar alignment. The magnitude of the voltage was such as to generate the same electric field strength E across all the samples and thus was varied in direct proportion to the sample thickness (eqn. 4.3). After holding at 80°C for 5 minutes, the sample was cooled at 10°C min^{-1} to -80°C, the voltage removed and the charging loop short-circuited via a recording pico-ammeter to measure the depolarisation current. After holding at -80°C for 5 minutes to equilibrate, the sample was heated at 10°C min^{-1} to 90°C to observe the depolarisation current as a function of temperature. The variation in depolarisation current as a

function of temperature for pure PET and the dendrimer/PET blends are shown in Figures 4.6 and 4.7.

Experimental DETA

A 3V a.c. voltage of frequency 1kHz was applied across the polymer film to create an oscillating electric field which was kept in place throughout the experiment. On cooling to -80°C and at appropriate temperature increments thereafter up to 110°C, the capacitance, C, and the dielectric loss angle, tan δ, were measured using a three-terminal cell and a General Radio capacitance bridge. The variation of tan δ as a function of temperature for pure PET and the dendrimer/PET blends are shown in Figures 4.8 and 4.9.

Discussion and Interpretation of Dielectric Measurements

On inspection of Figures 4.6, 4.7, 4.8 and 4.9 it is clear that DETA and TSC analysis of the dendrimer/PET blends yield relaxation spectra of broadly similar appearance comprising of a sharp peak at elevated temperature and a broader subambient peak of much lower intensity. In dielectric spectroscopy, such peaks are conventionally termed the α and β relaxations respectively and arise as a consequence of dipolar reorientation phenomena.

In an early attempt to correlate α and β relaxations in PET to specific dipolar rearrangements, Reddish[8] ascribed the α process to cis - trans ester linkage rearrangement and the β process to the influence of terminal group rotation. Both of these assignments have subsequently been discounted by later workers in the field.[9,10] Illers and Breuer attributed the α peak to the onset of cooperative segmental chain motion in the amorphous phase, relating to the glass transition temperature, T_g, and resolved the β peak into 3 components each of which was thought to be due to highly constrained localised motion within the polymer chain.[10]

TSC Analysis of Dendrimer (7) / PET Blends

Current / pA

Legend:
— PET
---- 2.5% (7)/PET w/w
— 5% (7)/PET w/w
— 10% (7)/PET w/w
— 20% (7)/PET w/w

Temperature /C
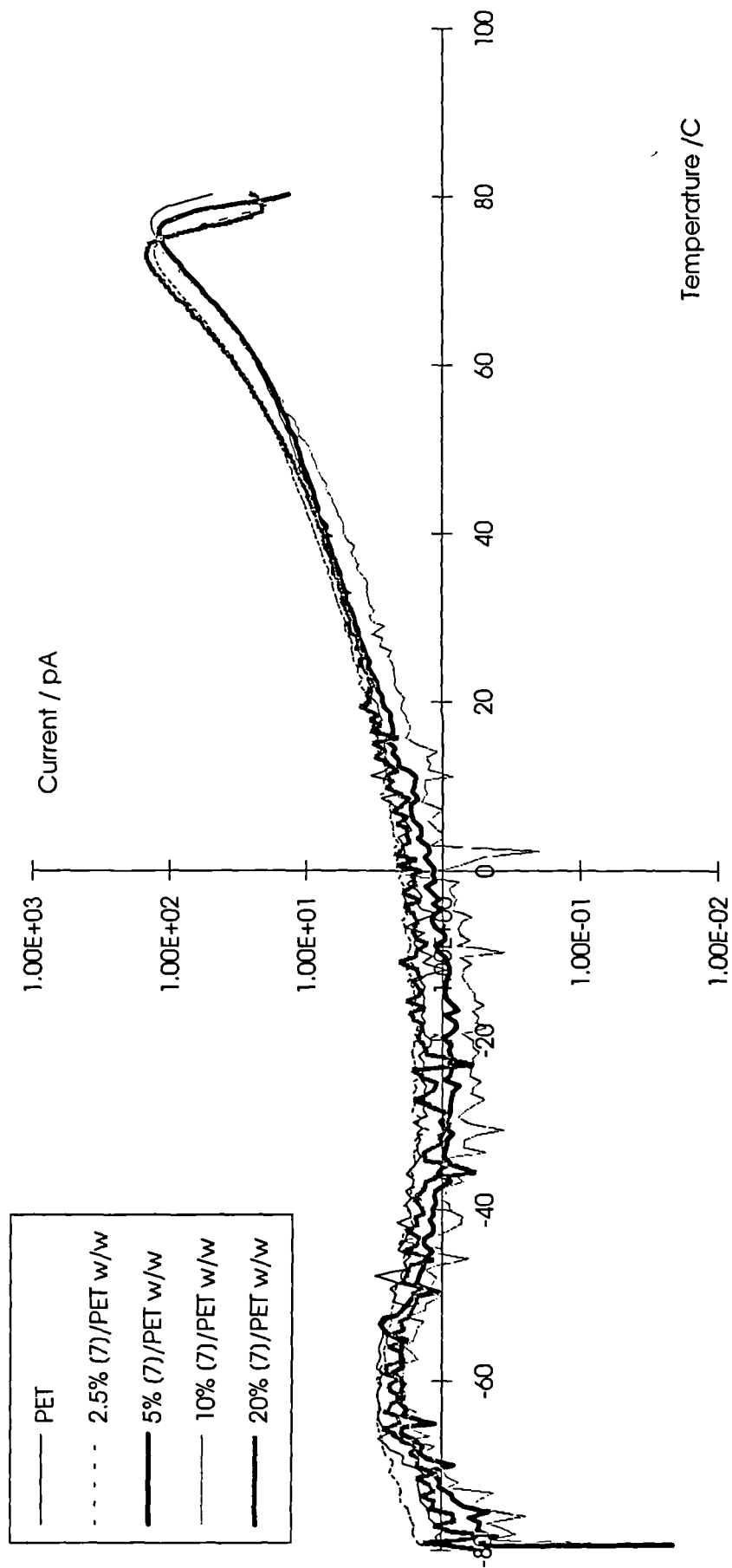
Figure 4.6

TSC Analysis of Dendrimer (16) / PET Blends

Current / pA

1.00E+03

1.00E+02

1.00E+01

1.00E+00

1.00E-01

Temperature /C

Legend:
— PET
---- 2.5% (16) / PET w/w
— 5% (16) / PET w/w
---- 10% (16) / PET w/w
— 20% (16) / PET w/w

Figure 4.7

78
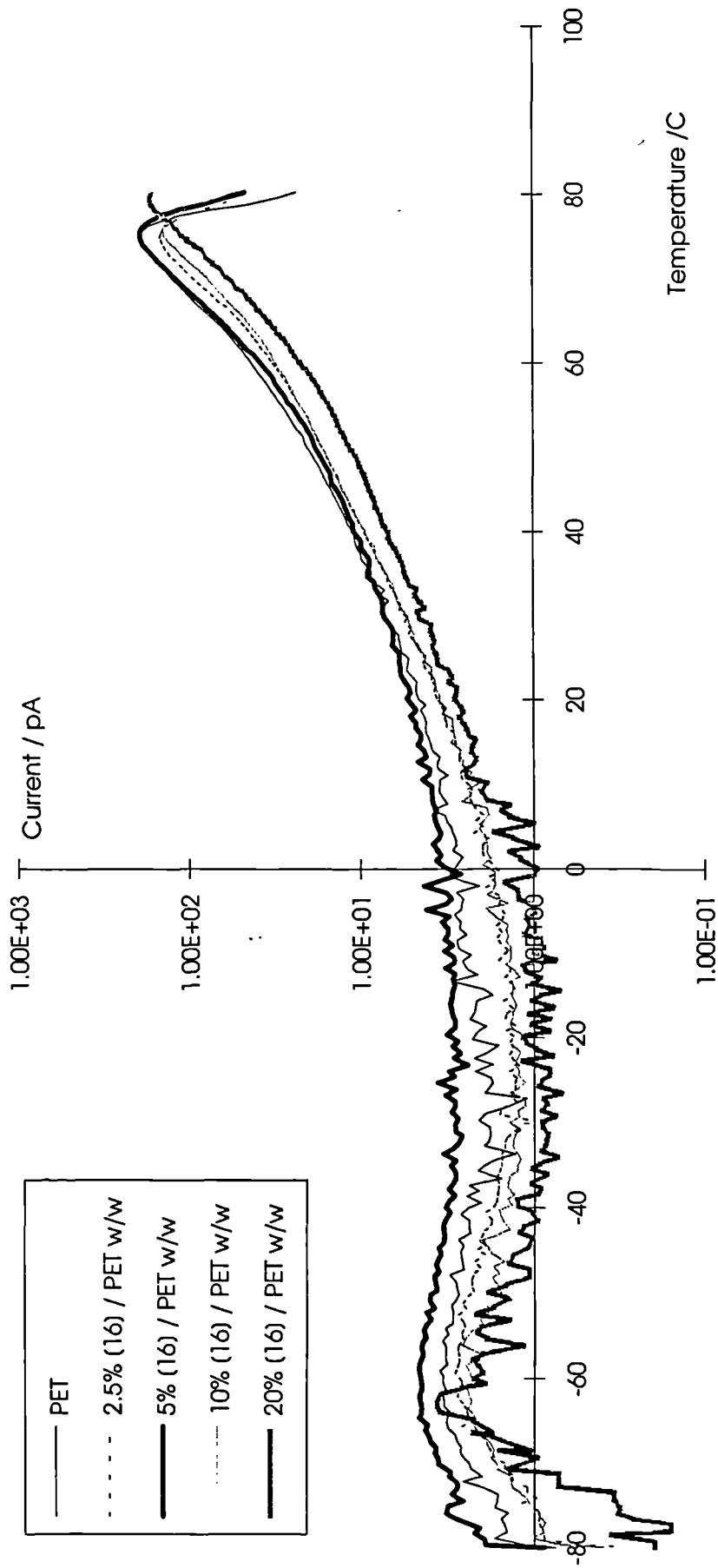
Dielectric Analysis of Dendrimer (7) / PET Blends
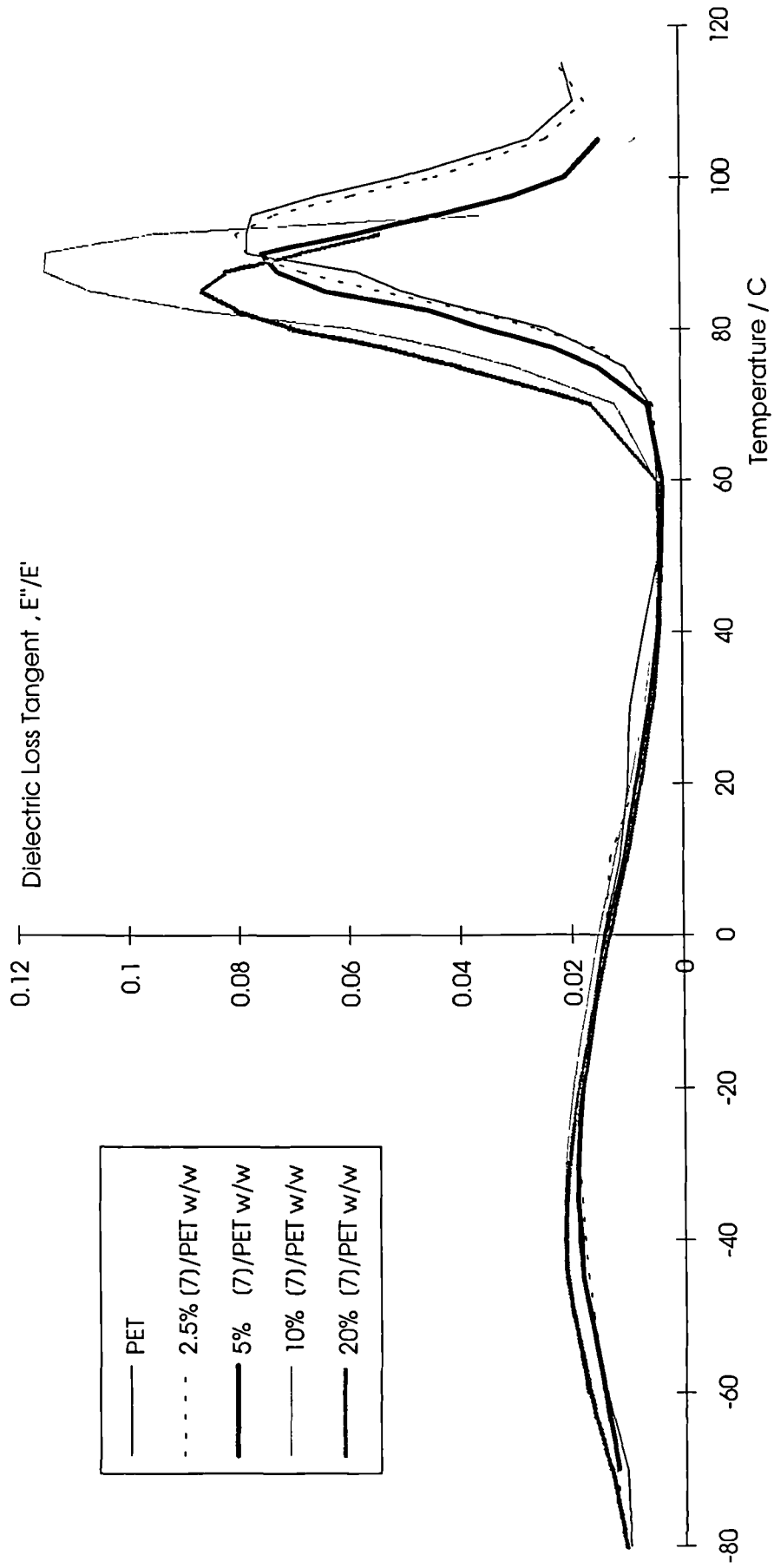
Figure 4.8

Dielectric Analysis of Dendrimer (16) / PET Blends

Dielectric Loss Tangent , E''/E'

Figure 4.9

Legend:
- PET
- 2.5% (16) / PET w/w
- 5% (16) / PET w/w
- 10% (16) / PET w/w
- 20% (16) / PET w/w
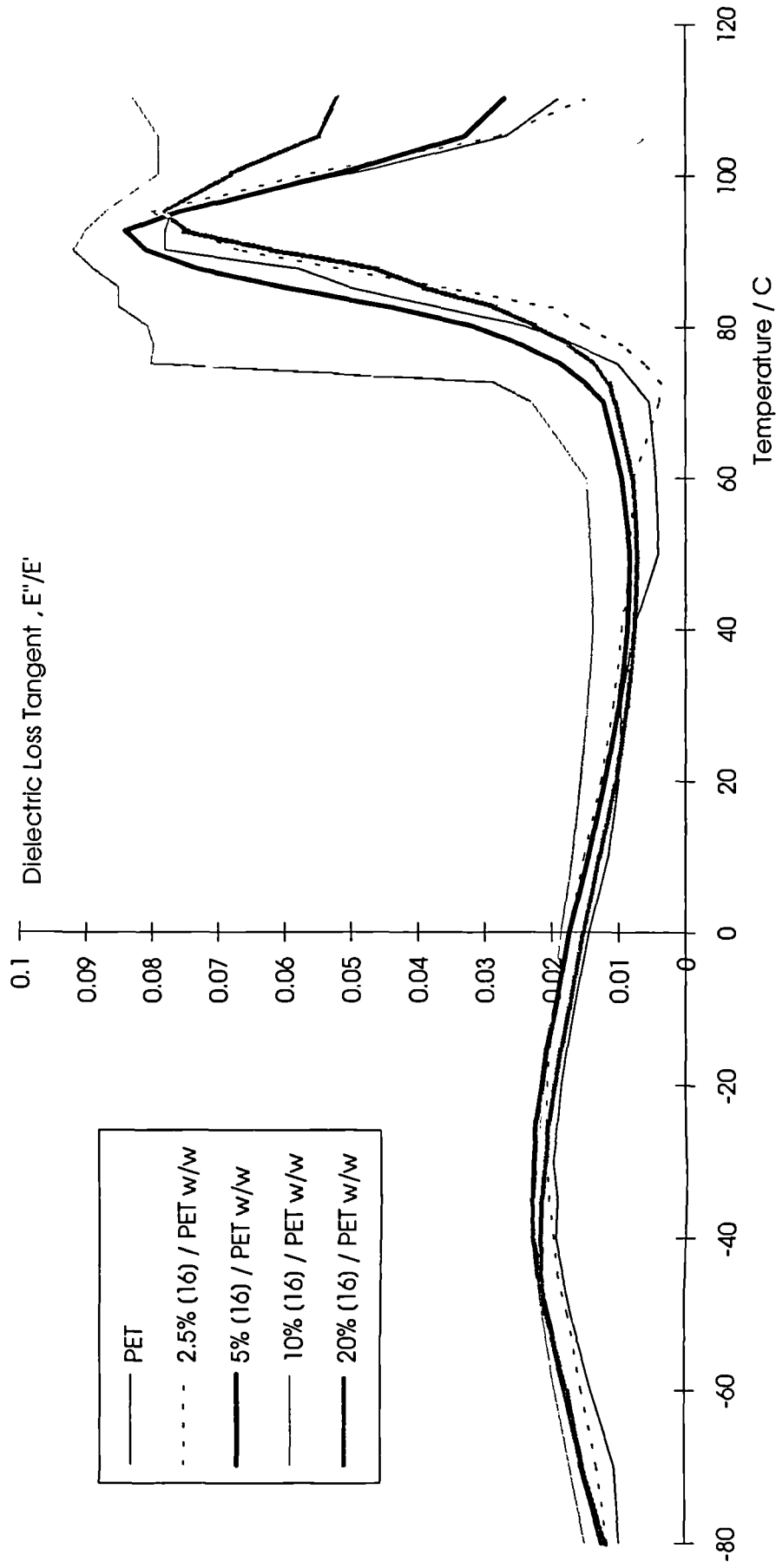
Temperature / C

It is noted that tan δ peaks in the 1kHz DETA spectra occur at higher temperatures than the corresponding peaks in the TSC analysis. Although such peaks arise as the consequence of the same underlying molecular motion of the polymer chain, the phenomenon is well known and arises since dipole relaxation is dependent on the applied experimental frequency.[5] Since in the dielectric analysis of the blended materials it is the relative change in blend properties as a function of composition that is of prime importance, this complication need not be considered further as the general trends in both DETA and TSC analysis are more significant.

On examination of the TSC analysis of dendrimer [7] and [16]/PET blends (Figures 4.6 and 4.7), increasing dendrimer incorporation appears to have little influence on peak intensity indicating little or no suppression of molecular relaxation processes. It is thought that the very small differences in β peak intensity are attributable to errors associated with film thickness measurement, resulting in small differences in the applied poling field.

Although all the peak positions determined by dielectric spectroscopy are subject to an error of around ±1°C, TSC analysis shows that the dendrimer [7]/PET blends show a slight depression of the α peak position with increased dendrimer incorporation whereas in the case of the [16]/PET blend series increasing the proportion of dendrimer within the blend appears to have the opposite effect.

A similar pattern is noted in the DETA spectra. Again dendrimer [7] blends tend to depress the α peak position with increasing dendrimer incorporation but in the case of dendrimer [16] blends the situation is less well defined (Figures 4.8 and 4.9).

The lowering of the α peak temperature, as observed for dendrimer [7] blends, is equivalent to a reduction in the glass transition temperature (T_g). Such behaviour is commonly associated with the effect of plasticisers, typically small molecules that separate the polymeric chains from one another and increase the free volume of the system, disrupting inter-chain interaction and making reptation easier. This aids chain slippage which at a macroscopic level leads to increased flexibility and mechanical toughness at the expense of lowering the mechanical strength.

Conversely, an increase in the α transition temperature is associated with enhanced intermolecular interaction such as an increase in cross-link density or sample

crystallinity however in the case of the latter, this is accompanied by a corresponding decrease in peak intensity.[11]

On the basis of the experimental data, dendrimer [7] appears to behave as a plasticiser in lowering the glass transition temperature whereas dendrimer [16] shows some evidence of antiplasticiser behaviour. In order to investigate this surprising observation bearing in mind the similarity of the dendrimer structures, a study of the deformation behaviour has been undertaken using mechanical testing techniques and is detailed in the following section.

Introduction to Mechanical Testing

Mechanical testing of polymeric materials enables the deformation induced by applied forces to be quantified and evaluated with respect to existing materials. This is an invaluable technique both in the development of new materials and for modification and improvement of existing ones.

In order to do this, it is necessary to define a number of terms to describe the behaviour of the materials under test:-

Tensile Stress :-	tensile force per unit area
Strain :-	change in length per unit original length
Initial Modulus:-	ratio of the tensile stress to the corresponding strain below the deviation from proportionality (a measure of stiffness)
Yield Stress :-	tensile stress at which the first inflection of the stress/strain curve occurs, where an increase in strain occurs without further increase in stress
Draw Ratio :-	ratio of drawn (oriented) sample length : original sample length
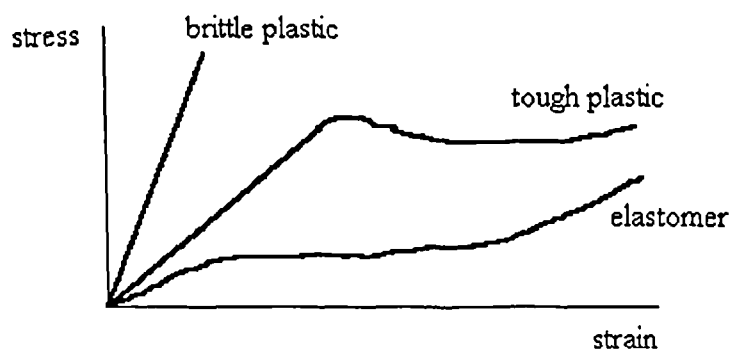
Figure 4.10 Stress-Strain Characteristics of Different Classes of Polymers.[11]

A number of common types of mechanical behaviour are illustrated in Figure 4.10. In the case of a brittle plastic, the stress-strain curve is linear with a steep gradient and thus high modulus, indicating the stiffness of the material. The strain at which mechanical failure occurs is small. In tough plastics, the initial modulus is lower than that of brittle plastics. Typically they exhibit a yield point at which further elongation occurs at constant stress. Elastomers, having a non-linear stress-strain curve and low modulus are capable of extending reversibly to large strain before mechanical failure occurs.

Oriented Polymers

In conventional linear polymer molecules, the intramolecular covalent bonding along the chain direction is much stronger than the intermolecular Van der Waals and hydrogen-bonded interactions acting between polymer chains which are in general perpendicular to the chain direction. This large difference in intra- and intermolecular forces gives rise to appreciable mechanical anisotropy at the molecular level however molecular anisotropy does not necessarily lead to anisotropy of bulk properties because of the random assembly of polymer chains in an unoriented sample.[12] Bulk anisotropy is induced into a sample by producing a preferred direction of molecular orientation. This may be achieved in a number of ways:-

The manufacture of conventional oriented polymer fibres is by use of a melt spinning process in which polymer is extruded through a spinneret and the resultant filament yarn collected on a rotating wind-up drum. The speed of the drum, the so-called "wind-up" rate, can be controlled so as to pull out or draw the fibre to the desired degree of orientation. Polymer films may be similarly oriented by drawing at temperatures above T_g either in a continuous or batch process.

In the case of a transparent oriented film, the degree of bulk orientation within the drawn sample is readily found by measuring the birefringence of the material. A pre-drawn or oriented material has a greater tensile modulus in the direction of alignment than a comparable unoriented sample on account of the greater number of polymer chains per unit cross-sectional area.

84

Sample Preparation for Tensile Testing

Solutions of dendrimer / PET blends in dichloroacetic acid (10% w/w) were cast onto glass slides to form thin, even films. Following the same drying procedure as for TSC and DETA samples, the samples were melted on a hotplate at 300°C for 15 seconds before removing and cooling rapidly in a stream of compressed air to minimise crystallisation. The films were removed from the glass substrate by soaking in water for 24 hours followed by prising them from the glass with a sharp blade.

Undrawn samples, typically 50mm × 2mm and 40μm thick, were cut from the amorphous films and drawn at 80°C in an Instron environmental chamber at a draw speed of 50mm min^{-1} to predetermined draw ratios of between 3 and 6. In all cases, the draw ratio was determined from the displacement of ink spots on the drawn film from their initial spacing of 2mm on the unoriented material. Thickness measurements of the oriented samples, typically 10-15μm, were derived from sample mass, length and width measurements, assuming a typical sample density of 1.35g cm^{-3}.[7] This was found to be a more reproducible procedure than direct measurement using a micrometer gauge and facilitated thickness measurement to ±1μm. Birefringence measurements were made using a Zeiss 'Polmi A' polarising microscope with an Ehringhaus tilting plate compensator attachment.

Note:- Due to the brittle nature of the 20% w/w dendrimer / PET blends, no mechanical properties have been determined for these materials since it has not been possible to remove them from the glass substrate in sufficiently large pieces.

Tensile Testing Apparatus[13]
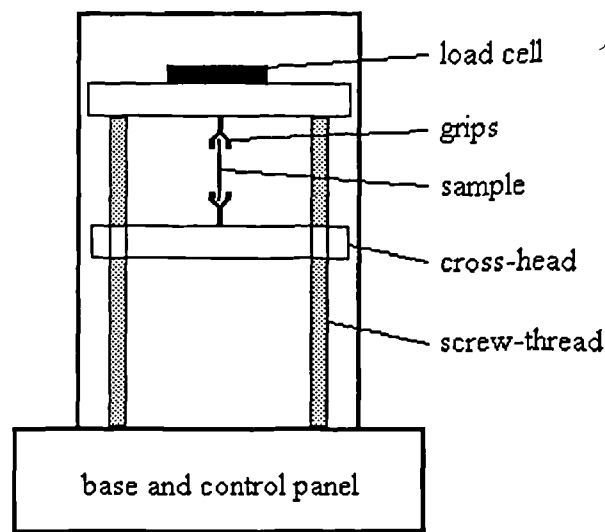
Figure 4.11 Schematic Diagram of Instron Tensile Testing Apparatus.

On securing the specimen firmly between a pair of grips to prevent slippage and ensuring that the sample is not bent or twisted in any way so as to restrict alignment in the direction of strain, the travelling cross-head height is adjusted such that the sample becomes taut. The separation between the pair of grips, equal to the initial length of the sample under test, is known as the gauge length. By selecting an appropriate cross-head speed, the extension of the sample may be carried out at a constant, pre-determined rate.

Such a procedure may be used for both orientation of samples, in which case the sample is drawn to a pre-determined draw ratio in an environmental chamber at a temperature above T_g then cooled rapidly to room temperature whilst still under strain, or alternatively to measure the tensile modulus of a test specimen when tested to destruction. In the case of the latter, the load cell is used to measure the tensile force applied to the specimen.

Results and Interpretation of Tensile Testing

Figure 4.12 shows the initial modulus of drawn samples as a function of birefringence, a measure of overall molecular orientation, for both dendrimer/PET blends and for pure PET control samples prepared in the same way. The solid line indicates the values obtained for PET film formed by melt extrusion followed by drawing at 80°C.[14] It is clear from Figure 4.12 that the incorporation of the dendrimers does not produce a significant change in the well-known correlation between modulus and overall molecular orientation.[14] The close correlation of the PET values with those previously determined, particularly at lower birefringence, indicates that the film casting procedure from dichloroacetic acid is a valid preparative method giving results comparable with those from other techniques. Until this point there had been some doubt as to the effectiveness with which the solvent could be removed from the films, which appears on the strength of this evidence to have been unfounded.

It is suggested that the deviation from the solid line at higher orientation may be due to the difficulty in obtaining uniformly drawn samples, a particular problem at higher draw ratio where the effects of yielding tend to produce variation in cross-section dimensions and anisotropy thus distorting the experimental result.

With some exceptions, notably the 2.5% dendrimer [7]/PET blends, Figure 4.13 shows that incorporation of dendrimer [16] within a blend produces a material of higher modulus than incorporation of dendrimer [7] for a given draw ratio. The graph is subject to considerable scatter due to the experimental difficulties encountered as a consequence of dealing with small, fragile specimens such as uneven drawing and sample slippage in the Instron clamps. Taken alone, such data cannot be used to provide firm evidence of different effects from the different dendrimer additives on the mechanical properties of PET but it was sufficient to initiate a more thorough investigation of the situation employing a more sensitive approach.

Tensile Testing of Dendrimer / PET Drawn Films (Initial Modulus vs. Birefringence)
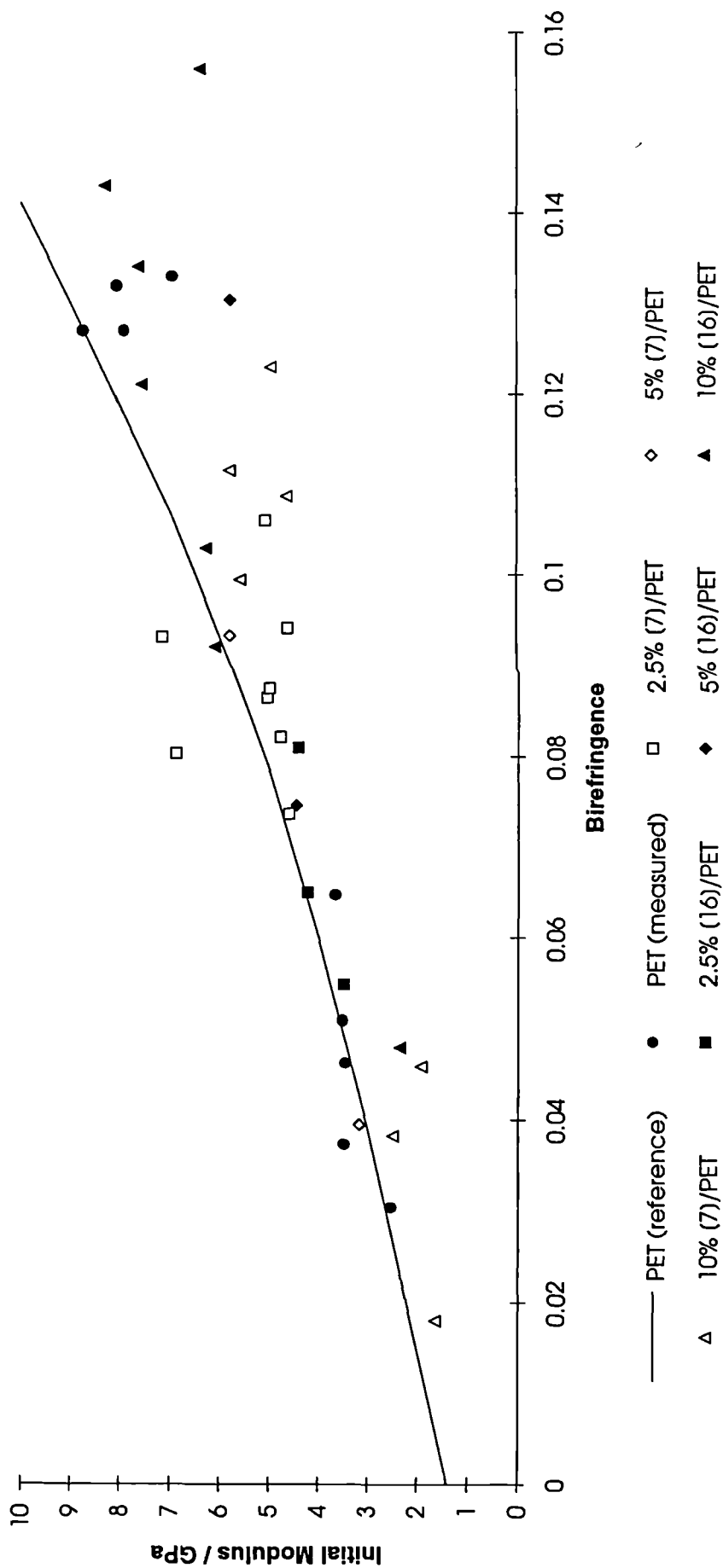
Figure 4.12

Tensile Testing of Dendrimer / PET Drawn Films (Initial Modulus vs. Draw Ratio)

Legend:
- □ 2.5% (7)/PET
- ◇ 5% (7)/PET
- △ 10% (7)/PET
- ■ 2.5% (16)/PET
- ◆ 5% (16)/PET
- ▲ 10% (16)/PET
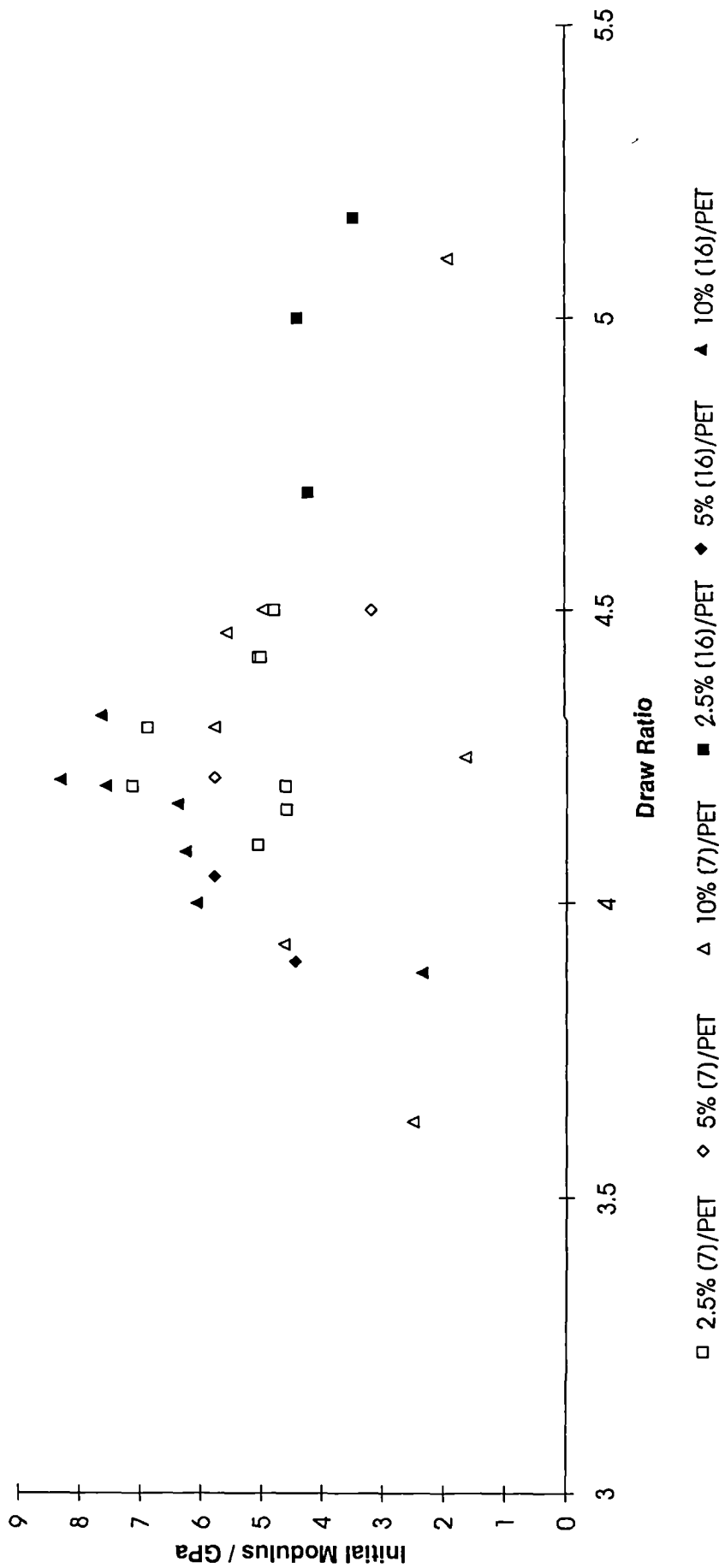
Figure 4.13

Rubber Elasticity Theory[15-17]

In the simple model of rubber elasticity used in this work, any polymer network may be regarded as a series of chain segments that are attached to one another by cross-links or entanglement points. Each chain segment can be considered to comprise of a number of freely-jointed rigid rods. These random rigid rod links correspond to a number of repeat units.
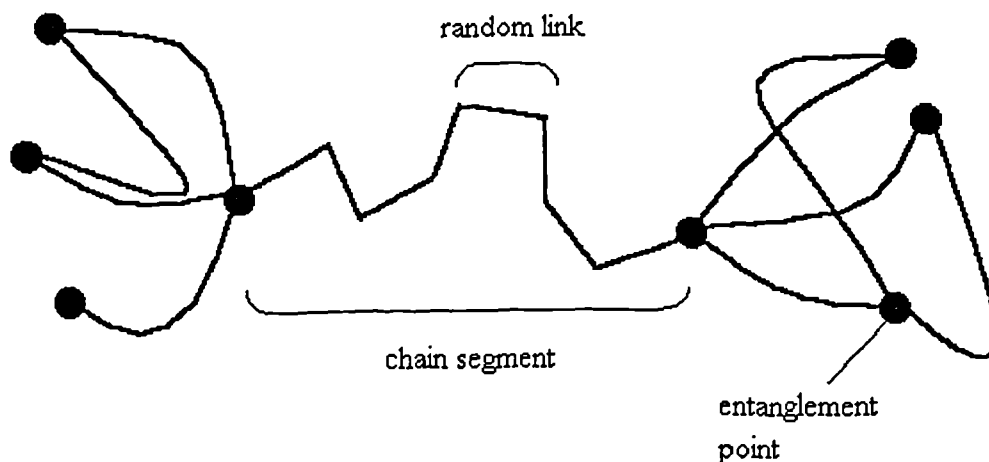
Figure 4.14 Simple Model of a Cross-Linked Network.

Entanglement points are not necessarily conventional covalent cross-links. Even in linear polymers, physical cross-links may arise as a consequence of trapped chains, loops and knots.

As has already been shown in the previous section, molecular orientation and thus stress may be frozen into samples during the drawing process if they are cooled below the glass transition temperature with the stress still in place. This may be recovered as a shrinkage stress on reheating above T_g whilst holding at constant strain.

According to the molecular theory of rubber elasticity, the tensile stress on the strained cross-section, σ, is given by

$$\sigma = NkT(\lambda^2 - 1/\lambda) \qquad \text{(eqn. 4.10)}$$

where N is the number of chain segments per unit volume, k is the Boltzmann constant, T is the drawing temperature and λ is the draw ratio.

The optical anisotropy, Δn, is given by

$$\Delta n = \frac{2\pi (\bar{n}^2 + 2)^2}{45\bar{n}} N(\alpha_1 - \alpha_2)(\lambda^2 - 1/\lambda) \quad \text{(eqn. 4.11)}$$

where $\bar{n}$ is the mean refractive index and $(\alpha_1 - \alpha_2)$ is the optical anisotropy of the random link.

Hence the stress-optical coefficient, $\Delta n/\sigma$ is given by

$$\frac{\Delta n}{\sigma} = \frac{2\pi(\bar{n}^2 + 2)^2}{45\bar{n}kT}(\alpha_1 - \alpha_2) \quad \text{(eqn. 4.12)}$$

If the rubber elasticity theory applies and uniaxially oriented film can be considered as a strained network, heating an optically anisotropic film above the T_g should release frozen-in strain that is proportional to the initial optical anisotropy, Δn.

Sample Preparation for Shrinkage Force Measurements

Films with draw ratios ranging between 1.6 and 5 were prepared using solvent casting and Instron drawing techniques under the same conditions as those used for tensile testing samples. Only pure PET and 10% dendrimer / PET w/w blends were used in the course of this study since changes in material properties due to dendrimer incorporation would be highlighted most readily in this way.

Shrinkage Force Measurement

to chart recorder

strain gauge

sample

silicone oil bath
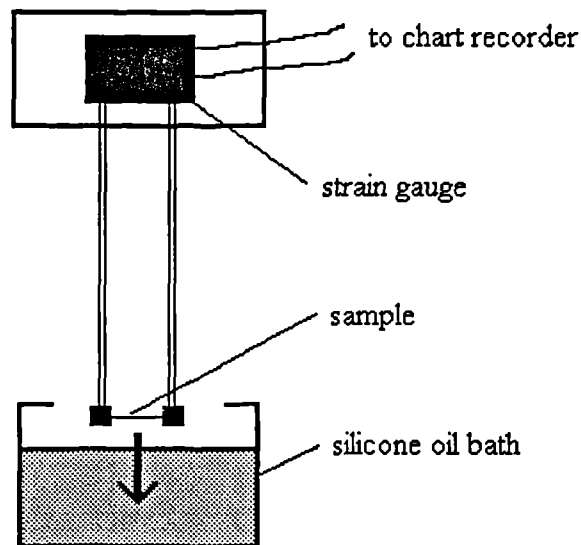
Figure 4.15 Schematic Diagram of Shrinkage Force Apparatus.[16]

On securing the sample loosely between the two clamps, the clamp separation is increased such that the film becomes taut and the gauge signal just starts to increase. The sample is then rapidly immersed in silicone oil at 90°C and the peak shrinkage force recorded on the chart recorder, from which the shrinkage stress may be calculated.

Results of Shrinkage Force Experiments

Figure 4.16 shows the birefringence of all the samples plotted as a function of draw ratio. Although for each sample type, birefringence is shown to be linearly dependent on $(\lambda^2 - 1/\lambda)$ as suggested by eqn. 4.11, there are clear differences between PET and the different dendrimer blends. Although these differences may at least in part be ascribed to the change in the effective draw temperature relative to the T_g of the blends, Padibjo and Ward[14] have indicated that this effect can only account for around 20% of the observed change in overall molecular orientation.

Shrinkage stress data shown as a function of birefringence (Figure 4.17) reveals a more complicated situation. These results suggest that PET and the blends behave in a similar way to one another and support the view expressed as a conclusion of the tensile testing work that dendrimer incorporation has little effect on modulus for a given degree of molecular orientation. The results are similar to published data[17] for PET (solid line) except that the plateau region in the range $0.02 < \Delta n < 0.06$ is less pronounced. The stress-optical coefficient, $\Delta n/\sigma$, is a constant only for $\Delta n < 0.02$. This indicates that the simple theory of rubber elasticity is only valid within this region.

Figure 4.18 shows shrinkage stress as a function of draw ratio for all the samples and illustrates differences between pure PET and the dendrimer blends in a similar way to Figure 4.16. The measured PET results lie close to literature values[17] indicating that the presence of any residual solvent does not affect the outcome significantly. Dendrimer [7] blends exhibit lower shrinkage stress for a given draw ratio than PET whereas for dendrimer [16] blends the opposite is true. Figure 4.19 is an expansion of the [7] and [16] blend plots in Figure 4.18 for low shrinkage stress and emphasises the difference between the two materials.

Mechanical Testing of Dendrimer / PET Drawn Films (Birefringence vs. $\lambda*\lambda - 1/\lambda$)
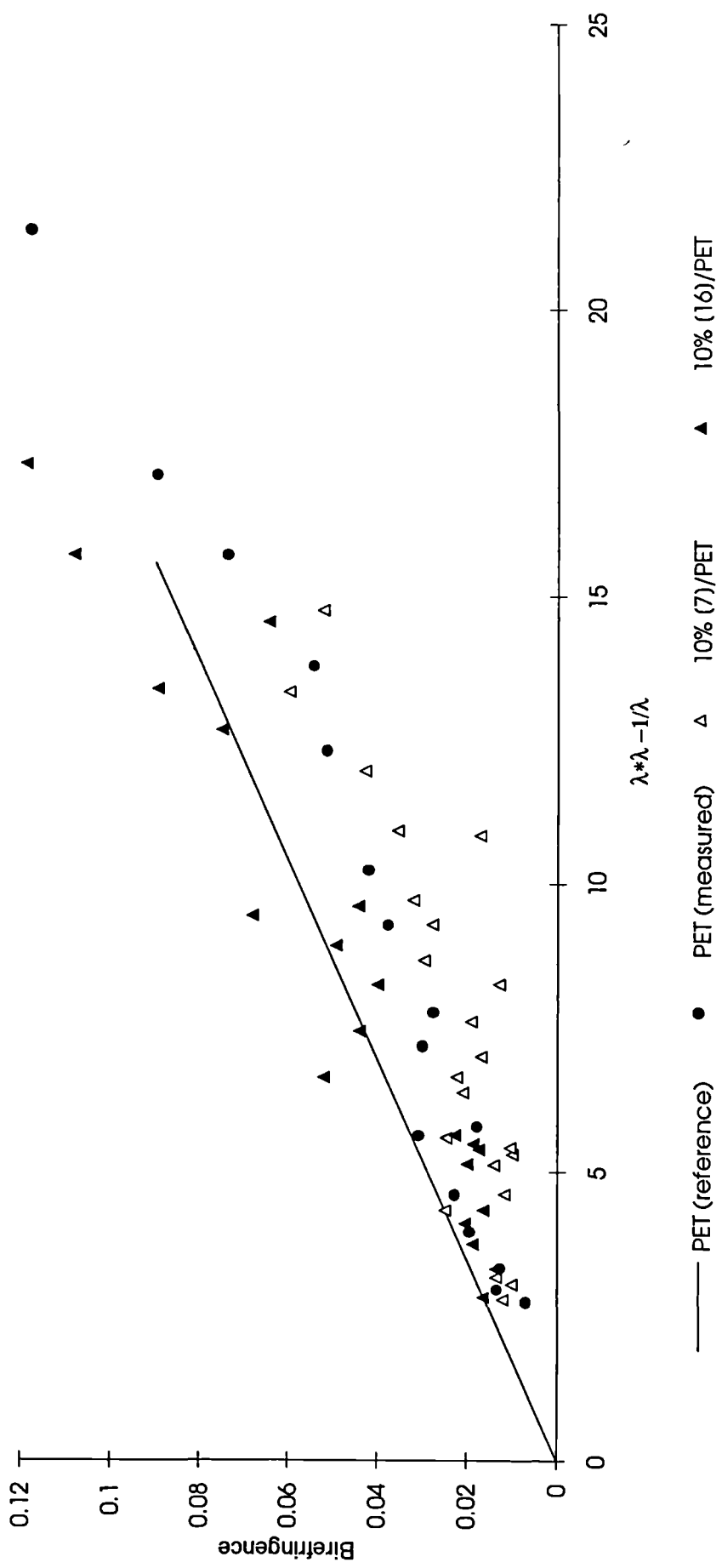
Birefringence

$\lambda*\lambda - 1/\lambda$

—— PET (reference)   ● PET (measured)   △ 10% (7)/PET   ▲ 10% (16)/PET

Figure 4.16

94

Mechanical Testing of Dendrimer / PET Drawn Films (Shrinkage Stress vs. Birefringence)
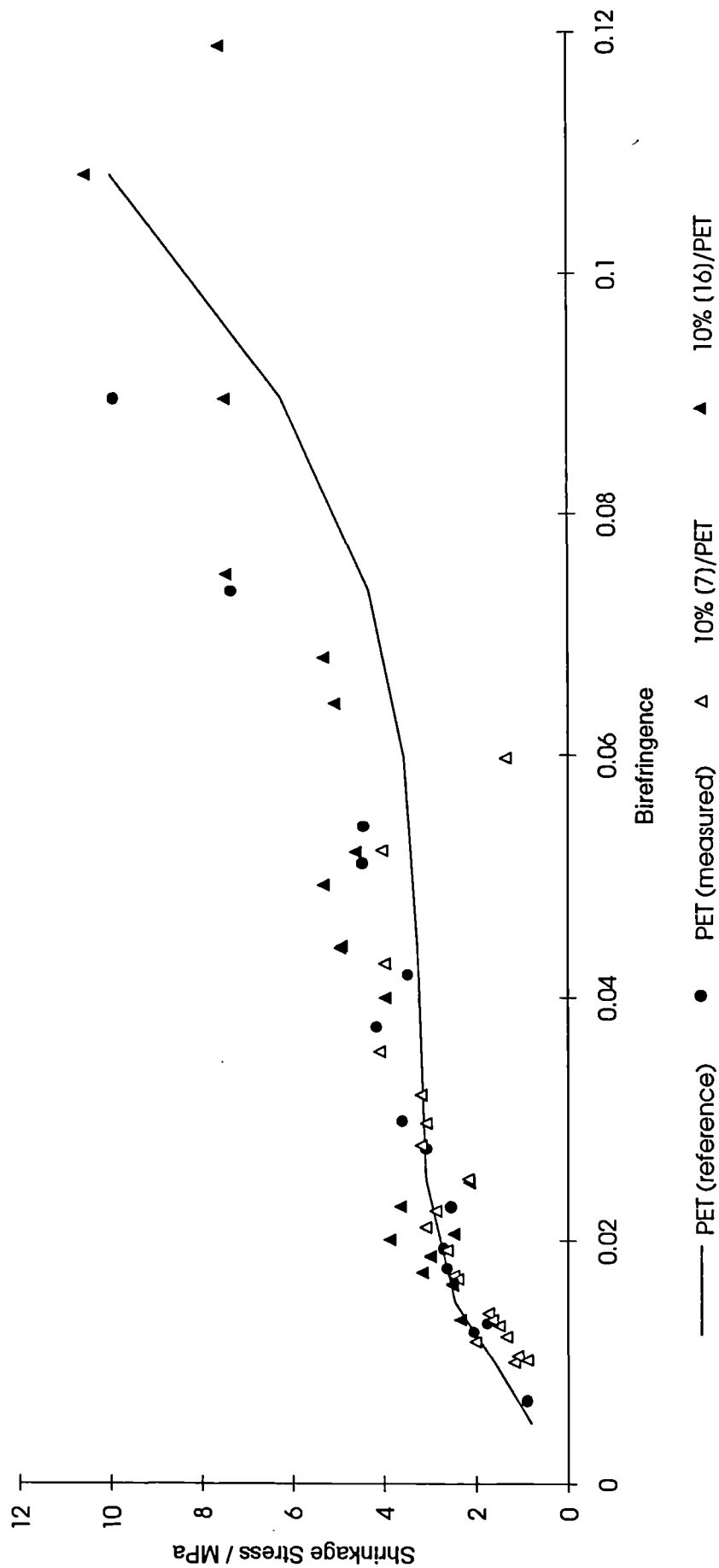
Figure 4.17

Mechanical Testing of Dendrimer / PET Drawn Films   (Shrinkage Stress vs. $\lambda * \lambda - 1/\lambda$)
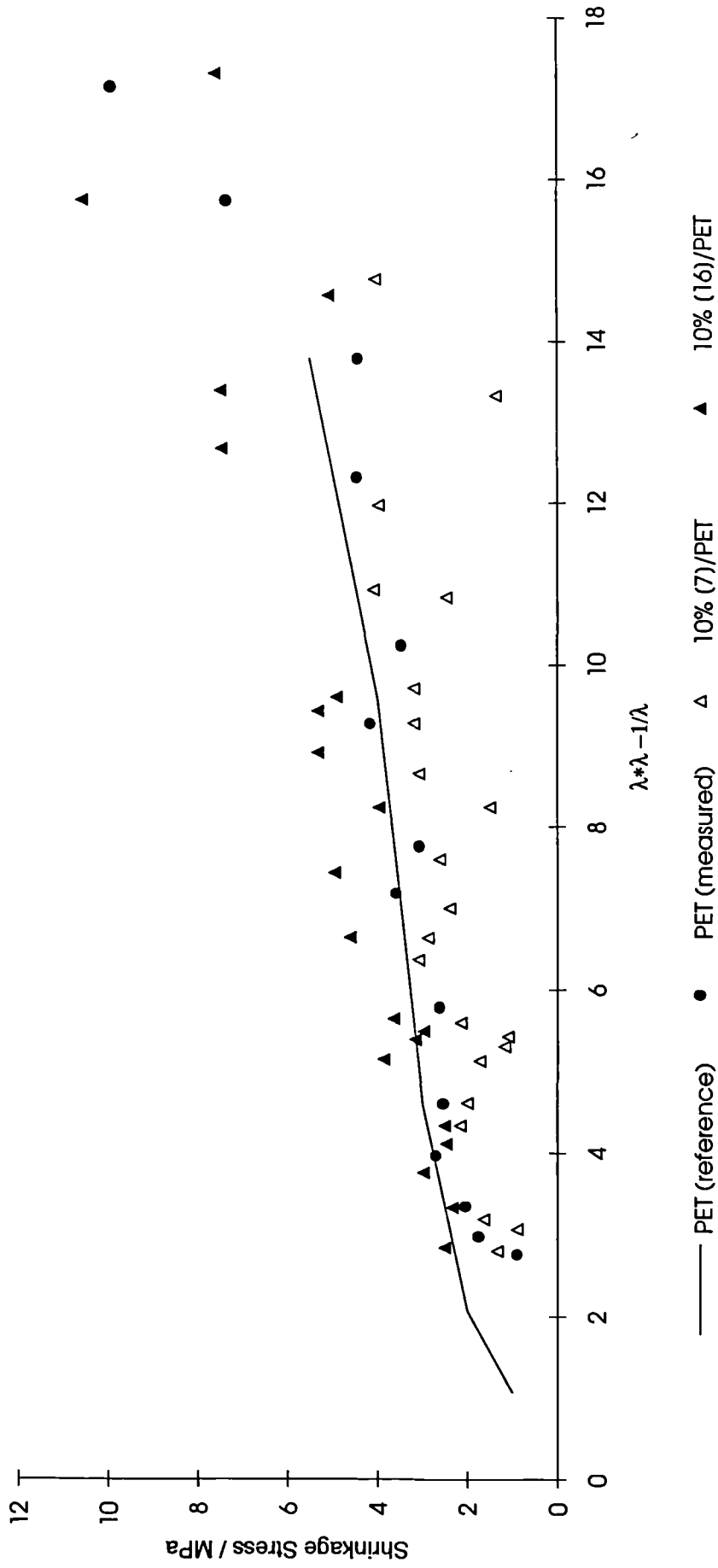
Figure 4.18

Mechanical Testing of Dendrimer / PET Drawn Films (Shrinkage Stress vs. $\lambda*\lambda - 1/\lambda$)

Shrinkage Stress / MPa

$\lambda*\lambda - 1/\lambda$

△ 10% (7)/PET   ▲ 10% (16)/PET

Figure 4.19

97
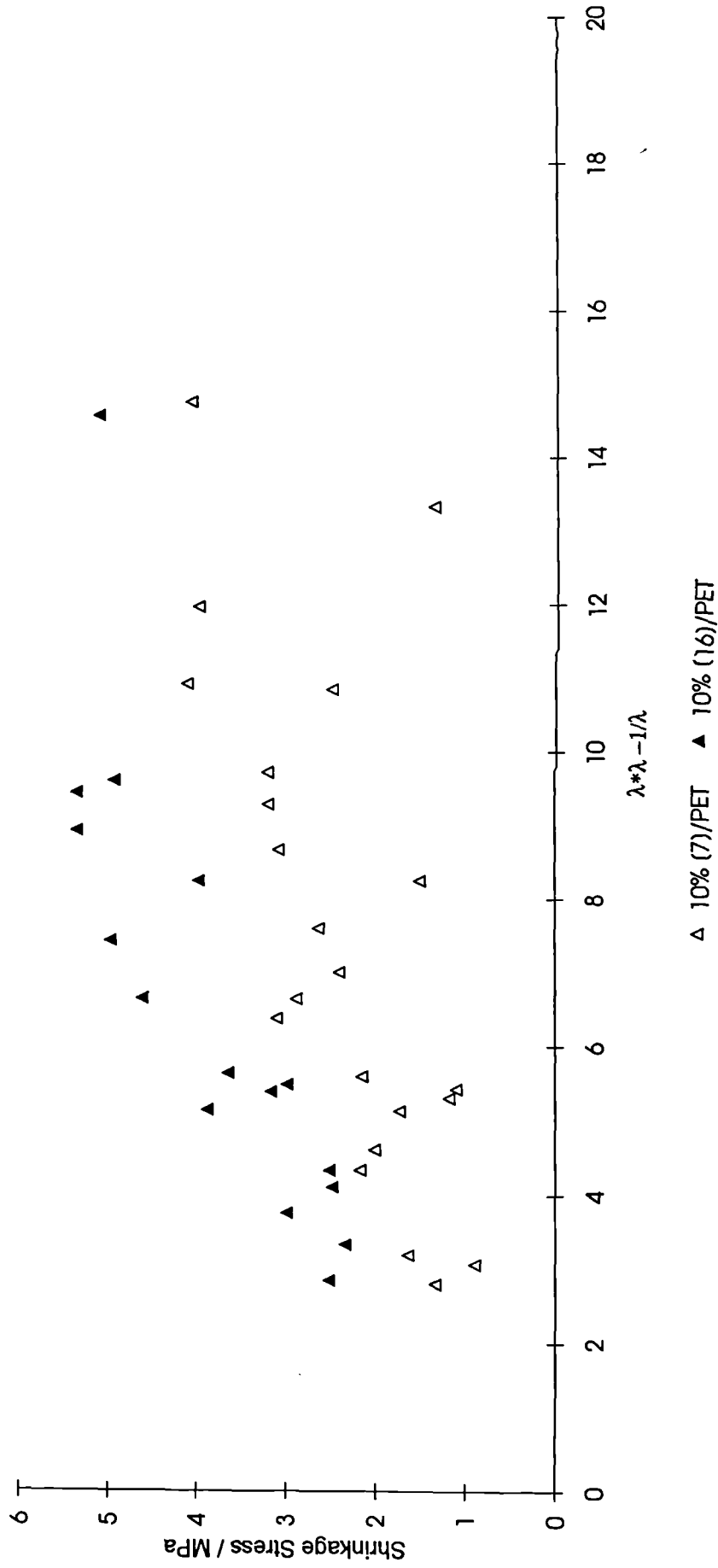
Discussion

Comparison of Figures 4.16 and 4.18 indicates that whilst optical anisotropy is linearly dependent on $(\lambda^2 - 1/\lambda)$ in accordance with eqn. 4.11, the shrinkage stress vs. $(\lambda^2 - 1/\lambda)$ curve deviates from the predicted linearity of eqn. 4.10. One possible explanation of this result is proposed in terms of partial network breakdown in which a limited number of entanglement points fail to be effective in the retention of stress yet are still able to contribute towards molecular orientation and bulk birefringence. The final rise in Figure 4.18 has been attributed to the finite extensibility of the molecular network.[17]

Given the differences in behaviour of PET and the dendrimer blends as illustrated in Figures 4.16, 4.18 and 4.19, dendrimer [7] appears to plasticise the PET in the conventional manner by increasing the free volume of the system and reducing chain interactions, which leads to increased chain slippage thus reducing chain orientation for a given draw ratio. In contrast, incorporation of dendrimer [16] leads to enhanced orientation for a given draw ratio thus exhibiting an antiplasticisation effect. It is possible that this is due to an interaction between the dendrimer and the PET chains that is sufficiently large to more than compensate for the reduced interaction between the PET chains themselves.

By consideration of the experimental data in terms of the molecular theory of rubber elasticity, it is possible to derive quantitative results relating to the chain entanglement at a molecular level:-

From Figure 4.17, it has already been noted that the simple molecular theory is valid for $\Delta n < 0.02$, where the curve gradient and hence the stress-optical coefficient, $\Delta n/\sigma$, is constant. An expansion of this region is shown in Figure 4.20, from which it can be deduced that the gradient and thus the polarisability of the random link, $(\alpha_1 - \alpha_2)$, is substantially the same for PET and the blended materials. A least squares fit of all the data points within this region passing through the origin yields a mean stress-optical coefficient of 6.90×10^{-9} $N^{-1}m^2$ from which eqn. 4.12 gives the polarisability of the random link, $(\alpha_1 - \alpha_2)$, as 1.85×10^{-29} m^3, taking the mean refractive index of the polymer film as 1.6^7 and the drawing temperature as 80°C. This value compares favourably with published data which indicates that $(\alpha_1 - \alpha_2)$ lies between 0.7 and 1.9 $\times 10^{-29}$ m^3.[16-18] Although it is recognised that the polarisation of each dendrimer is

Mechanical Testing of Dendrimer / PET Drawn Films (Shrinkage Stress vs. Birefringence)

Mean Gradient = 145 MPa

$\therefore (\alpha_1 - \alpha_2) = 1.85$ E-29 m³

Figure 4.20

Shrinkage Stress / MPa

Birefringence

——— PET (reference)   ● PET (measured)   △ 10% (7)/PET   ▲ 10% (16)/PET   – – – least squares fit
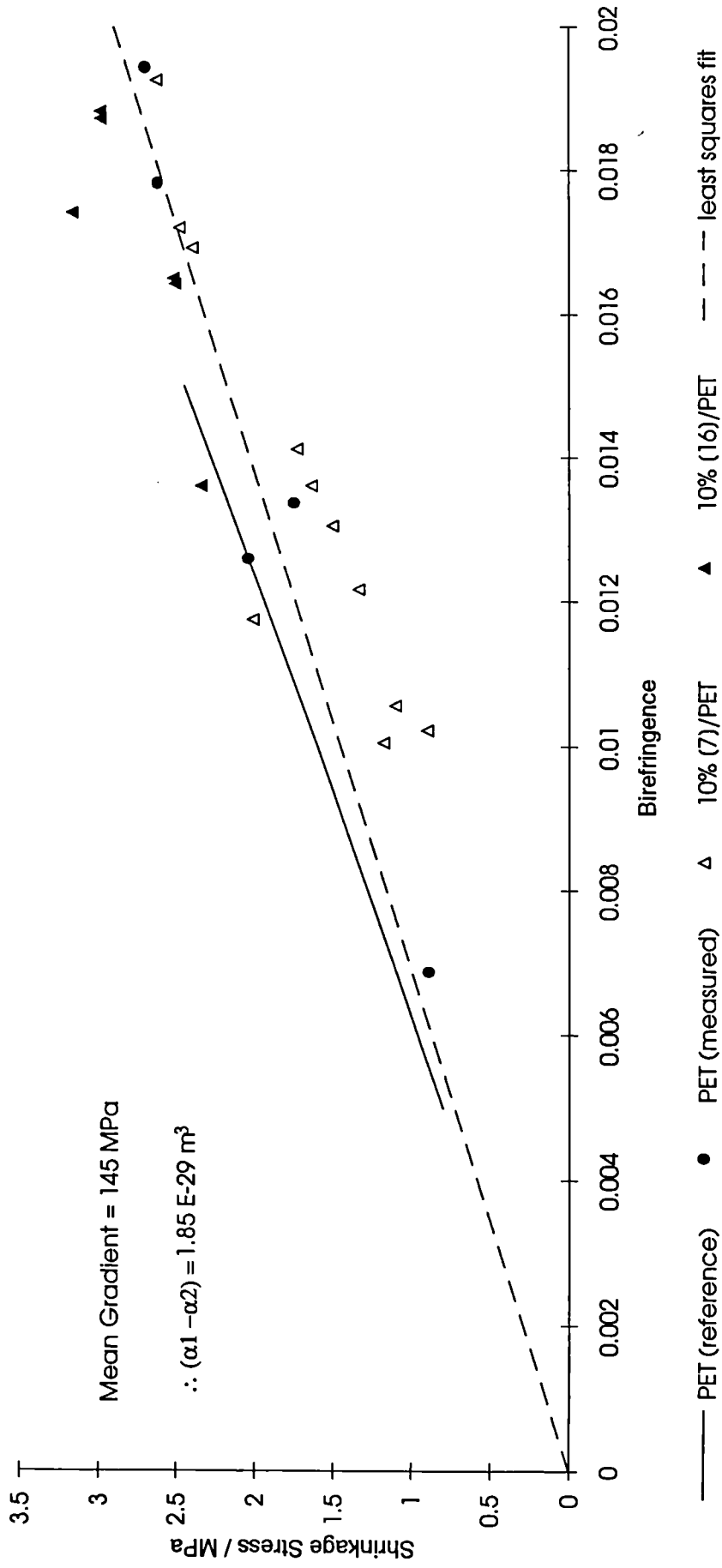
likely to be different to that of the PET random link, it is thought that the degree of dendrimer incorporation is sufficiently small such that it is unlikely to significantly affect the results.

Having determined the polarisability of the random link, the number of chain segments between entanglements per unit volume, N, has been calculated from the linear relationship between birefringence and $(\lambda^2 - 1/\lambda)$ in Figure 4.16 using eqn. 4.11 (Table 4.2). Least-squares fitting has been used to determine the line gradient for each sample type. These have not been constrained to pass through the origin since on inspection of the experimental data, it appears that in all cases, a degree of drawing has taken place without a corresponding increase in birefringence.

Sample	PET (ref)	PET (measured)	10% [7] / PET	10% [16] / PET
$N / 10^{26} \, m^{-3}$	1.72	1.58	1.02	2.07

Table 4.2 No. of Chain Segments per Unit Volume for Film Specimens.

From the experimentally determined N for PET, the volume occupied by each chain segment and thus the mass of a single chain can be determined. The mean molecular weight of a chain segment is calculated to be 5140 assuming a relative sample density of 1.35.[7] As each repeat unit has a mass of 192, this corresponds to approximately 27 repeat units per chain segment. The value of $(\alpha_1 - \alpha_2)$ can be compared to the value computed for a fully extended monomer[19] of $0.52 \times 10^{-29} \, m^3$ to yield a value of 3.6 repeat units per random link thus implying a mean chain composition of 7.5 random links.

Conclusion

Both dielectric measurements and tensile testing of dendrimer / PET blend films have indicated that incorporation of dendrimers has a noticeable effect on the material characteristics. Furthermore, the observed effect is dependent on the size or shape of the added dendrimer. Dendrimer [7] acts as a plasticiser and reduces the extent of chain interaction whereas dendrimer [16] acts as an antiplasticising agent and enhances the overall intermolecular interactions. These effects have been quantified by stress-

optical measurements. It has been shown that dendrimer [7] has the effect of reducing the number of effective physical cross-links or chain entanglements per unit volume with respect to a pure PET sample whereas dendrimer [16] incorporation leads to a substantial increase in chain entanglement density (Table 4.2), the increase in the number of entanglement points being almost equal to the number of added dendrimer [16] molecules, which suggests that on average, each dendrimer molecule creates an additional entanglement. This may be accounted for in a simplistic manner by envisaging the PET chains as becoming interwoven with [16], the larger, more highly branched dendrimer, thus increasing the extent of physical entanglement and overall interchain interaction. In contrast, [7], the smaller dendrimer, is less able to bind the PET chains together and disrupts the intrinsic chain interaction.

On a macroscopic scale, although the tensile modulus for given molecular alignment as measured by optical anisotropy is not noticeably influenced by dendrimer incorporation, the extent by which a film must be drawn to achieve that orientation shows a marked dependence on the type of dendrimer added. Dendrimer [7] / PET films must be drawn to a greater extent than the pure PET films to obtain the same degree of orientation whereas for dendrimer [16] / PET films the reverse is true. Although the behaviour of dendrimer [7] is typical of common plasticisers, the enhanced molecular orientation for a given draw ratio exhibited by blends containing dendrimer [16] is a desirable phenomenon that is much sought after in the production of PET fibres.

References

1. Connolly, M., Ma, B. and Karasz, F., PMSE Prep., Amer.Chem.Soc. Div.Polym.Mater. 69, 82 (1993)

2. Halliday, D. and Resnick, R., "Physics", (3rd edn.), Wiley (1978)

3. Pethig, R., "Dielectric and Electronic Properties of Biological Materials", Wiley (1979)

4. Chowdhury, B. in "New Characterization Techniques for Thin Polymer Films", Tong, H. and Ngugen, L.T. (eds.), Wiley (1990)

5. Wetton, R.E. in "Polymer Characterisation", Hunt, B.J. and James, M.I. (eds.), Blackie (1993)

6. Daniel, V.V., "Dielectric Relaxation", Academic Press (1967)

7. Lawton, E.L. and Ringwald, E.L. in "Polymer Handbook", (3rd edn.), Brandrup, J. and Immergut, E.H. (eds.), Wiley Interscience (1989)

8. Reddish, W., Trans. Faraday Soc. 46, 459 (1950)

9. Farrow, G., McIntosh, J. and Ward, I.M., Makromol. Chem. 38, 147 (1960)

10. Illers, K.H. and Breuer, H., J. Colloid. Sci. 18, 1 (1963)

11. Sperling, L.H., "Introduction to Physical Polymer Science", (2nd edn.), Wiley (1992)

12. Nomura, S. in "Comprehensive Polymer Science V2", Allen, G. and Bevington, J.C. (eds.), Pergamon (1989)

13. Flanagan, M. in "Polymer Characterisation", Hunt, B.J. and James, M.I. (eds.), Blackie (1993)

14. Padibjo, S.R. and Ward, I.M., Polymer 24, 1103 (1983)

15. Treloar, L.R.G., Trans. Faraday Soc. 50, 881 (1954)

16. Pinnock, P.R. and Ward, I.M., Trans. Faraday Soc. 62, 1308 (1966)

17. Rietsch, F., Duckett, R.A. and Ward, I.M., Polymer 20, 1133 (1979)

18. Savvon, S.M. and Turovenov, K.K., Geterotsepnye Vysokomolekul. Soedin. 205 (1964) (C.A. 61 4505d)

19. Pinnock, P.R. and Ward, I.M., Br. J. Appl. Phys. 15, 1559 (1964)

CHAPTER 5

Hyperbranched Polymers

Introduction

In linear condensation polymers, each molecule, regardless of size, possesses no more than two terminal units. Each molecule will contain exactly two terminal units provided that no intramolecular cyclisation reactions take place. Such molecules are capable of reacting with other molecules in a stepwise manner to increase the molecular chain length. Polymers of this type may be formed by the homopolymerisation of A-B type molecules or by the copolymerisation of A-A and B-B units, in which reactions are restricted to those between an A and a B group. The incorporation of polyfunctional monomers in the polymerisation reaction may although will not necessarily lead to extensive cross-linking and the formation of network structures.

Consider a trifunctional monomer of the type AB_2. Polycondensation of such a monomer leads to structures such as that shown in Figure 5.1.
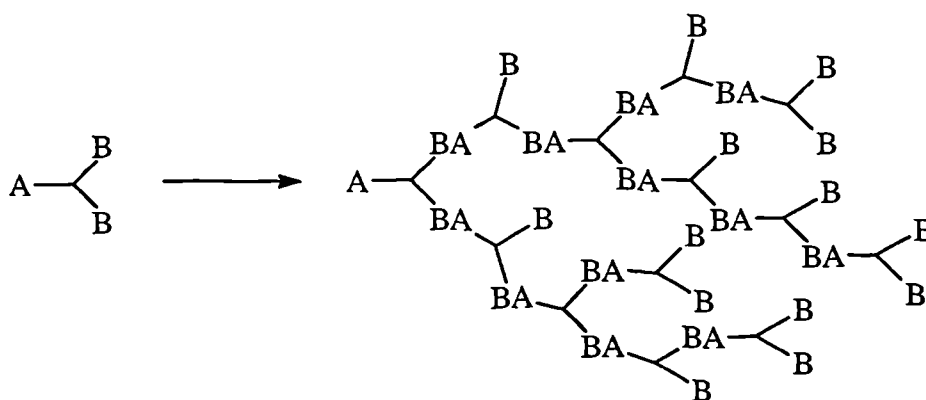
Figure 5.1 A Schematic View of AB_2-type Polymerisation

In such a situation, each molecule will contain at most one unreacted A functionality and exactly one provided the approximation is made that no intramolecular condensation takes place. If this is the case, there will be one unreacted A group and (x+1) B groups in a molecule comprising of x monomer units. In the more general case of an f-functional monomer of the type $AB_{(f-1)}$, each x-mer molecule

will possess a single A functionality and (fx - 2x +1) unreacted B units. Such molecules have been termed "hyperbranched polymers".

Until recently, there have been few reported examples of polymers with hyperbranched topology. Of those that have been prepared, little or no investigation of their unusual molecular connectivity appears to have been carried out. The elimination of metal halides from trihalophenol salts to form polyaryl ethers[1] and the Friedel-Crafts condensation of benzyl halides[2] provide two early examples of polymers of this type.

Perhaps the most widely known example of a hyperbranched polymer is that of the naturally occurring polyglucose, amylopectin, which is the major constituent of starch. Starch is a carbohydrate which provides a source of energy in many living organisms. The evidence of its extensively branched structure has been obtained by degradation and analysis of the reaction products using conventional polysaccharide methods.[3]

Following the rapid growth of activity in the field of dendrimer synthesis within the last 10 years, there has been a resurgence of interest in hyperbranched polymers, largely on account of their structural similarity yet greatly simplified method of preparation with respect to dendrimer molecules. Although there have been numerous suggestions for the exploitation of dendrimers for a host of speciality applications,[4] in practical terms, the laborious and time-consuming iterative procedures necessary to make such materials have detracted from their widespread acceptance. If, as suggested, some of the unusual and potentially useful properties of dendrimer molecules arise on account of their extensively branched geometry rather than their well-defined monodisperse nature, it may be possible to replicate these properties by employing polydisperse analogues thus making the use of such structures a more commercially viable proposition.

Within the last few years, many groups have reported work directed towards the synthesis of hyperbranched polymers.[5-7] Although there have been a few groups that have made considerable progress in the characterisation and control of the molecular weight of such structures, there have also been examples in the literature in which there appears to have been little or no appreciation of such subtleties. Amongst the more fully characterised materials produced via a polycondensation route have been the wholly aromatic polyphenylenes of Kim and Webster.[5] The coupling of

arylboronic acids or arylmagnesium halides with aryl halides in the presence of organometallic catalysts has produced rigid hyperbranched structures that are soluble in common organic solvents. These may be converted to water-soluble polycarboxylate salts on treatment with butyllithium and carbon dioxide (Figure 5.2).
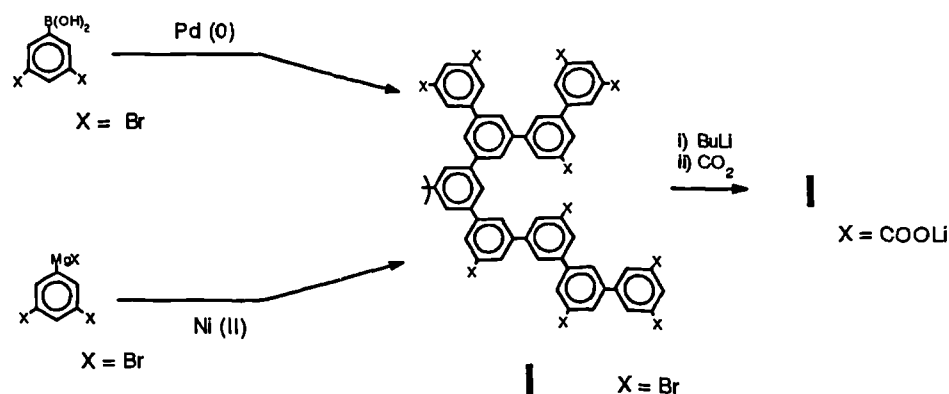
Figure 5.2 Synthesis of the polyphenylene hyperbranched polymers

In a continuation of their related work on the synthesis of monodisperse dendrimers, Fréchet and co-workers have been involved in the synthesis of hyperbranched polyester[6] and polyether[8] analogues. In both cases, all the polymers have been found to be highly soluble in organic solvents. By modification of reaction conditions such as polymerisation time and temperature, some degree of control of molecular weight and polydispersity has been demonstrated.

Unlike their monodisperse dendrimer equivalents, AB_2 hyperbranched polymers are formed by a random sequence of events resulting in extended structures in which there are four different types of structural unit that may be present. In common with dendrimers, each hyperbranched polymer may contain fully branched (type b) monomer units and terminal (type t) units. In addition, there is also the possibility of the incorporation of linear (type l) units, in which only one of the B functionalities has reacted thus leading to branching irregularity, and the monomer unit at the focal point of the hyperbranched wedge, of which there is only one per molecule (subject to there being no intramolecular reaction as described earlier). Depending on its connectivity, the unit at the focal point may be regarded as a special case of a branched or linear

106

unit, the influence of which becomes insignificant with increasingly high molecular weight.
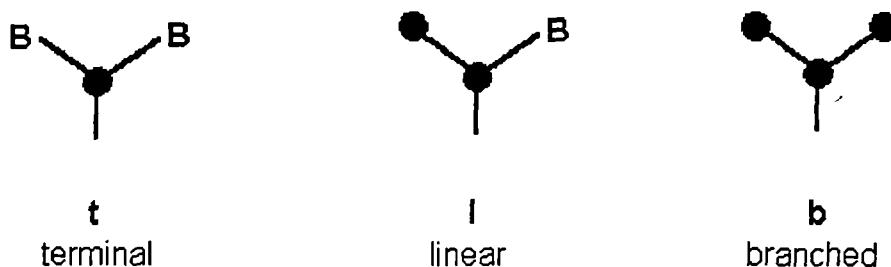
Figure 5.3 Schematic representation of types of monomer unit

In principle, although statistically unlikely, it is possible to prepare both linear polymers and perfect or fully branched dendritic wedges from AB_x type monomers. Since it is clear that the extent of branching will have a profound influence on the physical properties of a material, a branching factor, f_{br}, has been defined to give an indication of the degree of branching as shown below.[6]

$$f_{br} = \frac{N_t + N_b}{N_t + N_b + N_l}$$ (eqn. 5.1)

where N_x is the number of type x units in the structure.

Both terminal (type t) and branched (type b) units contribute to the fully branched structure whilst linear (type l) units reduce the branching factor hence

$$0 \le f_{br} \le 1$$ (eqn. 5.2)

where $f_{br} = 0$ represents the case of an infinitely long linear polymer and $f_{br} = 1$ represents the case of a perfectly branched macromolecule.

From geometric considerations, in any AB_2-type hyperbranched polymer, the number of terminal units, N_t, is given by

$$N_t = N_b + 1$$ (eqn. 5.3)

irrespective of the number of linear units, N_l, in the structure. As such, in favourable cases in which the proportion of linear units can be determined with respect to the either the number of terminal or branching units directly, the branching factor, f_{br}, can be readily calculated. In less favourable cases, it is necessary to make derivatives[7] or in more extreme cases, to fragment the polymer in order to determine the degree of branching. Extreme care must be taken in such cases so as not to disrupt the evidence of the original branching pattern in the subsequent analysis. Branching factors for the more fully characterised hyperbranched polymers have typically been within the range 0.6 - 0.7 indicating that there are approximately equal numbers of terminal, linear and branching units within the structures.

Another feature in which hyperbranched polymers differ markedly from their dendrimer counterparts is that of molecular symmetry. For a hyperbranched molecule of given molecular weight and branching factor, a large number of geometric isomers can be envisaged. Consequently, for a collection of such molecules of variable molecular weight and branching factor, the number of different possible structures is practically infinite. Such a multiplicity of components leads to the expectation of a largely amorphous structure, which is what has been found in the limited number of cases in which this aspect of characterisation has been investigated.[9]

Molecular Weight Distribution in Hyperbranched Polymers

Flory[10,11] has shown that the molecular weight distribution of an AB condensation polymer may be predicted using a statistical approach. In the absence of undesirable side reactions and provided that the reactivity of each functional group is independent of its position in a molecule, this leads to the expressions

$$n_x = (1-p).p^{x-1} \qquad \text{(eqn. 5.4)}$$

$$w_x = x.(1-p)^2.p^{x-1} \qquad \text{(eqn. 5.5)}$$

$$\overline{x}_n = \frac{1}{1-p} \qquad \text{(eqn. 5.6)}$$

$$\overline{x}_w = \frac{1+p}{1-p} \qquad \text{(eqn. 5.7)}$$

where n_x and w_x are the mole fraction and weight fraction of x-mer and $\overline{x}_n$ and $\overline{x}_w$ are the number average and weight average degree of polymerisation respectively. The term p is the probability that a given functionality has reacted, which in this case is equal to the extent of reaction. The polydispersity of such a polymer is given by the ratio $\overline{x}_w/\overline{x}_n$ or $\overline{M}_w/\overline{M}_n$, where $\overline{M}_n$ and $\overline{M}_w$ are the number and weight average molecular masses respectively. The polydispersity tends to 2 as the reaction proceeds.

For a non-linear condensation polymerisation, the situation is significantly more complex. In the general case of the polymerisation of an f-functional monomer of the form AB_{f-1}, the equivalent terms have been calculated by Flory to be:-

$$n_x = \frac{(fx-x)!}{(fx-2x+1)!\,x!}\alpha^{x-1}.(1-\alpha)^{(fx-2x+1)} \qquad \text{(eqn. 5.8)}$$

$$w_x = [1-\alpha(f-1)].x.\frac{(fx-x)!}{(fx-2x+1)!\,x!}\alpha^{x-1}.(1-\alpha)^{(fx-2x+1)} \qquad \text{(eqn. 5.9)}$$

$$\bar{X}_n = \frac{1}{[1-\alpha(f-1)]}$$

(eqn. 5.10)

$$\bar{X}_w = \frac{[1-\alpha^2(f-1)]}{[1-\alpha(f-1)]^2}$$

(eqn. 5.11)

where α is the probability that a given B functionality has reacted, which is equal to $p/(f-1)$, where p is the extent of reaction as before. Simplification of equations 5.8 - 5.11 to yield the equations for linear polymerisation (equations 5.4 - 5.7) may be made by making the substitutions $\alpha = p$ and $f = 2$.
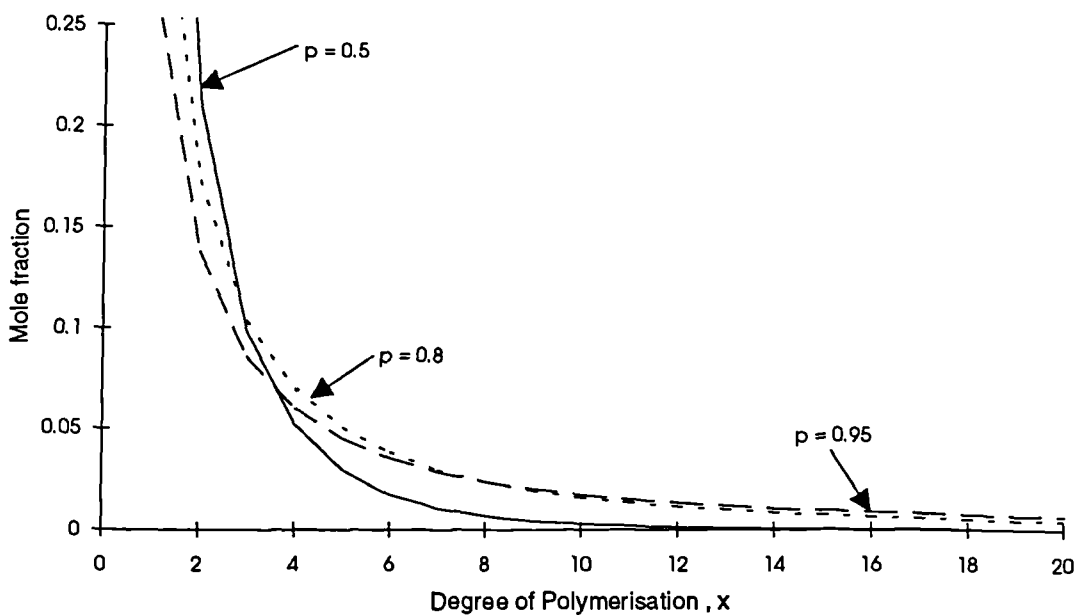
Figure 5.4 Mole Fraction Distribution for AB_2 Polymers
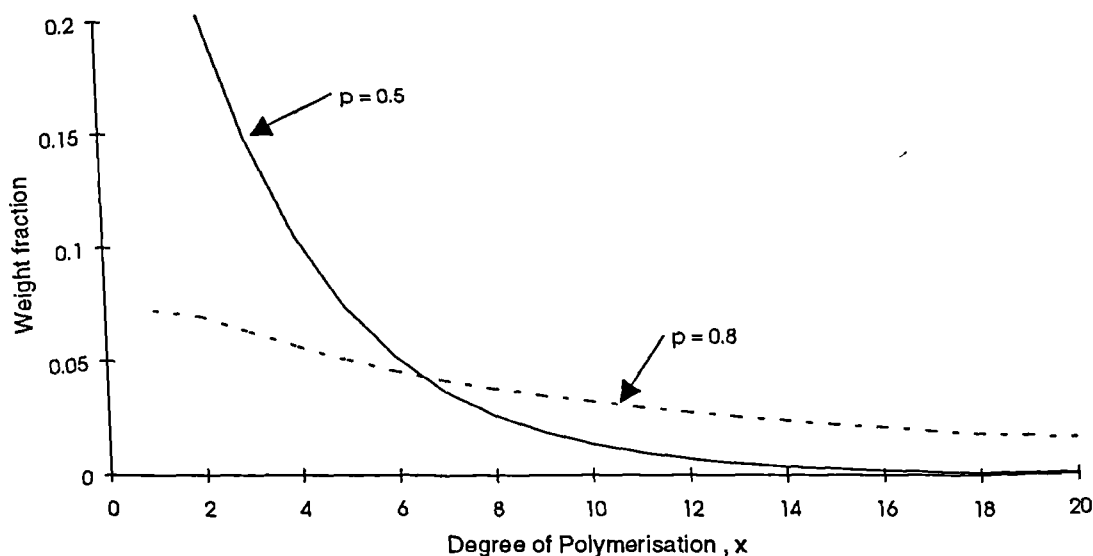
Figure 5.5 Weight Fraction Distribution for AB_2 Polymers

Figures 5.4 and 5.5, based on equations 5.8 and 5.9 respectively, show that for a trifunctional monomer, a considerable broadening in the molecular weight distribution occurs as the reaction proceeds. It is noted that even at high conversion the most numerous species is still the unreacted monomer unit. As α approaches α_{max} (= 0.5), the weight fraction of each species tends to zero and since for all α, the total number of monomer units is constant, the weight distribution must become infinitely broad.

The broadening of the distribution is best illustrated by consideration of the change in polydispersity of the system as the reaction proceeds. For AB_2 polymerisation, equations 5.10 and 5.11 can be combined to give the corresponding polydispersity expression equation 5.12.

$$\frac{\overline{x}_w}{\overline{x}_n} = \frac{1 - 2\alpha^2}{1 - 2\alpha} \qquad \text{(eqn. 5.12)}$$
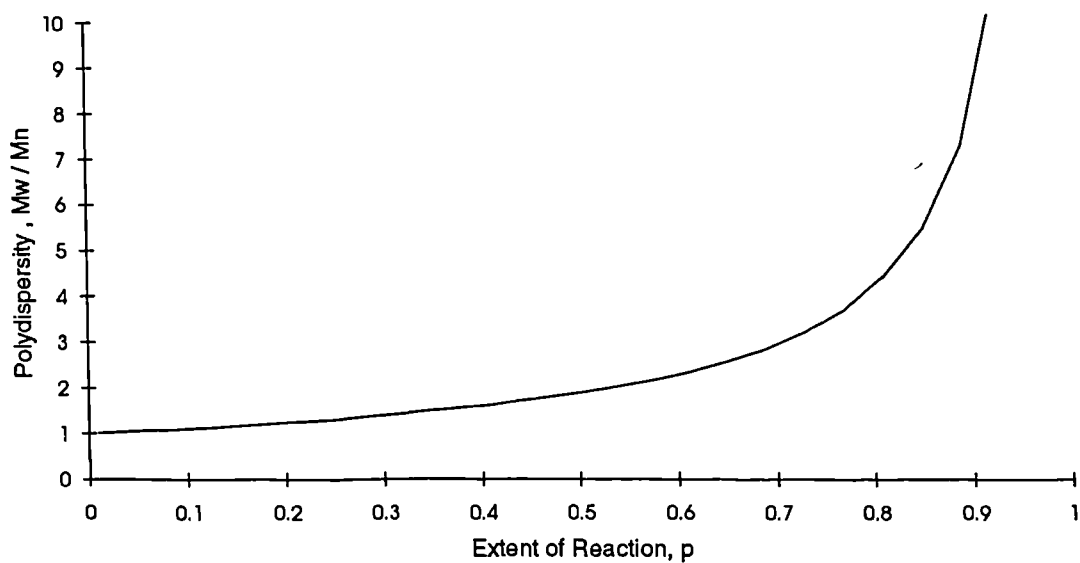
Figure 5.6 Increase in Polydispersity as a Function of Reaction Conversion

in AB_2 Polymerisation

As shown in Figure 5.6, although the increase in polydispersity is initially small, it grows rapidly as the reaction proceeds to completion, tending to infinity as $\alpha \rightarrow \alpha_{max}$ and $p \rightarrow 1$.

Hyperbranched Polyester Macromolecules

As a natural extension of the monodisperse dendrimer work detailed in earlier sections, the synthesis of hyperbranched polyesters via single-step condensation polymerisation has been investigated with a view to replicating some of the unusual properties of dendrimer molecules whilst avoiding the difficulties associated with their step-wise synthesis. In the course of this work, a new approach to the control of the molecular weight and polydispersity of hyperbranched polymers has been demonstrated. This facilitates the production of new families of hyperbranched materials and also allows for an experimental assessment of some of the points made by Flory in his theoretical treatment of the subject.

In the design of new polymeric materials, the ease of monomer production and the selection of appropriate polymerisation conditions both play a significant role in the determination of the success of a project. In the synthesis of the hyperbranched molecules described in this chapter, the considerable wealth of experience acquired in the preparation of aromatic polyester dendrimers based on 5-hydroxyisophthalic acid has been drawn upon to produce a monomer that would be expected to undergo a high yielding polymerisation reaction under similar conditions to those involved in the preparation of the commodity polymer PET. This monomer is similar to a monomer recently described by Walter and co-workers[12] however the characterisation of the corresponding polymer has not been discussed.
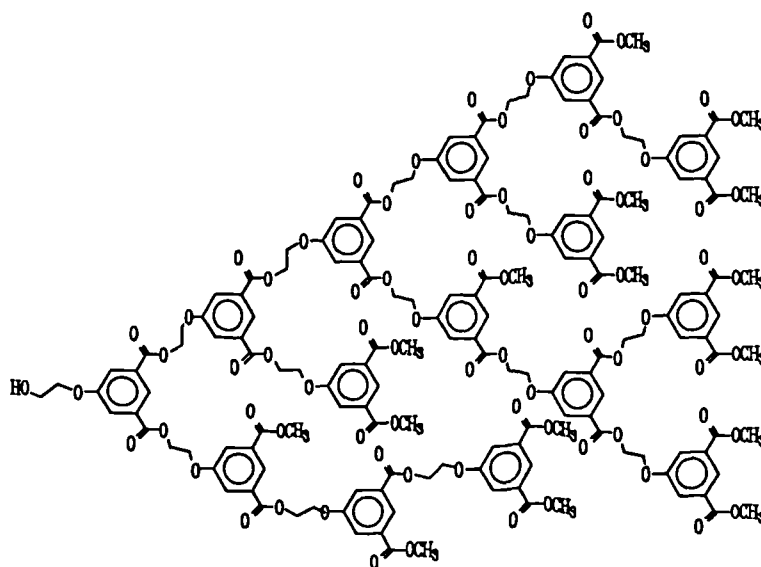
Figure 5.7 Generalised Structure of the AB_2 Hyperbranched Polyester

Monomer Synthesis

The esterification of 5-hydroxyisophthalic acid is carried out cleanly and in high yield (>89%) on treatment with commercially available boron trifluoride-methanol complex in methanol solution[13] to produce the white fibrous solid dimethyl-5-hydroxyisophthalate (see Scheme 5.1). Direct etherification of this with 2-bromoethanol in the presence of potassium fluoride on alumina[14] results in the recovery of a small quantity of the desired product, dimethyl-5-(2-hydroxyethoxy)isophthalate however the yield is unsatisfactory (<10%). This has been ascribed to the difficulty involved in the removal of the unreacted phenolic species during the purification procedure. Removal of dimethyl-5-hydroxyisophthalate by the conventional technique of extraction into aqueous base also results in the uptake of the substituted alcohol into the aqueous layer. In contrast, 2-bromoethyl acetate, obtained from the reaction of 2-bromoethanol with acetic anhydride under sulphuric acid catalysis, can be readily coupled with the phenolic diester, dimethyl-5-hydroxyisophthalate, to give dimethyl-5-(2-acetoxyethoxy)isophthalate by refluxing the components with a suspension of anhydrous potassium carbonate in acetone.[15] The improved etherification procedure has an appreciable cost advantage over the potassium fluoride on alumina route, which becomes increasingly important in larger scale reactions.

The hydrolysis of dimethyl-5-(2-acetoxyethoxy)isophthalate to the target monomer, dimethyl-5-(2-hydroxyethoxy)isophthalate is carried out cleanly with a catalytic amount of potassium hydroxide in methanol solution. The selective cleavage of the alkyl acetate ester is assured by the judicious choice of reaction solvent. Following precipitation into dilute aqueous acid and recrystallisation from toluene, the desired product is prepared as a white crystalline solid in excellent yield (>93%). The preparation of the monomer via its acetate derivative is thus justified in terms of the higher overall yield of product despite the need for an additional synthetic step.
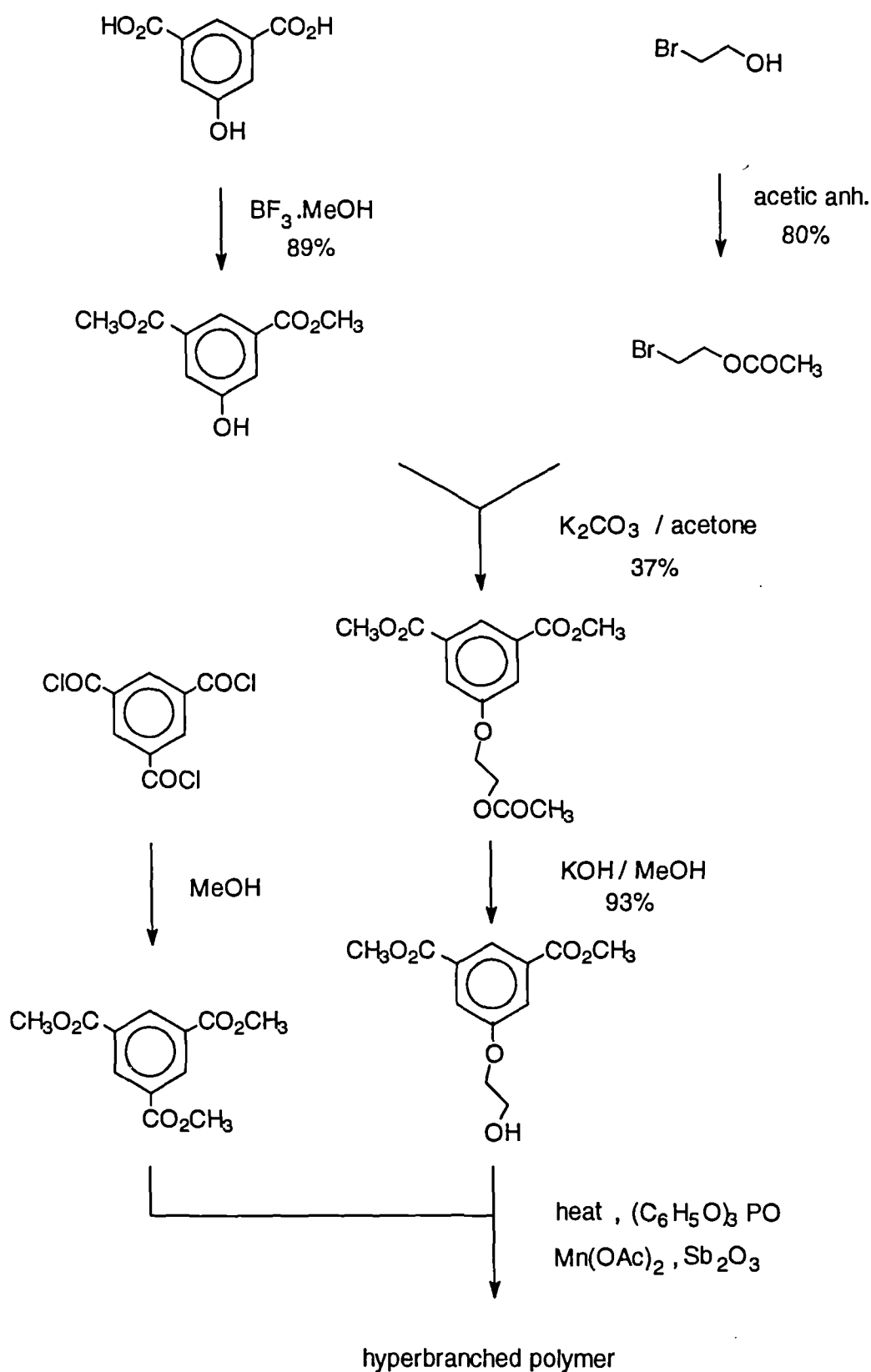
Scheme 5.1 Synthesis of the Hyperbranched Polyesters

Polymerisation

Given the structural similarity of the monomer unit dimethyl-5-(2-hydroxyethoxy)isophthalate to bis -(2-hydroxyethyl)terephthalate, an intermediate in the manufacture of poly(ethylene terephthalate), it was anticipated that the use of a similar catalyst system to those used in that process would be effective in the melt polycondensation of the AB_2-type monomer to produce high molecular weight material.

A mixture of antimony trioxide and manganese acetate has been used as the catalyst system in the preparation of the hyperbranched polyesters. The use of this system is well documented for the catalysis of the analogous linear polycondensation reaction.[16] Triphenylphosphate is added to the reaction mixture to restrict the degree of thermal degradation.

The polycondensation reaction is carried out using specially designed apparatus as shown in Figure 5.8. The reaction vessel is made so as to allow only slight clearance (~1mm) of the revolving paddle and thus facilitate intimate mixing.

Whilst stirring the solid monomer under a flow of nitrogen, the reaction vessel is lowered into the preheated Woods metal bath at 100°C. With continued stirring, the bath temperature is increased at a rate of 10°C/min to 240°C where it is held for two hours.

On removal of the flow of nitrogen, the pressure in the reaction vessel is reduced to 1mmHg and heating continued for a further hour at 240°C to remove residual methanol and drive the reaction to higher conversion. On completion of the reaction, the vacuum is removed and the reaction mixture cooled to room temperature under a flow of nitrogen. The dark-coloured oil solidifies to give a brittle brown glass which is readily soluble in chloroform. Addition of a chloroform solution of the polymer to a large excess of methanol results in the precipitation of the polymer that is collected by filtration and dried under vacuum to yield a white powdery solid.

116
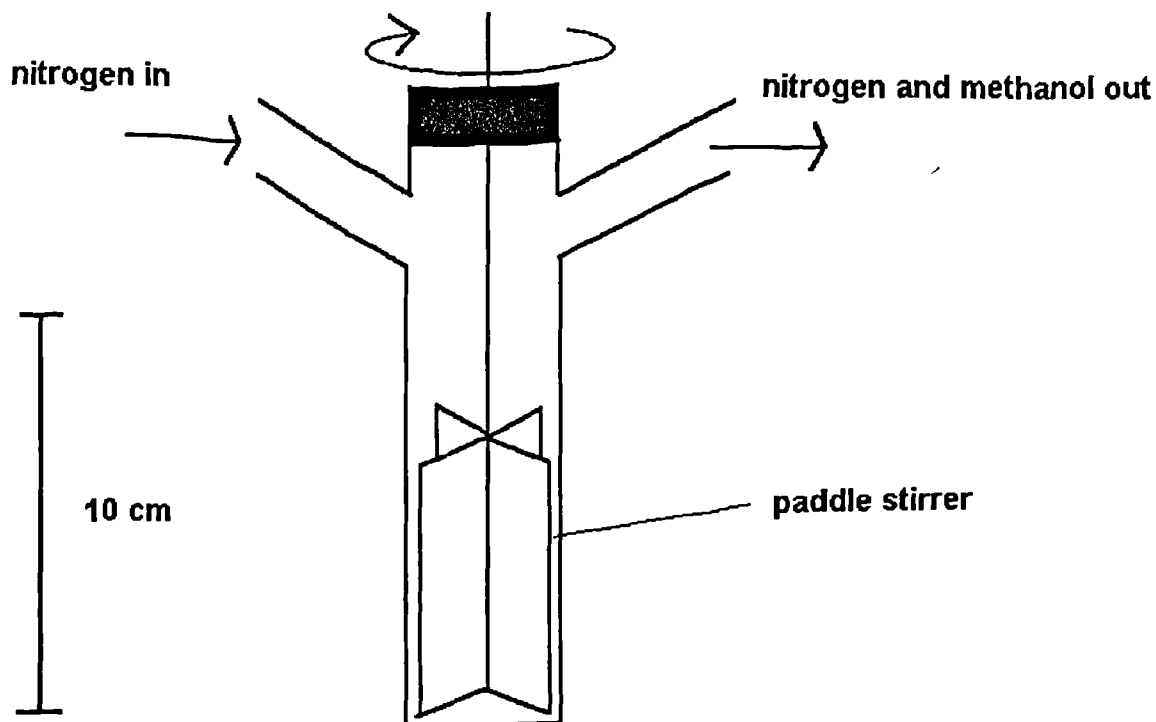
Figure 5.8 Polymerisation Apparatus

Copolymerisation

The copolymerisation of the branched monomer with increasing proportions of trimethyl-1,3,5-benzene tricarboxylate, which is readily made by the addition of 1,3,5-benzene tricarbonyl trichloride to excess methanol, has also been carried out using the same general polymerisation technique. It was anticipated that trimethyl-1,3,5-benzenetricarboxylate, a B_3-type monomer, would act as a trifunctional terminator unit, thereby restricting the hyperbranched growth. Drawing an analogy with the case of the monodisperse dendrimer systems, this may be viewed as a 'terminator core' as opposed to the initiator core molecules used at the outset of growth by the divergent route. Copolymerisation of the monomer and core molecule has been carried out in the ratios of 9:1, 21:1, 45:1 and 93:1. These values represent the increasing monomer:core ratios that would exist in consecutive generations of monodisperse dendrimers prepared by an iterative stepwise route. This series of materials, together with the wholly AB_2 polymer, will form the basis of the discussion in the following section.

Characterisation and Discussion

In contrast to the ease with which the well-defined dendrimers may be characterised using conventional organic chemistry techniques, for hyperbranched polymers it is necessary to rely more heavily on the characterisation techniques used for the investigation of more typical polymeric materials. Infra-red analysis is of little use in the characterisation of such structures since this merely confirms the presence of the incorporated ether and ester linkages as expected. No significant differences can be detected between the samples using this technique.

All of the samples are highly soluble in common organic solvents such as chloroform and tetrahydrofuran. It is suggested that their enhanced solubility with respect to that of linear polyesters is attributable to their extensively branched molecular geometry, which prevents close packing and crystallisation of the materials.[9] This view is supported by evidence from X-ray powder diffraction studies, which indicate that all of the polymers are largely amorphous materials (Figure 5.9).
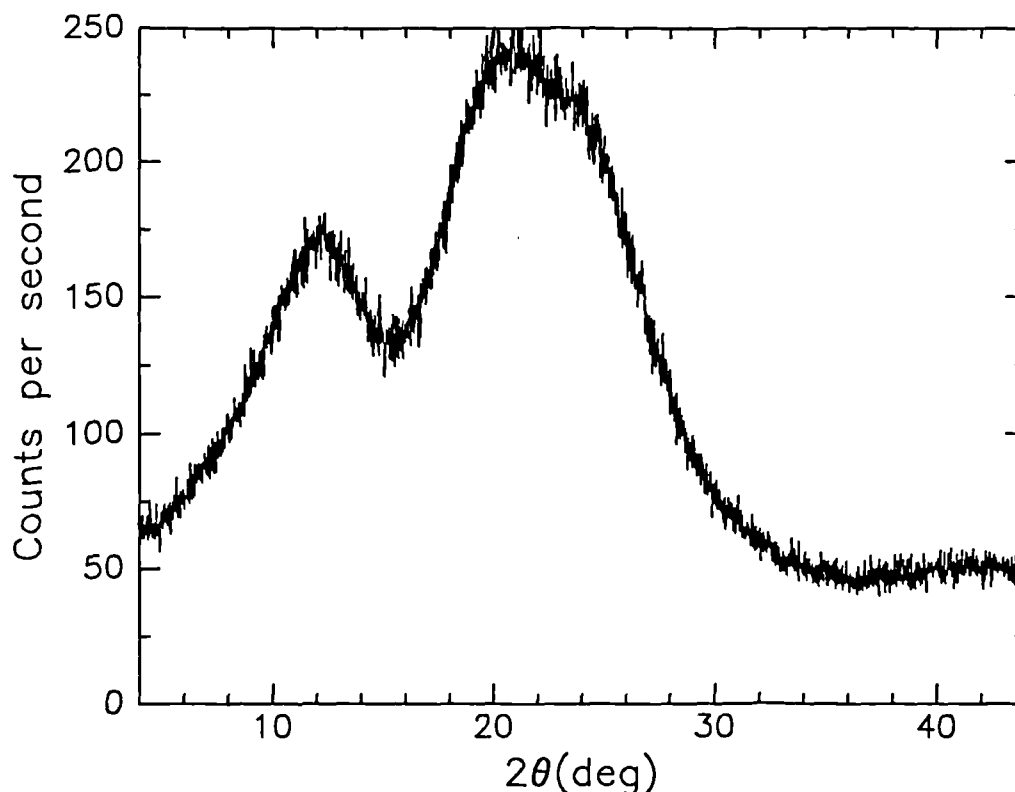
Figure 5.9 Wide Angle X-Ray Diffraction Trace of the AB_2 Hyperbranched Polyester

In the solution state ^{1}H n.m.r. spectrum of the homopolymer, 5 distinct regions are present and are readily assigned with reference to the monomer spectrum. The broad nature of the peaks is characteristic of polymeric materials and is due to the resonance from protons in very similar although unique environments. The other major difference between the monomer and homopolymer spectra is the relative intensity of the methyl peak, which is reduced with respect to the rest of the spectrum as a consequence of the elimination of methanol in the polycondensation process. In addition, the ^{1}H spectra of the copolymers have a peak at around $\delta 8.8$ attributable to the terminator core protons, the intensity of this peak approximately reflecting the ratio of monomer:core incorporation in the polymerisation reaction (Figure 5.10).

^{13}C n.m.r. spectra of the polymers are consistent with the general structure shown in Figure 5.7. The peaks show only slight line broadening and reveal a degree of fine structure arising from the linear, branched and terminal monomer units within the polymer (Figure 5.10). A low intensity peak at around $\delta 68$ appears in all the spectra and has been attributed to unreacted monomer and/or monomer units with free alcohol functionality at the focal point of wedges that are not bound to a terminator core. With reference to model compounds and correlation tables, further analysis of these peaks using a Bruker AMX500 n.m.r. instrument has facilitated their detailed assignment in favourable cases. The use of quantitative ^{13}C n.m.r. and subsequent peak deconvolution by numerical methods has enabled an independent determination of the degree of branching to be made from different regions of the same spectrum (see Supplement 5.1). Irrespective of the monomer:core ratio, the branching factor f_{br} for each hyperbranched polymer has been determined to be within the range 0.60 - 0.67, which from equations 5.1 and 5.3 indicates that there are approximately equal numbers of linear, branched and terminal monomer units within the structures. The fact that the branching factor is essentially independent of the copolymerisation ratio suggests that the steric constraints imposed by hyperbranched growth are not appreciably influenced by the incorporation of terminator core units.
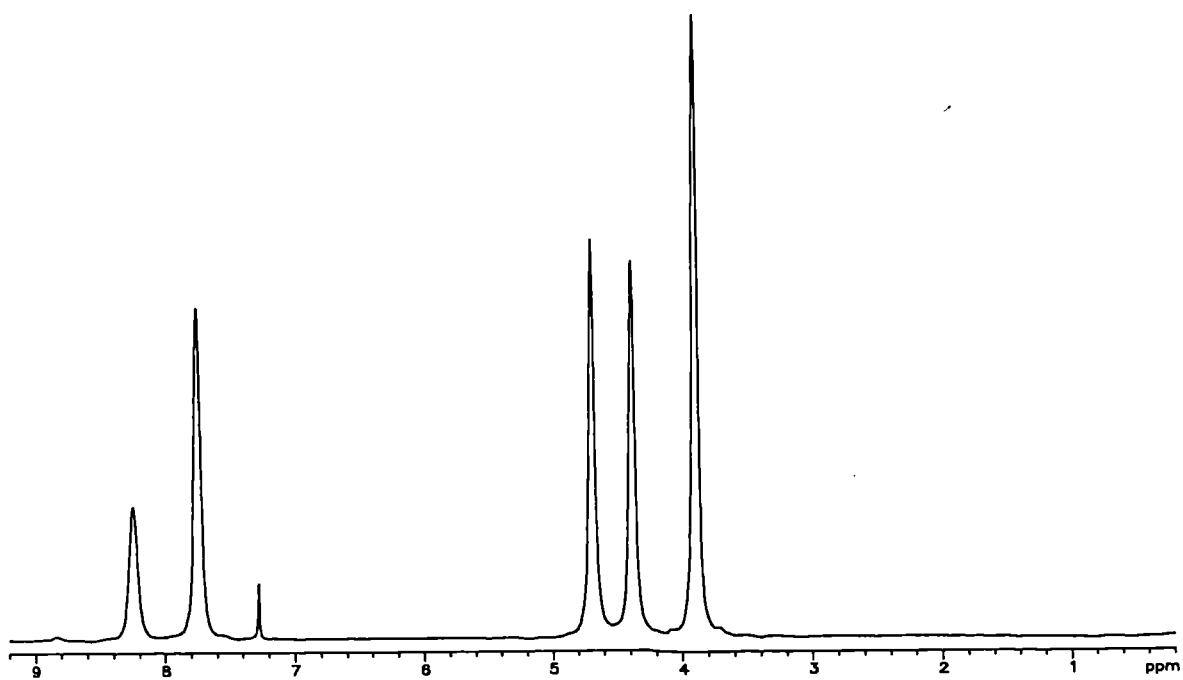
(a)
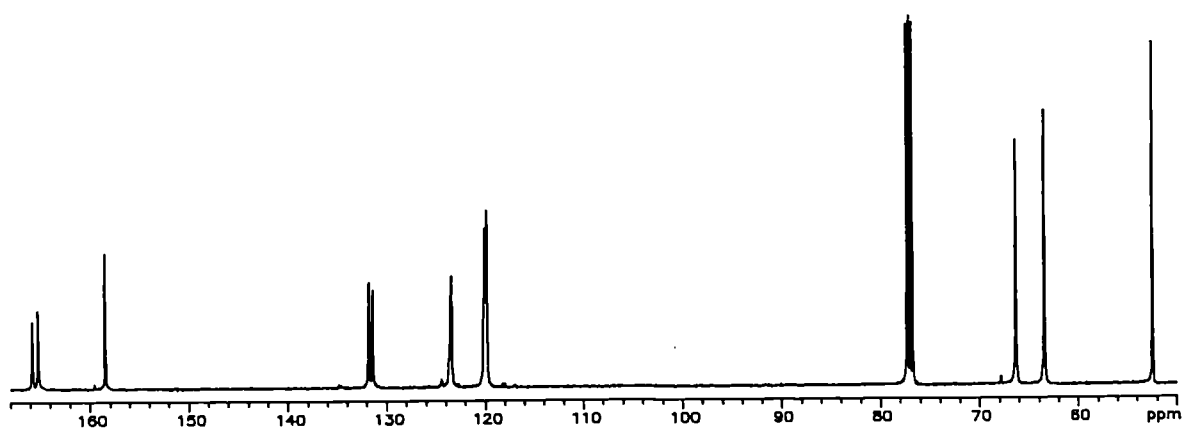
(b)

Figure 5.10 ^{1}H and ^{13}C n.m.r. spectra of 93:1 monomer:core copolymer in CDCl$_3$

120

The routine determination of the molecular mass of the hyperbranched polymers has been carried out by gel permeation chromatography with reference to conventional polystyrene calibration standards of low polydispersity. The analysis has been carried out in both chloroform and tetrahydrofuran solution and the polystyrene-equivalent molecular masses in each case are shown in Table 5.1.

Core:monomer ratio	Chloroform			Tetrahydrofuran			Dendrimer
	M_n	M_w	M_w/M_n	M_n	M_w	M_w/M_n	M^*
0.1111 (1:9)	3220	6150	1.91	3060	5060	1.65	2250
0.0476 (1:21)	4740	9390	1.98	3590	8360	2.33	4914
0.0222 (1:45)	7080	17830	2.52	9250	21770	2.36	10242
0.0108 (1:93)	8040	25260	3.14	10260	28600	2.79	20898
0 (AB$_2$)	9450	31500	3.33	12600	36050	2.86	-----

* Absolute mass for perfect dendrimer analogue with the same core:monomer ratio

Table 5.1 GPC Data for the Hyperbranched Polymers

For each sample, there is a discrepancy of ~25% in M_n and ~15% in M_w determination between the two solvent systems. Analysis in chloroform yields higher polystyrene-equivalent molecular masses than those in tetrahydrofuran for polymers with a relatively high core:monomer ratio whereas for polymers with a greater proportion of monomer incorporation the reverse is the case. Since GPC analysis effects separation according to molecular volume rather than molecular mass, this evidence indicates that the polymers have a variable hydrodynamic radius dependent on the nature of the solvent and suggests that solvent type influences the hydrodynamic radius of the structurally similar polymers in a different manner according to molecular size. Furthermore, the suggestion that linear polystyrene standards may be used to determine accurate molecular masses for this extensively branched type of polymeric material must be regarded with some scepticism. Support for this view may be drawn from the work of the Fréchet group[8] which has shown that the determination of weight-average molecular mass values for several hyperbranched aromatic polyethers by the absolute technique of low angle laser light scattering (LALLS) yields values that

are generally 3 - 5 times higher than the respective values from GPC. Consequently, GPC must be regarded as giving only a rough estimate of absolute molecular mass yet may provide valuable information on the more general molecular mass distribution profile.

From a consideration of our own data in Table 5.1 and illustrated in Figures 5.11 and 5.12, GPC analysis in chloroform and in tetrahydrofuran yield broadly similar trends. As anticipated, both number- and weight-average molecular mass increases smoothly as a function of decreasing core incorporation. This can be rationalised by consideration of the core molecule as a B_3 trifunctional terminator unit. Reaction of the A functionality of a hyperbranched wedge, irrespective of size, with such a unit will prevent further growth at the focal point of that wedge. There is the potential for a single B_3 terminator core to react with up to three wedge molecules thus forming structures reminiscent of dendrimers. An increase in terminator concentration in the polymerisation reaction has been clearly demonstrated to lead to lower molecular mass products and thus provides an effective means of controlling the molecular mass of hyperbranched polymers.
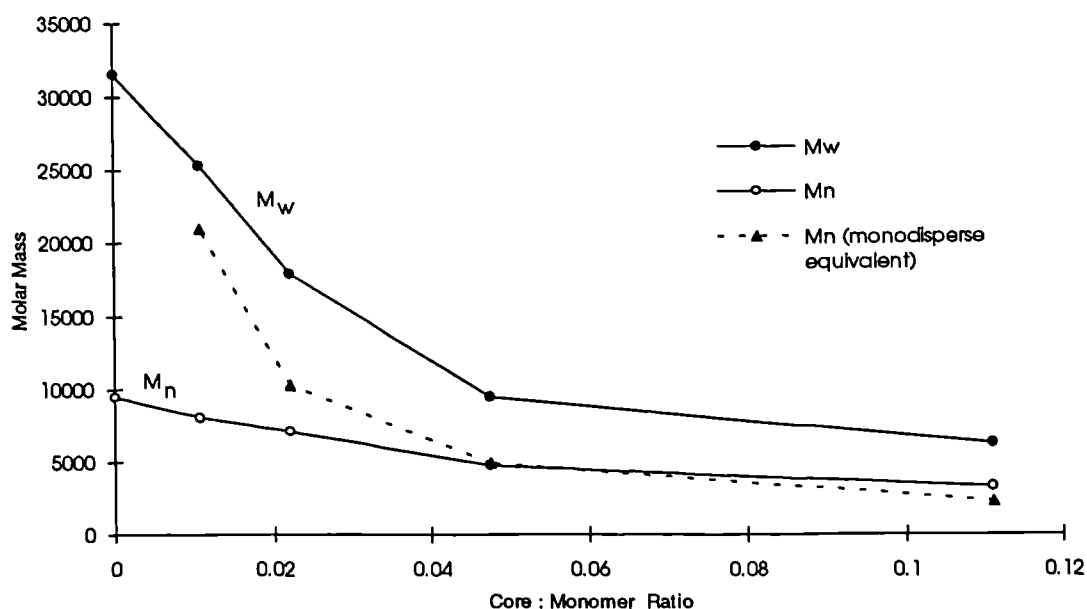
Figure 5.11 Variation in Molar Mass as a Function of Core:Monomer Ratio (as determined by chloroform GPC)
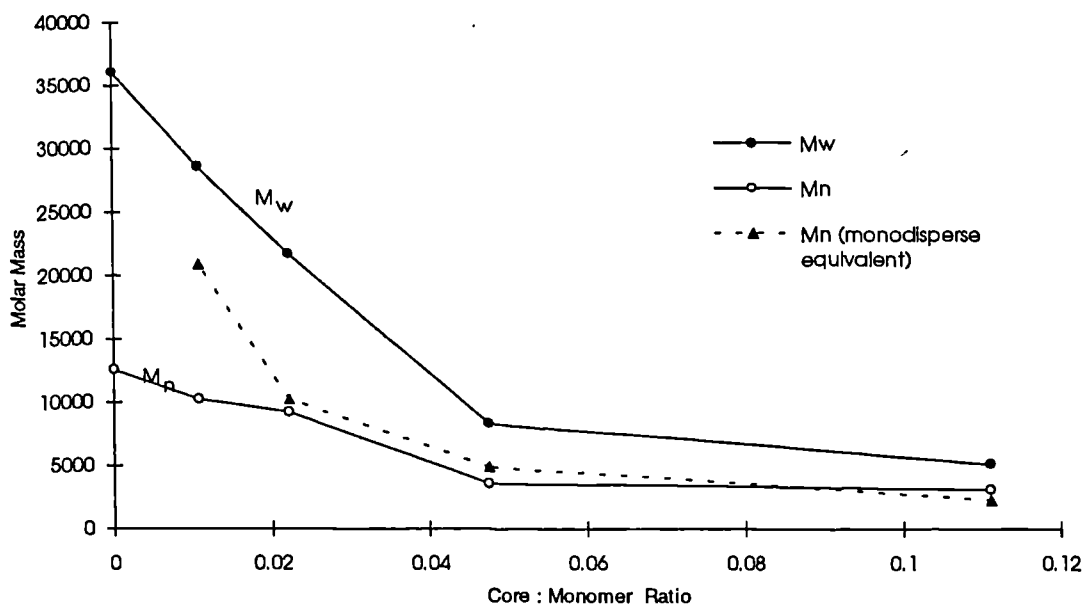
Figure 5.12 Variation of Molar Mass as a Function of Core:Monomer Ratio
(as determined by THF GPC)

At high core:monomer ratios, the polystyrene-equivalent number-average
molecular mass is found to be relatively close to the calculated absolute mass of a
perfectly branched dendrimer of the same composition. With increasing molecular
weight, the dendrimer mass increases at a greater rate than that of its hyperbranched
analogue. Notwithstanding the earlier discussion relating to the interpretation of GPC
data, this observation may be viewed in terms of the likelihood of the polycondensation
reaction approaching completion. For hyperbranched polymers, the maximum
attainable degree of polymerisation rises as the proportion of terminator core
decreases. As a consequence, after a given number of reaction steps, although the
degree of polymerisation is independent of core:monomer ratio, the extent of reaction
is higher for hyperbranched polymers with a greater core:monomer ratio. In the case
of any monodisperse dendrimer, the degree of polymerisation is always equal to the
maximum attainable value for such a structure, irrespective of molecular size. This
suggests that the ratio of the hyperbranched polymer polystyrene-equivalent number-
average molecular mass to the calculated absolute mass of the dendrimer analogue

with the same structural composition provides a qualitative measure of the extent of reaction for the hyperbranched polymer.

The polydispersity of the hyperbranched polymers rises smoothly with increasing molecular mass brought about by a reduction of the core:monomer ratio. The data presented in Figure 5.13 indicates that the relatively low mass polymers have a polydispersity of around 2, which is the same as that found in linear polymerisation reactions as the extent of reaction, p, approaches unity. With decreasing core:monomer ratio, the polydispersity rises at an increasing rate initially before tailing off to a finite value of approximately 3. Using a statistical approach, Flory[10,11] predicted that for AB_2 systems, the polydispersity would rise at an increasing rate with the increasing fraction of reacted B groups, α, (equation 5.12), tending to infinity as $\alpha \rightarrow \alpha_{max}$. By incorporation of a variable proportion of B_3 terminator core, it has been possible to restrict the value of α and so provide evidence to support the Flory model at low and intermediate conversion.
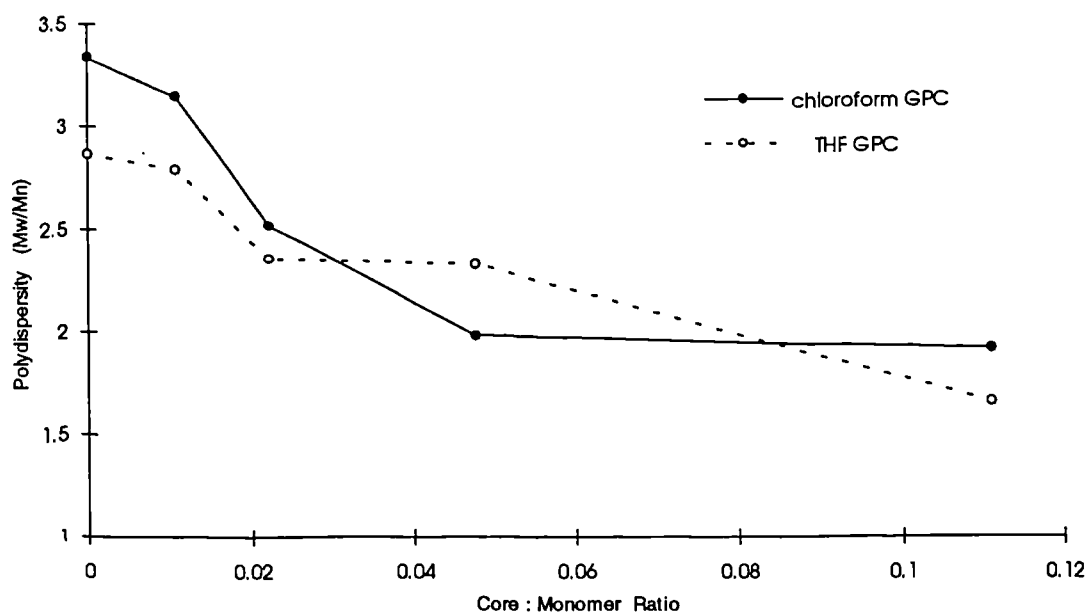
Figure 5.13 Polydispersity as a Function of Core:Monomer Ratio

(as determined by chloroform and THF GPC)

In the Flory statistical approach, the assumption is made that intramolecular condensation reactions do not occur. Clearly, as the polymerisation progresses, the number of unreacted B groups in any chosen molecule increases with respect to the total number of unreacted B groups. As such, the likelihood of intramolecular condensation and consequent termination increases with increased molecular mass and compounds the already serious problem of growth inhibition due to congestion of the reactive site at the focal point of the hyperbranched wedge. This leads to a failure to achieve 100% conversion resulting in a deviation from the Flory model.

Fréchet[8] has suggested that the broad polydispersity of hyperbranched materials may be accounted for, at least partially, by the presence of both linear (type l) and branched (type b) repeat units within their structures however examination of the recent literature provides little or no evidence in support of this view. In view of the results presented above, it is proposed that it is the statistical nature of stepwise polycondensation with respect to the extent of reaction that is the dominant influence in determining the polydispersity.

Thermogravimetric analysis has shown that at a constant heating rate of $10°C$ min^{-1} in a nitrogen atmosphere, all of the hyperbranched polymers retain 98% of their mass up to $365 \pm 5°C$.

On annealing each polymer at $300°C$ for 2 minutes and cooling at a rate of $10°C$ min^{-1} to $25°C$, where it was held for a further 5 minutes, a DSC thermogram was recorded at a heating rate of $10°C$ min^{-1} to $300°C$. This procedure was repeated twice for each polymer using a new sample each time. In each case, no melting peak was observed indicating little or no sample crystallinity as confirmed by X-ray powder diffraction studies and discussed earlier.

A glass transition temperature has been observed for each polymer and the results are displayed in Figure 5.14.
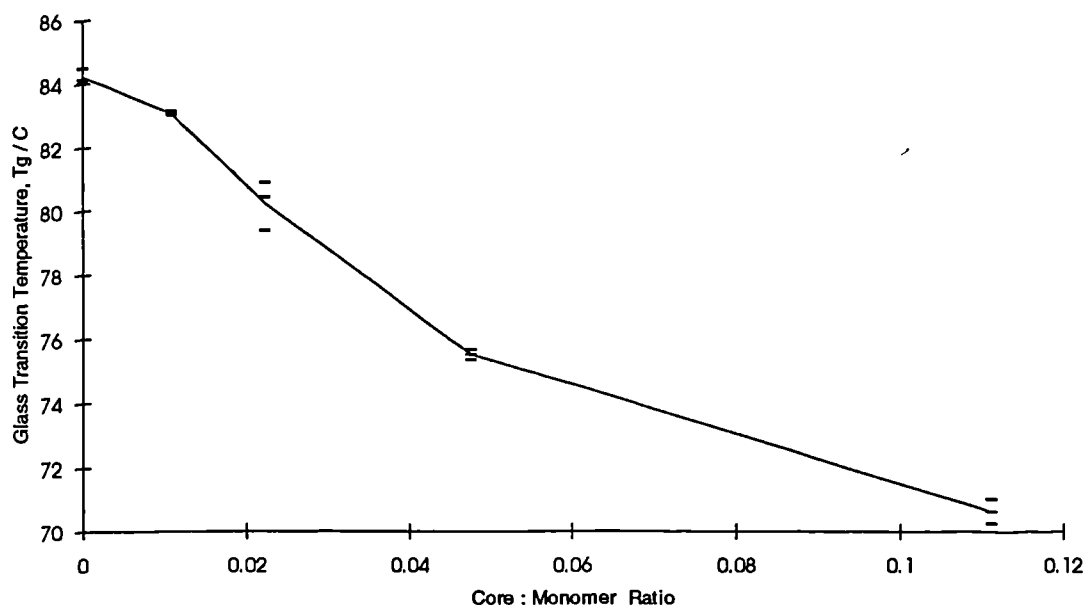
Figure 5.14 Glass Transition Temperature as a Function of Core:Monomer Ratio

(as determined by DSC)

For conventional linear polymers, the glass transition temperature, T_g,

increases with increasing molecular mass up to a limiting value, $T_{g\infty}$, which according

to the chain-end free volume theory may be described by the relationship

$$T_g = T_{g\infty} - K / M_n \qquad \text{(eqn. 5.13)}$$

where K is a constant for a given polymer since the number of chain ends in a linear

polymer is always equal to 2.[17] This follows from the decrease in the free volume of

the system with increasing molecular mass caused by a reduction in the number of end

groups per unit volume.[18]

In a recent investigation into the variation of glass transition temperature with

molecular weight for dendritic polyethers and polyesters, Fréchet and co-workers[19]

concluded that the conventional plot of T_g against $1/M_n$ has little meaning for dendritic

macromolecules since the number of chain ends, n_e, in each molecule increases as a

function of molecular weight. They proposed a modified expression (equation 5.14) to

126

account for this phenomenon and suggested that hyperbranched polymers such as the polyesters described by Voit and Turner[20] also conform to this modified expression.

$$T_g = T_{g\infty} - K'(n_e / M_n)$$ (eqn. 5.14)
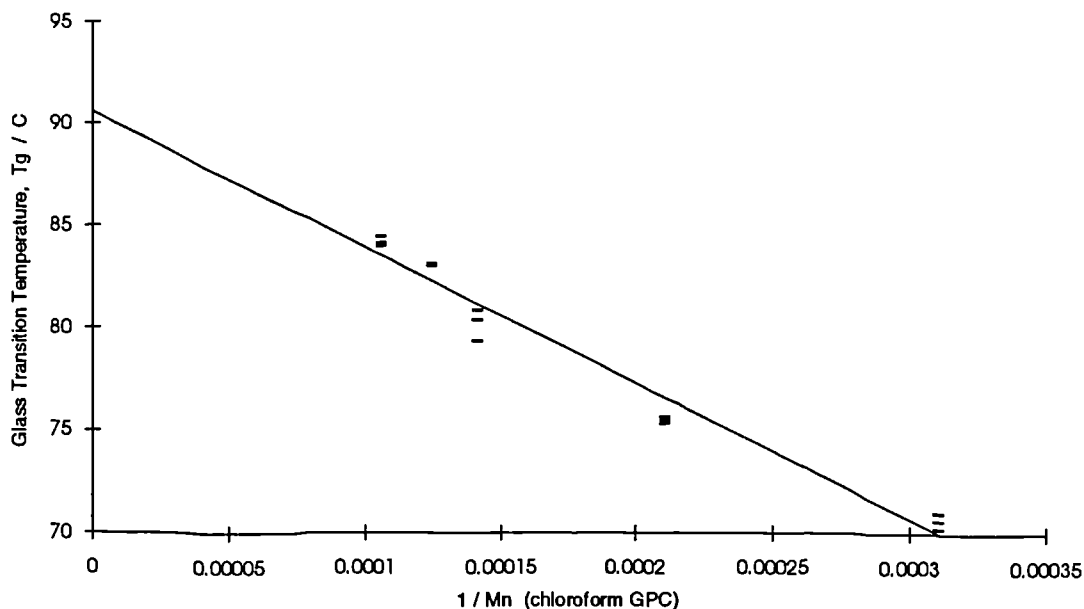
Figure 5.15 Glass Transition Temperature as a Function of $1 / M_n$

Analysis of data from our own hyperbranched polymers indicates that there is a linear relationship between the measured T_g and the reciprocal of the polystyrene-equivalent number-average molecular weight (Figure 5.15). If the Fréchet modification of the T_g / M_n relationship is to hold for our materials, this implies that there is a linear relationship between T_g and n_e/M_n, i.e. the number of chain ends is constant irrespective of molecular size. It has already been shown that this is not the case since the determination of a constant branching factor, f_{br}, irrespective of molecular mass implies that the proportion of terminal units, or chain ends, is also constant and that the chain end density is independent of molecular mass. This leads to the conclusion that for a series of hyperbranched polymers with the same branching factor irrespective of molecular weight, the value of n_e/M_n will also be independent of molecular weight. Equation 5.14 thus predicts that for hyperbranched polymers, T_g is independent of molecular mass, which has quite clearly been shown not to be the case.

Thus our work suggests that for hyperbranched polymers, it is not possible to account for the change in glass transition temperature as a function of molecular mass solely in terms of the simple chain-end free volume model.

The linearity of the graph in Figure 5.15 indicates that the effective chain end density of our hyperbranched molecules decreases with increasing molecular mass in a similar way to that for linear polymers (equation 5.13) although it is known that the actual chain end density remains unchanged. It is proposed that this situation may arise as a consequence of the extensively branched nature of our materials. As can be envisaged from Figure 5.7, terminal groups located on or near the surface of a hyperbranched molecule will have a greater mobility and thus a larger free volume than those buried within the branching structure.

The situation may be rationalised in terms of an increasing number of buried chain ends as a proportion of the whole with increasing molecular size. If this is the case then the increase in T_g with increasing molecular mass for hyperbranched polymers may be regarded as a physical consequence of the imperfect branching structure of such materials.

Hyperbranched Polyester/PET Blends

The work described in Chapter 4 demonstrated that the blending of a dendrimer with PET can lead to an increase in the overall interchain interaction resulting in enhanced molecular orientation for a given draw ratio. This has been rationalised in terms of the increased chain entanglement brought about by the incorporation of the dendrimer structure. If this is the case, it may be that the effect is dependent on the extensively branched topology of the dendrimer and not necessarily on its monodisperse nature. As a result, it may be possible to obtain similar effects by incorporation of less well-defined yet highly branched additives such as the hyperbranched polyesters described earlier.

Blend Preparation

Mixtures of hyperbranched polymers and PET were dissolved in dichloroacetic acid ($CHCl_2CO_2H$) to form 10% w/w hyperbranched polymer/PET (hyperblend) solutions. After stirring to ensure complete mixing, each solution was poured into a large excess of distilled water from which a white solid was precipitated. This was collected by filtration, washed several times with water and extracted using a Soxhlet apparatus with distilled water for 24 hours to remove any residual traces of dichloroacetic acid. The solid was dried under vacuum (50°C,0.1Torr) to constant mass. A sample of pure PET was prepared in a similar manner in order to provide an appropriate control sample. PET ($M_w \approx 20,000$) was supplied by ICI p.l.c.

Differential Scanning Calorimetry Analysis of the Hyperblends

Each sample was heated at a rate of $200°Cmin^{-1}$ to 280°C at which it was held for 2 minutes. After cooling at a rate of $10°Cmin^{-1}$ to 25°C, at which it was held for a further 5 minutes, a DSC thermogram was recorded at a heating rate of $10°Cmin^{-1}$ to 280°C. This procedure was repeated twice for each blend composition, using a new specimen each time. Although the PET melting point is virtually unchanged by the addition of the hyperbranched polymers, the glass transition temperature rises with incorporation of the larger hyperbranched polymers (Figure 5.16). This suggests that the larger hyperbranched polymers are acting as antiplasticising agents and enhancing

the overall interchain interactions in the same way as was found in the dendrimer[16]/PET blends whereas the smaller additives do not behave in this way.
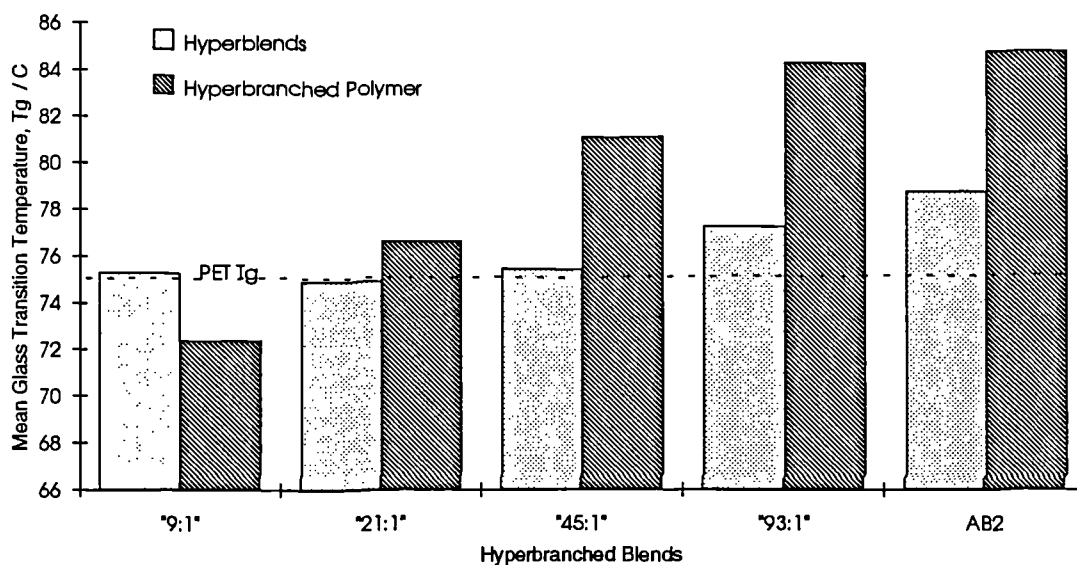
Figure 5.16 Glass Transition Temperatures of the 10% w/w Hyperblends and their Components

Mechanical Characterisation

On the basis of the thermal characterisation of the hyperblends, blends incorporating the larger hyperbranched materials have been selected to assess the potential of hyperbranched polyesters for modification of the drawing behaviour of PET. The same sample preparation methods and experimental techniques have been used as those described in Chapter 4. Preliminary work has focused on the change in molecular orientation as a function of draw ratio and a comparison made with the results obtained from studies of the dendrimer/PET blends.

Figure 5.17 shows the birefringence of blends incorporating the larger hyperbranched polymers as a function of draw ratio. On comparison with Figure 4.16, it is noted that all of these hyperblends appear to behave in a similar way to the dendrimer [16]/PET blend in that incorporation of the branched polymer leads to enhanced orientation for a given draw ratio with respect to the PET control sample. It is reasonable to suggest that as in the dendrimer case, this effect may be attributed to the greater degree of chain entanglement brought about by the presence of the

130

Mechanical Testing of Hyperbranched Polymer / PET Drawn Films (Birefringence vs. $\lambda*\lambda - 1/\lambda$)

$\lambda*\lambda - 1/\lambda$

○ PET (measured) ● 10% AB2/PET ■ 10% 93:1/PET
▲ 10% 45:1/PET
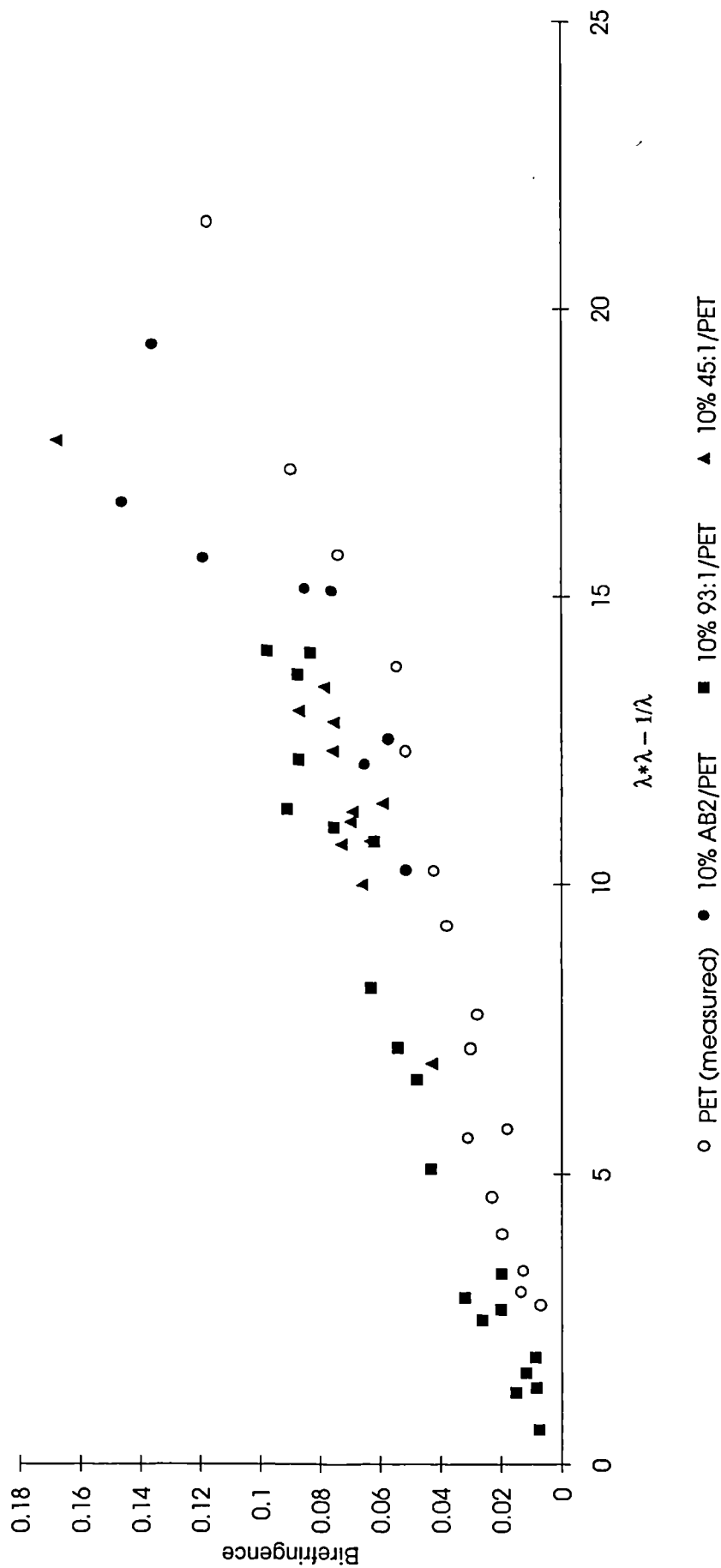
Figure 5.17

extensively branched structures. Furthermore, the extent of orientation enhancement appears to be largely unaffected by the size of the incorporated hyperbranched polymer which indicates that the effective entanglement density may be ascribed to the localised branching structure rather than the hyperbranched polymer size however it is clear that further work in this area is necessary to understand this phenomenon.

Summary

A new approach to the controlled synthesis of hyperbranched polymers has been demonstrated. This technique has facilitated the production of a new series of hyperbranched materials without the need to resort to the laborious and time-consuming methods employed in the synthesis of their dendrimer analogues.

This work has allowed for an experimental assessment of some of the points made in the theoretical treatment of the subject and also describes the use of such randomly branched structures to replicate the effects brought about by the blending of well-defined species into the commodity polymer PET.

Experimental

All organic reagents were obtained from Aldrich Chemical Co. and used without further purification. Melting points were obtained on an Electrothermal digital melting point apparatus unless otherwise stated and reported without correction. Infra-red spectra were recorded on a Perkin-Elmer 1600 series FTIR. Thermogravimetric analyses were carried out using a Stanton Redcroft TG 760 Thermobalance. Differential scanning calorimetry was performed on a Perkin-Elmer DSC-7 at a scanning rate of 10°C/min. ^{1}H and ^{13}C n.m.r. spectra were recorded on a Varian 200MHz Gemini or Varian 400MHz spectrometer as indicated and were referenced to TMS. Gel permeation chromatography was carried out in chloroform using three 5μm columns of PL gel with pore size 100Å, 10^3Å and 10^5Å and a Waters differential refractometer detector and in tetrahydrofuran using two 10μm mixed columns and a Viscotek differential refractometer / viscometer. X-ray diffraction was carried out on a Siemens Diffraktometer D5000.

The I.R. and n.m.r. spectra for all compunds are shown in Appendix 2.

Synthesis of dimethyl-5-hydroxyisophthalate. Boron trifluoride-methanol complex in excess methanol (450ml,50%BF$_3$w/w) was added to a stirred suspension of 5-hydroxyisophthalic acid (240g,1.32mol) in anhydrous methanol (1200ml) and the mixture refluxed with stirring for 24h. On cooling the hot solution to room temperature, a white slurry formed. After removal of the solvent by filtration under reduced pressure, the residue was recrystallised from distilled water (5000ml), filtered and washed with cold hexane. The residue was dried under vacuum (50°C,0.1mmHg) to yield dimethyl-5-hydroxyisophthalate as a fine white fibrous solid (247.78g,1.18mol,89.4%,mp.164-165°C lit[21] 159-160°C) which was characterised by ^{1}H n.m.r. (d^6-acetone, 200MHz) δ3.91 (s,6H,C$\underline{H}_3$), δ7.68 (d,1.48Hz,2H,Ar$\underline{H}$), δ8.10 (t,1.48Hz,1H,Ar$\underline{H}$), δ9.08 (s,1H,O$\underline{H}$), ^{13}C n.m.r. (d^6-acetone, 50MHz) δ52.63 ($\underline{C}$H$_3$), δ121.11, δ122.16 (aromatic $\underline{C}$-H), δ132.90 (aromatic $\underline{C}$-R), δ158.58 (aromatic $\underline{C}$-O), δ166.38 ($\underline{C}$=O), I.R. (KBr disc) 3361.5 cm^{-1} (broad, H-bonded O-H stretch), 3012.8 cm^{-1} (w, aryl-H C-H stretch), 2963.3 cm^{-1} (w, saturated C-H stretch),

1704.8 cm^{-1} (s, aromatic ester C=O vibration), 1600.0 cm^{-1} (s, aryl-H C-H vibration),

736.4 cm^{-1} (s, aryl-H C-H out-of-plane vibration).

Synthesis of 2-bromoethyl acetate. Concentrated sulphuric acid (6ml) was

added to a mixture of acetic anhydride (600.00g,5.88mol) and 2-bromoethanol

(200.00g,1.60mol) and the mixture refluxed with stirring overnight. On cooling, the

mixture was poured into water (2000ml) and extracted with dichloromethane

(4×500ml). The combined organic layers were washed with water (3×2000ml), dried

(MgSO$_4$) and the solvent removed by evaporation. The residue was distilled at

atmospheric pressure (158-160°C lit[21] 159°C) to yield 2-bromoethyl acetate as a

colourless oil (214.92g,1.29mol,80.4%) which was characterised by ^{1}H n.m.r. (CDCl$_3$,

200MHz) δ2.04 (s,3H,C$\underline{H}_3$), δ3.46 (t,6.09Hz,2H,C$\underline{H}_2$Br), δ4.32 (t,6.16Hz,2H,C$\underline{H}_2$O),

^{13}C n.m.r. (CDCl$_3$, 50MHz) δ21.19 ($\underline{C}H_3$), δ29.19 ($\underline{C}H_2$Br), δ64.24 ($\underline{C}H_2$O), δ170.92

($\underline{C}$=O), I.R. (liquid) 2969.3 cm^{-1} (w, saturated C-H stretch), 1746.6 cm^{-1} (s, aliphatic

ester stretch).

Synthesis of dimethyl-5-(2-acetoxyethoxy)isophthalate. Anhydrous

potassium carbonate (161.00g,1.17mol) was added to a stirred solution of dimethyl-5-

hydroxyisophthalate (245.00g,1.17mol) and 2-bromoethyl acetate (183.70g,1.10mol)

in anhydrous acetone (1600ml) and the mixture stirred and refluxed for 72h. with a

potassium hydroxide drying tube attached to the top of the condenser.

On cooling, the mixture was filtered and the residue washed with acetone. Acetone

was removed from the combined filtrate by evaporation to yield a light tan-coloured

slurry. Dichloromethane (1000ml) was added and the solution washed with aqueous

sodium hydroxide solution (10×400ml,2M), dried (MgSO$_4$) and the solvent evaporated

to give a yellow oil that solidified on cooling. This was recrystallised from hot hexane

to yield dimethyl-5-(2-acetoxyethoxy)isophthalate as a fine white powder

(120.51g,0.407mol,37.0%,mp.79.5-80.5°C) which was characterised by ^{1}H n.m.r.

(CDCl$_3$, 200MHz) δ2.11 (s,3H,C$\underline{H}_3$), δ3.94 (s,6H,C$\underline{H}_3$), δ4.27 (t,4.84Hz,2H,C$\underline{H}_2$O),

δ4.46 (t,5.16Hz,2H,C$\underline{H}_2$O), δ7.78 (d,1.32Hz,2H,Ar$\underline{H}$), δ8.30 (m,1H,Ar$\underline{H}$), ^{13}C n.m.r.

(CDCl$_3$, 100MHz) δ20.84 (acetate $\underline{C}H_3$), δ52.45 (CO$_2$$\underline{C}H_3$), δ62.50 ($\underline{C}H_2$OC=O),

δ66.92 ($\underline{C}H_2$OAr), δ119.87, δ120.28 (aromatic $\underline{C}$-H), δ131.82 (aromatic $\underline{C}$-R),

$\delta158.51$ (aromatic $\underline{C}$-O), $\delta165.97$ (Ar$\underline{C}$=O), $\delta170.90$ (CH$_2$O$\underline{C}$=O), I.R. (KBr disc) 3090.5 cm^{-1} (w, aryl-H C-H stretch), 2959.5 cm^{-1} (w, saturated C-H stretch), 1735.1 cm^{-1} (s, aliphatic C=O stretch), 1716.3 cm^{-1} (s, aromatic C=O stretch), 1599.0 cm^{-1} (m, aryl-H C-H vibration), 1254.6 cm^{-1} (s, aryl C-O stretch), 757.7 cm^{-1} (s, aryl-H out-of-plane vibration).

Synthesis of dimethyl-5-(2-hydroxyethoxy)isophthalate. Dimethyl-5-(2-acetoxyethoxy)isophthalate (117.00g,0.395mol) was added to a stirred solution of potassium hydroxide (0.87g,0.0155mol) in dry methanol (900ml) and the mixture stirred at 30°C overnight. The solution was poured into distilled water (3000ml) and the solution acidified to pH1 with aqueous hydrochloric acid solution (10% v/v).

On cooling in an ice-bath, the mixture was filtered and the residue washed with cold hexane. The residue was dried under vacuum (40°C,0.1mmHg) to yield dimethyl-5-(2-hydroxyethoxy)isophthalate as a white crystalline solid (93.51g,0.368mol,93.2%,mp.112-112.5°C) which was characterised by ^{1}H n.m.r. (CDCl$_3$, 400MHz) $\delta2.42$ (broad,1H,O$\underline{H}$), $\delta3.95$ (m,6H,C$\underline{H}_3$), $\delta4.02$ (m,2H,C$\underline{H}_2$OH), $\delta4.18$ (m,2H,C$\underline{H}_2$OAr), $\delta7.76$ (m,2H,Ar$\underline{H}$), $\delta8.28$ (m,1H,Ar$\underline{H}$), ^{13}C n.m.r. (CDCl$_3$, 100MHz) $\delta52.48$ ($\underline{C}$H$_3$), $\delta61.20$ ($\underline{C}$H$_2$OH), $\delta69.84$ ($\underline{C}$H$_2$OAr), $\delta119.83$, $\delta123.31$ (aromatic $\underline{C}$-H), $\delta131.79$ (aromatic $\underline{C}$-R), $\delta158.71$ (aromatic $\underline{C}$-O), $\delta166.05$ ($\underline{C}$=O), I.R. (KBr disc) 3318.9 cm^{-1} (broad, O-H stretch), 3086.6 cm^{-1} (w, aryl-H C-H stretch), 2951.7 cm^{-1} (s, saturated C-H stretch), 1727.4 cm^{-1} (s, C-O absorption), 1596.0 cm^{-1} (s, aryl-H vibration), 1250.7 cm^{-1} (s, aryl C-O stretch), 754.1 cm^{-1} (s, C-H out-of-plane vibration).

Synthesis of trimethyl-1,3,5-benzenetricarboxylate. 1,3,5-Benzene tricarbonyl trichloride (5.00g,0.0188mol) was added to sodium-dried methanol (50ml) and the mixture stirred for 30 minutes to form a white suspension. On cooling in an ice-bath, the precipitate was collected by filtration and washed with cold methanol to yield trimethyl-1,3,5-benzenetricarboxylate as a white crystalline solid (4.25g,0.0169mol,89.7%,mp.147.0-148.0°C lit[21] 144°C) which was characterised by ^{1}H n.m.r. (CDCl$_3$, 200MHz) $\delta3.99$ (s,9H,C$\underline{H}_3$), $\delta8.86$ (s,3H,Ar$\underline{H}$), ^{13}C n.m.r. (CDCl$_3$, 50MHz) $\delta53.11$ ($\underline{C}$H$_3$), $\delta131.67$ (aromatic $\underline{C}$-R), $\delta135.06$ (aromatic $\underline{C}$-H), $\delta165.88$

(C=O), I.R. (KBr disc) 3097.8 cm^{-1} (w, aryl-H C-H stretch), 3015.5 cm^{-1} (w, aryl-H C-H stretch), 2956.7 cm^{-1} (s, saturated C-H stretch), 2848.3 cm^{-1} (w, saturated C-H stretch), 1731.3 cm^{-1} (s, ester C=O absorption), 1432.3 cm^{-1} (s, saturated C-H deformation).

References

1. Hunter, W.H. and Woolett, G.H., J.Am.Chem.Soc. 43, 135 (1921)

2. Jacobson, R.A., J.Am.Chem.Soc. 54, 1513 (1932)

3. Bolker, H.I., "Natural and Synthetic Polymers", Marcel Dekker (1974)

4. Tomalia, D.A., Naylor, A.M. and Goddard, W.A. III, Angew.Chem.Int.Ed.Engl. 29, 138 (1990)

5. Kim, Y.H. and Webster, O.W., Macromolecules 25, 5561 (1992)

6. Hawker, C.J., Lee, R. and Fréchet, J.M.J., J.Am.Chem.Soc. 113, 4583 (1991)

7. Turner, S.R., Voit, B.I. and Mourey, T.H., Macromolecules 26, 4617 (1993)

8. Uhrich, K.E., Hawker, C.J., Fréchet, J.M.J. and Turner, S.R., Macromolecules 25, 4583 (1992)

9. Kim, Y.H., Macromol.Symp. 77, 21 (1994)

10. Flory, P.J., J.Am.Chem.Soc. 74, 2718 (1952)

11. Flory, P.J., "Priciples of Polymer Chemistry", Cornell University Press (1953)

12. Walter, F., Turner, S.R. and Voit, B.I., Polym.Prep.Am.Chem.Soc. Div.Polym.Chem. 33, 79 (1992)

13. Hallas, G., J.Chem.Soc. 5770 (1965)

14. Ando, T., Yamawaki, J., Kawate, T., Sumi, S. and Hanafusa, T., Bull.Chem.Soc.Jpn. 55, 2504 (1982)

15. Furniss, B.S., Hannaford, A.J., Smith, P.W. and Tatchall, A.R., "Vogel's Textbook of Practical Organic Chemistry" (5th edn.), Longman (1989)

16. Gümther, B. and Zachmann, H.G., Polymer 24, 1008 (1983)

17. Richardson, M.J. in "Comprehensive Polymer Science V1", Allen, G. and Bevington, J.C. (Eds.), Pergamon (1989)

18. Sperling, L.H., "Introduction to Physical Polymer Science" (2nd edn.), Wiley (1992)

19. Wooley, K.L., Hawker, C.J., Pochan, J.M. and Fréchet, J.M.J., Macromolecules 26, 1514 (1993)

20. Voit, B.I. and Turner, S.R., Polym. Prepr.,Am.Chem.Soc., Div.Polym.Chem. 33, 184 (1992)

21.	"Dictionary of Organic Compounds" (5th edn.), Buckingham, J. and Donaghy, S.M. (Eds.), Chapman and Hall (1982)

In principle, the degree of branching of a hyperbranched polymer may be determined by consideration of the relative peak intensities in quantitative n.m.r. spectroscopy. In favourable cases, where the peaks associated with terminal, linear and branched units are distinct and may be identified by the use of model compounds and correlation tables, the branching factor f_{br} can be calculated from the peak integrals using equation 5.1.[1-3]
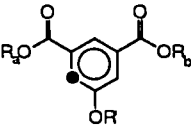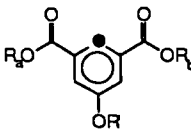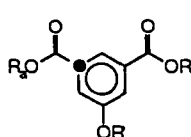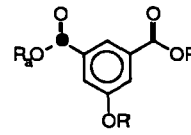
Using a Bruker AMX500 spectrometer, the ^{1}H and ^{13}C n.m.r. spectra of the hyperbranched polyesters studied in the course of this work are not resolved sufficiently well to allow the branching factor to be calculated as described above although the ^{13}C n.m.r. spectra do show appreciable fine structure. With reference to the spectra of the model compounds dimethyl-5-(2-acetoxyethoxy)isophthalate and dimethyl-5-(2-hydroxyethoxy)isophthalate and the use of appropriate correlation tables,[4] in most cases, peaks from terminal (dimethyl ester), linear (methyl / substituted ethyl ester) and branched (di-(substituted ethyl ester)) units (Figure S5.1.1) have been identified.
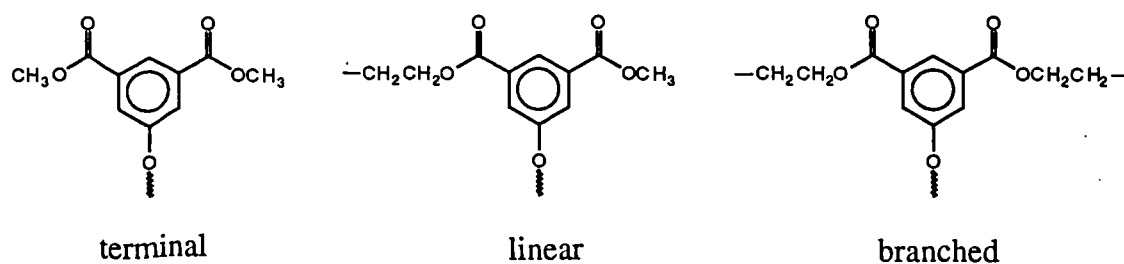
Figure S5.1.1 Types of Repeat Unit in the Hyperbranched Polyesters

Quantitative ^{13}C n.m.r. spectra have been recorded using a pulse relaxation delay of 10 seconds (Figure S5.1.2). Peak deconvolution has been carried out using a non-linear least squares Lorentzian curve fitting routine[5] (Figures S5.1.3 - S5.1.5). Integration of the deconvoluted peaks has enabled an independent determination of the degree of branching to be made from different regions of the same spectrum.

Where it has not possible to assign fully the peaks in a region of the spectrum, a number of possible values for the branching factor can be calculated (Table S5.1.1).

Peak Position	R_a, R_b	Assignment	Possible f_{br}	Likely f_{br}
δ52.38	—	$\underline{C}H_3$	—	—
δ63.41	—	$\underline{C}H_2OCO$	—	—
δ66.30	—	$\underline{C}H_2OAr$	—	—
δ119.78[c] δ119.95[c] δ120.01* δ120.11*	$(CH_2)_2$-, $(CH_2)_2$- Me, Me Me, $(CH_2)_2$- $(CH_2)_2$-, Me		0.40, 0.49, 0.60	0.60
δ123.34 δ123.42 δ123.60	Me, Me Me, $(CH_2)_2$- $(CH_2)_2$-, $(CH_2)_2$-		0.61	0.61
δ131.36[d] δ131.43[d] δ131.76[e] δ131.81[e]	$(CH_2)_2$-, $(CH_2)_2$- $(CH_2)_2$-, Me Me, Me Me, $(CH_2)_2$-		0.33, 0.67	0.67
δ158.44	—	aromatic C-O	—	—
δ165.16[f] δ165.23[f] δ165.76[g] δ165.82[g]	$(CH_2)_2$-, $(CH_2)_2$- $(CH_2)_2$-, Me Me, Me Me, $(CH_2)_2$-		0.37, 0.63	0.63

c,d,e,f,g   These pairs of peaks can only be assigned unambiguously as a result of the need for self-consistency of the data from different regions of the spectrum.

*   This pair of peaks cannot be assigned unambiguously using this technique.

Table S5.1.1 Peak Assignments and Branching Factor Determination from Different Regions of the AB_2 Polyester Quantitative [13]C Spectrum

In each case, one of the possible solutions for f_{br} is approximately equal to the unique solution $f_{br} = 0.61$ derived from calculations on the aromatic ring apex carbon atom signals ($\delta 123 - 124$). In order to be self-consistent, the degree of branching of the polymer should be independent of the region of the spectrum from which it was calculated. Further peak assignments can be made on the basis of this necessary constraint (Table S5.1.1). Consequently, the degree of branching of the AB_2 hyperbranched polyester has been determined to be within the range 0.60 - 0.67.

52.25
52.38
52.50
52.63

63.28
63.41
63.65
66.30
76.53
76.65
76.70
76.77
76.90
77.03
77.09
77.10
77.15
77.23
77.28
77.40
77.53
77.65

119.78
120.01
120.11
123.34
123.42
123.60

131.36
131.43
131.76
131.81

158.44
158.69
159.51
165.16
165.23
165.76
165.82
ppm
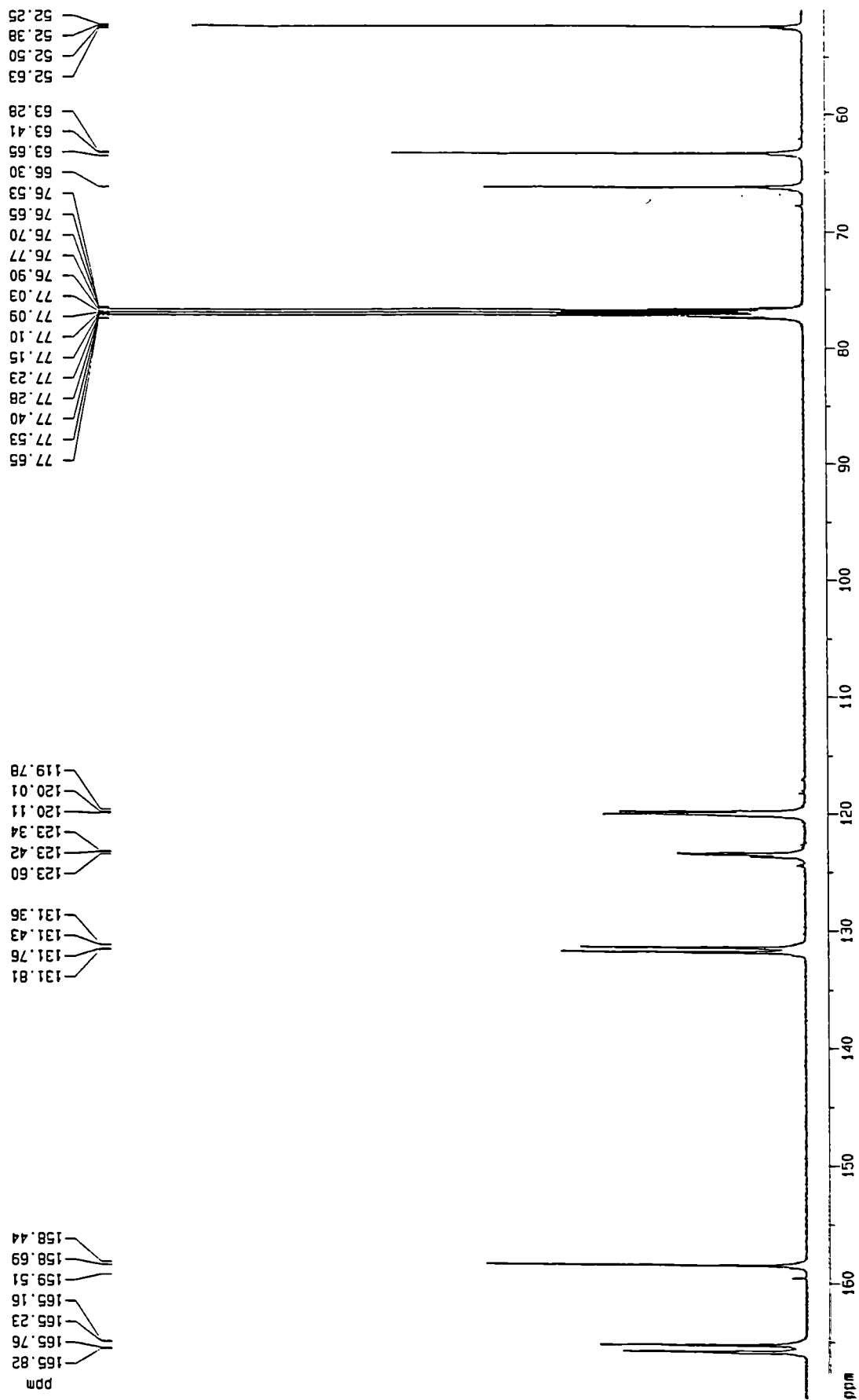
Figure S5.1.2 ^{13}C n.m.r. Spectrum of the AB_2 Hyperbranched Polyester in $CDCl_3$

Recorded on a Bruker AMX 500 Spectrometer

119.78 ——

119.93 ——
120.01 ——
120.12 ——

123.34 ——
123.42 ——

123.60 ——

120

ppm

ppm
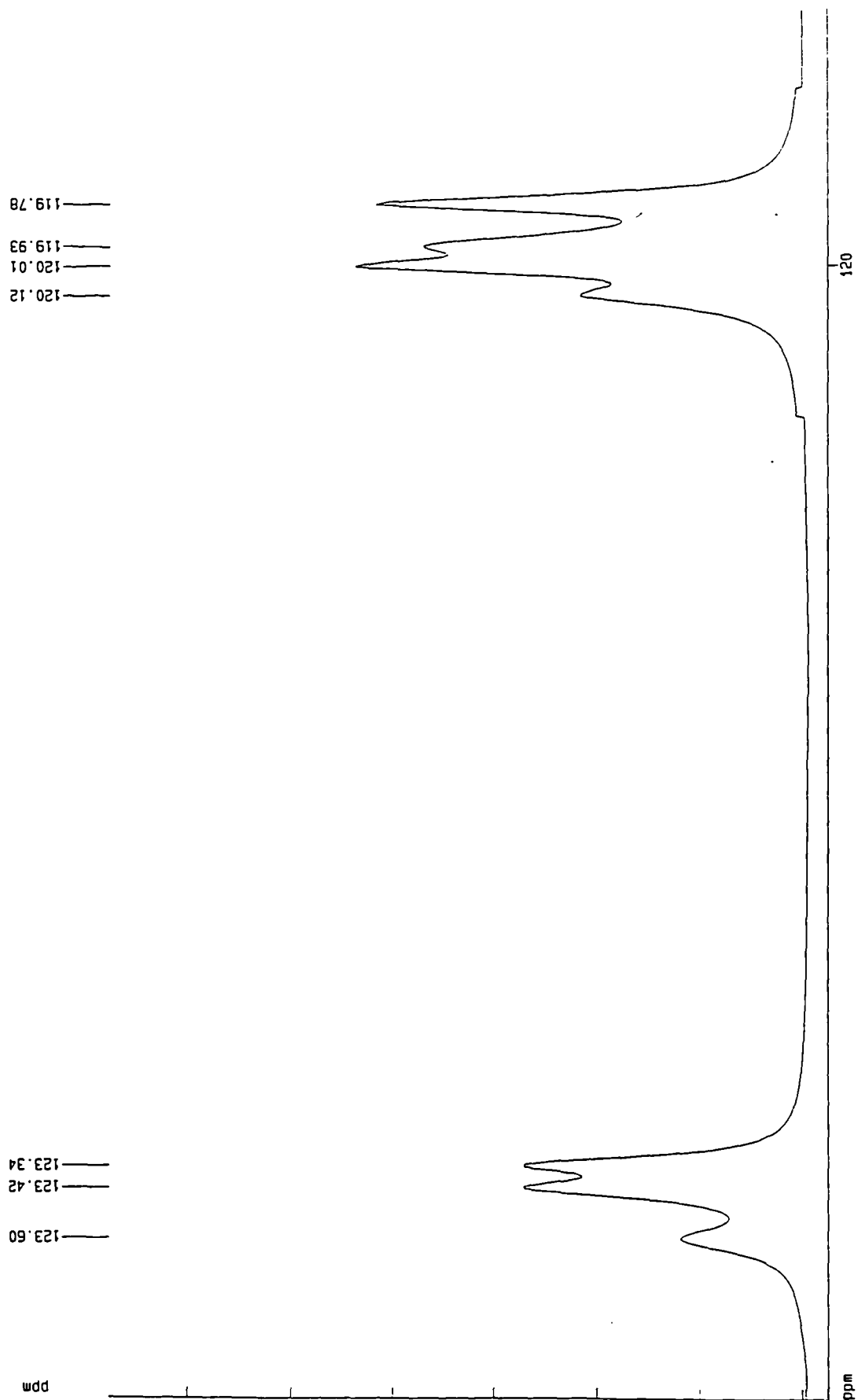
Figure S5.1.3 Lorentzian Curve Fit of Figure S5.1.2 (Region δ119 - 124)
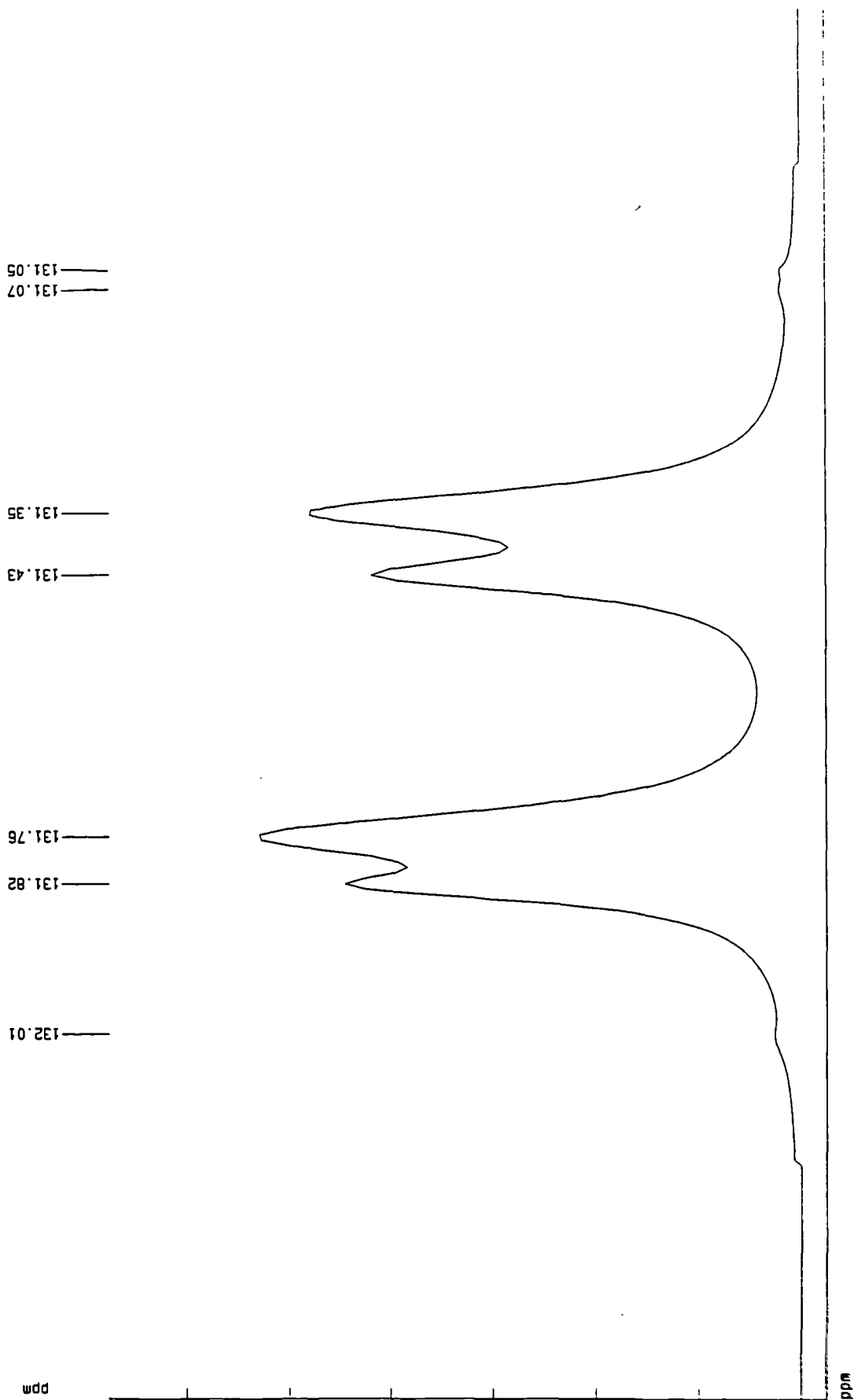
143

131.05 ——
131.07 ——

131.35 ——

131.43 ——

131.76 ——

131.82 ——

132.01 ——

ppm

Figure S5.1.4 Lorentzian Curve Fit of Figure S5.1.2 (Region δ130 - 133)

165.16

165.23

165.47

165.76

165.82

ppm

Figure S5.1.4 Lorentzian Curve Fit of Figure S5.1.2 (Region δ164 - 167)

145
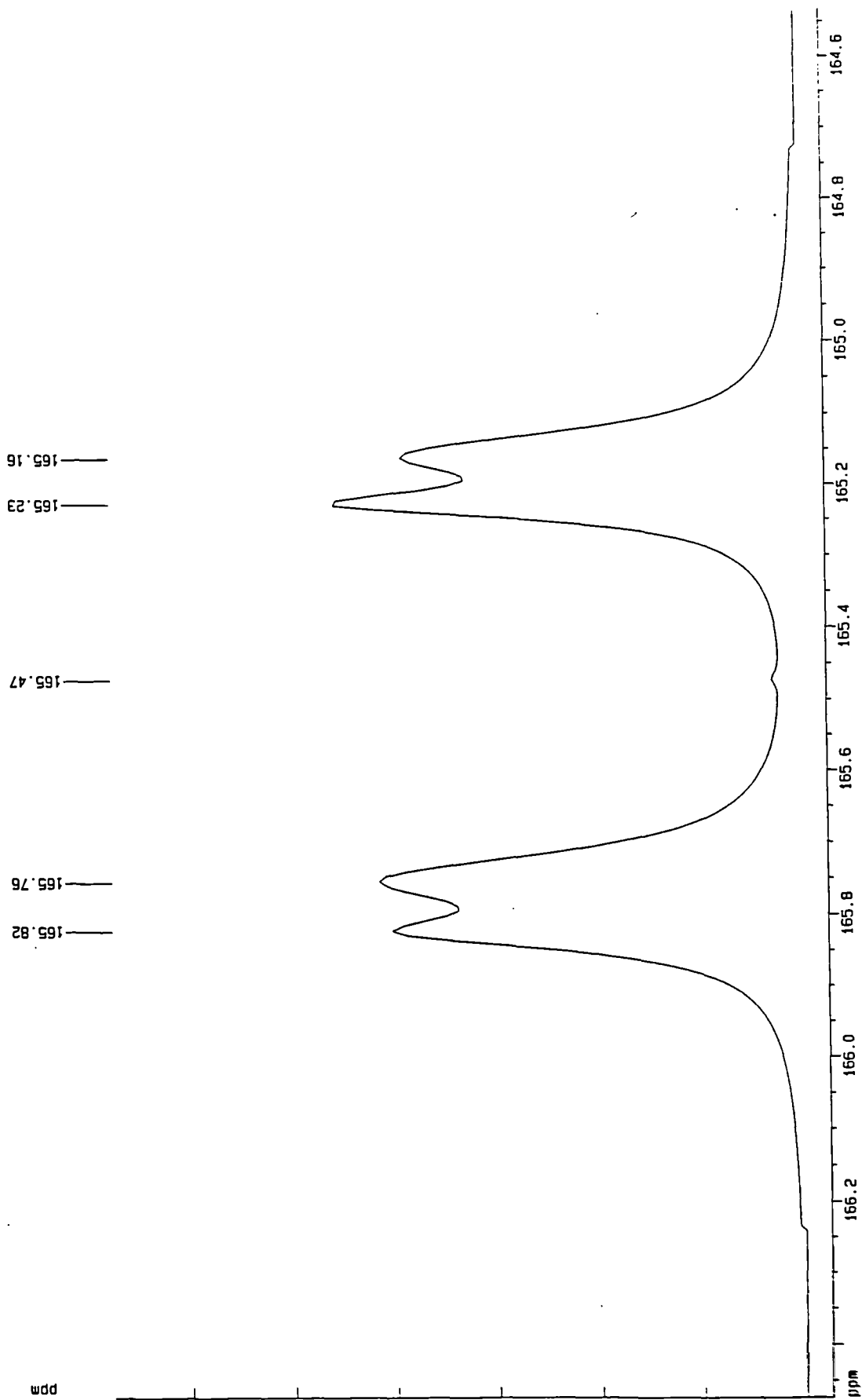
References

1. Hawker, C.J., Lee, R. and Fréchet, J.M.J., J.Am.Chem.Soc. 113 4583 (1991)

2. Kim, Y.H. and Webster, O.W., Macromolecules 25 5561 (1992)

3. Turner, S.R., Voit, B.I. and Mourey, T.H., Macromolecules 26 4617 (1993)

4. Kalinowski, H., Berger, S. and Braun, S., "Carbon-13 NMR Spectroscopy", Wiley (1988)

5. Bruker UXNMR (Proprietary software)

146

Overview and Suggestions for Further Work

During the course of this project, it has become apparent that the synthesis of monodisperse dendrimers is a time-consuming and laborious process yet such work has been essential for the determination of the structure-property relationships of such extensively branched structures and in the characterisation of their blends with PET.

For the development of our understanding of the hyperbranched polyesters, it is important to address the question of accurate mass determination using such absolute techniques as light scattering and osmometry in the characterisation of these materials. Optimisation of polymerisation conditions may extend the range of molecular mass attainable and provide a means of changing the branching factor for a given series. There is also great scope for the control of physical parameters by the copolymerisation of the AB_2 monomer units with their linear analogues in varying proportions which suggests that chain mobility and thus glass transition temperature may be regulated in this way. By combination of this approach with the addition of an appropriate quantity of terminator core molecule to control the molecular mass, it would be possible, as least in principle, to prepare polymers of pre-determined and independently controlled mass and glass transition temperature.

The continued study of the blending of hyperbranched polyesters with PET and with other commercially important polymers is to be encouraged since this may reveal practical processing advantages. The investigation of melt blending to assess the feasibility of continuous production techniques is also highly desirable. During conventional melt processing, it seems likely that transesterification will occur and this may be a problem.

It is possible that the preparation of hyperbranched polymers will become an increasingly important activity both from an academic and an industrial standpoint bearing in mind both the structural insight and technological benefits that may be realised during the course of such work.

APPENDIX 1

N.M.R. and I.R. spectra (Chapter 2)
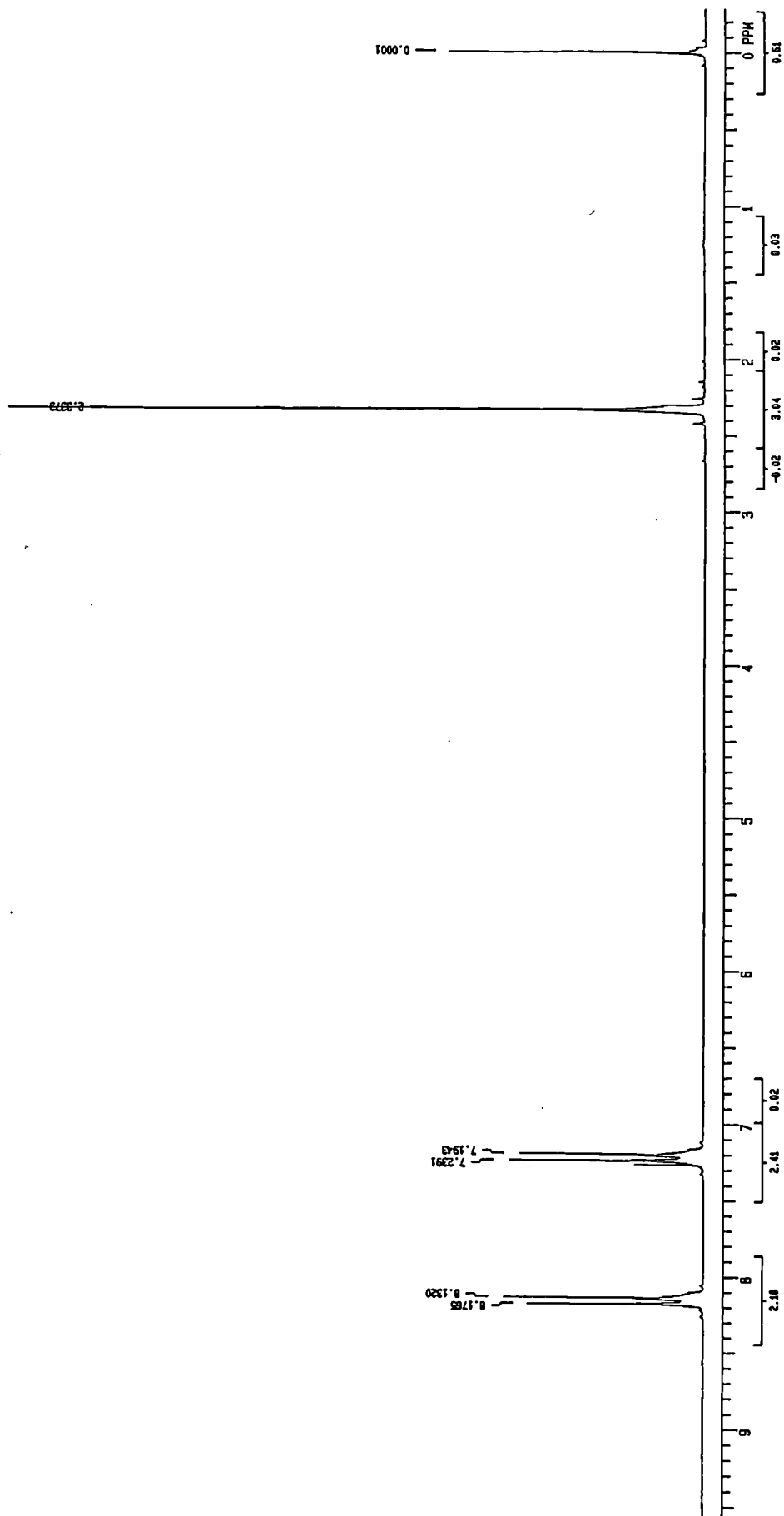
Figure A1.1 ^{1}H n.m.r. spectrum of 4-acetoxybenzoic acid (CDCl$_3$, 200MHz)
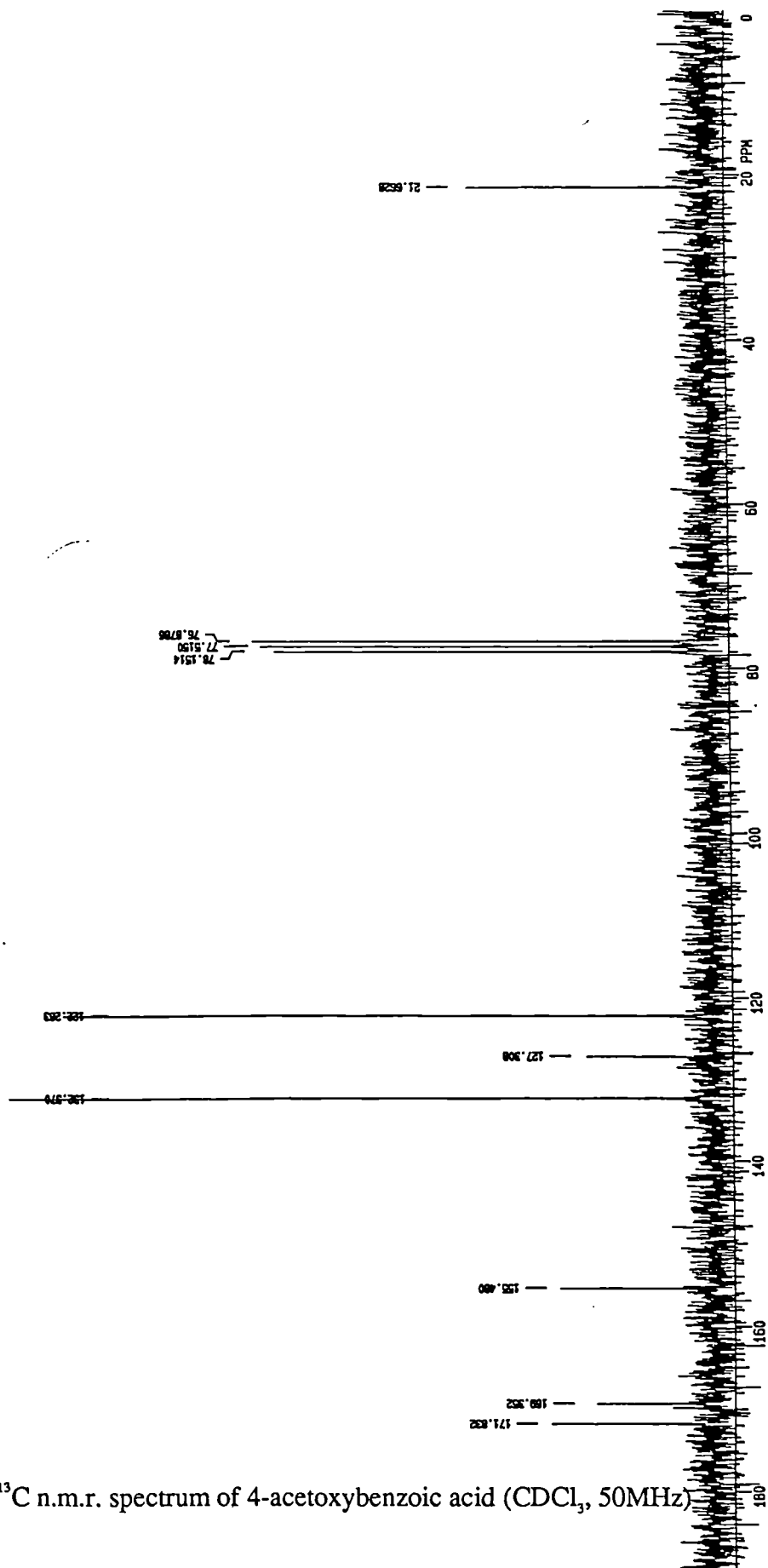
Figure A1.2 ^{13}C n.m.r. spectrum of 4-acetoxybenzoic acid (CDCl$_3$, 50MHz)
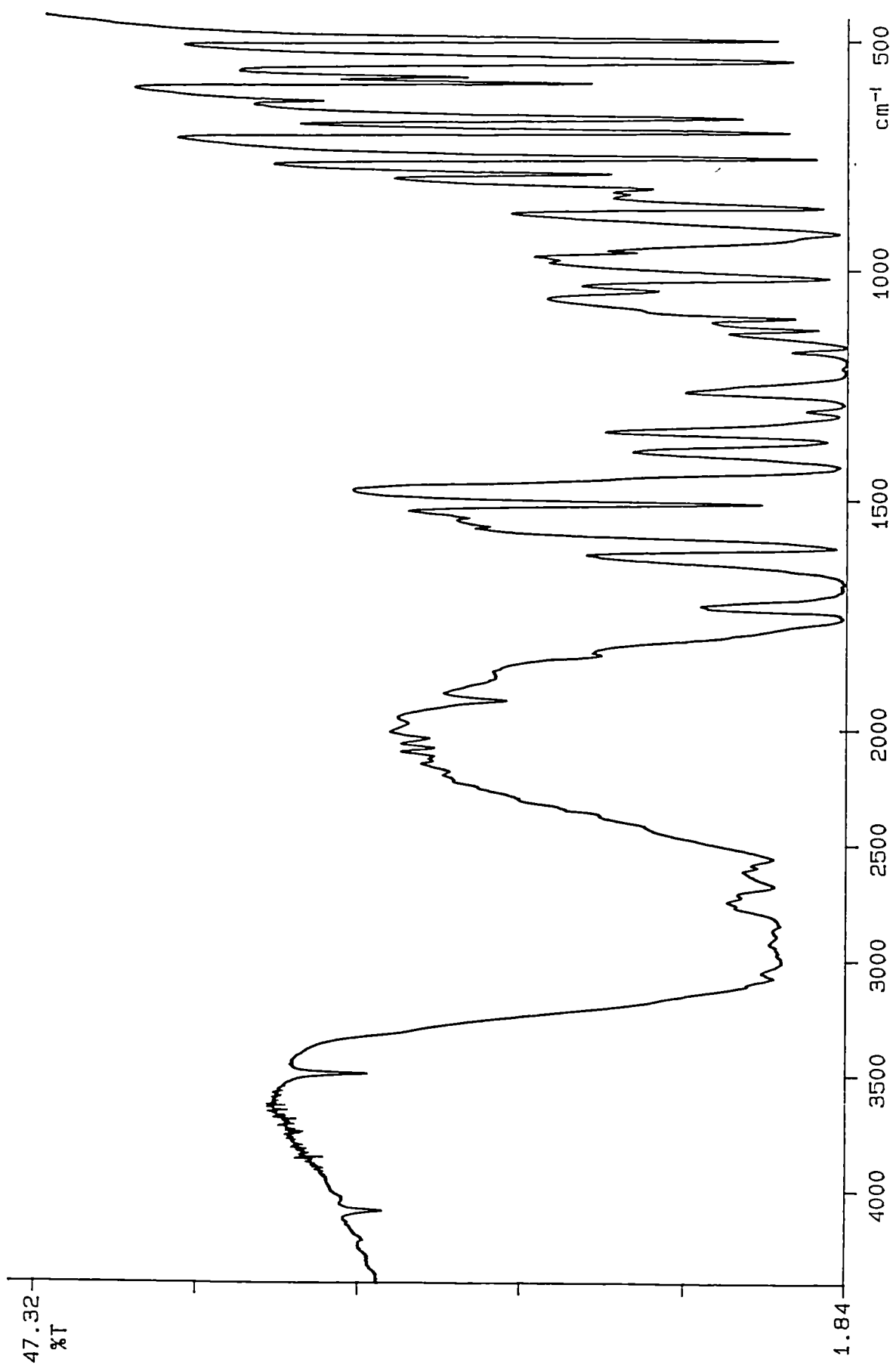
Figure A1.3 I.R. spectrum of 4-acetoxybenzoic acid (KBr disc)

Figure A1.4 ^{1}H n.m.r. spectrum of 4-acetoxybenzoyl chloride (d^6-acetone, 200MHz)
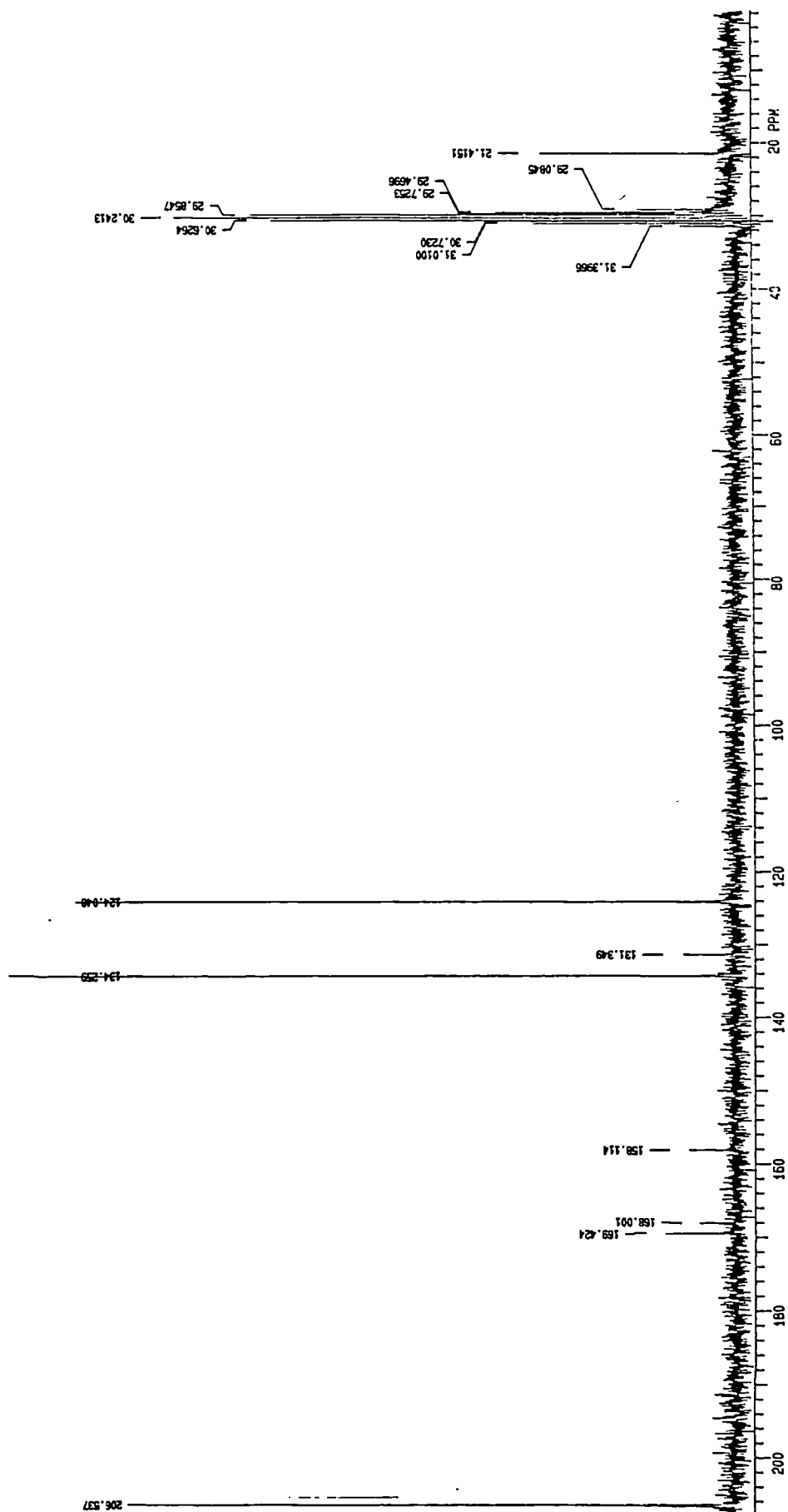
Figure A1.5 ^{13}C n.m.r. spectrum of 4-acetoxybenzoyl chloride (d^6-acetone, 50MHz)
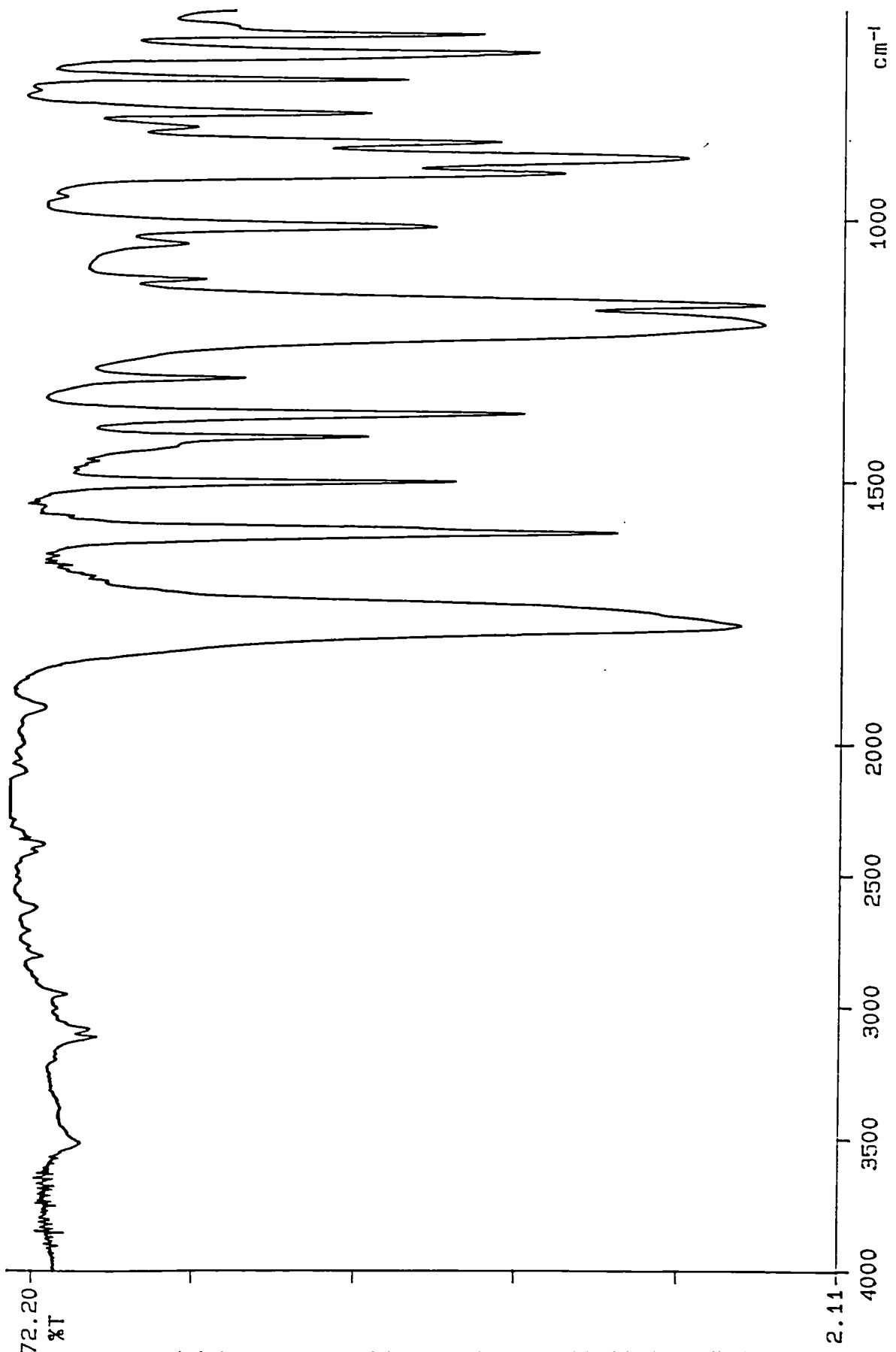
Figure A1.6 I.R. spectrum of 4-acetoxybenzoyl chloride (KBr disc)
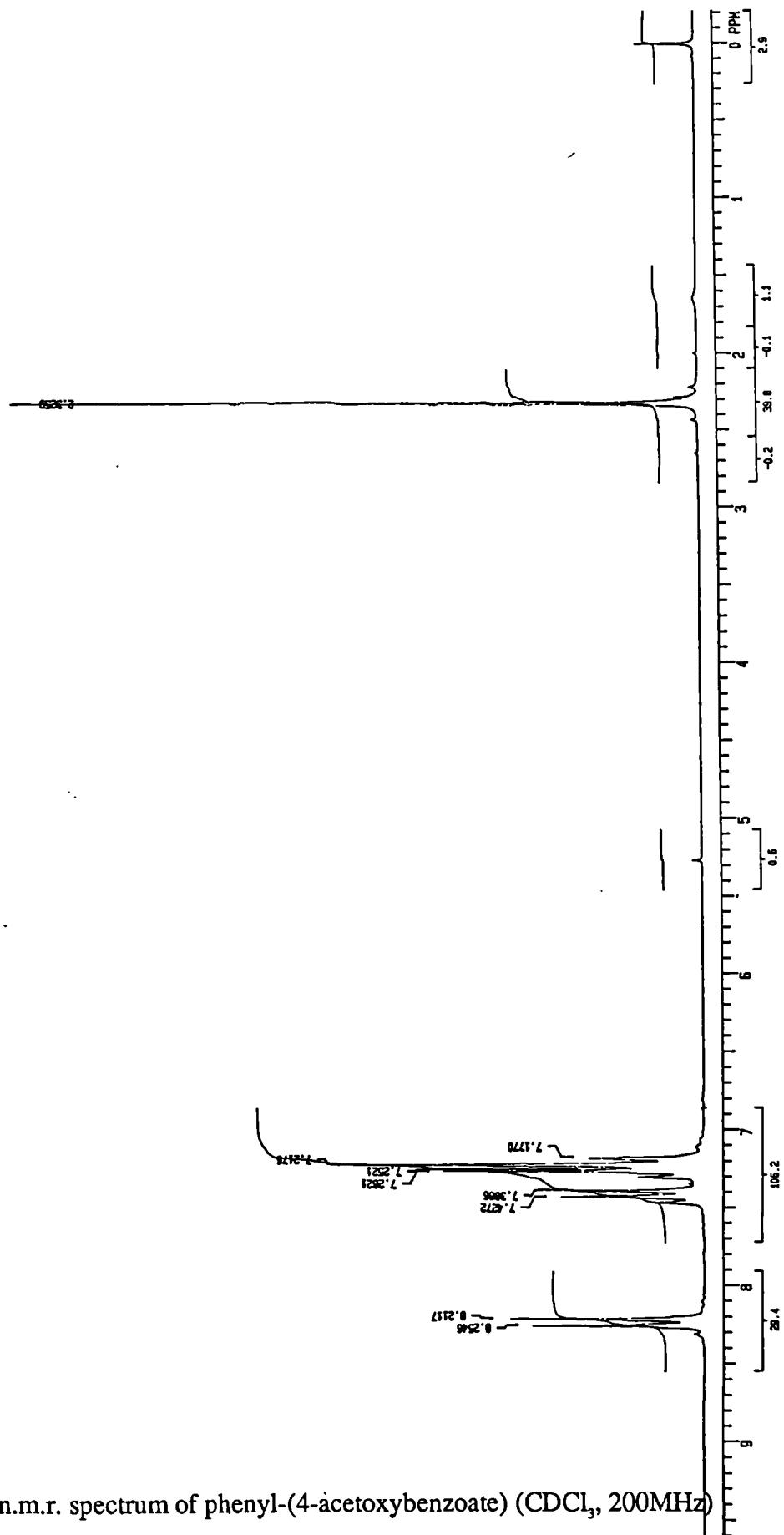
Figure A1.7 ¹H n.m.r. spectrum of phenyl-(4-acetoxybenzoate) (CDCl₃, 200MHz)
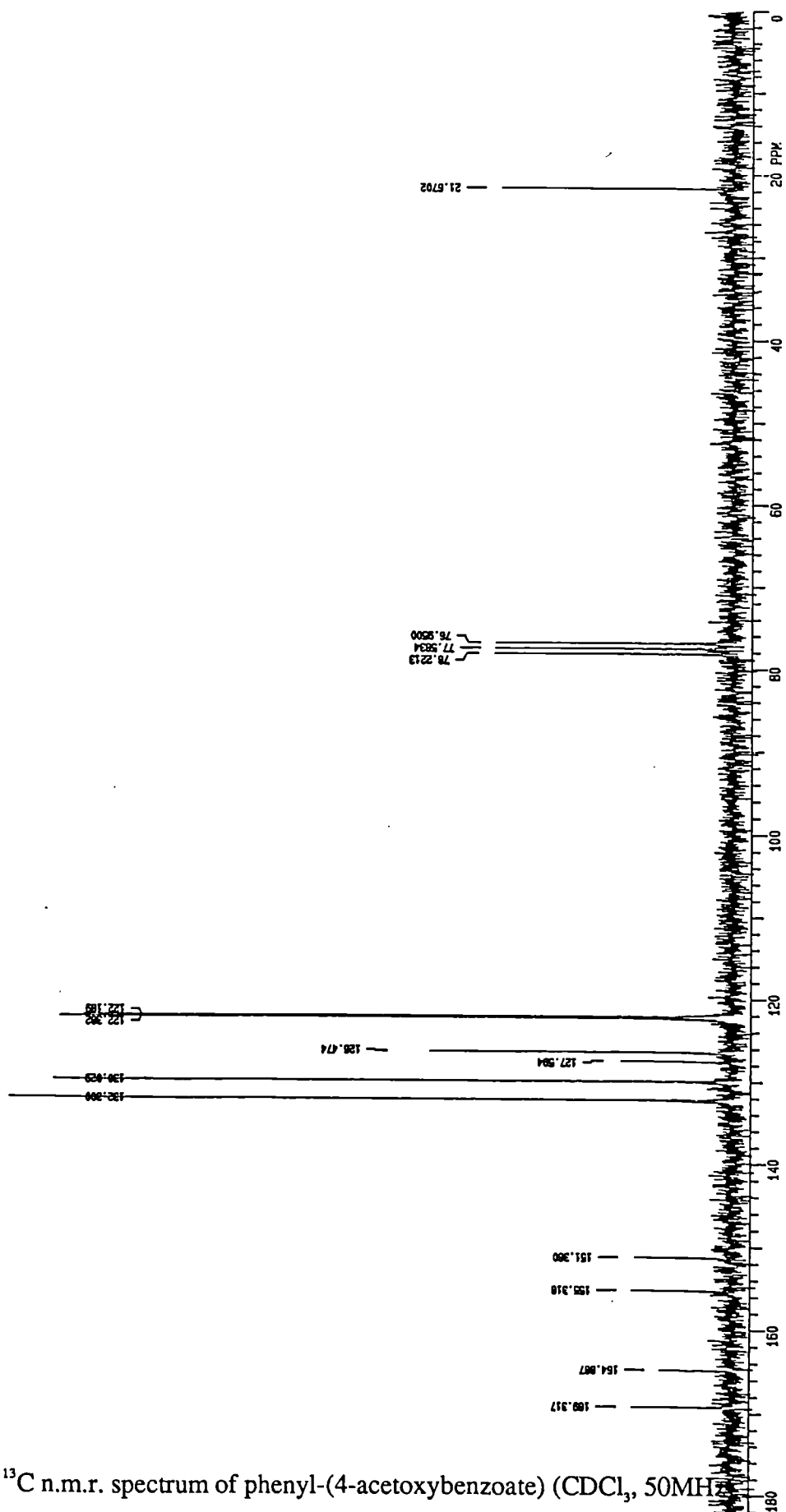
Figure A1.8 ^{13}C n.m.r. spectrum of phenyl-(4-acetoxybenzoate) (CDCl$_3$, 50MHz)
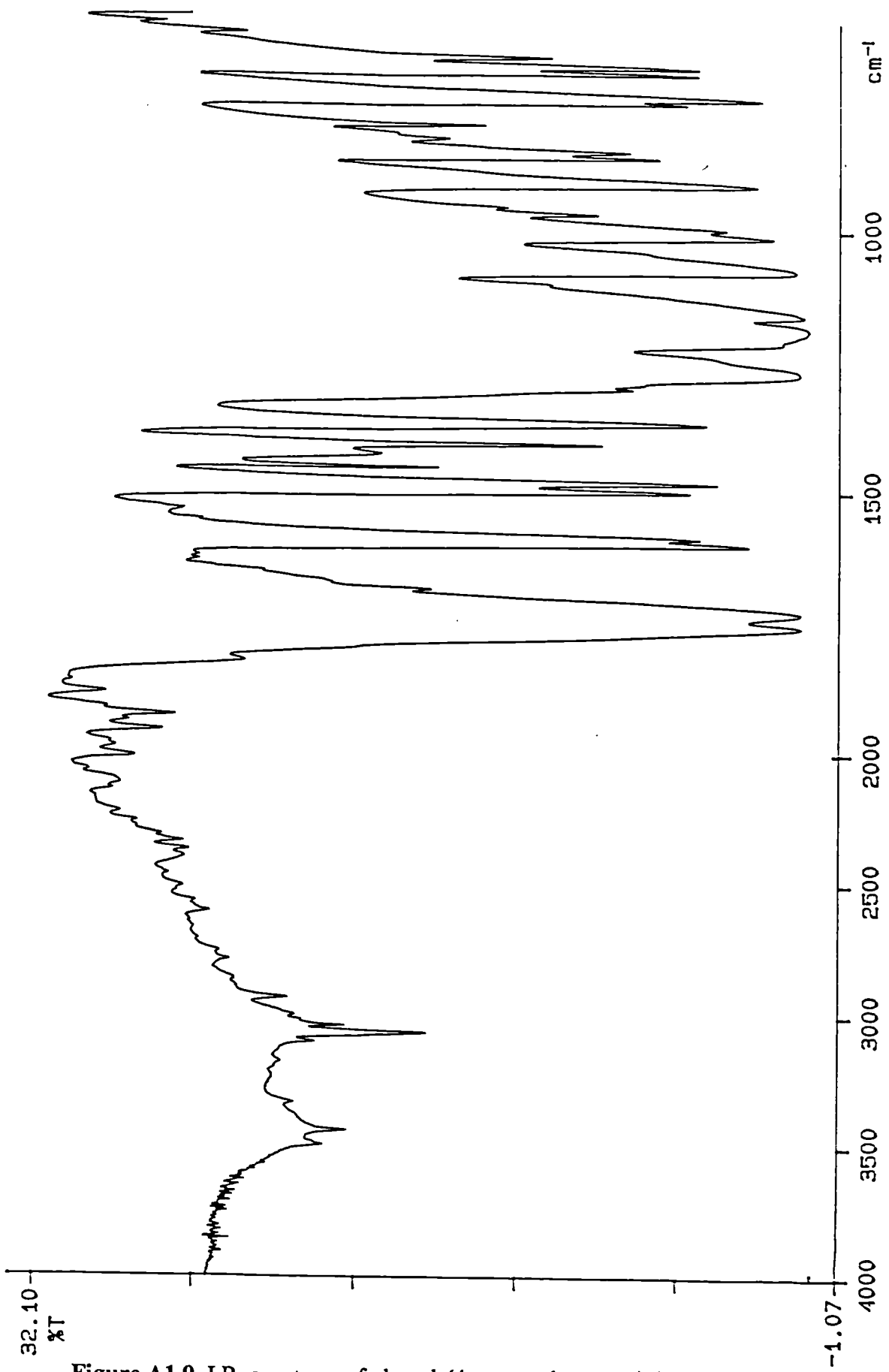
Figure A1.9 I.R. spectrum of phenyl-(4-acetoxybenzoate) (KBr disc)
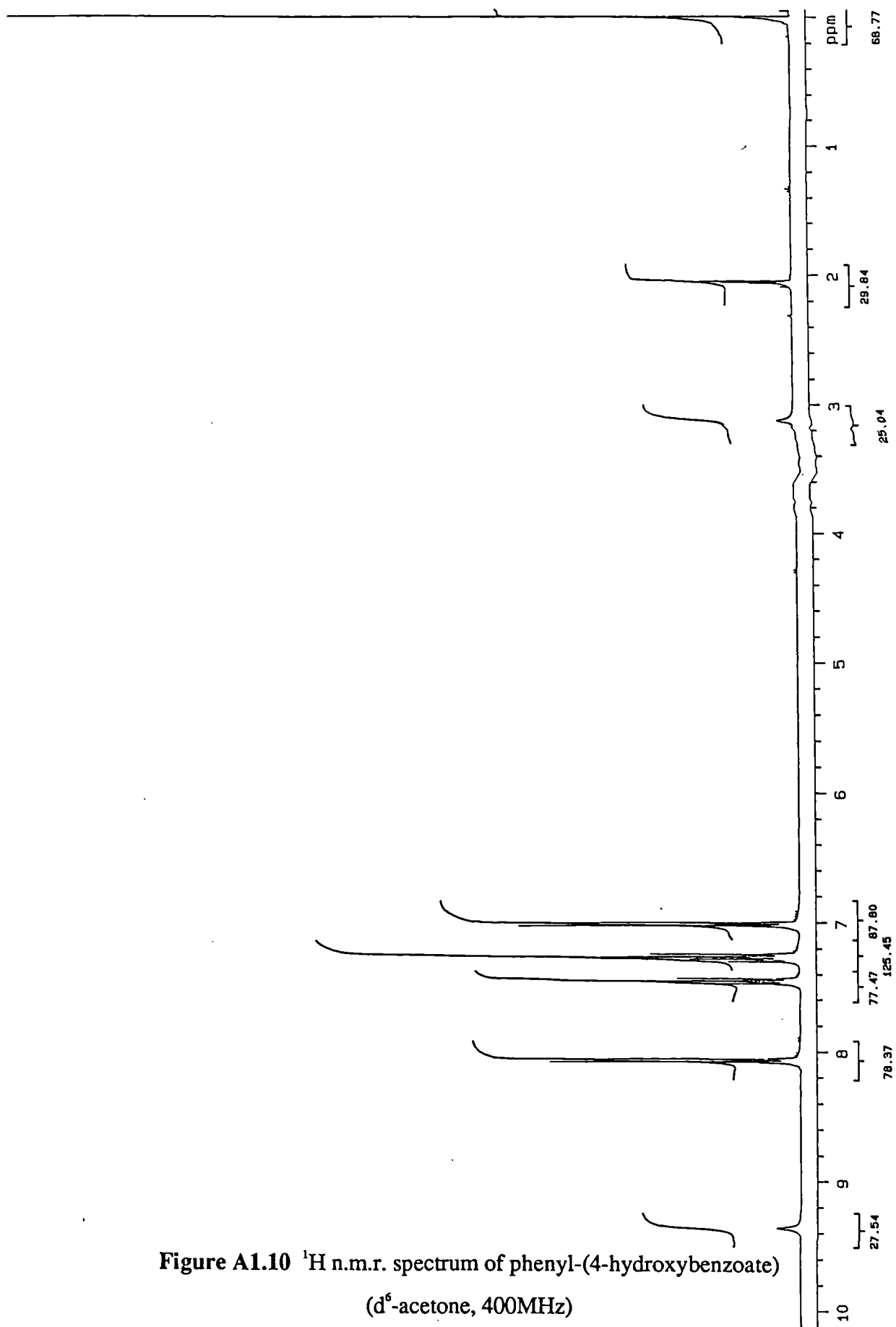
Figure A1.10 ¹H n.m.r. spectrum of phenyl-(4-hydroxybenzoate)

(d⁶-acetone, 400MHz)
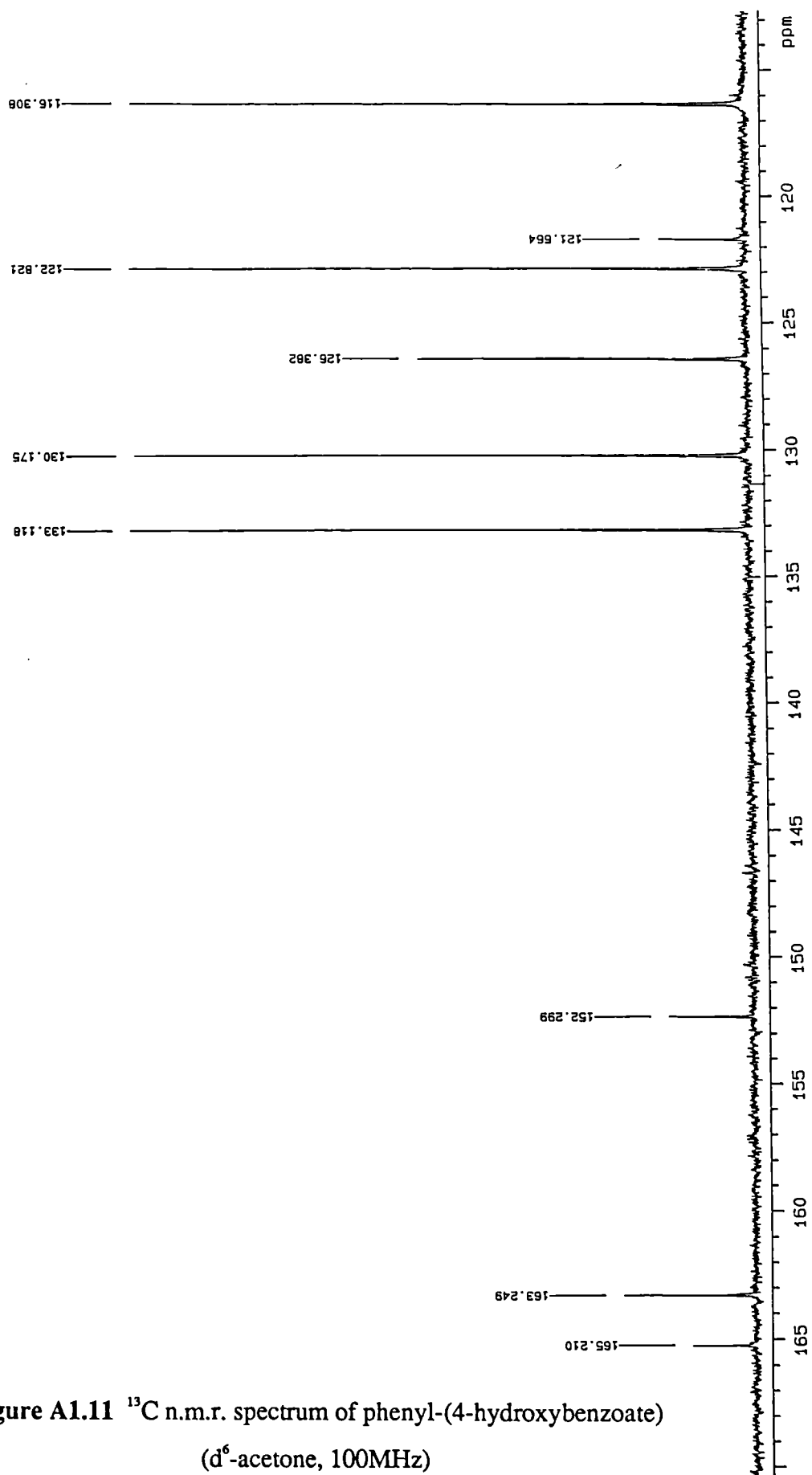
Figure A1.11 ¹³C n.m.r. spectrum of phenyl-(4-hydroxybenzoate)

(d⁶-acetone, 100MHz)
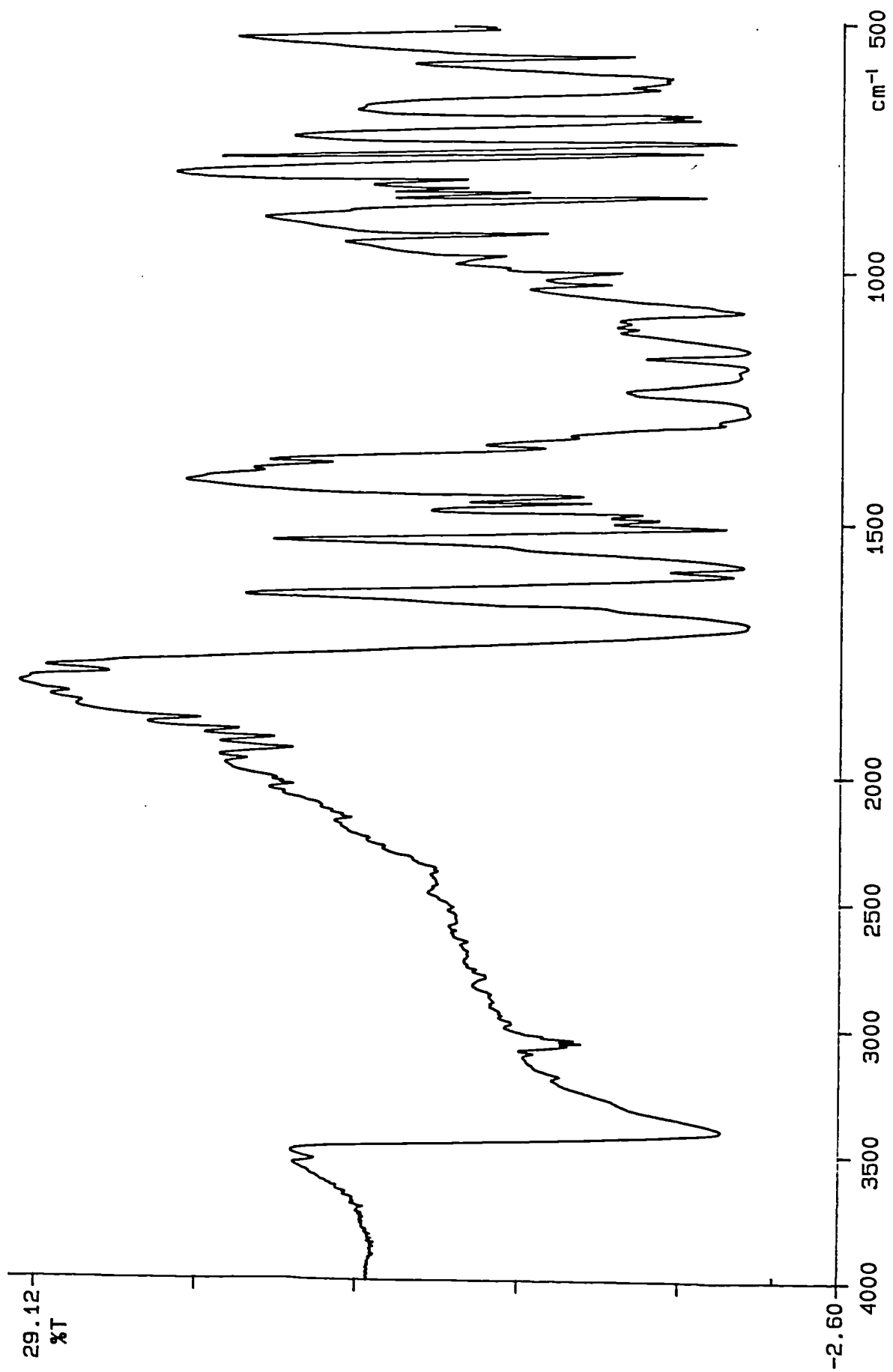
Figure A1.12 I.R. spectrum of phenyl-(4-hydroxybenzoate) (KBr disc)
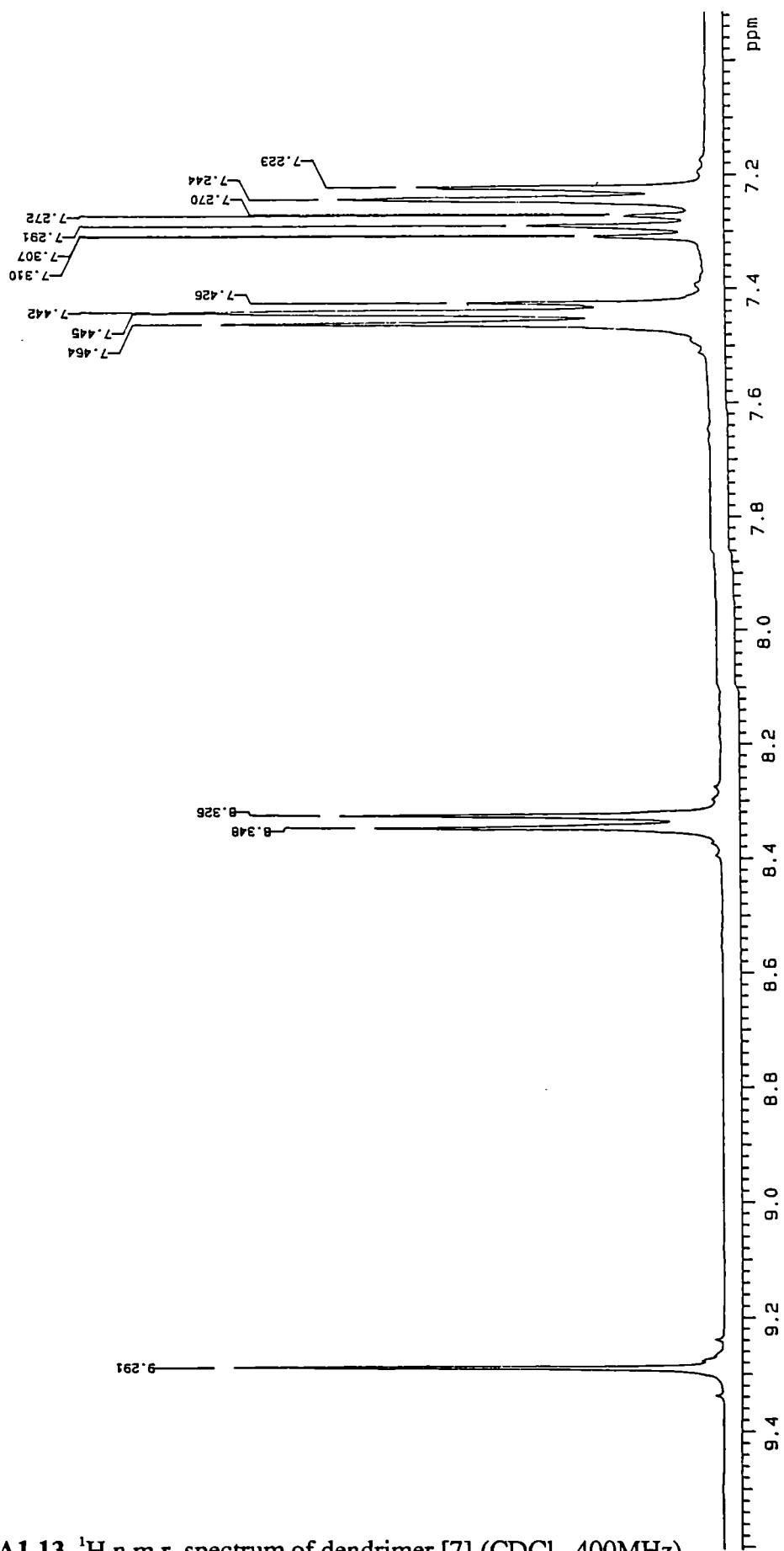
Figure A1.13 ^{1}H n.m.r. spectrum of dendrimer [7] (CDCl$_3$, 400MHz)
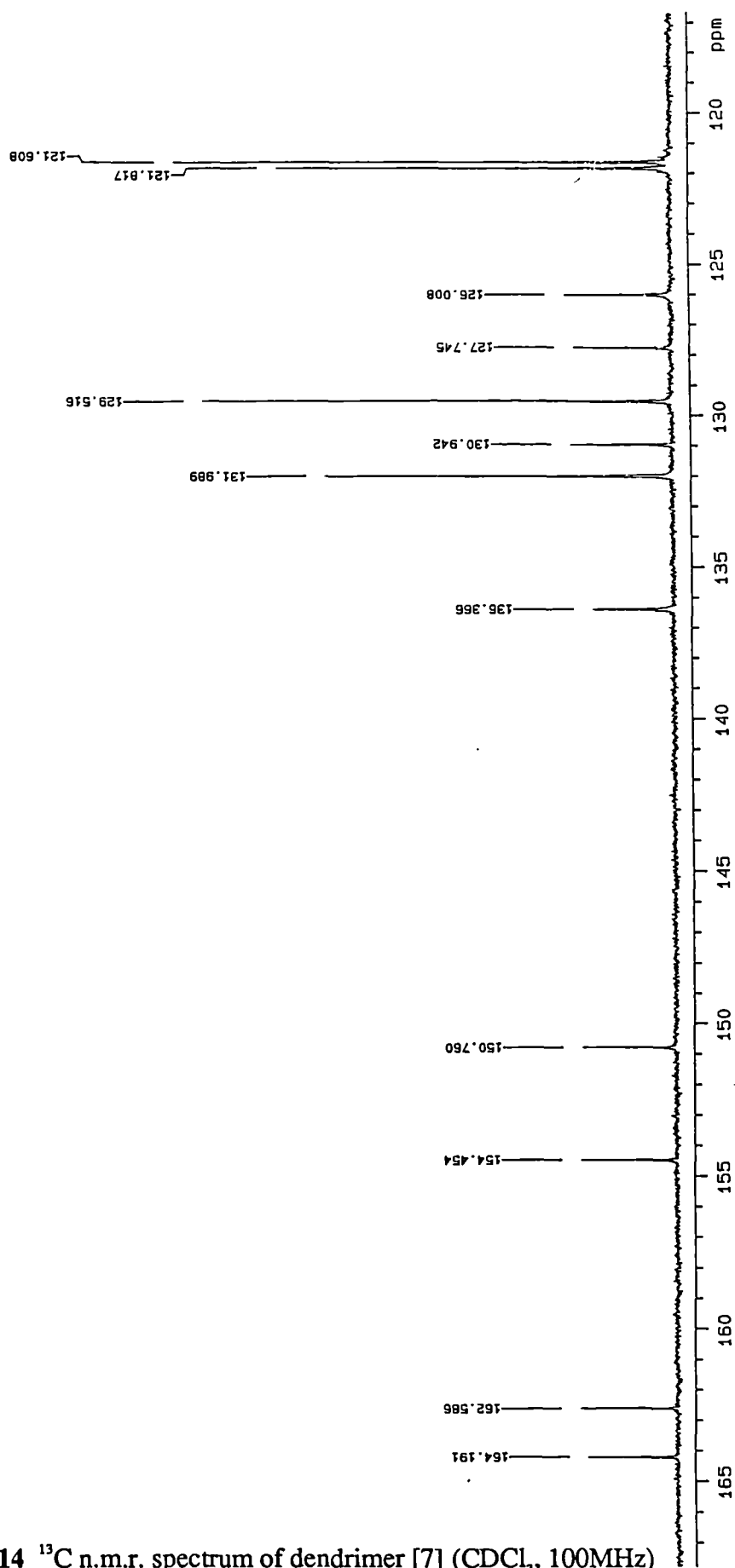
Figure A1.14 ^{13}C n.m.r. spectrum of dendrimer [7] (CDCl$_3$, 100MHz)
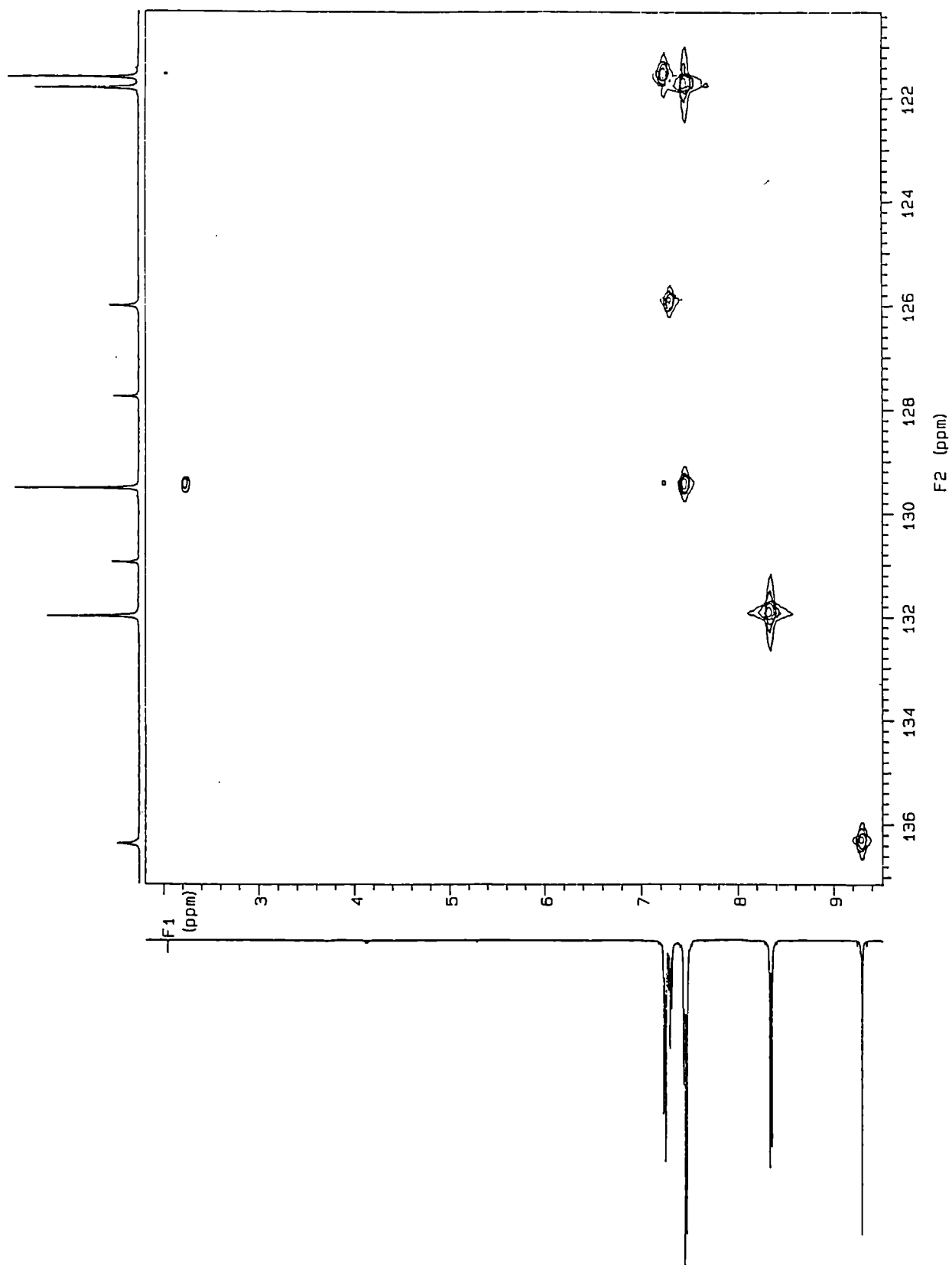
Figure A1.15 ^{1}H - ^{13}C hetcor spectrum of dendrimer [7] (CDCl$_3$)
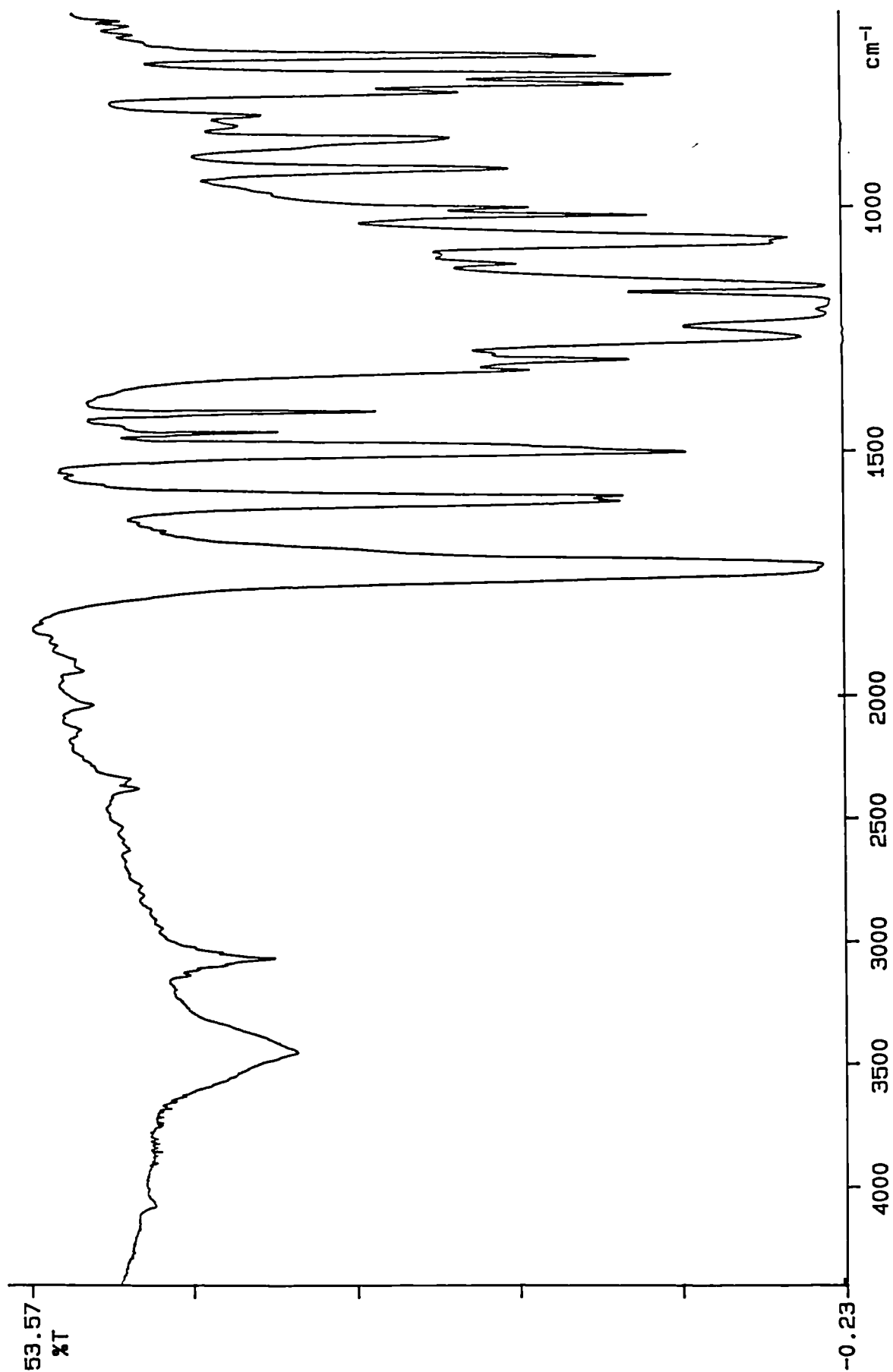
Figure A1.16 I.R. spectrum of dendrimer [7] (KBr disc)
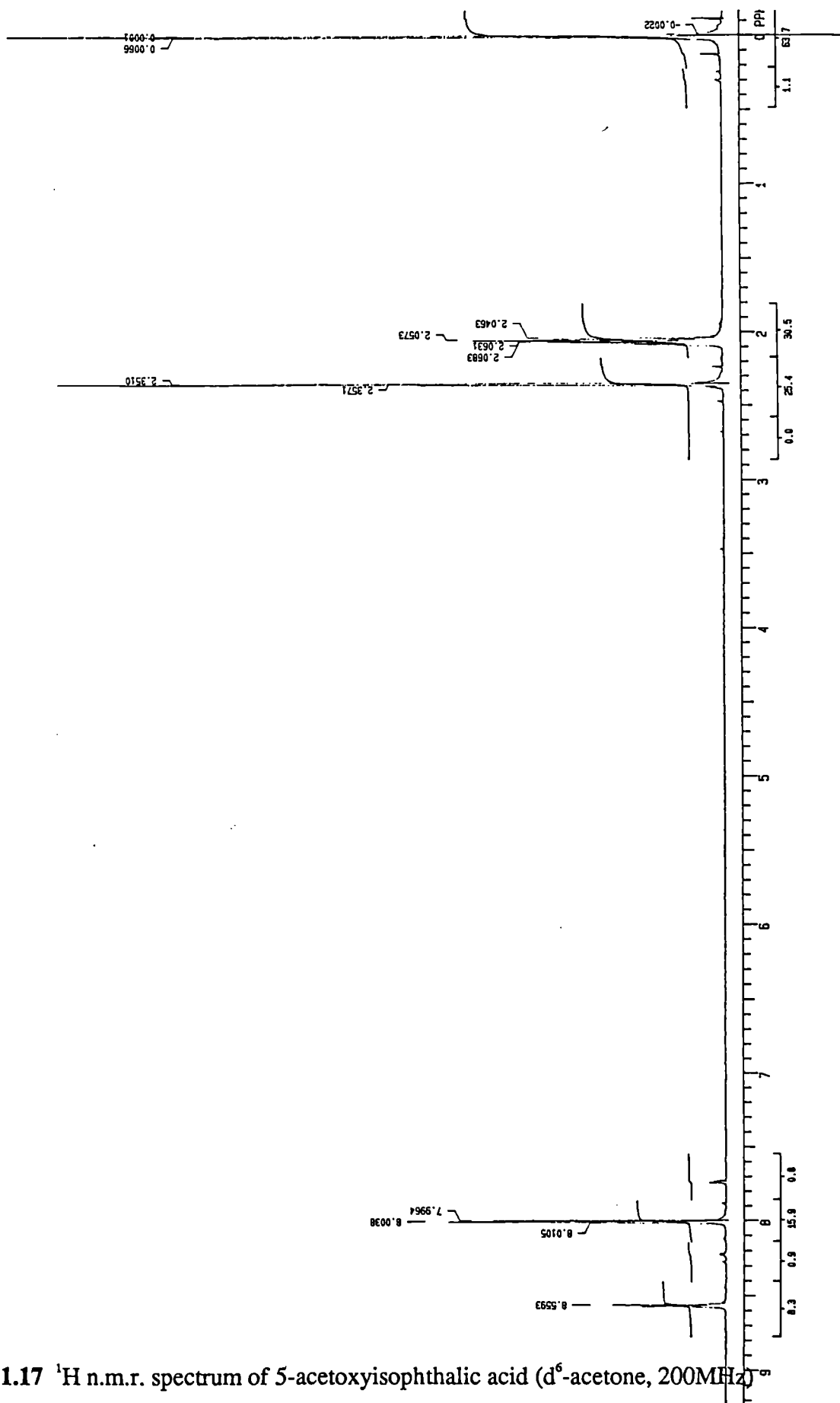
Figure A1.17 ^{1}H n.m.r. spectrum of 5-acetoxyisophthalic acid (d^6-acetone, 200MHz)
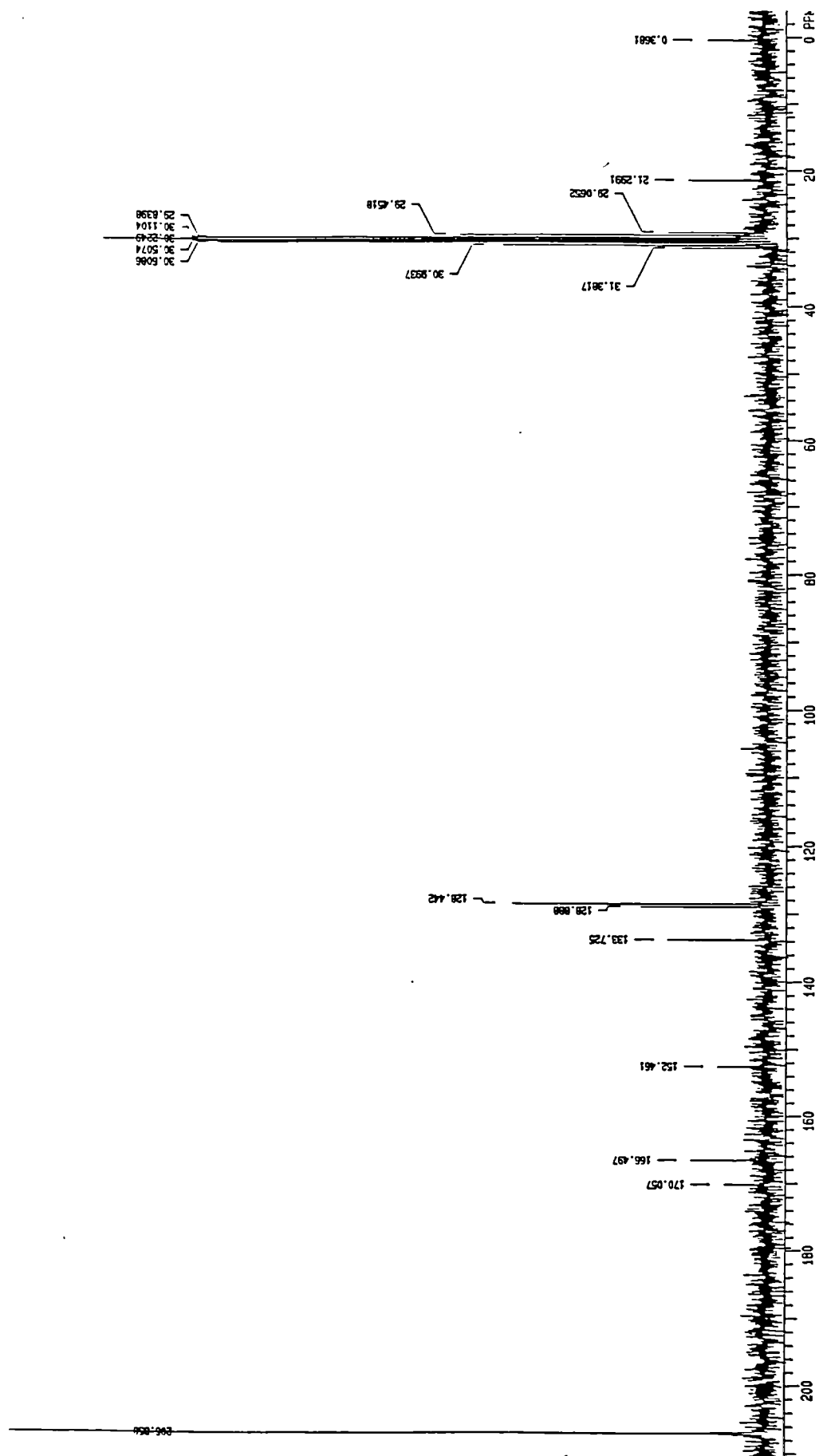
Figure A1.18 ^{13}C n.m.r. spectrum of 5-acetoxyisophthalic acid (d^6-acetone, 50MHz)
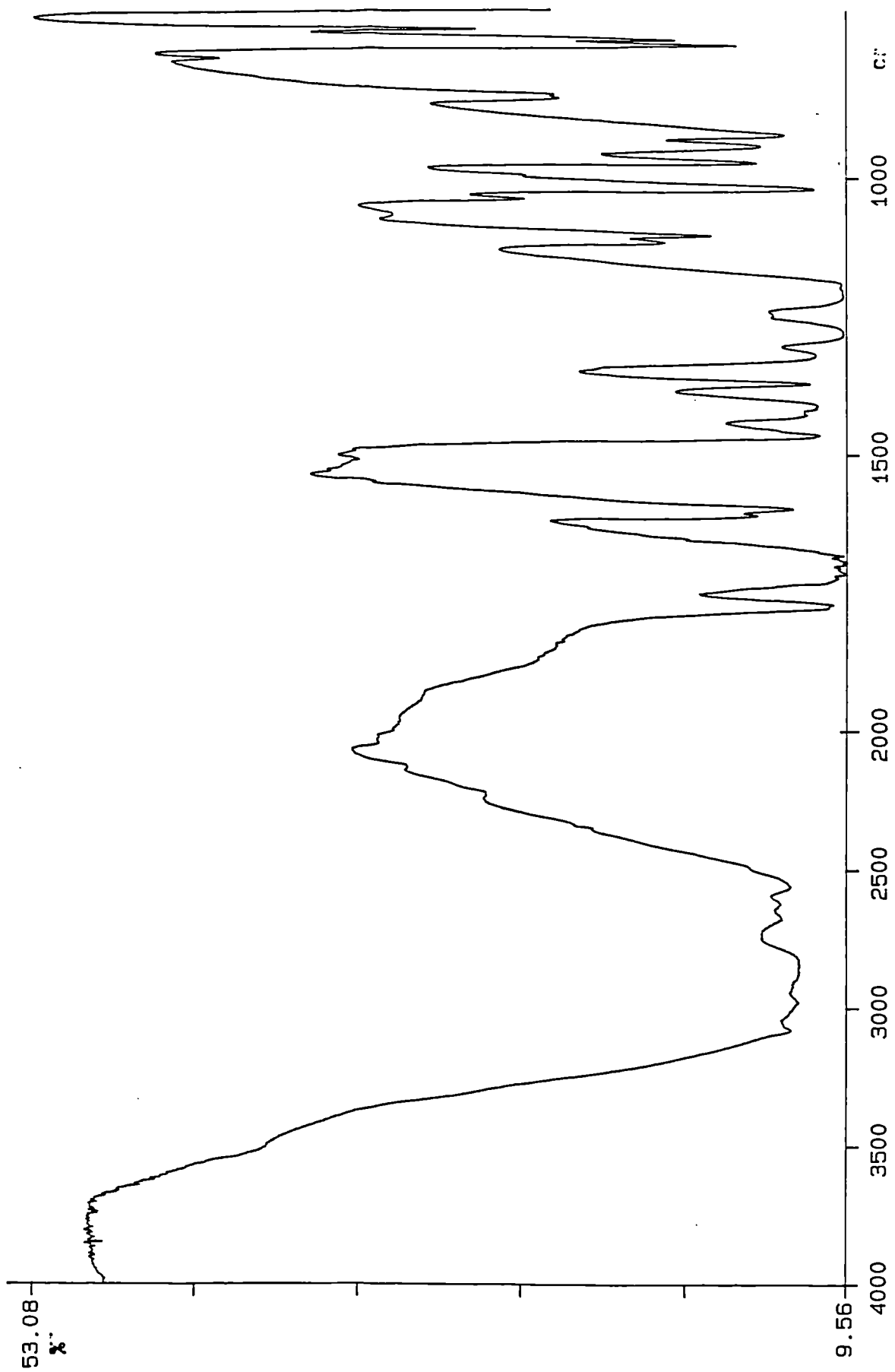
Figure A1.19 I.R. spectrum of 5-acetoxyisophthalic acid (KBr disc)
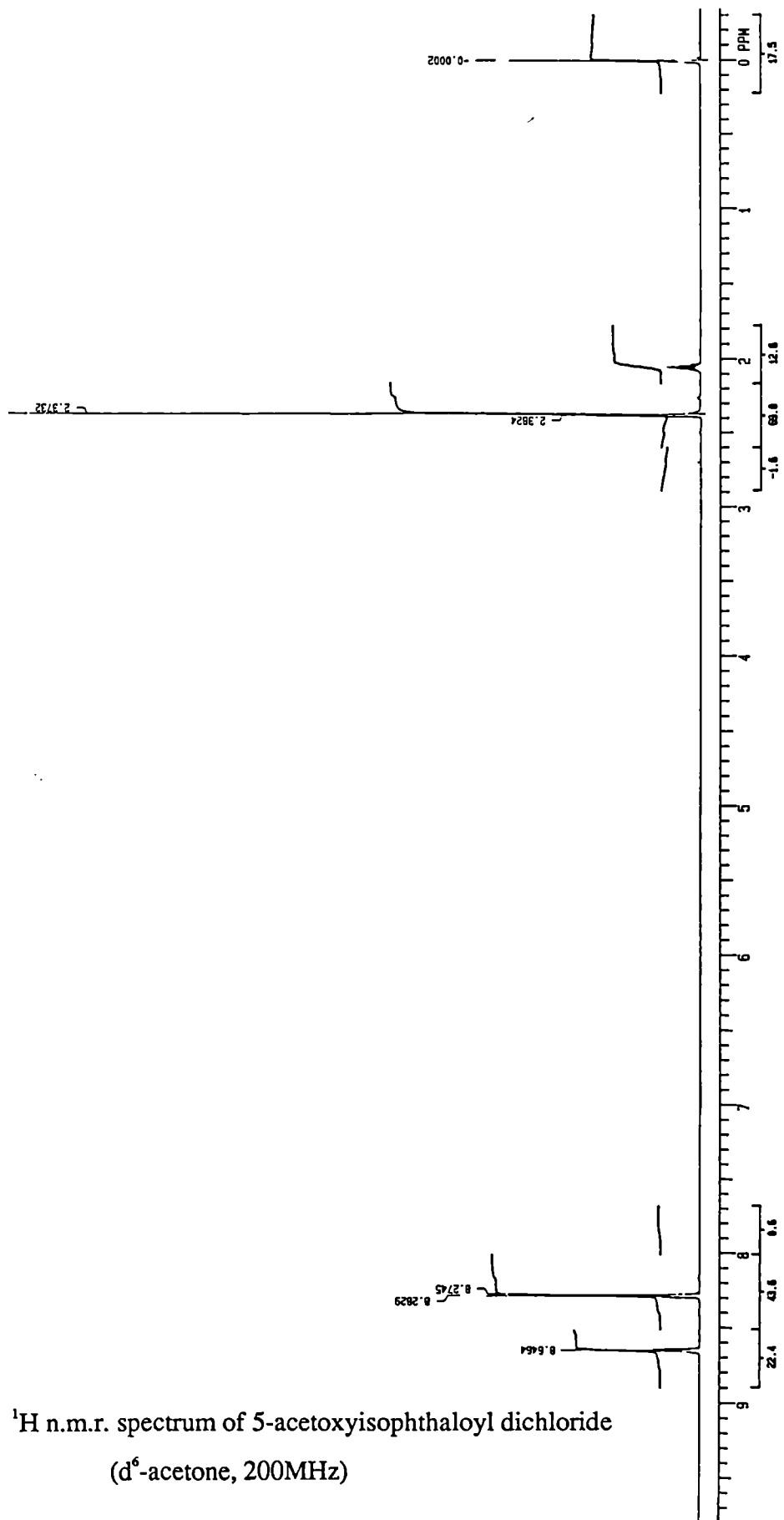
Figure A1.20 ^{1}H n.m.r. spectrum of 5-acetoxyisophthaloyl dichloride
(d^6-acetone, 200MHz)
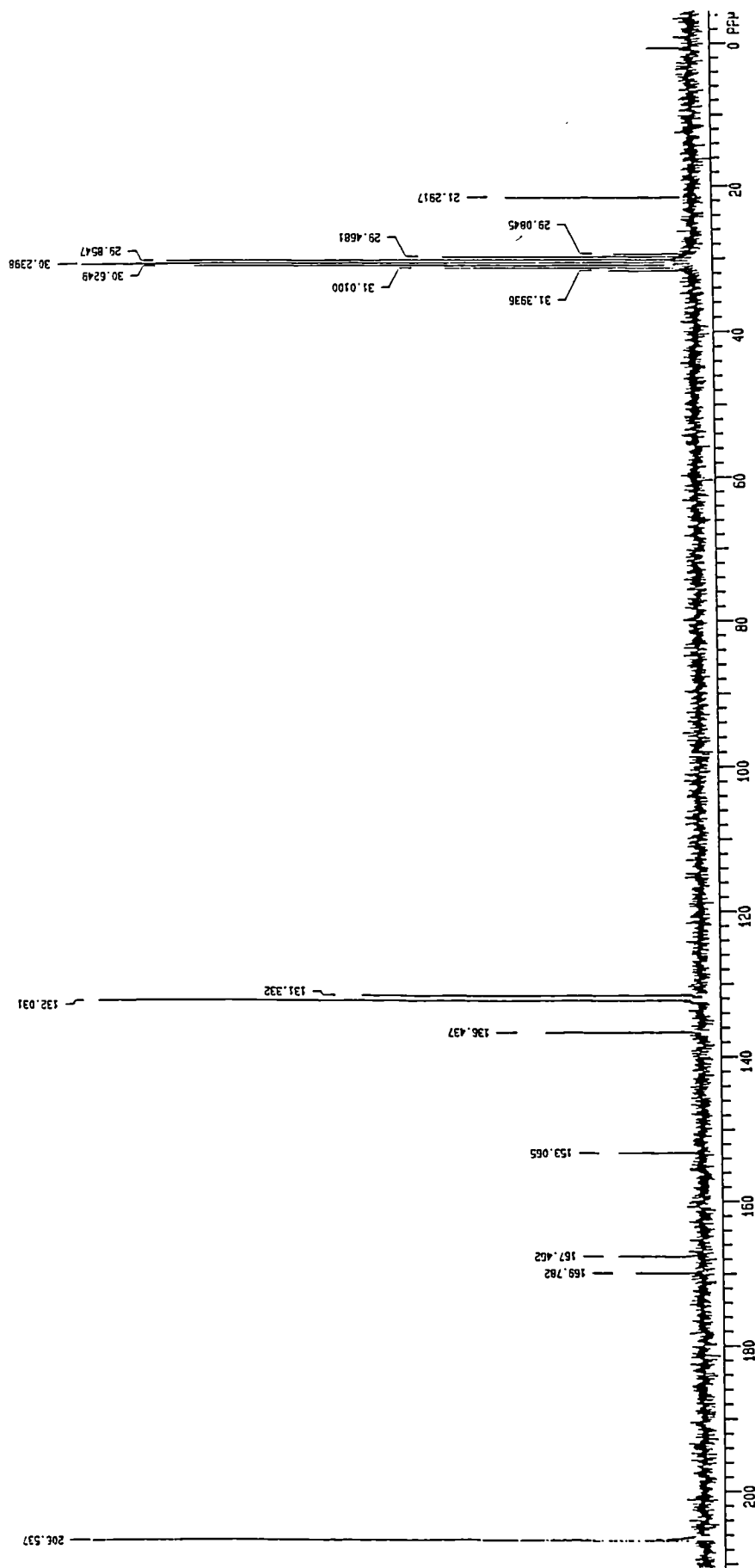
Figure A1.21 ^{13}C n.m.r. spectrum of 5-acetoxyisophthaloyl dichloride

(d^6-acetone, 50MHz)
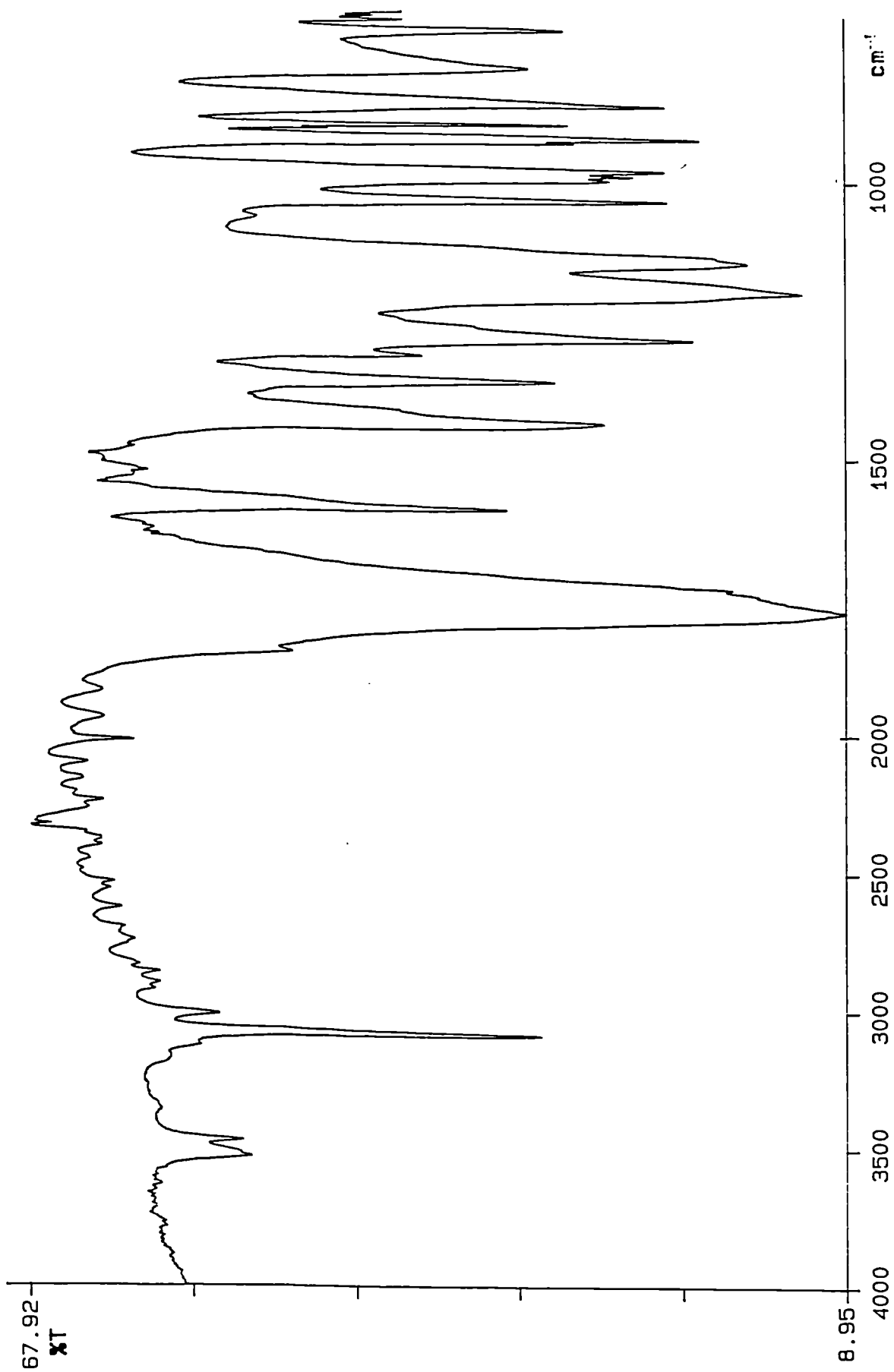
Figure A1.22 I.R. spectrum of 5-acetoxyisophthaloyl dichloride (liquid)
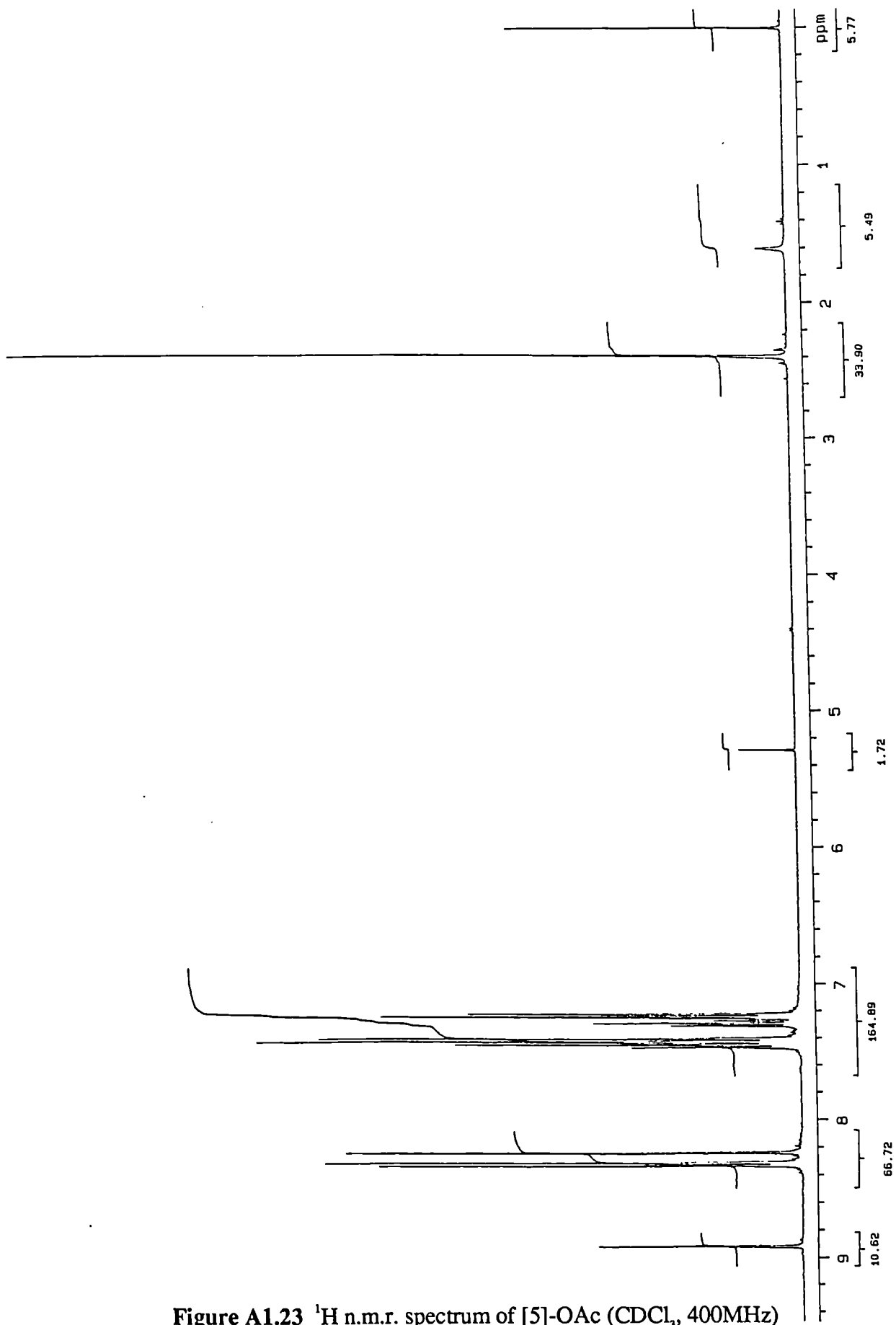
Figure A1.23 ^{1}H n.m.r. spectrum of [5]-OAc (CDCl$_3$, 400MHz)
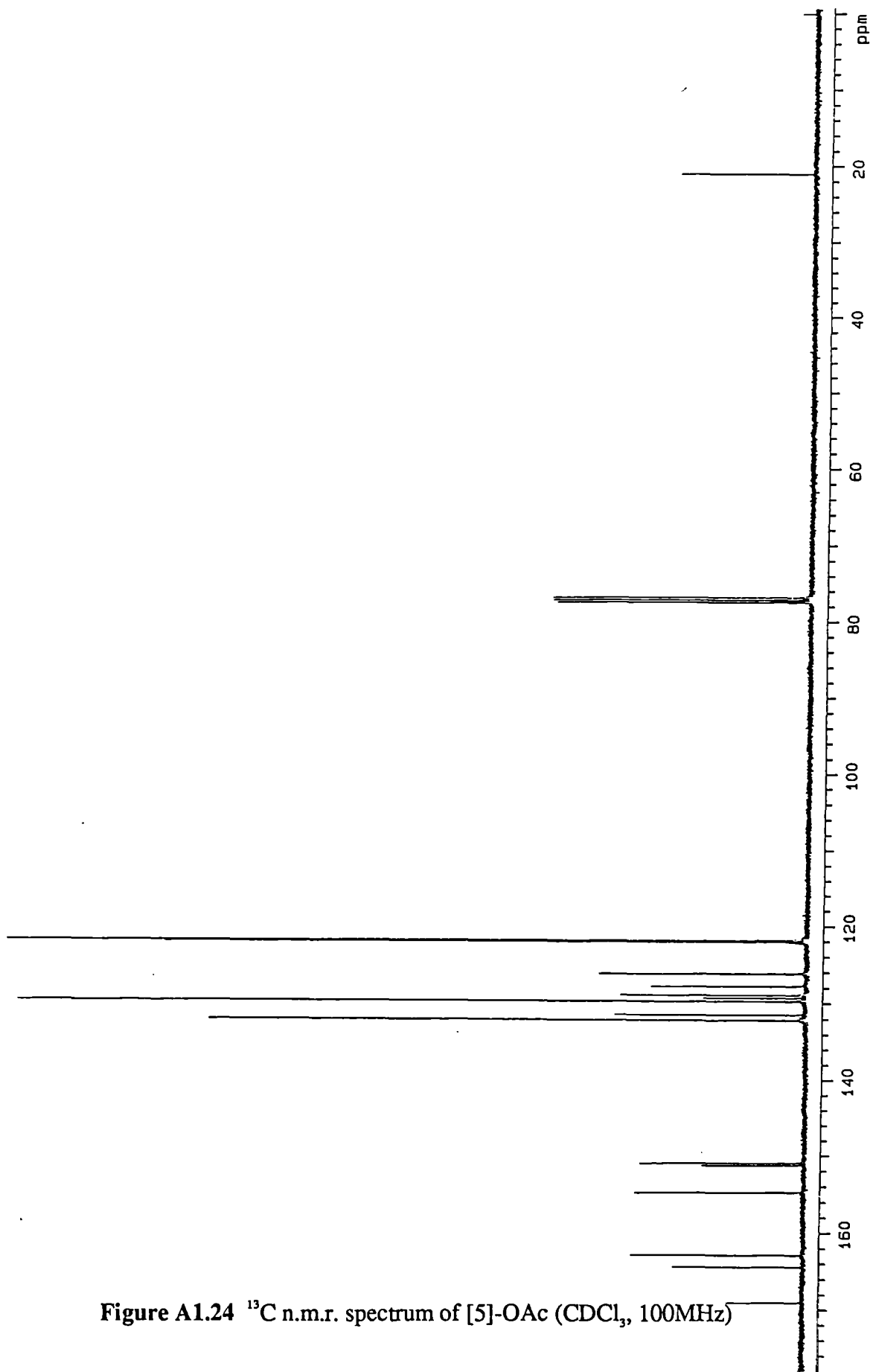
A1-24

Figure A1.24 ^{13}C n.m.r. spectrum of [5]-OAc (CDCl$_3$, 100MHz)
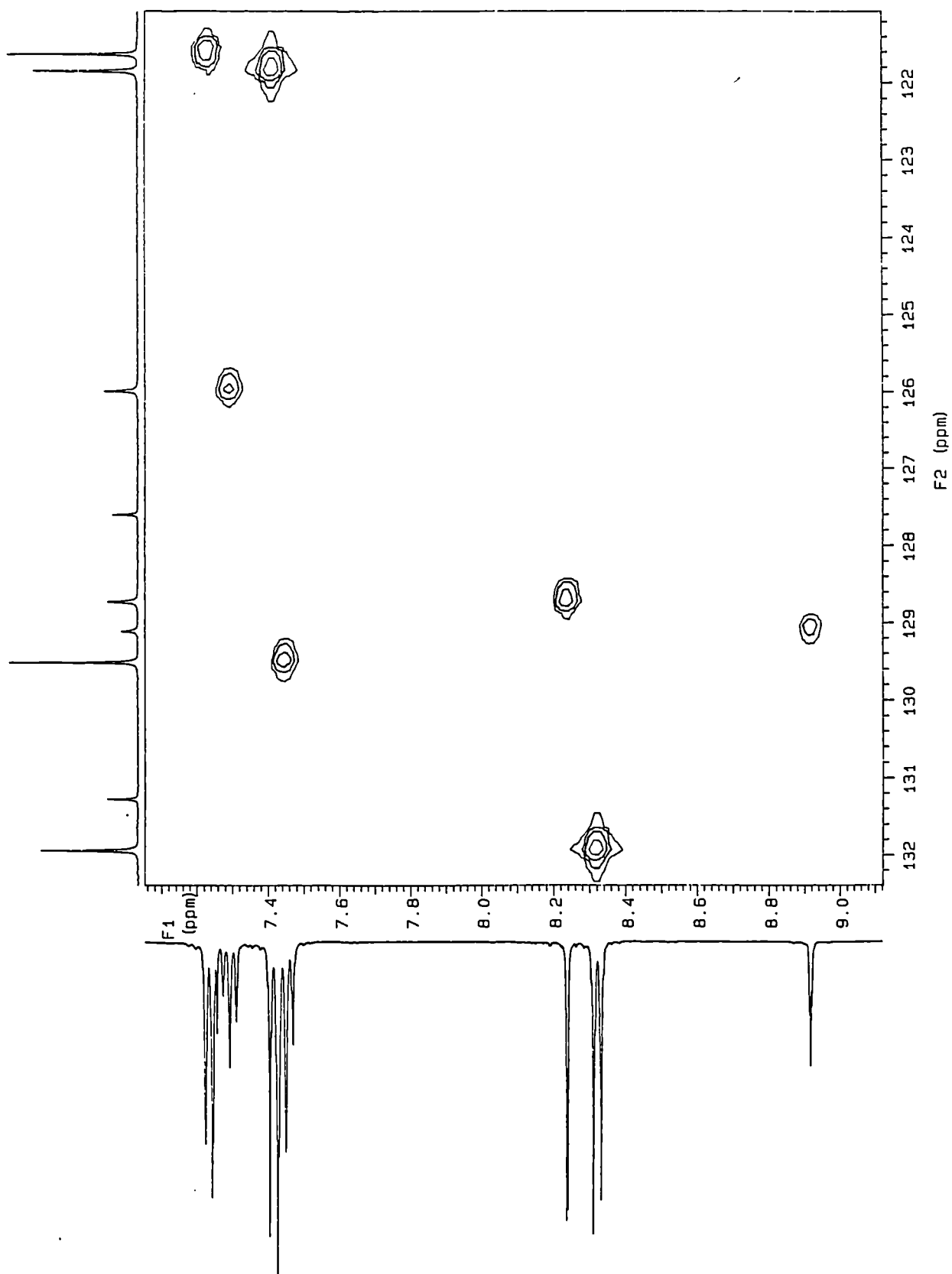
Figure A1.25 ^{1}H - ^{13}C hetcor spectrum of [5]-OAc (CDCl$_3$)
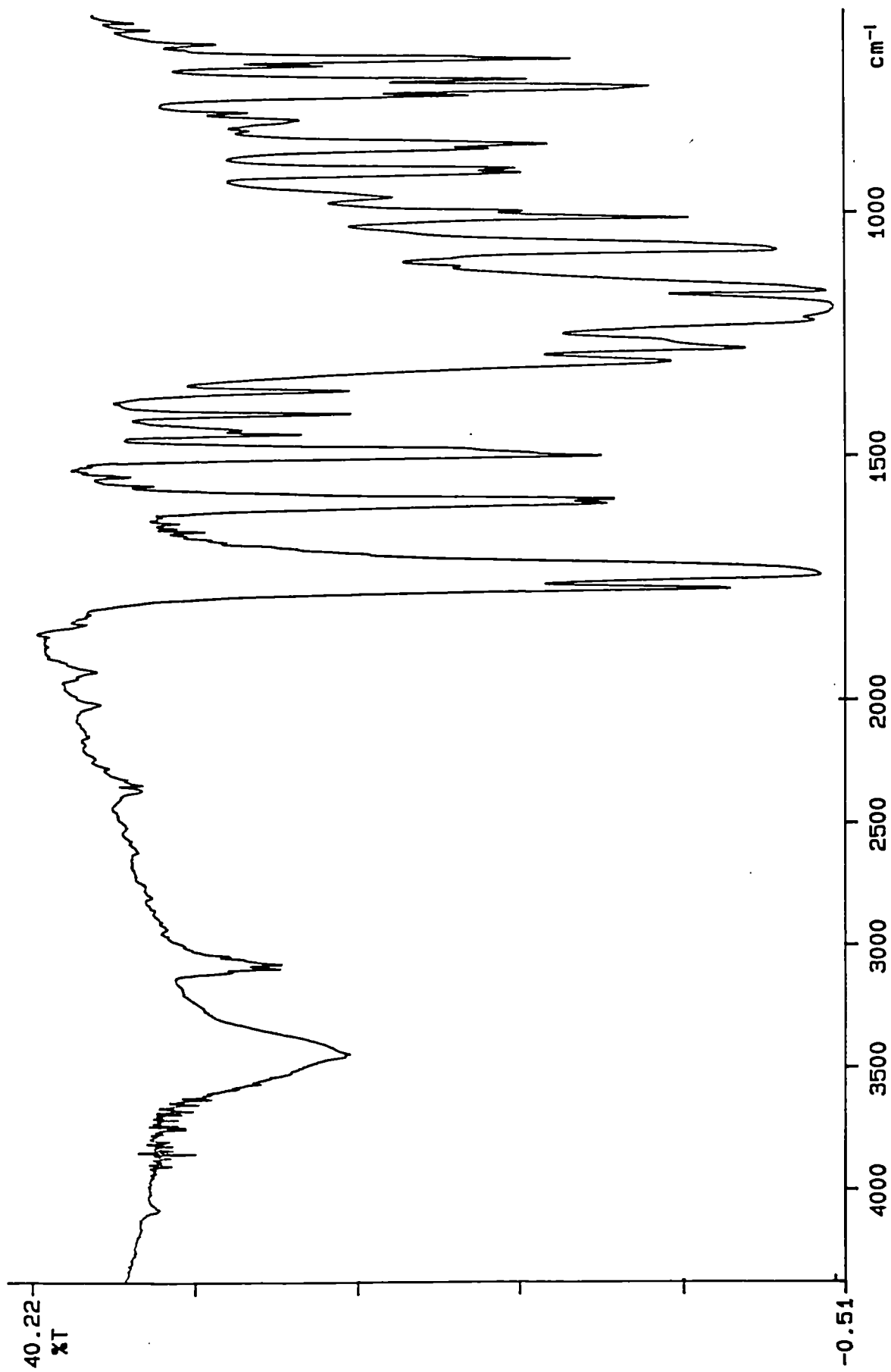
Figure A1.26 I.R. spectrum of [5]-OAc (KBr disc)

9.499

9.40
9.45
9.50
9.55
9.60
9.65

ppm

7.318
7.321
7.326
7.341
7.343

7.474
7.492
7.494
7.495
7.514

7.584
7.606

7.977
7.981

8.305
8.328

8.488

7.3
7.4
7.5
7.6
7.7
7.8
7.9
8.0
8.1
8.2
8.3
8.4
8.5

ppm
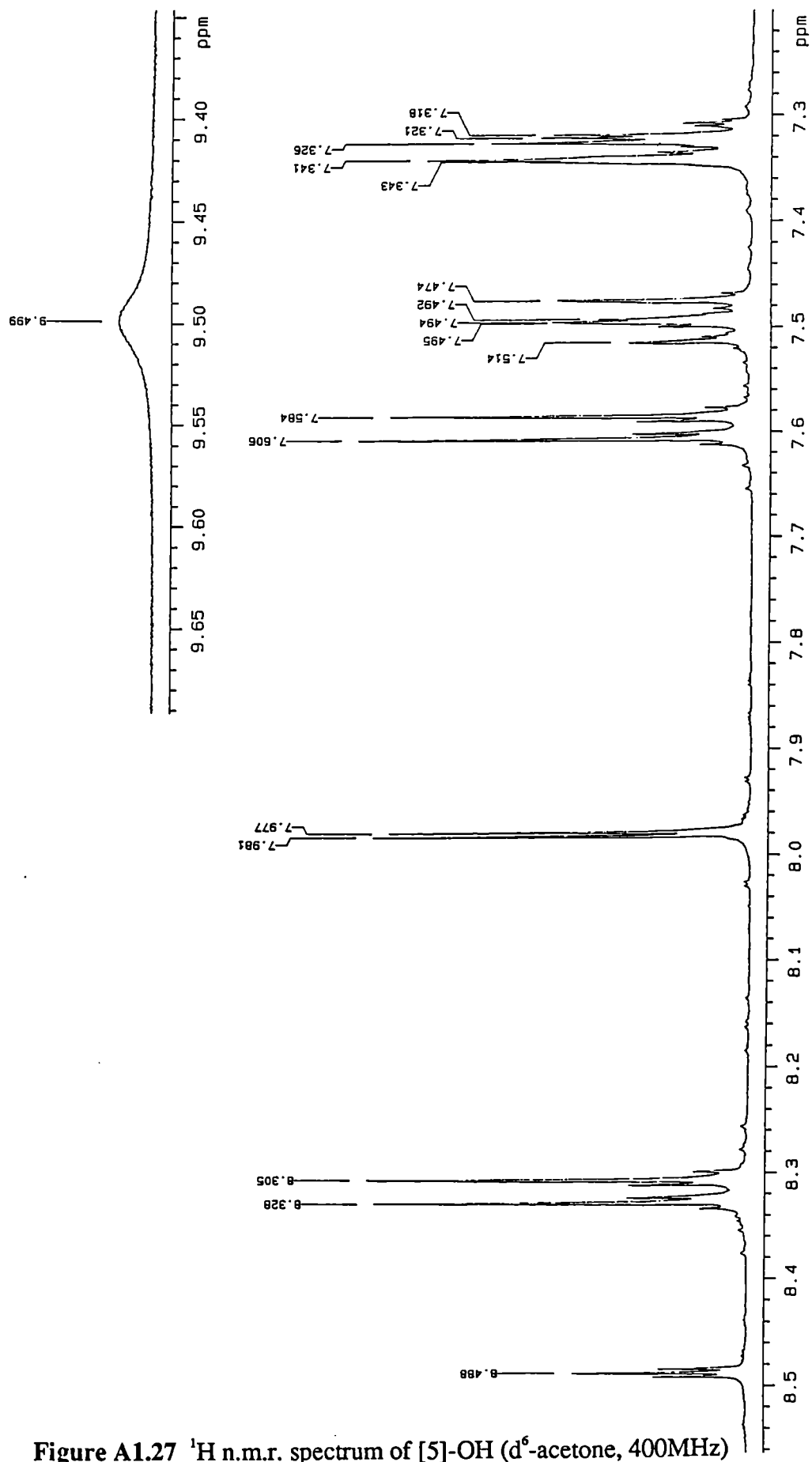
Figure A1.27 ^{1}H n.m.r. spectrum of [5]-OH (d^6-acetone, 400MHz)
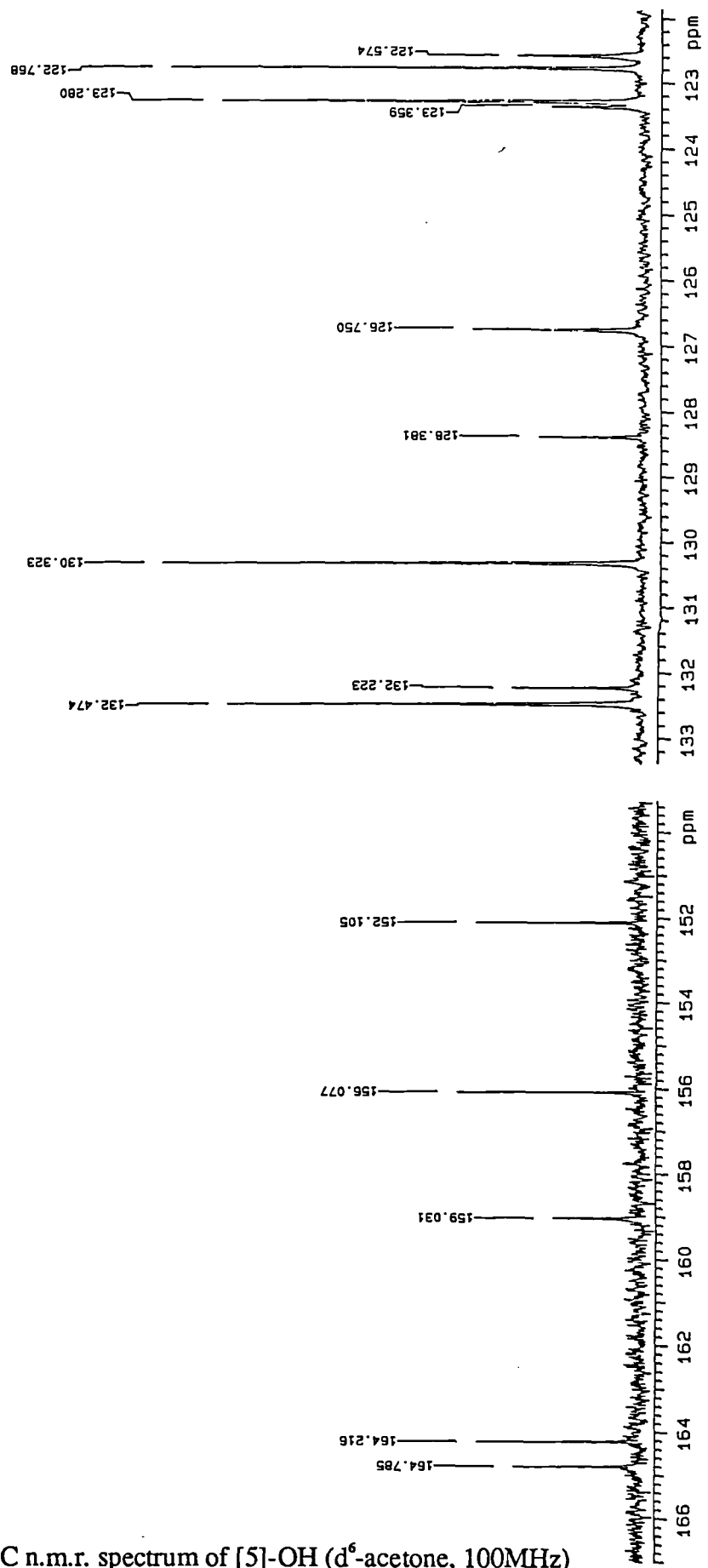
Figure A1.28 ^{13}C n.m.r. spectrum of [5]-OH (d^6-acetone, 100MHz)

122.574
122.768
123.280
123.359
126.750
128.381
130.323
132.223
132.474

152.105
156.077
159.031
164.216
164.785
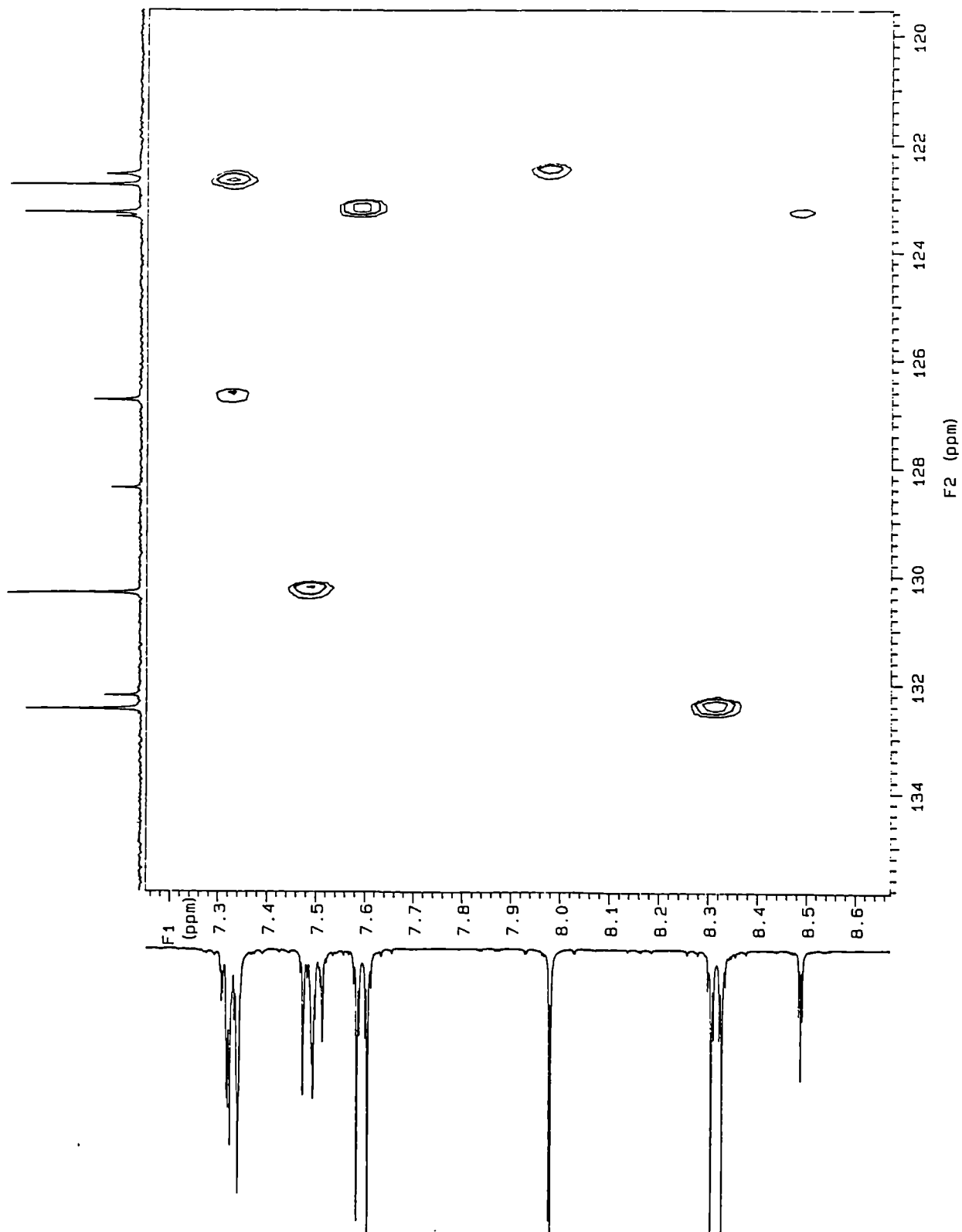
Figure A1.29 ^{1}H - ^{13}C hetcor spectrum of [5]-OH (d^6-acetone)
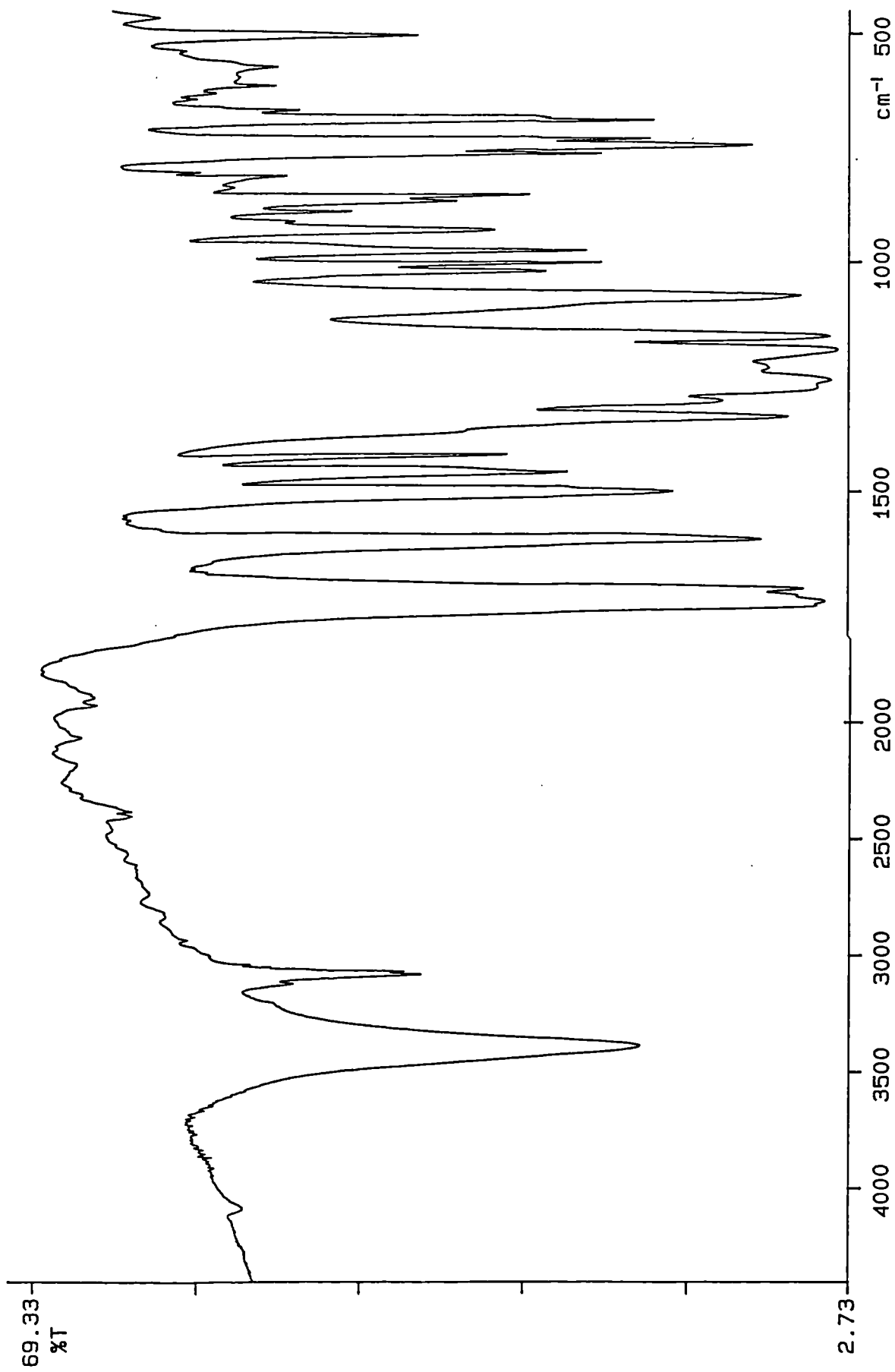
Figure A1.30 I.R. spectrum of [5]-OH (KBr disc)
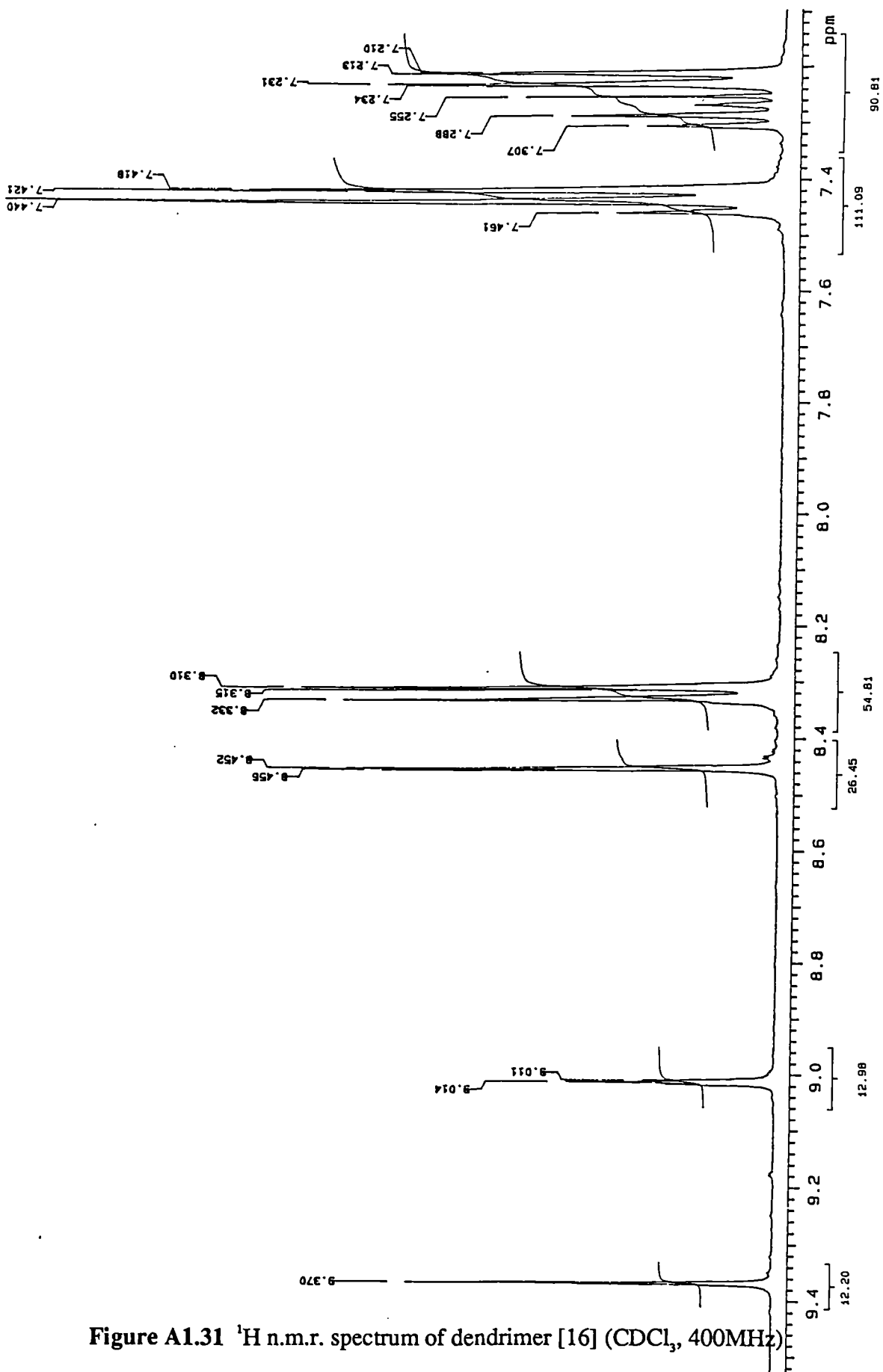
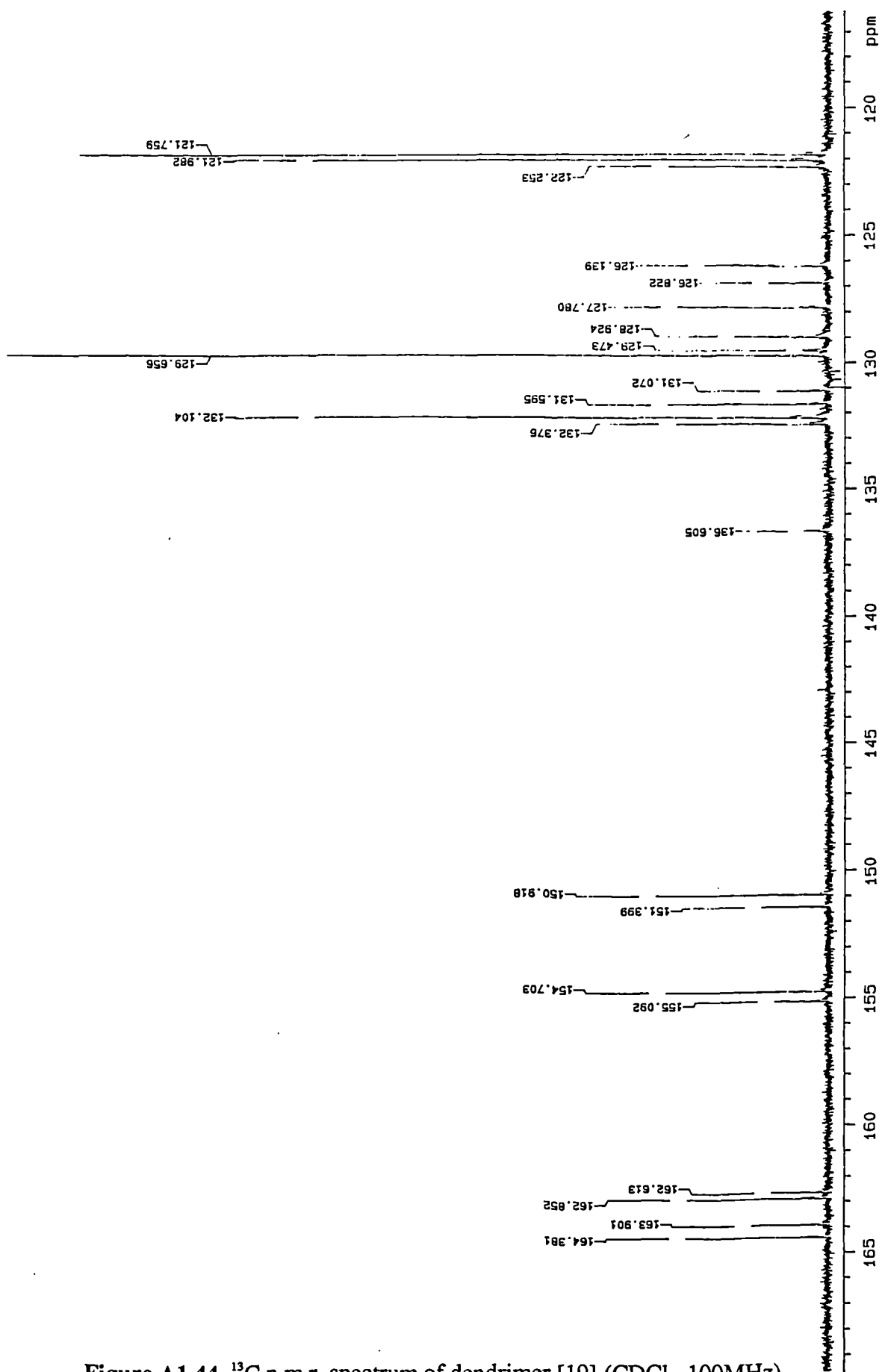**Figure A1.31** ^{1}H n.m.r. spectrum of dendrimer [16] (CDCl$_3$, 400MHz)

121.634
121.835
126.045
127.744
128.597
128.549
129.731
130.740
131.696
132.007
136.718
150.782
150.842
154.506
162.597
164.228

125
130
135
140
145
150
155
160
165
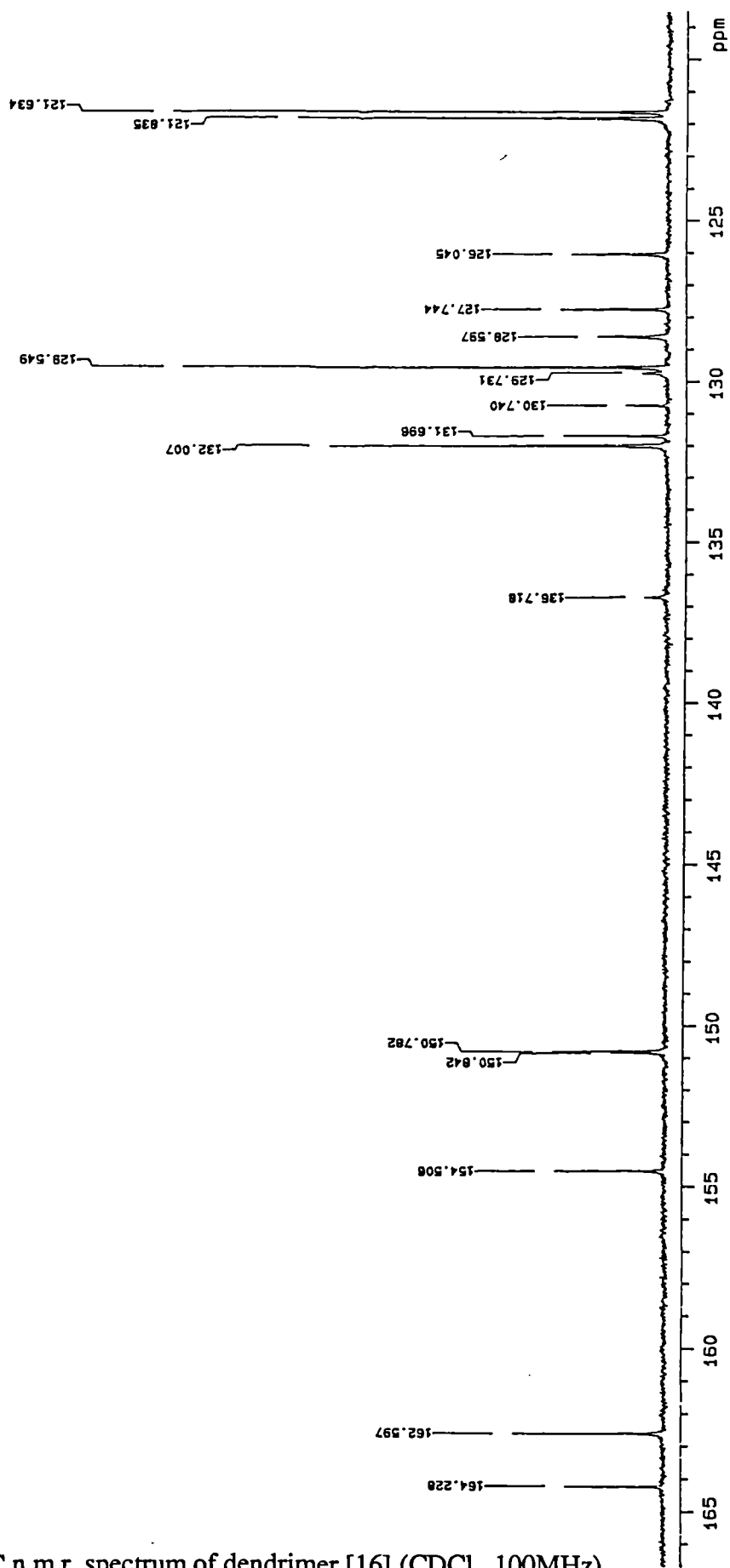
Figure A1.32 ^{13}C n.m.r. spectrum of dendrimer [16] (CDCl$_3$, 100MHz)
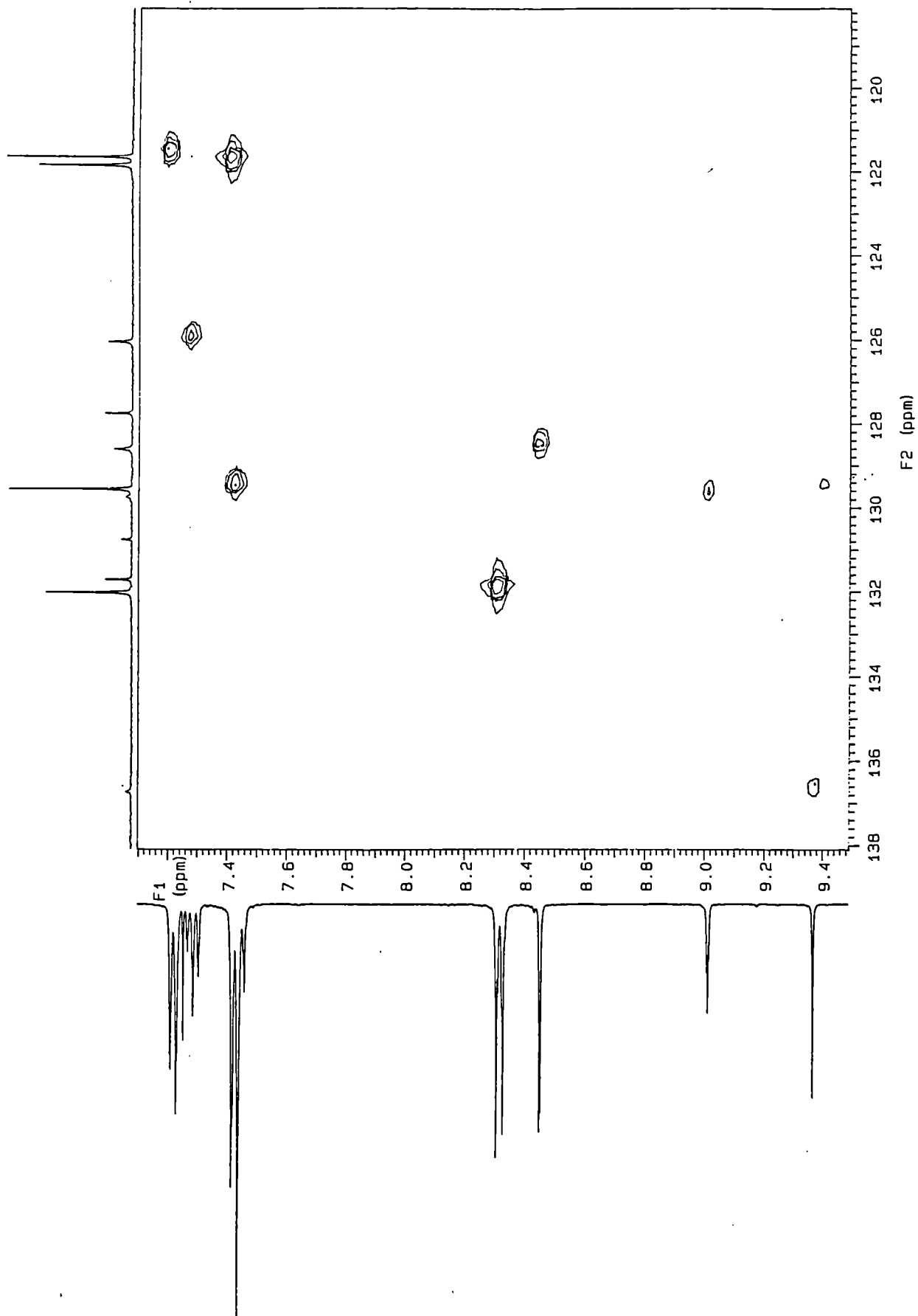
A1-33

Figure A1.33 ^1H - ^{13}C hetcor spectrum of dendrimer [16] (CDCl$_3$)
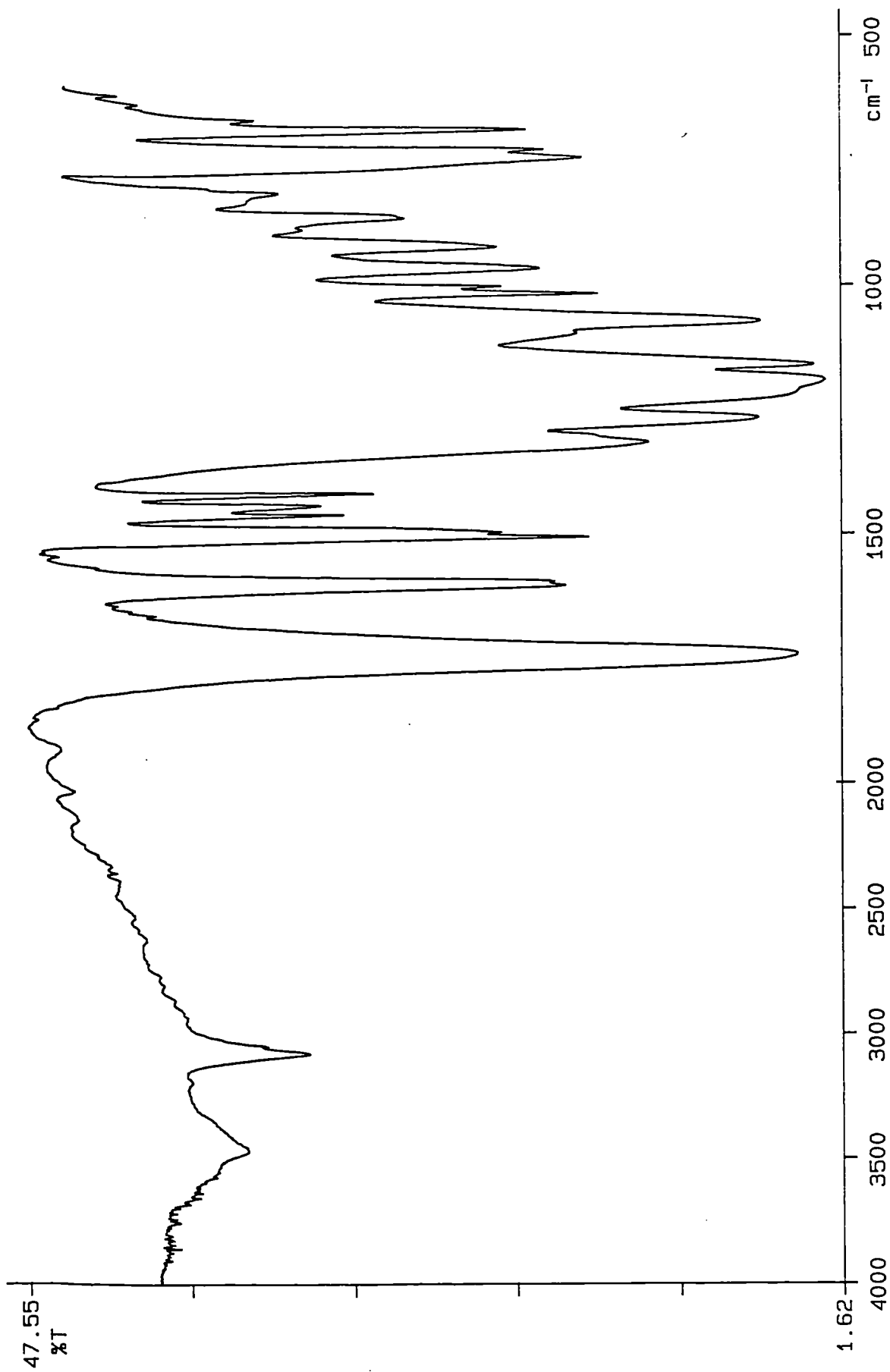
Figure A1.34 I.R. spectrum of dendrimer [16] (KBr disc)
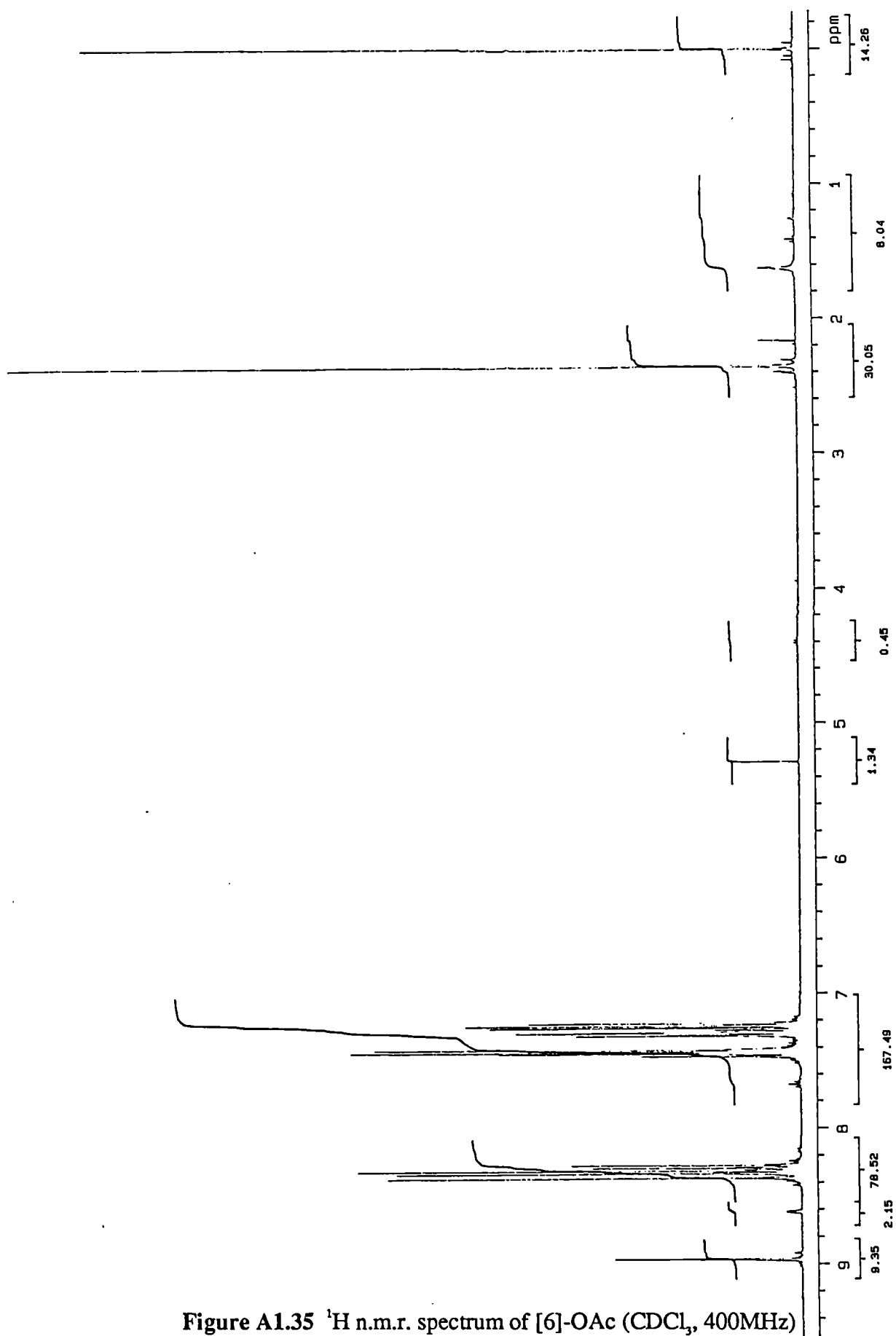
Figure A1.35 ¹H n.m.r. spectrum of [6]-OAc (CDCl₃, 400MHz)
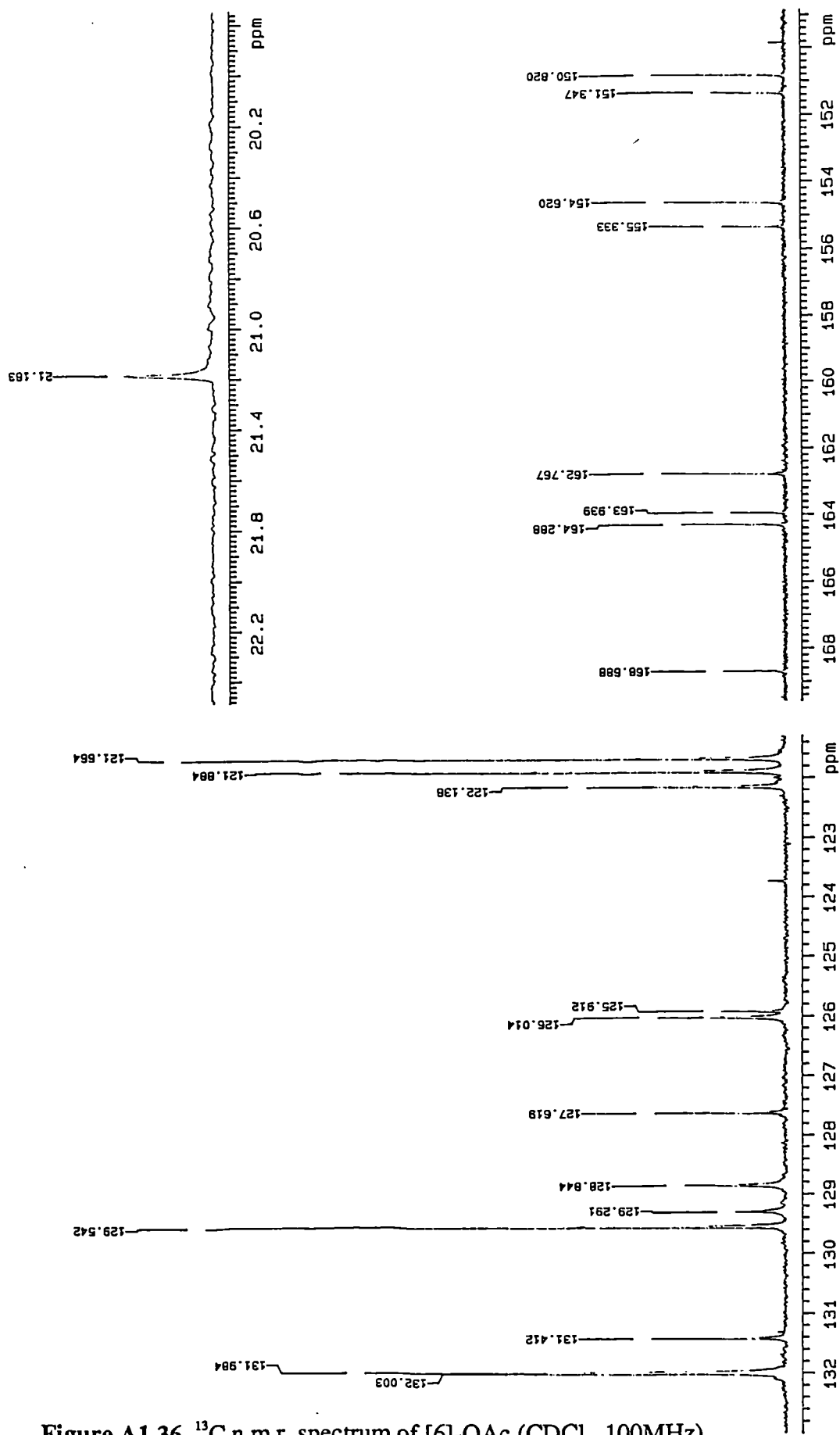
A1-36

Figure A1.36 ^{13}C n.m.r. spectrum of [6]-OAc (CDCl$_3$, 100MHz)
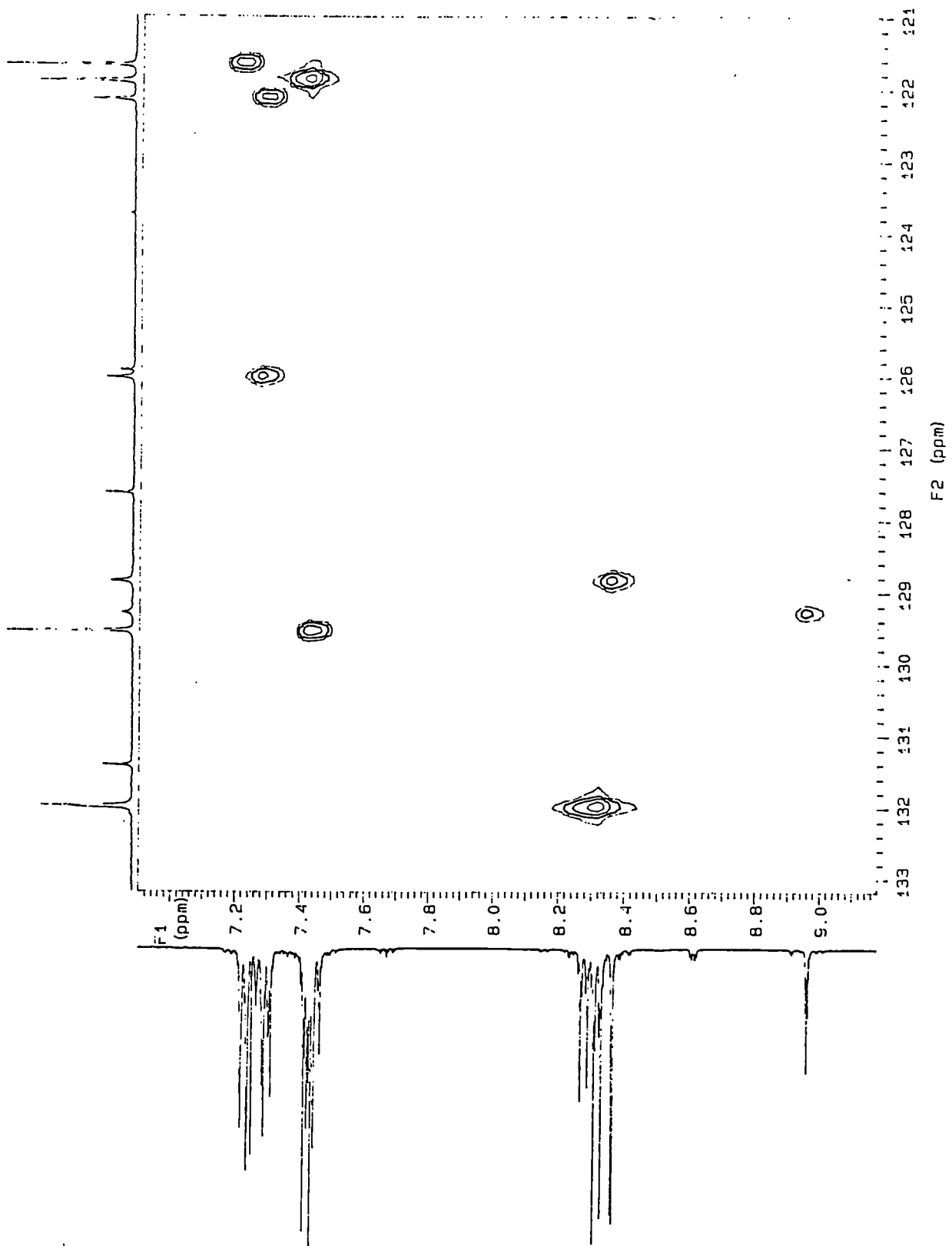
Figure A1.37 ^1H - ^{13}C hetcor spectrum of [6]-OAc (CDCl$_3$)
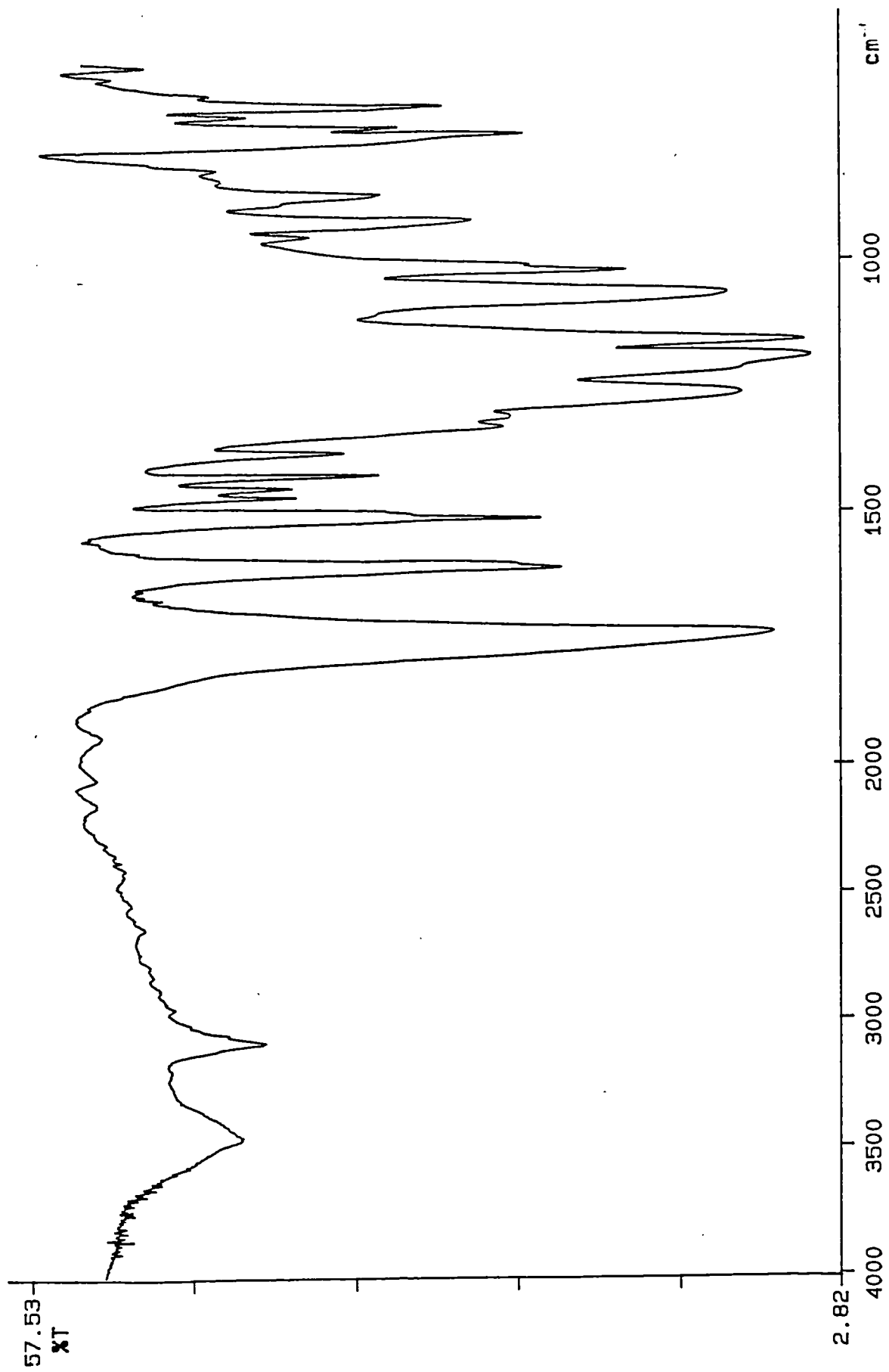
Figure A1.38 I.R. spectrum of [6]-OAc (KBr disc)
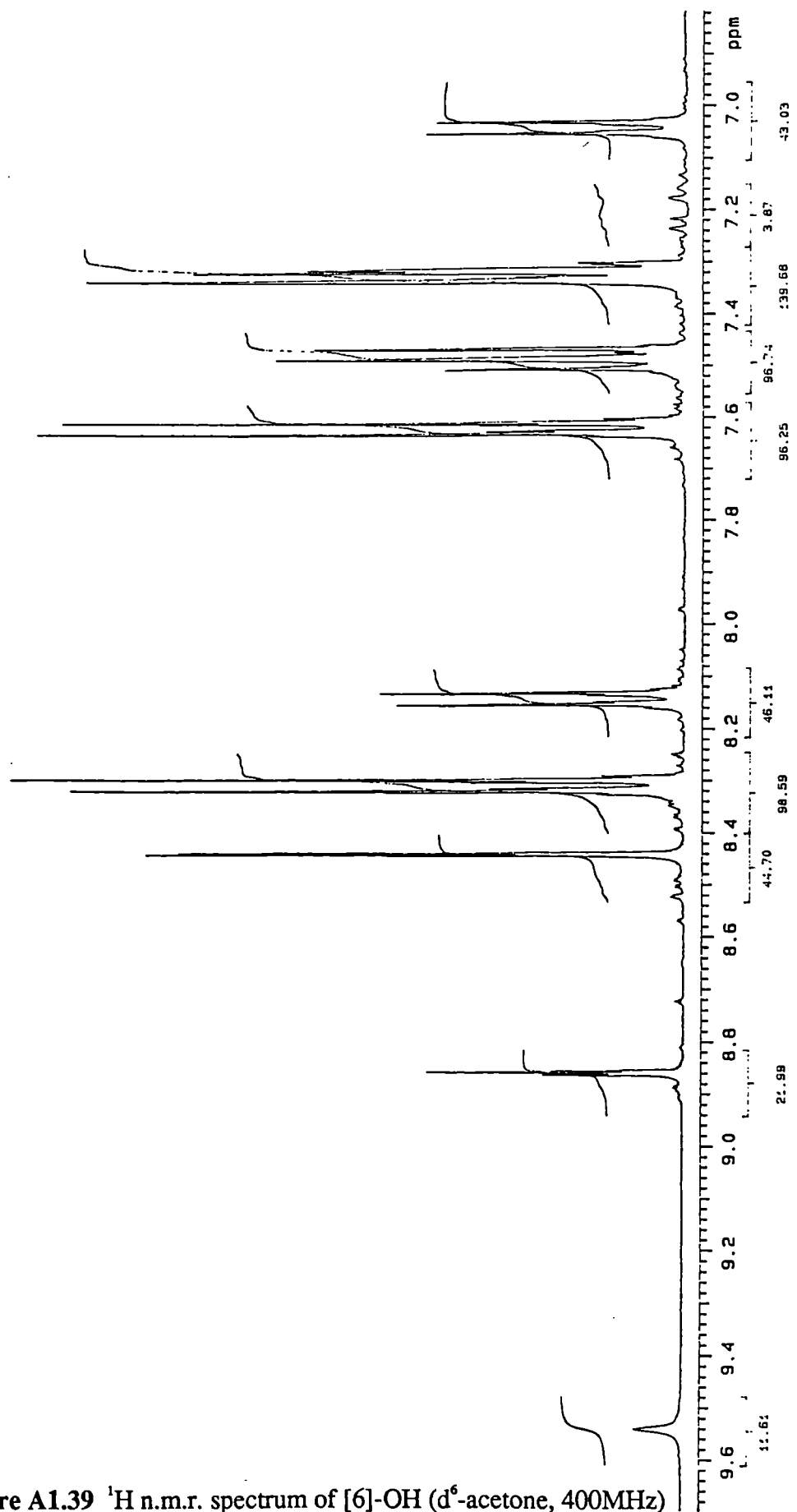
Figure A1.39 ^{1}H n.m.r. spectrum of [6]-OH (d^6-acetone, 400MHz)
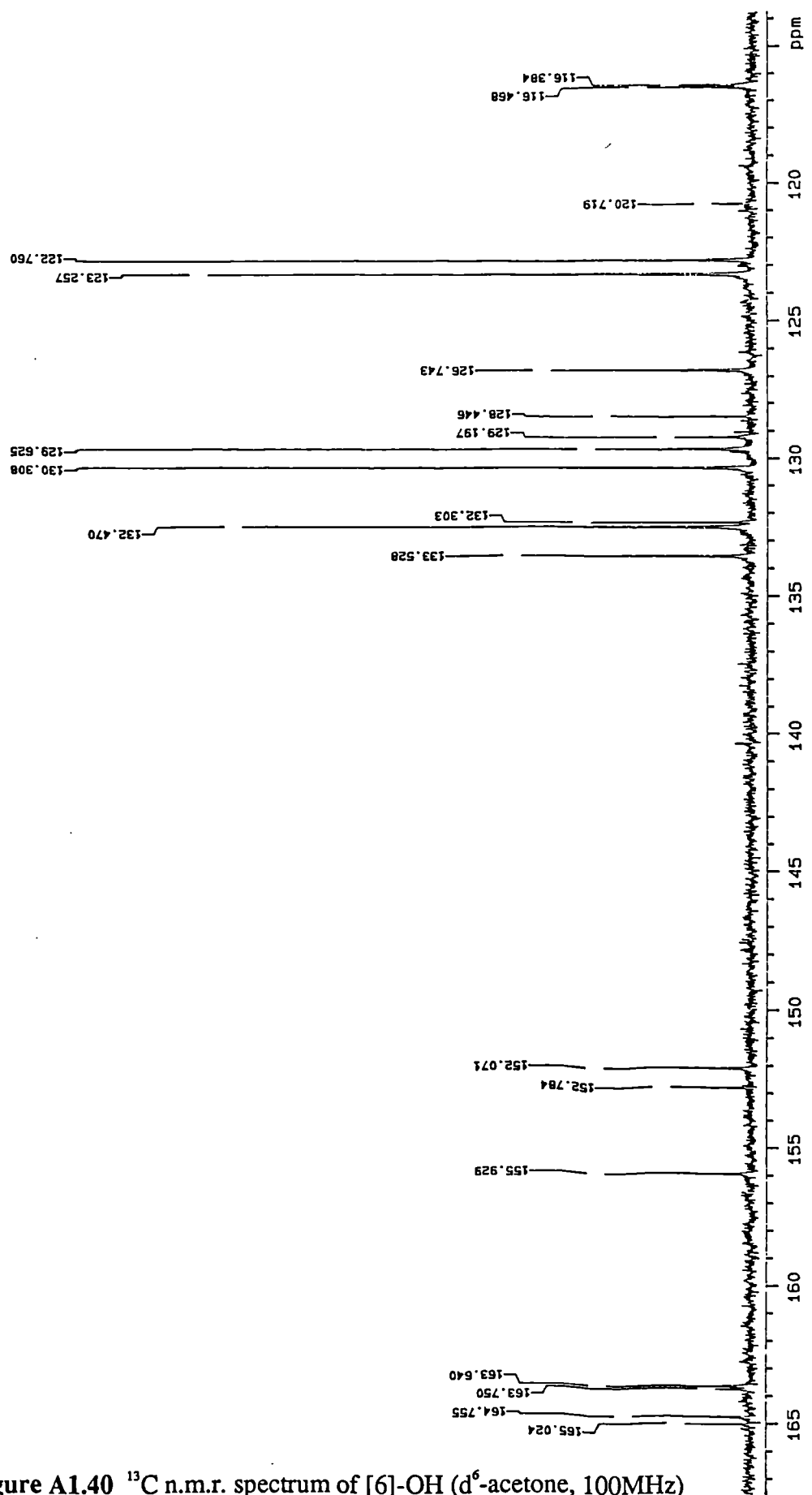
Figure A1.40 ^{13}C n.m.r. spectrum of [6]-OH (d^6-acetone, 100MHz)
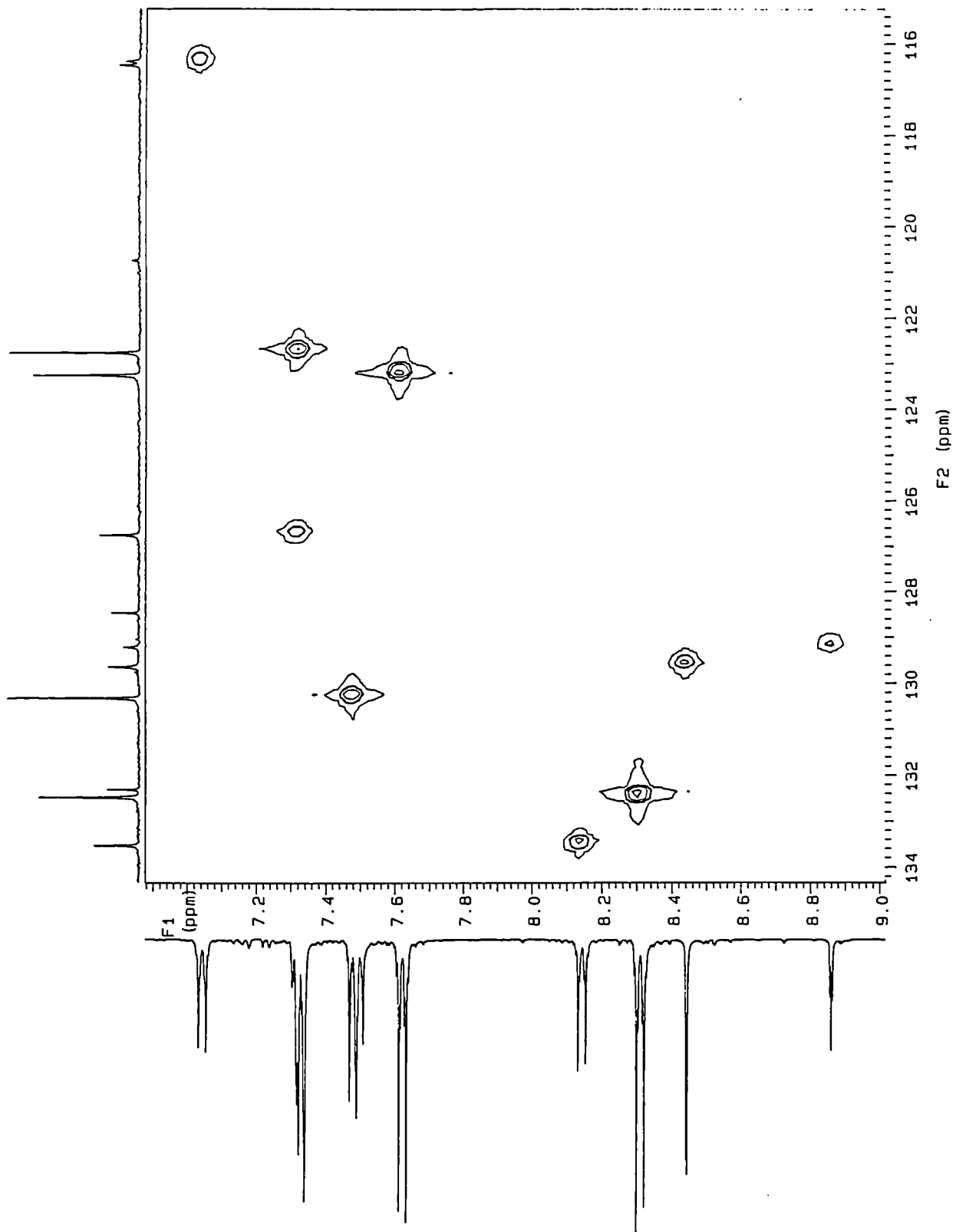
Figure A1.41 ^{1}H - ^{13}C hetcor spectrum of [6]-OH (d^{6}-acetone)
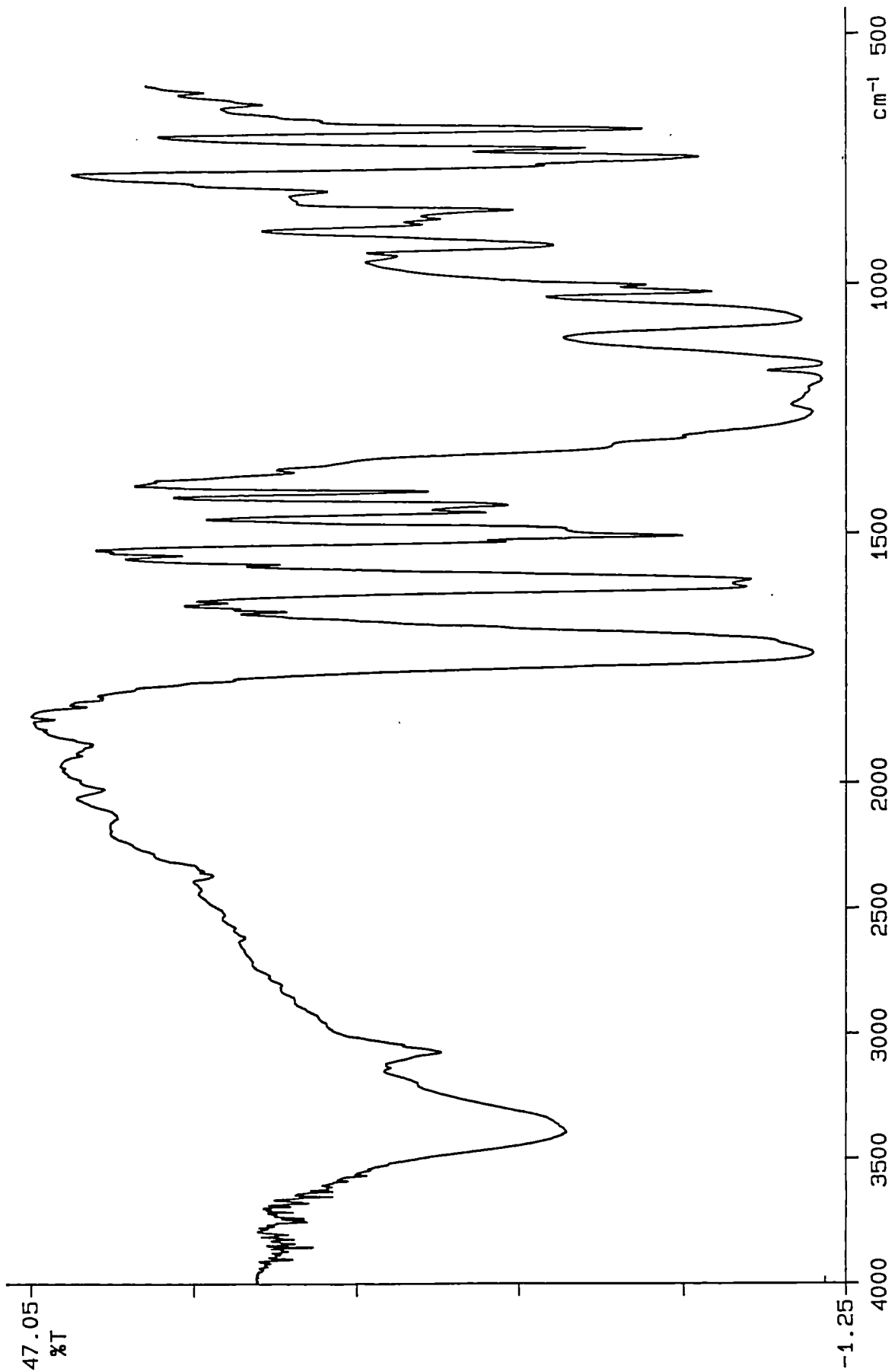
Figure A1.42 I.R. spectrum of [6]-OH (KBr disc)
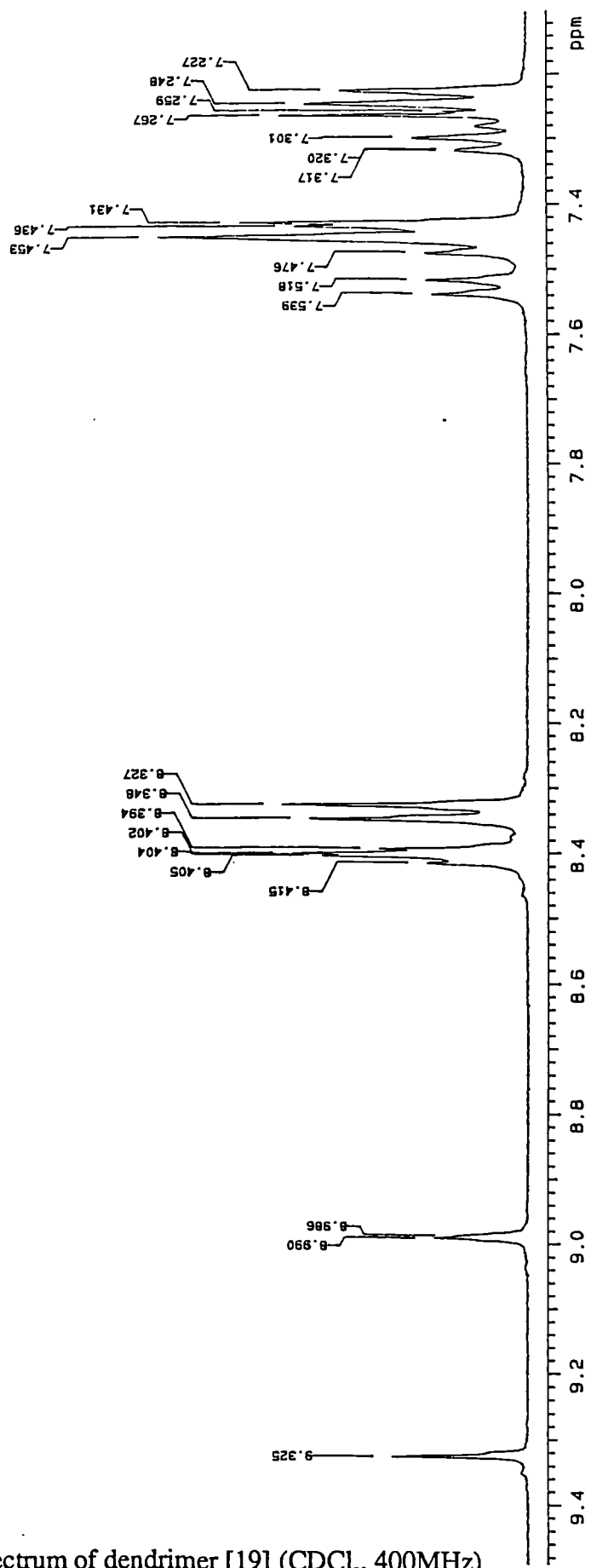
A1-43

Figure A1.43 ^{1}H n.m.r. spectrum of dendrimer [19] (CDCl$_3$, 400MHz)

Figure A1.44 ^{13}C n.m.r. spectrum of dendrimer [19] (CDCl$_3$, 100MHz)
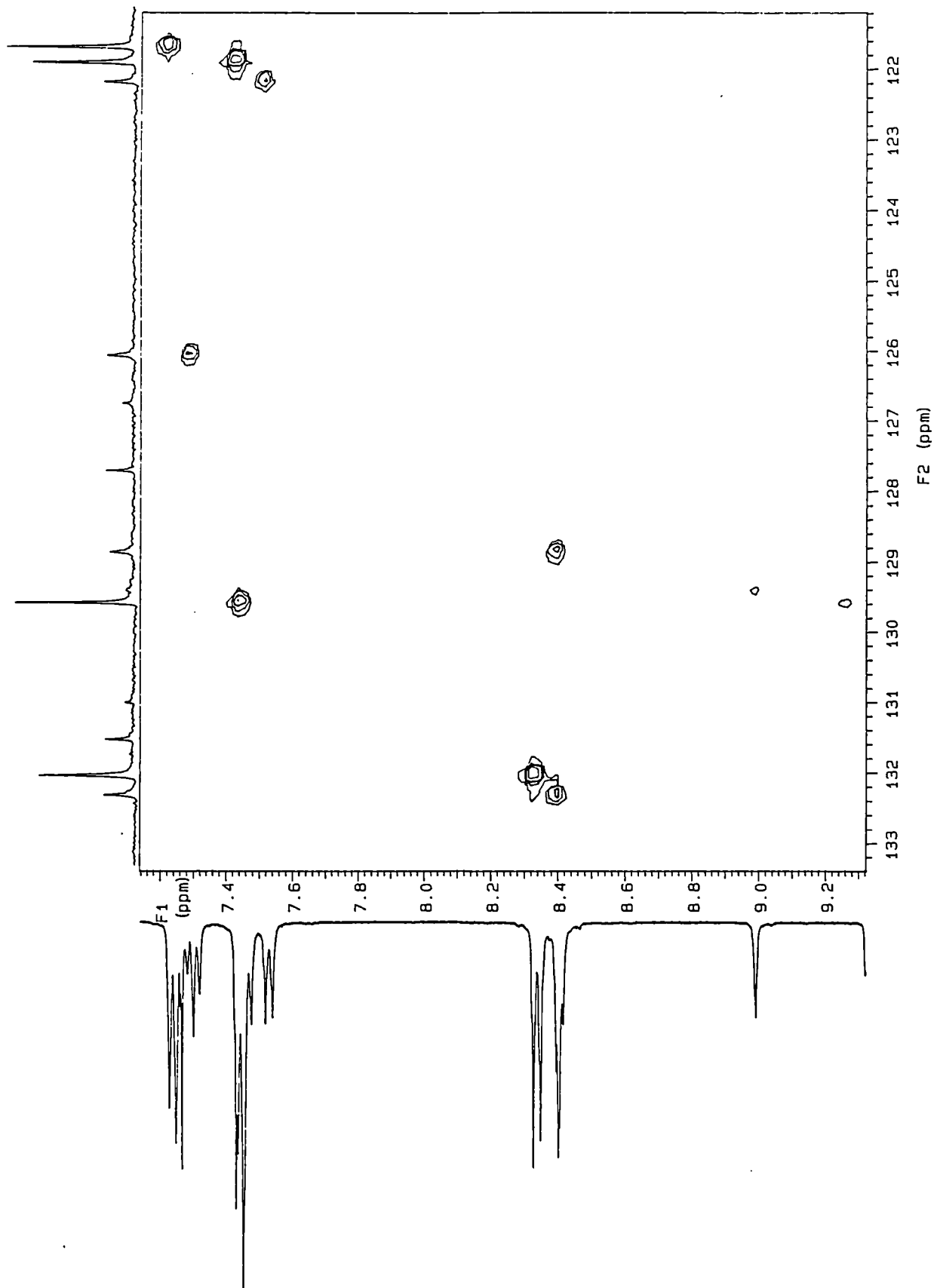
Figure A1.45 ^1H - ^{13}C hetcor spectrum of dendrimer [19] (CDCl$_3$)
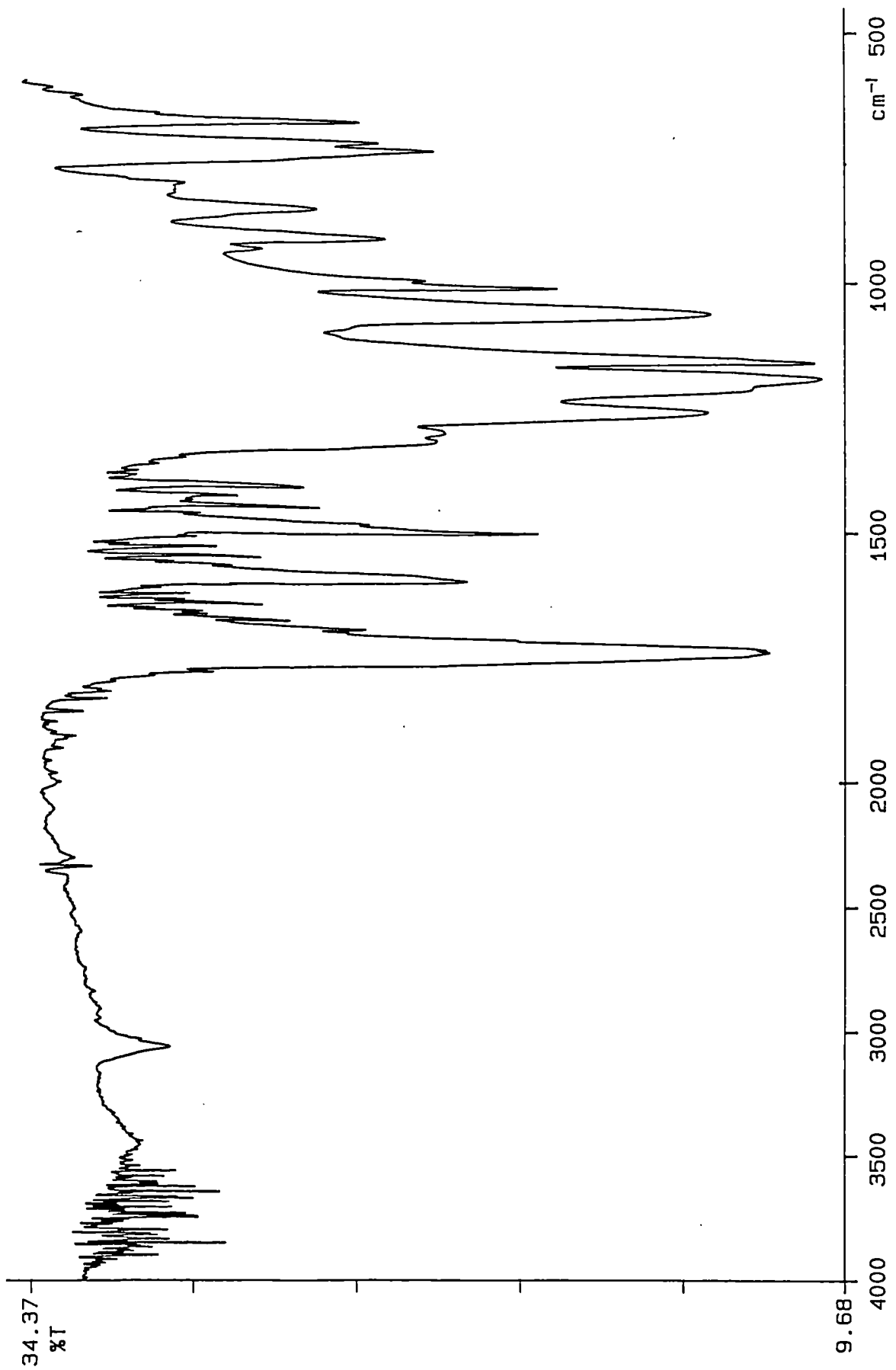
Figure A1.46 I.R. spectrum of dendrimer [19] (KBr disc)
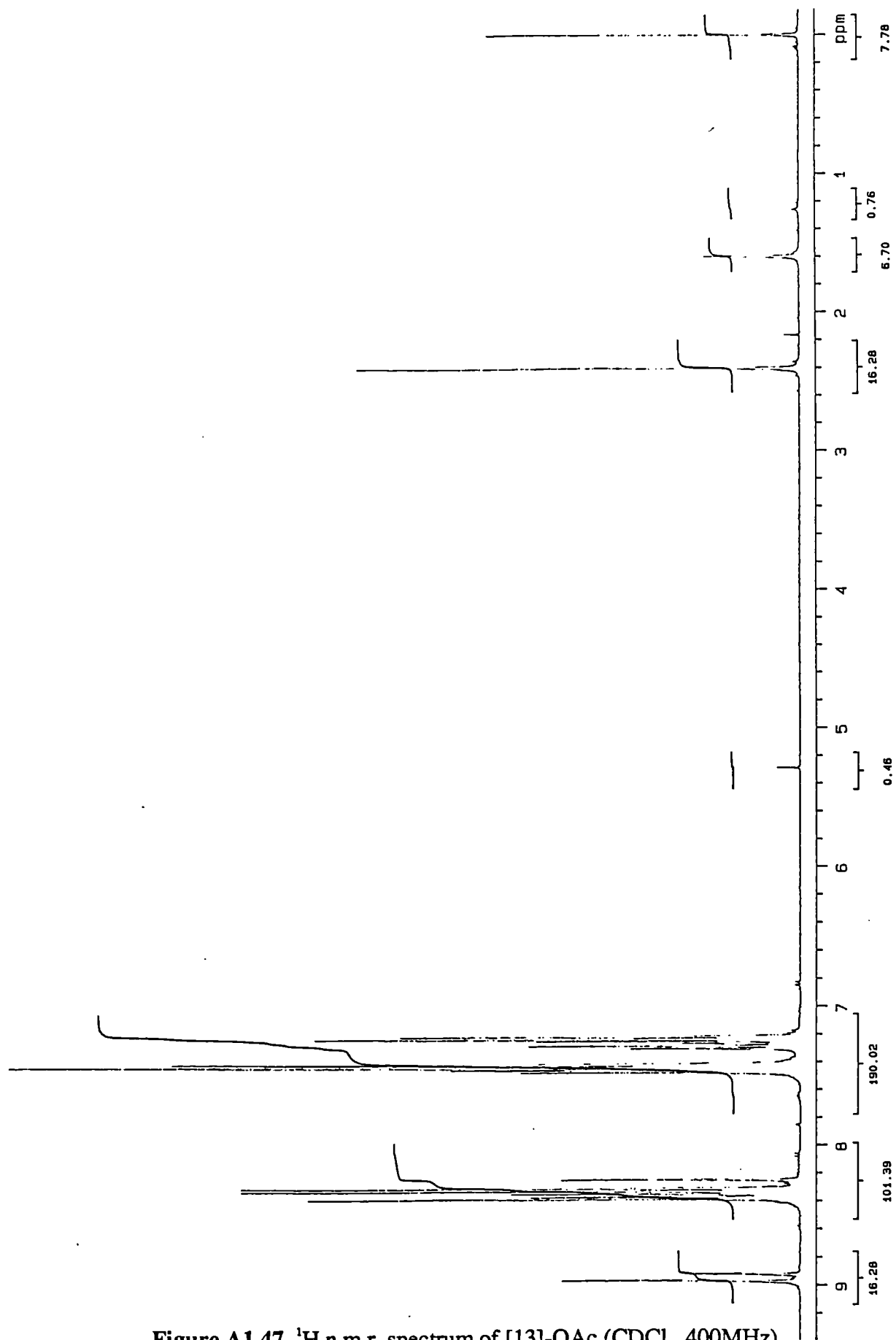
A1-47

Figure A1.47 ^{1}H n.m.r. spectrum of [13]-OAc (CDCl$_3$, 400MHz)
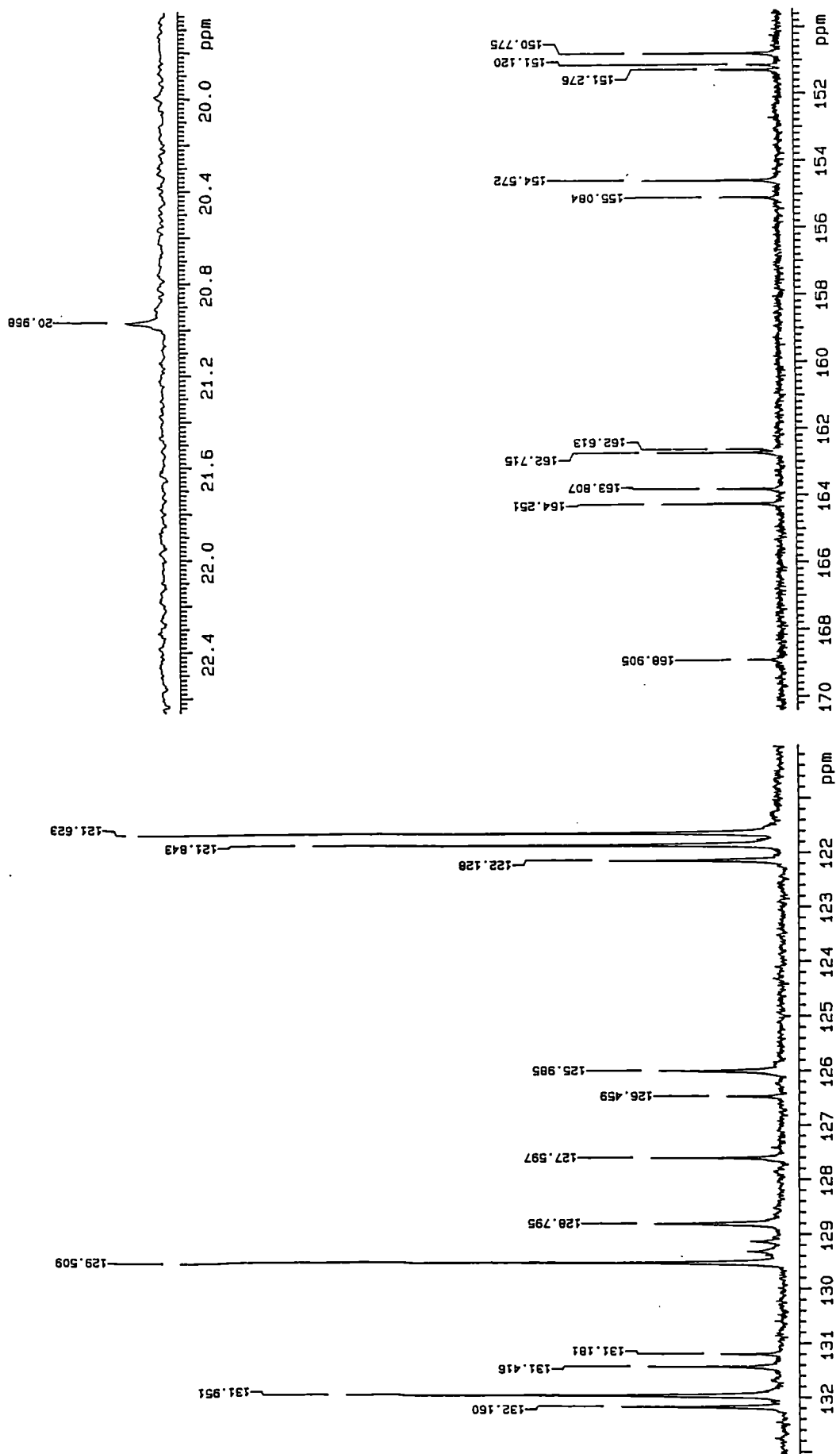
Figure A1.48 ^{13}C n.m.r. spectrum of [13]-OAc (CDCl$_3$, 100MHz)
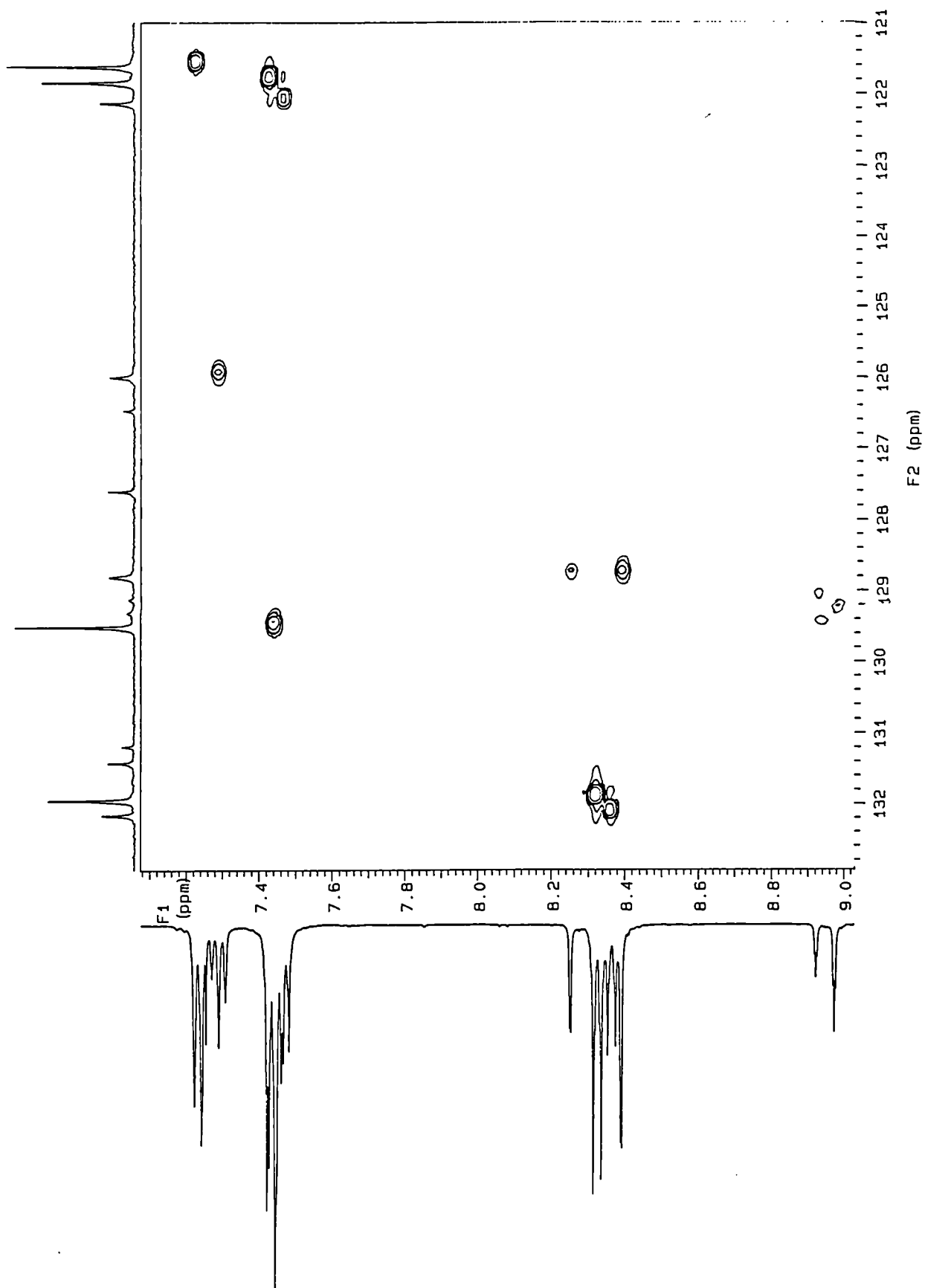
Figure A1.49 ^{1}H - ^{13}C hetcor spectrum of [13]-OAc (CDCl$_3$)
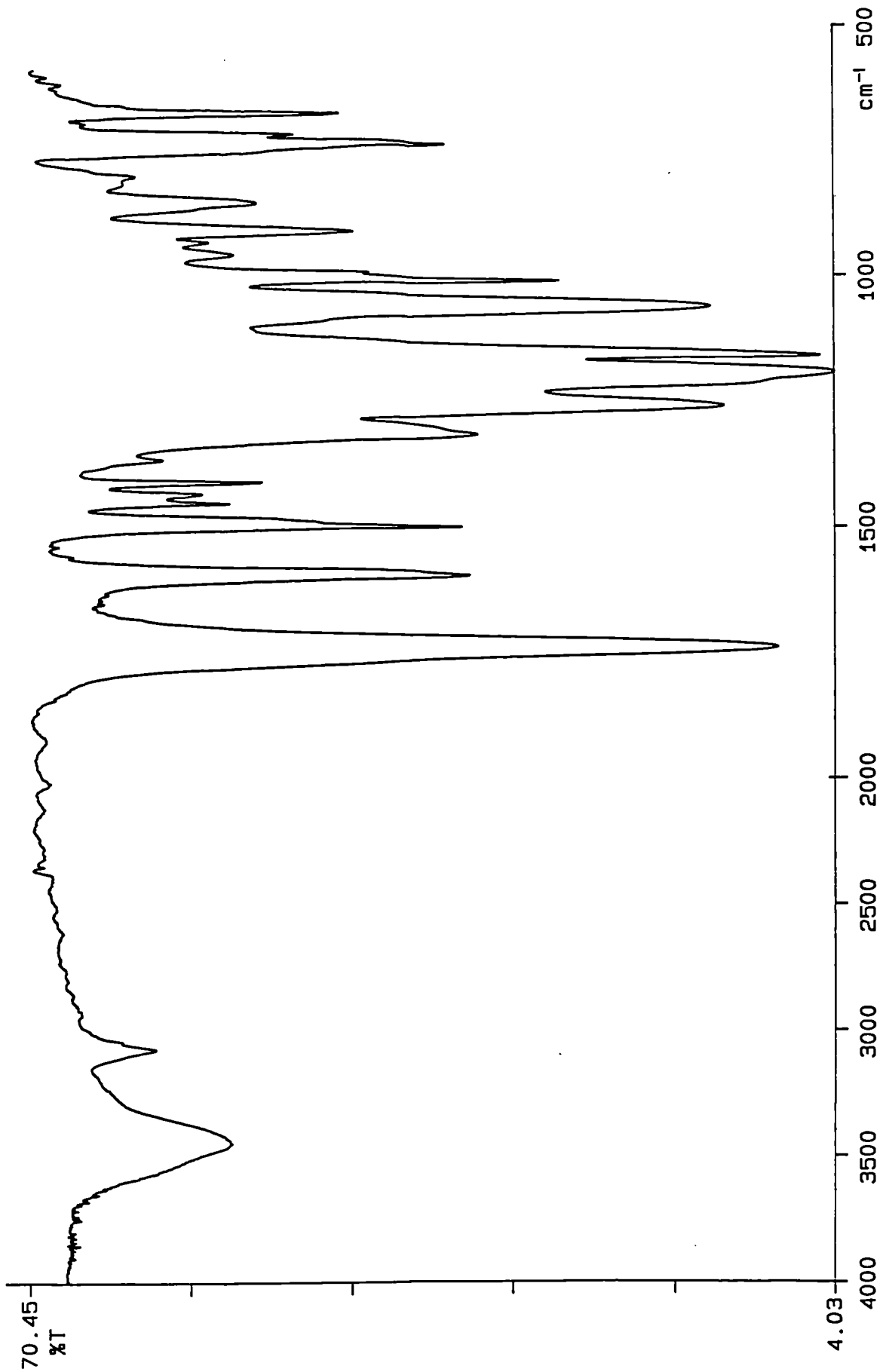
Figure A1.50 I.R. spectrum of [13]-OAc (KBr disc)

APPENDIX 2

N.M.R. and I.R. spectra (Chapter 5)
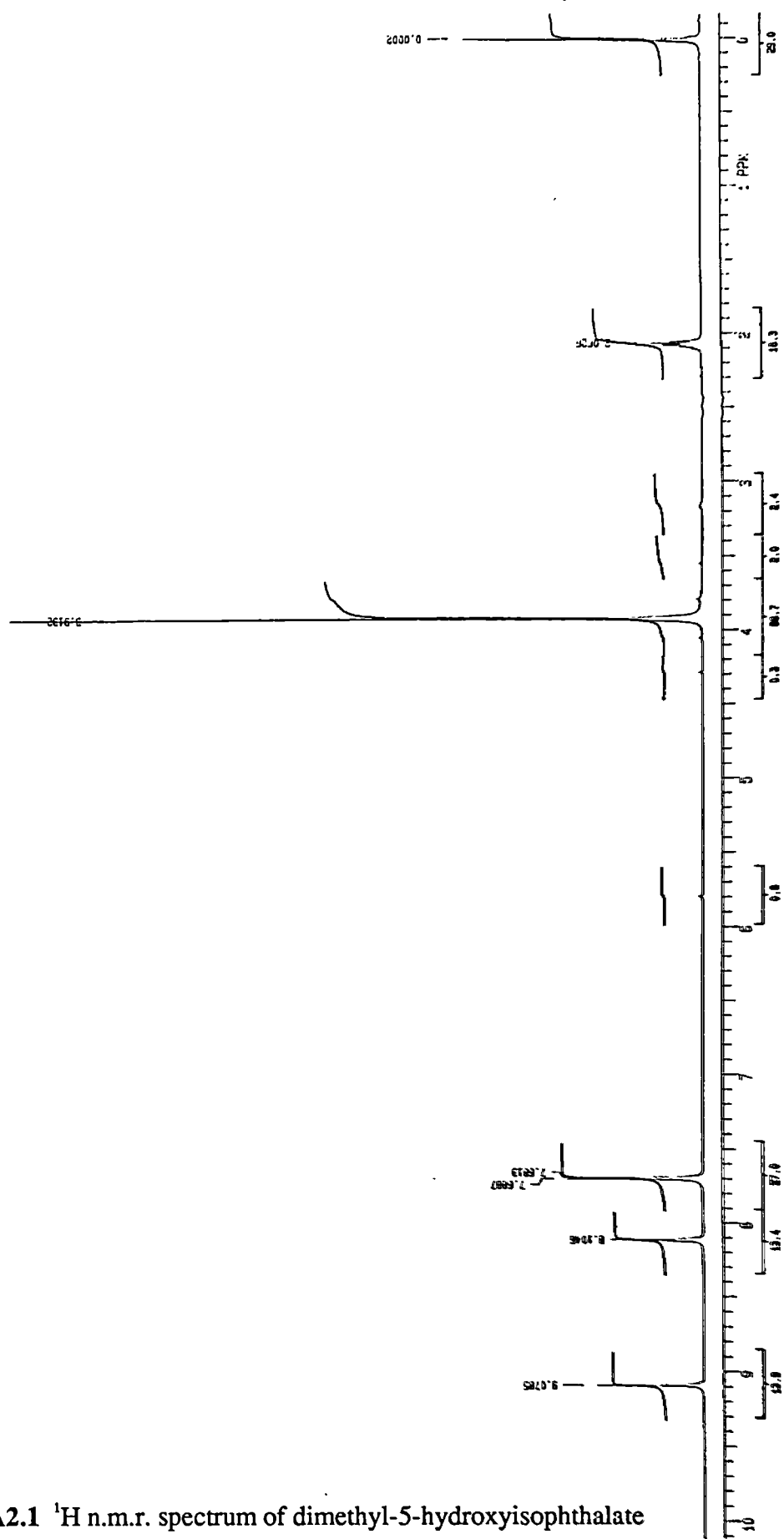
Figure A2.1 ^{1}H n.m.r. spectrum of dimethyl-5-hydroxyisophthalate
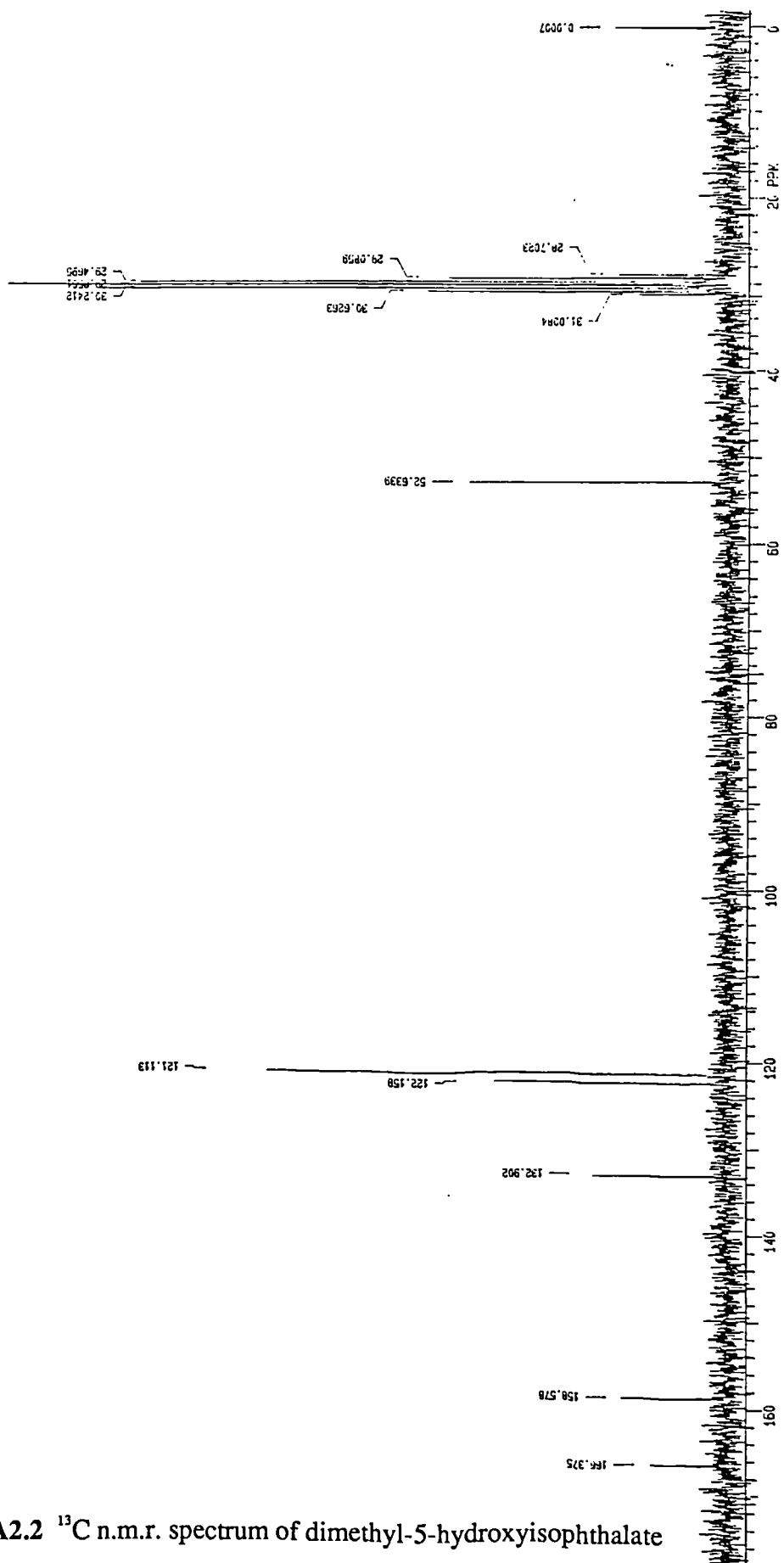(d^6-acetone, 200MHz)

0.0007

29.7023

29.4690
30.3663
32.2412
29.0658
30.6263
31.0284

52.6339

121.113
122.158

132.902

158.578

166.375

20 PPM

40

60

80

100

120

140

160

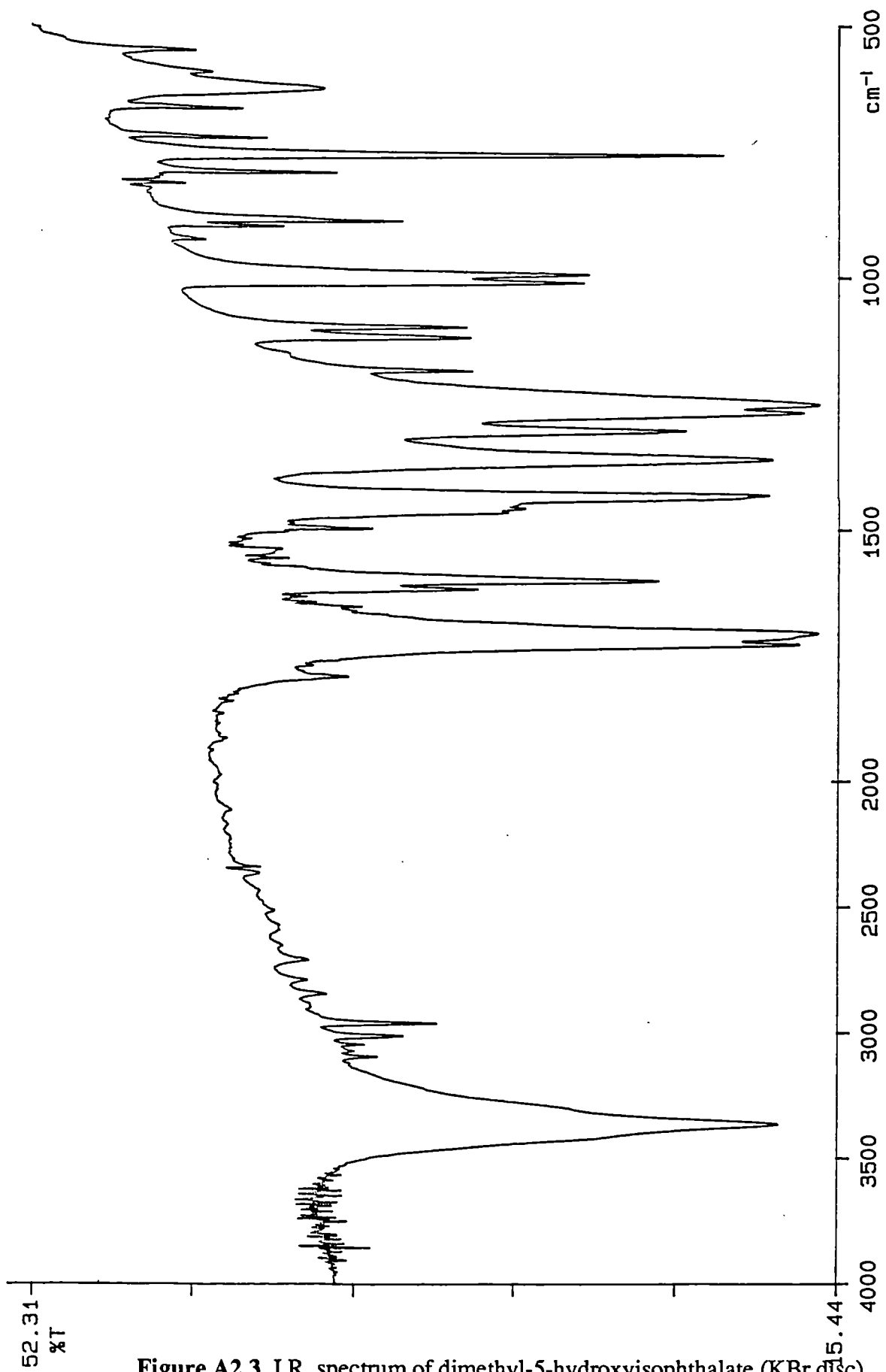**Figure A2.2** ^{13}C n.m.r. spectrum of dimethyl-5-hydroxyisophthalate
(d^6-acetone, 50MHz)

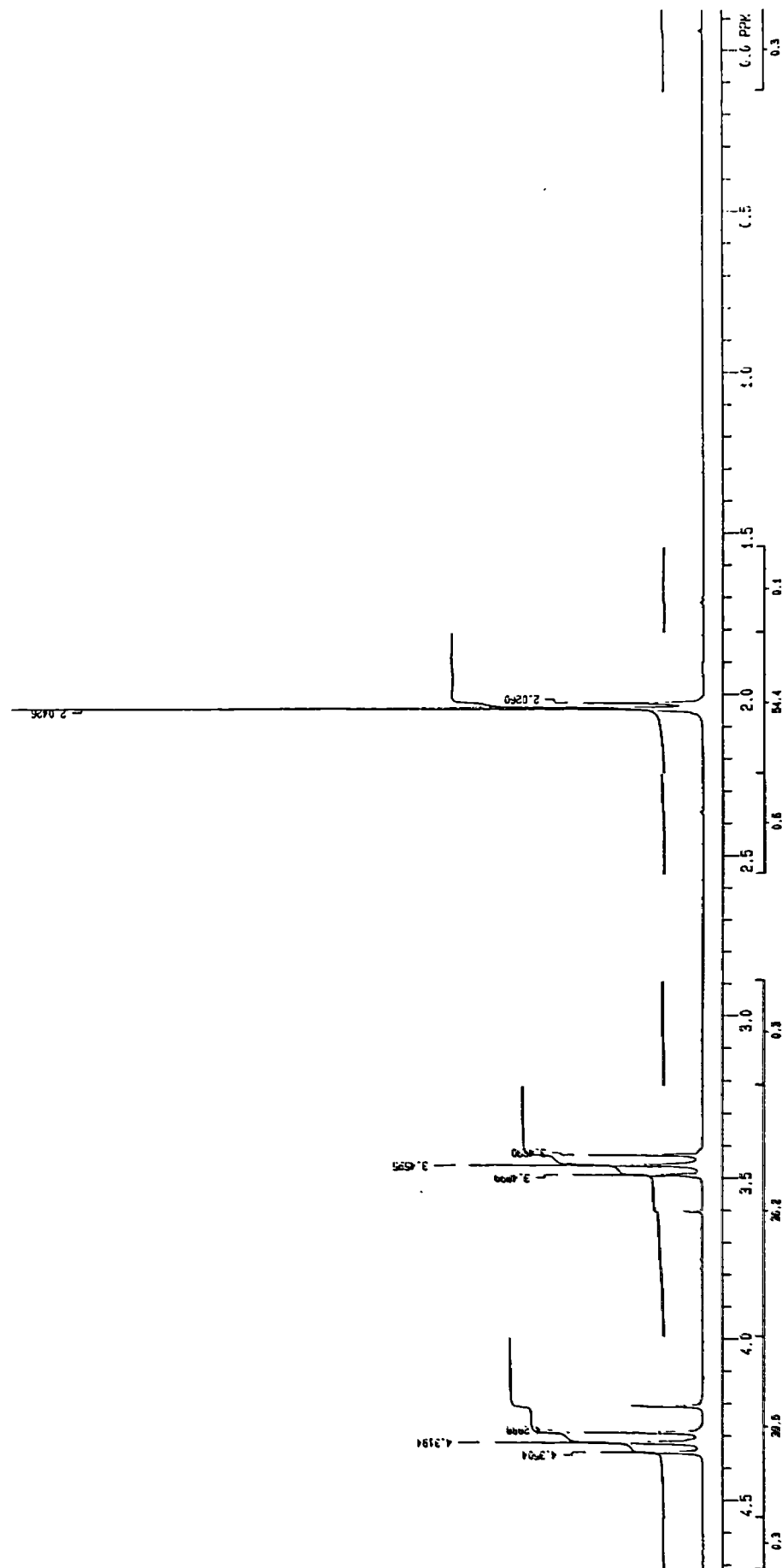**Figure A2.3** I.R. spectrum of dimethyl-5-hydroxyisophthalate (KBr disc)

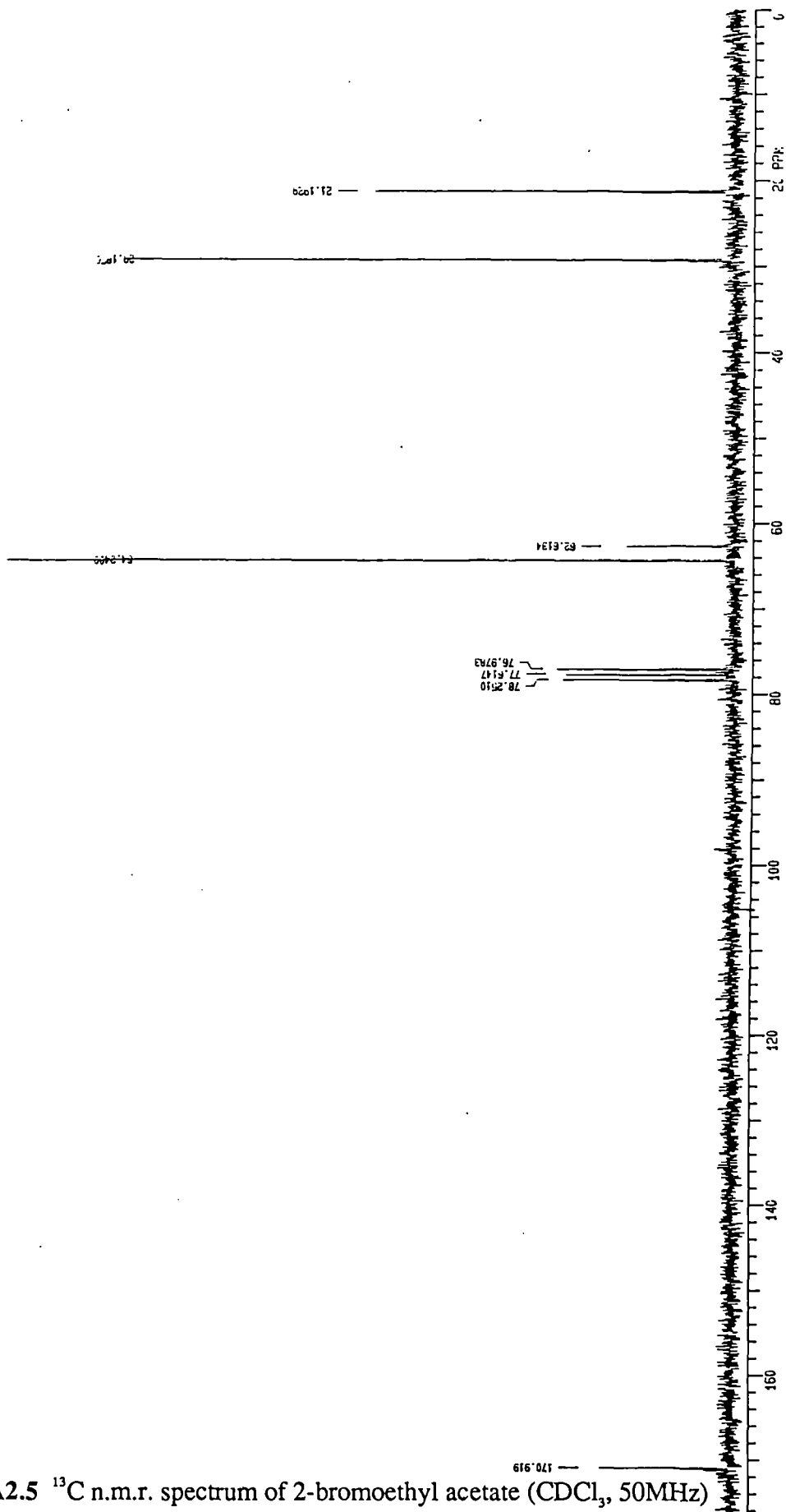**Figure A2.4** ^{1}H n.m.r. spectrum of 2-bromoethyl acetate (CDCl$_3$, 200MHz)

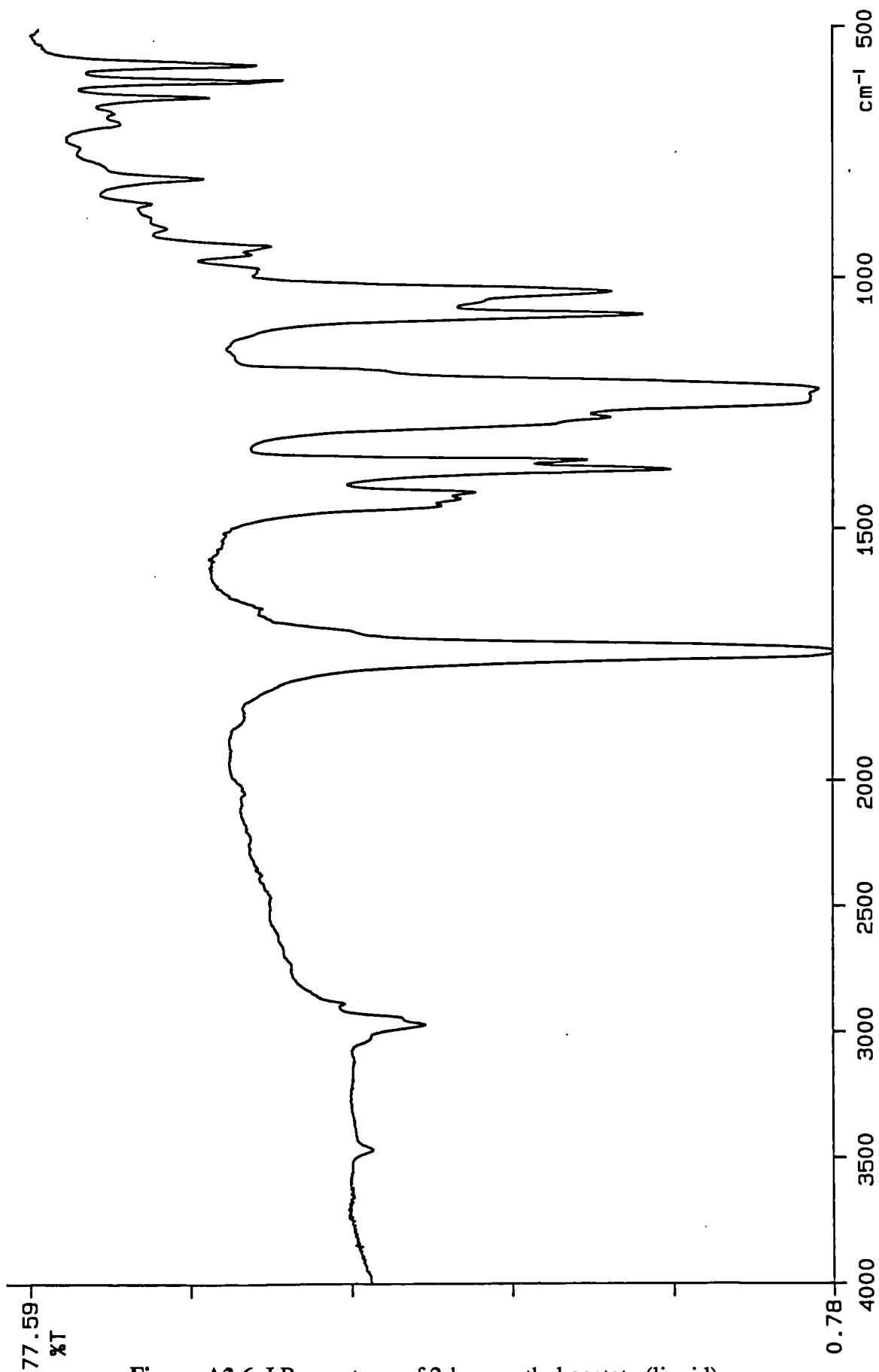**Figure A2.5** ^{13}C n.m.r. spectrum of 2-bromoethyl acetate (CDCl$_3$, 50MHz)

Figure A2.6 I.R. spectrum of 2-bromoethyl acetate (liquid)

Figure A2.7 ^{1}H n.m.r. spectrum of dimethyl-5-(2-acetoxyethoxy)isophthalate

(CDCl$_3$, 200MHz)

A2-8

Figure A2.8 ^{13}C n.m.r. spectrum of dimethyl-5-(2-acetoxyethoxy)isophthalate (CDCl$_3$, 100MHz)
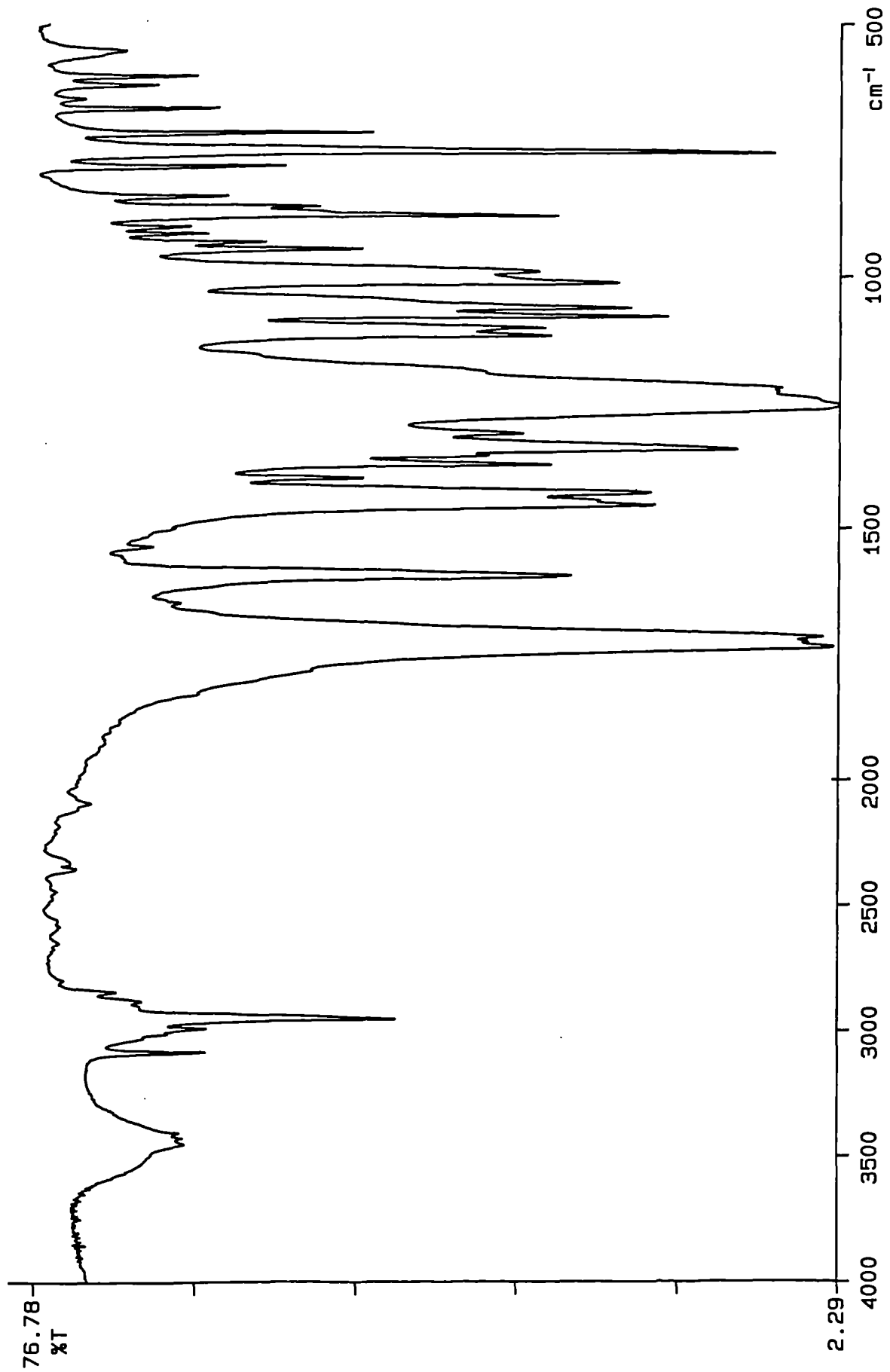
Figure A2.9 I.R. spectrum of dimethyl-5-(2-acetoxyethoxy)isophthalate (KBr disc)
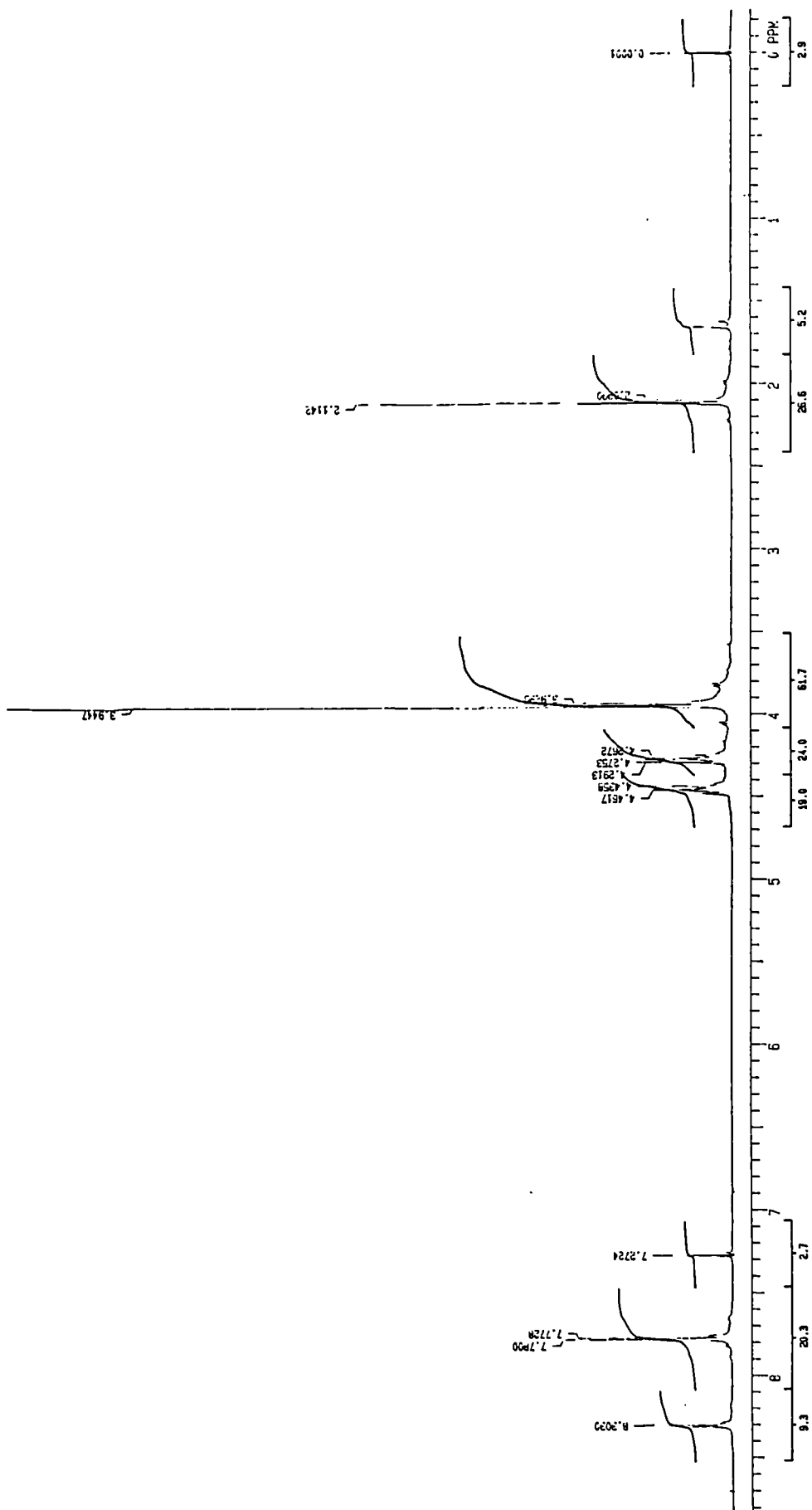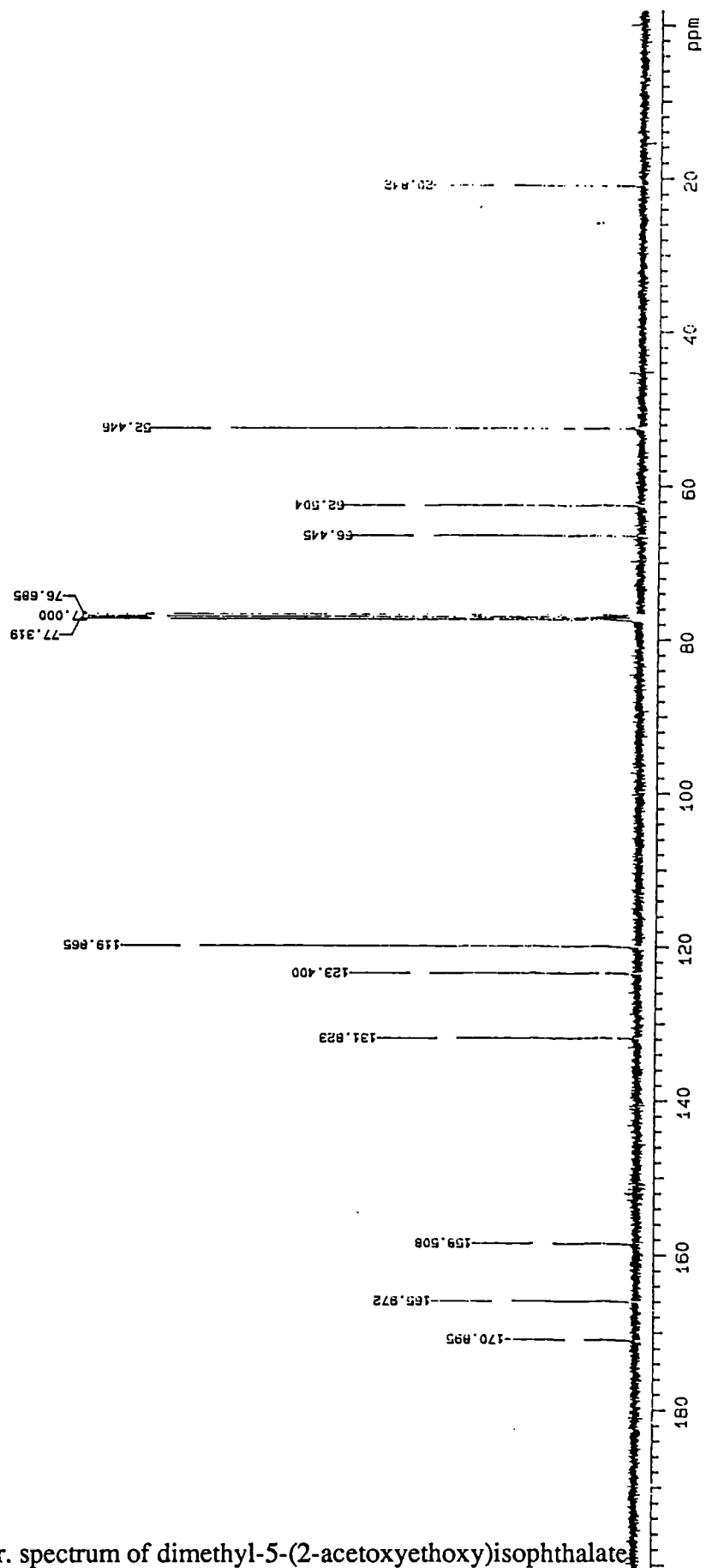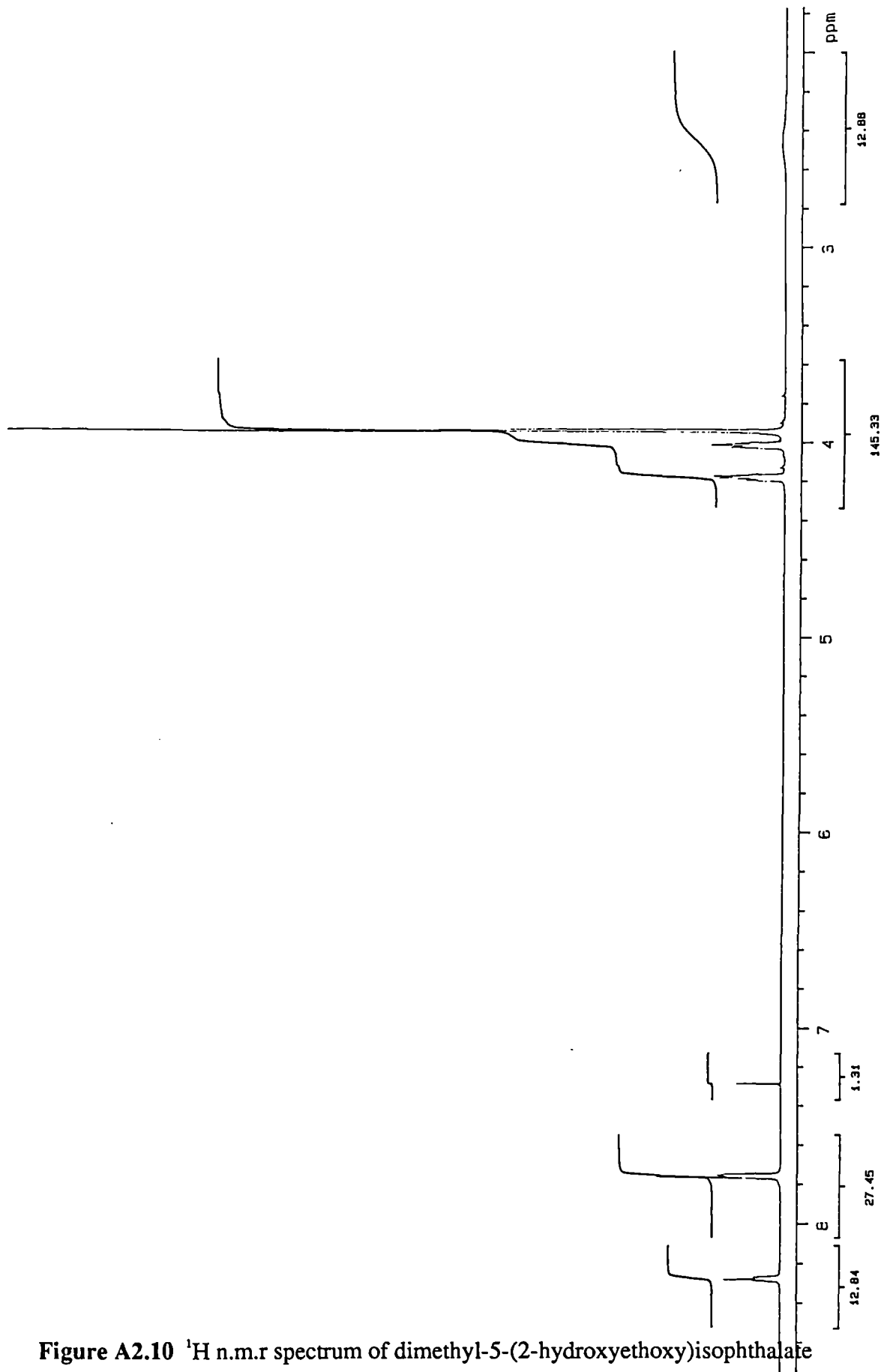
Figure A2.10 ^{1}H n.m.r spectrum of dimethyl-5-(2-hydroxyethoxy)isophthalate
(CDCl$_3$, 400MHz)
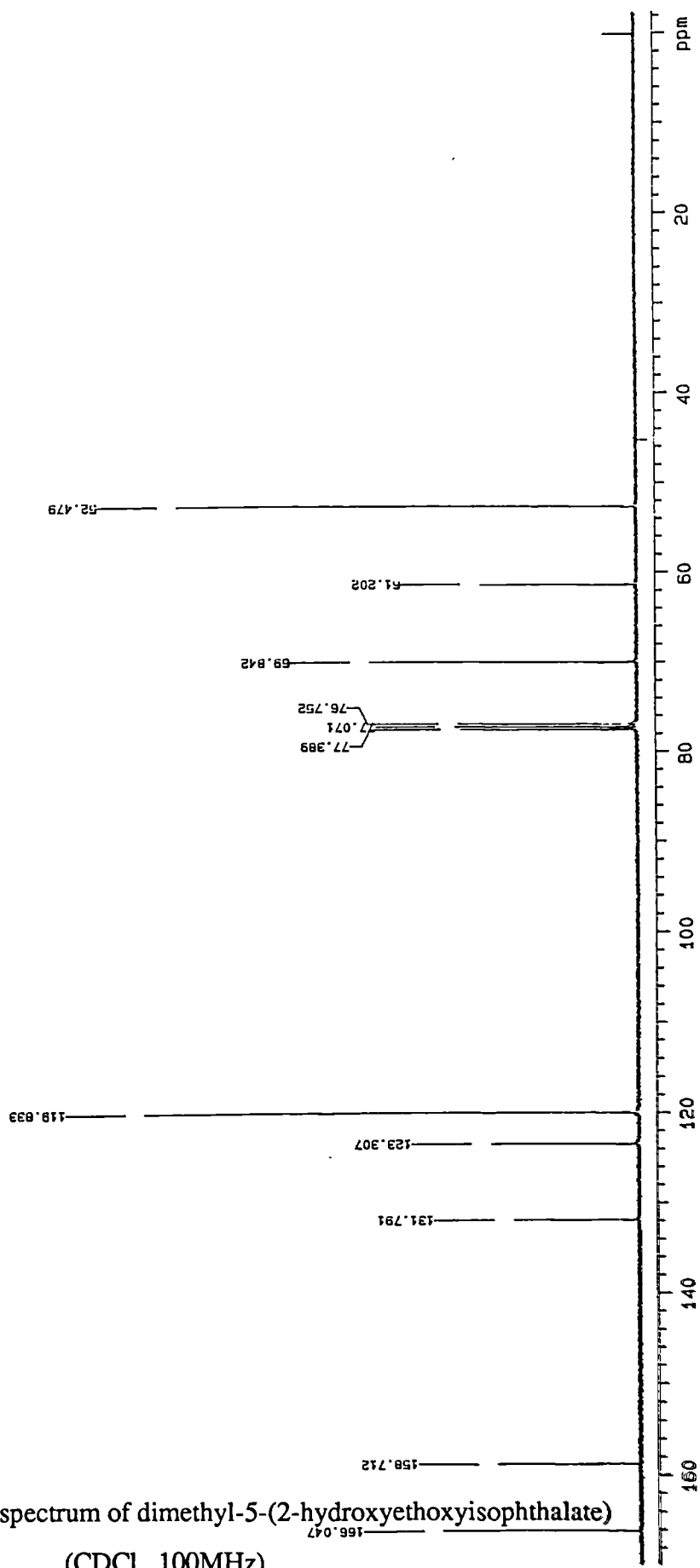
Figure A2.11 ^{13}C n.m.r. spectrum of dimethyl-5-(2-hydroxyethoxyisophthalate) (CDCl$_3$, 100MHz)

Figure A2.12 I.R. spectrum of dimethyl-5-(2-hydroxyethoxy)isophthalate (KBr disc)

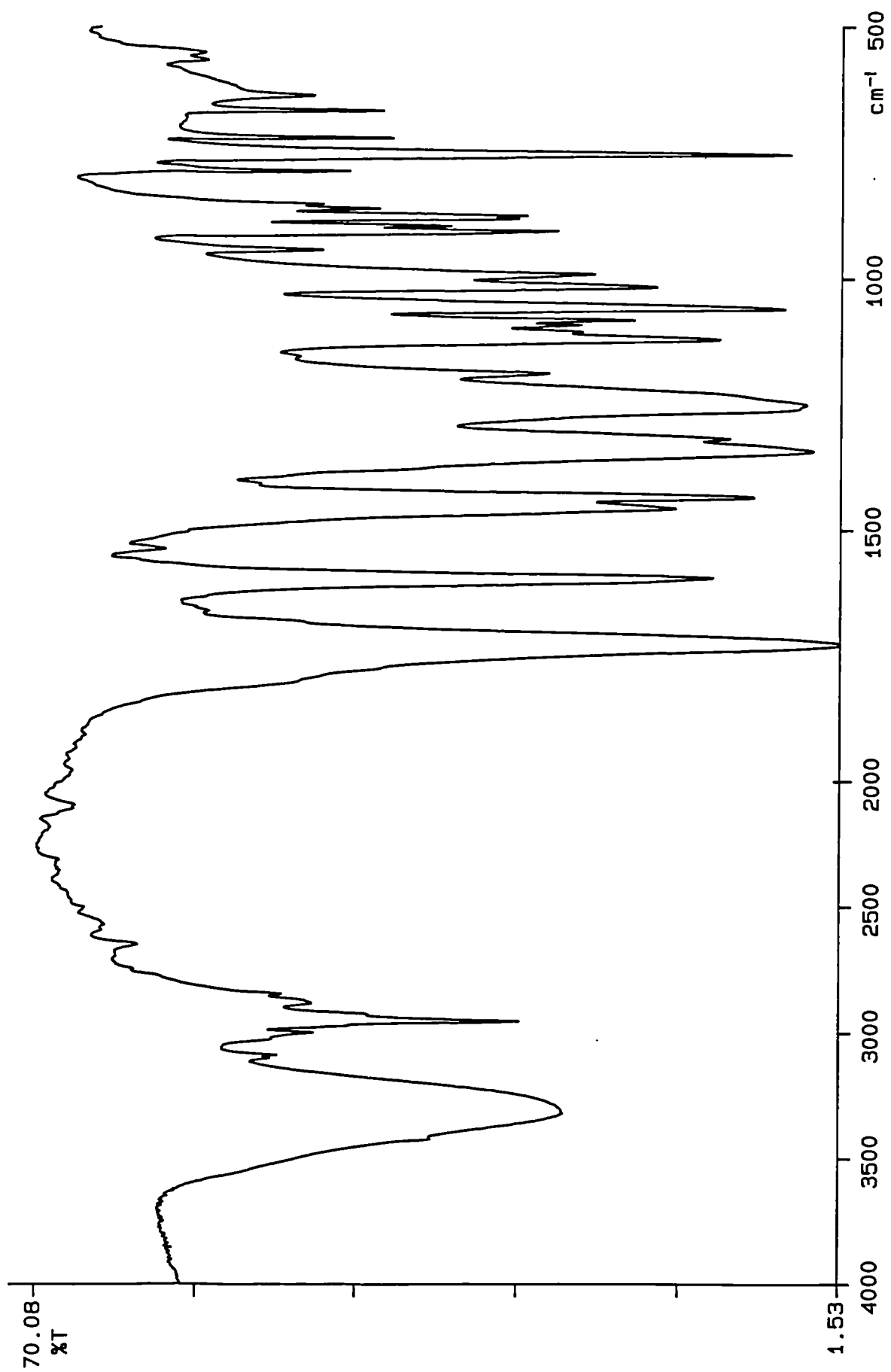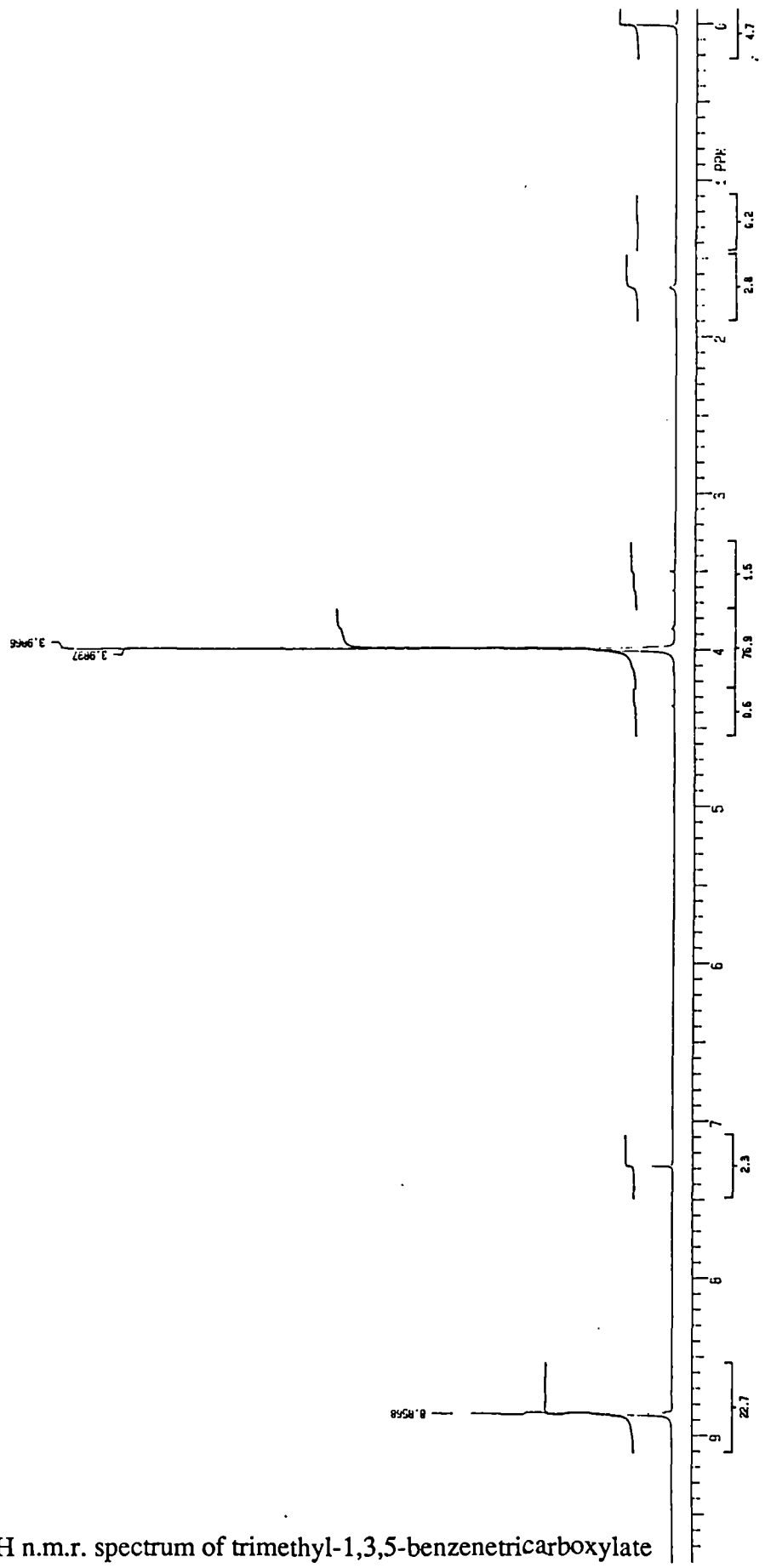**Figure A2.13** ^{1}H n.m.r. spectrum of trimethyl-1,3,5-benzenetricarboxylate
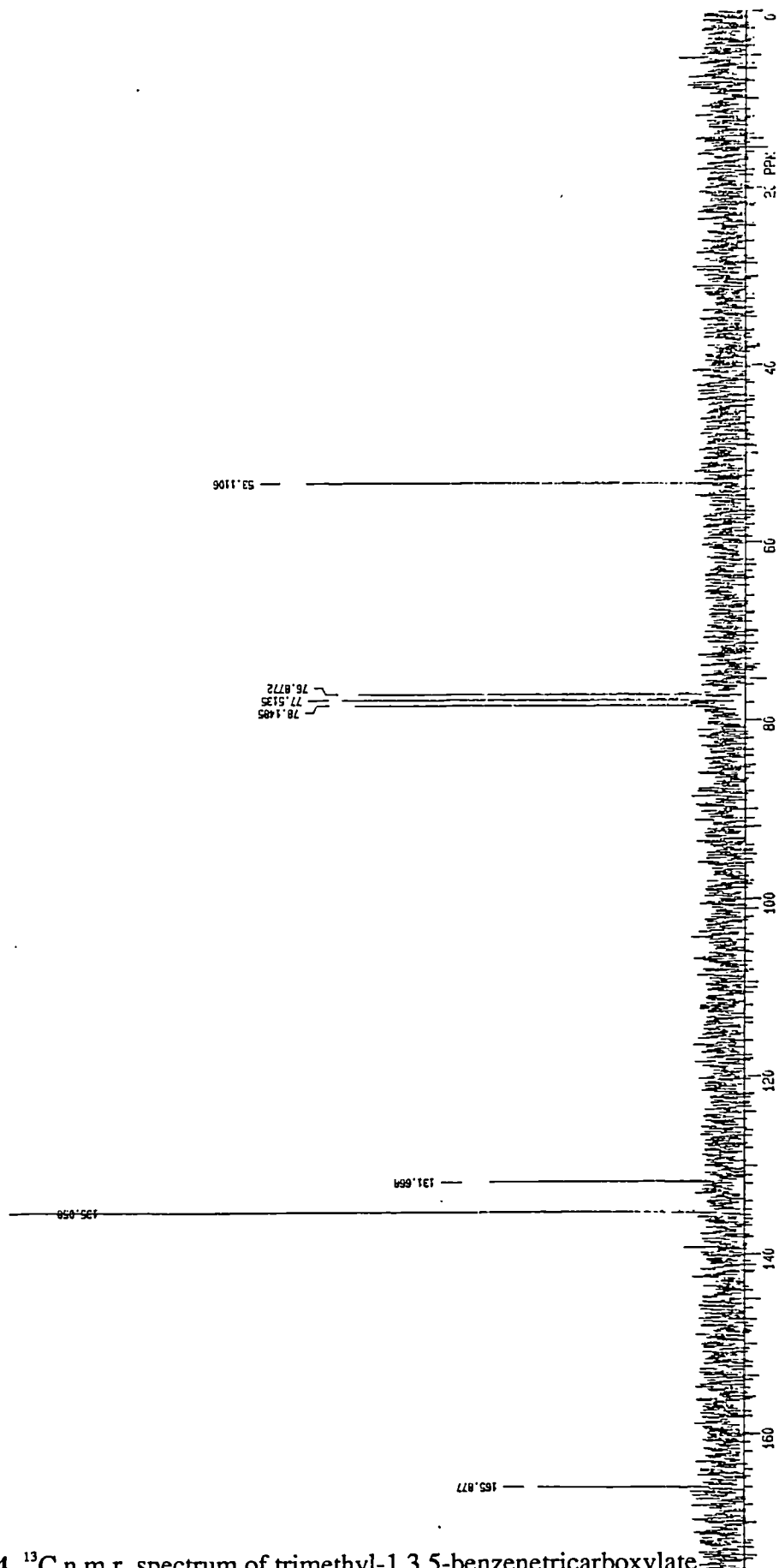
(CDCl$_3$, 200MHz)

Figure A2.14 ^{13}C n.m.r. spectrum of trimethyl-1,3,5-benzenetricarboxylate (CDCl$_3$, 50MHz)
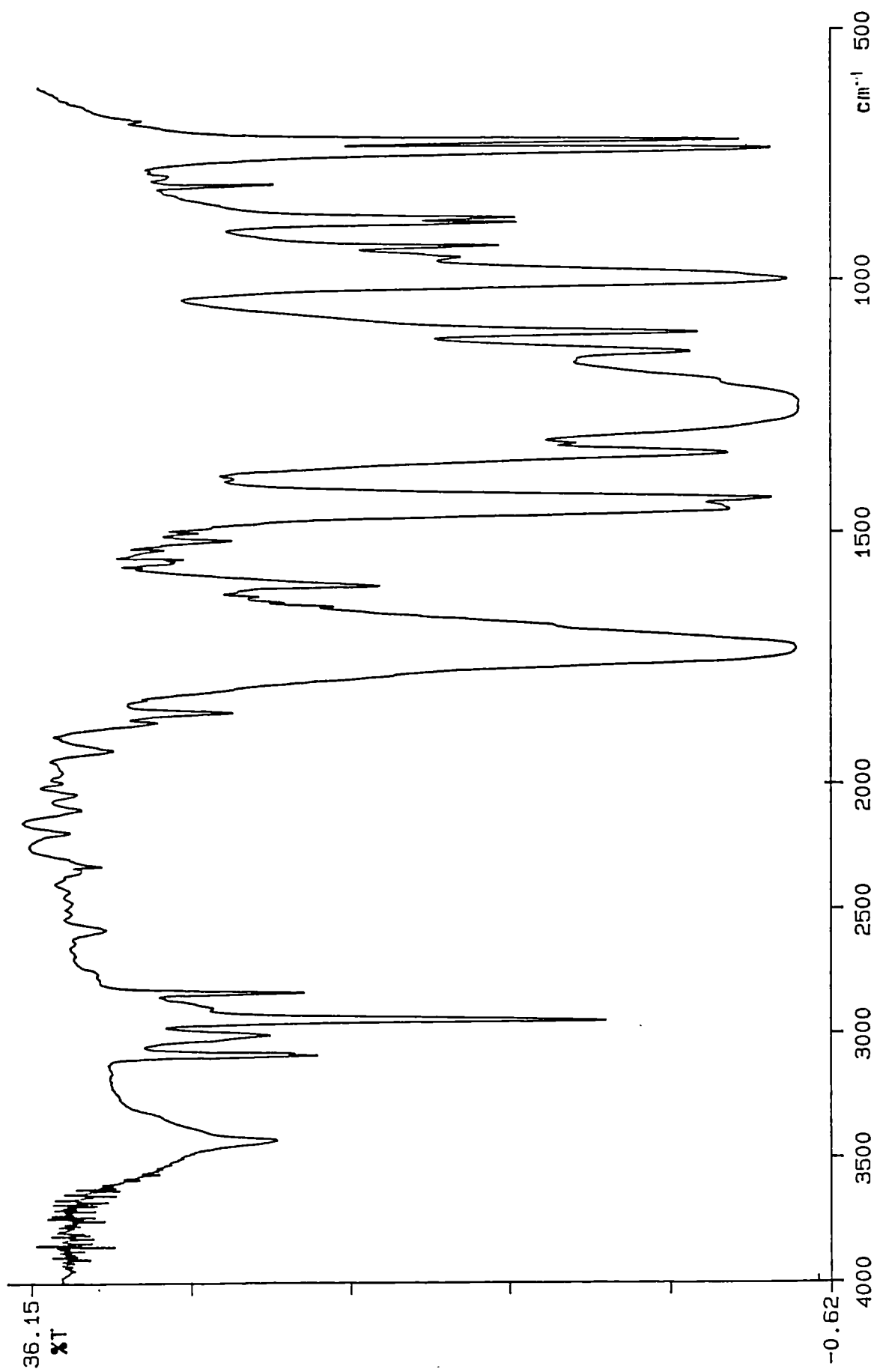
Figure A2.15 I.R. spectrum of trimethyl-1,3,5-benzenetricarboxylate (KBr disc)

Colloquia, Lectures and Seminars

1991

October 17   Dr. J.A.Salthouse, University of Manchester

Son et Luminere - A Demonstration Lecture

October 31   Dr. R.Keeley, Metropolitan Police Forensic Science Unit

Modern Forensic Science

November 6   Prof. B.F.G.Johnson, Edinburgh University

Cluster - Surface Analogues

November 7   Dr. A.R.Butler, St.Andrews University

Traditional Chinese Herbal Drugs: A Different Way of Treating Disease

November 13   Prof. D.Gani, St.Andrews University

The Chemistry of PLP Dependent Enzymes

November 20   Dr. R.More O'Ferrall, University College Dublin

Some Acid-Catalysed Rearrangements in Organic Chemistry

November 28   Prof. I.M.Ward, IRC in Polymer Science, Leeds University

The SCI Lecture: The Science and Technology of Oriented Polymers

December 5   Prof. A.L.Smith, ex-Unilever

Soap, Detergents and Black Puddings

December 11   Dr. W.D.Cooper, Shell Research

Colloid Science: Theory and Practice

1992

January 22   Dr. K.D.M.Harris, St.Andrews University

Understanding the Properties of Solid Inclusion Compounds

January 30   Dr. M.Anderson, Shell Research

Recent Advances in the Safe and Selective Chemical Control of Insect Pests

February 12   Prof. D.E.Fenton, Sheffield University

                 Polynuclear Complexes of Molecular Clefts as Models for Copper Biosites

February 13   Dr. J.Saunders, Glaxo Group Research Ltd.

                 Molecular Modelling in Drug Discovery

February 19   Prof. E.J.Thomas, Manchester University

                 Applications of Organostannanes to Organic Synthesis

February 20   Prof. E.Vogel, Cologne University

                 Porphyrins: Molecules of Interdisciplinary Interest

February 26   Prof. M.L.Hitchman, Strathclyde University

                 Chemical Vapour Deposition

March 5   Dr. N.C.Billingham, Sussex University

                 Degradable Plastics- Myth or Magic?

March 12   Dr. R.A.Hann, ICI Imagedata

                 Electronic Photography- An Image of the Future

March 17   Prof. Sir S.Edwards, Cavendish Laboratory, Cambridge

                 Phase Dynamics and Phase Changes in Polymer Liquid Crystals

March 18   Dr. H.Maskill, Newcastle University

                 Concerted or Stepwise Fragmentation in a Deamination-Type Reaction

March 25   Prof. H.Cherdron, Hoechst-Aktiengesellschaft Centrale Polymerforschung

                 Structural Concepts and Synthetic Methods in Industrial Polymer Science

May 11   Prof. W.Burchard, Freiburg University

                 Recent Developments in the Understanding of Reversible and Irreversible Network

                 Formation

May 13   Dr. J-C.Gehret, Ciba Geigy

                 Some Aspects of Industrial Agrochemical Research

September 21   Prof. E.Thomas, MIT

Interface Structures in Copolymer-Homopolymer Blends

October 15   Dr. M.Glazer and Dr. S.Tarling, Oxford University and Birbeck College

It Pays to be British! - The Chemist's Role as an Expert Witness in Patent Litigation

October 20   Dr. H.E.Bryndza, Du Pont Central Research

Synthesis, Reactions and Thermochemistry of Metal-Alkyl Cyanide Complexes and

Their Impact on Olefin Hydrocyanation Catalysts.

October 22   Prof. A.G.Davies, University College London

The Behaviour of Hydrogen as a Pseudometal

October 28   Dr. J.K.Cockcroft, Durham University

Recent Developments in Powder Diffraction

October 29   Dr. J.Emsley, Imperial College London

the Shocking History of Phosphorus

November 5   Dr. C.J.Ludman, Durham University

Explosions, a Demonstration Lecture

November 12   Prof. M.R.Truter, University College London

Luck and Logic in Host-Guest Chemistry

December 2   Prof. A.F.Hegarty, University College Dublin

Highly Reactive Enols Stabilised by Steric Protection

December 2   Dr. R.A.Aitken, St.Andrews University

The Versatile Cycloaddition of $Bu_3P.CS_2$

December 3   Prof. P.Edwards, Birmingham University

SCI Lecture: What is a Metal?

December 9   Dr. A.N.Burgess, ICI Runcorn

The Structure of Perfluorinated Ionomer Membranes

1993

January 20   Dr. D.C.Clary, Cambridge University

                     Energy Flow in Chemical Reactions

January 21   Prof. L.Hall, Cambridge University

                     NMR- Window to the Human Body

February 3   Prof. S.M.Roberts, Exeter University

                     Enzymes in Organic Synthesis

February 10   Dr. D.Gilles, Surrey University

                     NMR and Molecular Motion in Solution

February 18   Dr. I.Fraser, ICI Wilton

                     Reactive Processing of Composite Materials

March 3   Dr. K.J.P.Williams, BP

                     Raman Spectroscopy for Industrial Analysis

March 16   Prof. J.M.G.Cowie, Herriot-Watt University

                     High Technology in Chains: The Role of Polymers in Electronic Applications and

                     Data Processing

April 1   Prof. H.Spiess, Max Planck Intitut fur Polymerforschung

                     Multidimensional NMR Studies of Structure and Dynamics of Polymers

June 2   Prof. F.Ciardelli, Pisa University

                     Chiral Discrimination in the Stereospecific Polymerisation of Alpha Olefins

June 7   Prof. R.S.Stein, Massachusetts University

                     Scattering Studies of Crystalline and Liquid Crystalline Polymers

June 8   Prof. B.E.Eichinger, Biosym Technologies

                     Recent Polymer Modelling Results and a Look into the Future

June 16   Prof. A.K.Covington, Newcastle University

                     Use of Ion Selective Electrodes as Detectors in Ion Chromatography

July 6   Prof. C.W.Macosko, Minnesota University

Morphology Development in Immiscible Polymer Blending

October 20   Dr. P.Quayle, Manchester University

Aspects of Aqueous ROMP Chemistry

October 23   Prof. R.Adams, South Carolina University

The Chemistry of Metal Carbonyl Cluster Complexes Containing Platinum and Iron, Ruthenium or Osmium and the Development of a Cluster Based Alkyne Hydrogenation Catalyst

October 30   Dr. R.A.L.Jones, Cavendish Laboratory, Cambridge

Perambulating Polymers

November 24 Dr. P.G.Bruce, St.Andrews University

Synthesis and Applications of Inorganic Materials

December 1   Prof. M.A.McKervy, Queens University Belfast

Functionalised Calixerenes

1994

January 26   Prof. J.Evans, Southampton University

Shining Light on Catalysts

February 23   Prof. P.M.Maitlis, Sheffield University

Why Rhodium in Homogeneous Catalysis

March 2   Dr. C.Hunter, Sheffield University

Non-Covalent Interactions between Aromatic Molecules

Conferences and Courses Attended

March 1992	Macro Group (UK) Family Meeting Durham University
September 1992	IRC Club Meeting Leeds University
January 1993	IRC Polymer Engineering Course Bradford University
March 1993	IRC Polymer Physics Course Leeds University
April 1993	Macro Group (UK) Family Meeting Lancaster University
April 1993	High Polymer Group Conference Moretonhampstead
July 1993	SERC Graduate School Sheffield University
September 1993	IRC Club Meeting Durham University
April 1994	Macro Group (UK) Family Meeting Birmingham University
July 1994	MacroAkron '94 IUPAC Meeting University of Akron, Ohio, U.S.A.